

AsiaIntervention

CORONARY INTERVENTIONS

- **105** Obstructive sleep apnoea and coronary revascularisation outcomes *A.Y.H. Chew, C.-H. Lee*
- 114 Clinical prognostic value of a novel quantitative flow ratio from a single projection in patients with coronary bifurcation lesions treated with the provisional approach

J. Kan, S.-L. Chen, et al

- **124** Impact of real-time optical coherence tomography and angiographic coregistration on the percutaneous coronary intervention strategy *R.M. Kadavil, V. Subban, et al.*
- 133 Safety and efficacy of a novel 3D-printed bioresorbable sirolimuseluting scaffold in a porcine model

Q. Shi, M. Chen, et al

143 A simple mathematical method to identify optimal biplane fluoroscopic angulations for chronic total occlusion percutaneous coronary intervention using CT angiography

H. Kamiunten

152 Excimer laser coronary atherectomy for acute myocardial infarction with coronary artery ectasia and massive thrombosis

T. Hiruma, M. Isobe, et al

154 Myocardial ischaemia caused by two remote non-cardiac stenoses *M.S. Guérios, Z. Demartini Jr, E.E. Guérios*

INTERVENTIONS FOR VALVULAR DISEASE AND HEART FAILURE

156 Commissural alignment in the Evolut TAVR procedure: conventional versus hat marker-guided shaft rotation methods

Y. Konami, J. Yamaguchi, et al

166 Paracentral MitraClip implantation technique in a mitral valve with a small area due to rheumatic change

K. Kito, K. Kozuma, et al

168 Attention when performing transcatheter valve-in-valve procedures in degenerative INSPIRIS RESILIA valves: a case of malfunction in the expansion zone

H. Hioki, K. Kozuma, et al

170 Calcification with a figure of eight appearance found in routine coronary angiography

R. Velayutham, A. Shaheer Ahmed, S. Banerjee

PERIPHERAL INTERVENTIONS

172 Carotid artery interventions - endarterectomy versus stenting *S. Kedev*

EDITORIALS

97 Sharing knowledge and defining partnerships across boundaries through AICT-AsiaPCR

A. Seth

99 A novel quantitative flow ratio in coronary bifurcations: a simpler way to a real-time functional provisional stenting strategy

A. Tommasino, E. Navarra, E. Barbato

101 Angiography coregistration: time to fight clinician inertia *G. Guagliumi, D. Pellegrini*

103 New opportunities for bioresorbable scaffold technology A. Kastrati, M. Seguchi

LETTER TO THE EDITOR

180 Letter: Limitless suffixes for bifurcation classification with the Movahed coronary bifurcation lesion classification system

M. Reza Movahed

REPLY TO THE LETTER TO THE EDITOR

182 Reply: Limitless suffixes for bifurcation classification with the Movahed coronary bifurcation lesion classification system

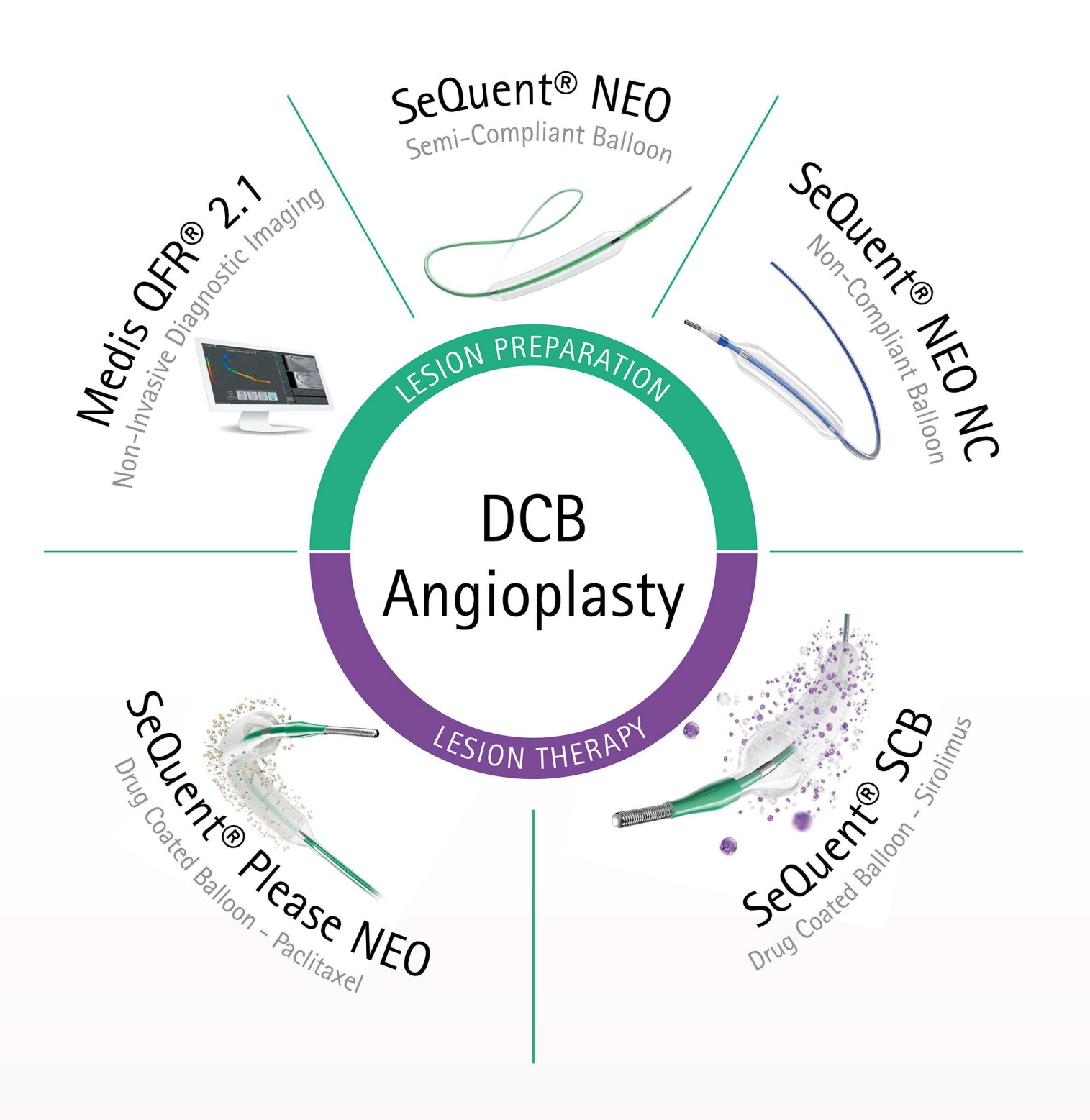
S.-L. Chen



Getting to the heart of the matter







SeQuent® DCBs

The proven performers in coronary angioplasty

Backing up cardiologists with unparalleled clinical data and proven performance for both paclitaxel and sirolimus coated balloons.



AsiaIntervention

The official journal of the Asian-Pacific Society of Interventional Cardiology and the Interventional Cardiology Foundation of India



Would you like to see your research featured in the AsiaIntervention Journal?

SUBMIT NOW!
AsiaIntervention.org

Follow us on:





WeChat









Sharing the best practice of Japan, Asia and beyond in valvular interventions

Share Your WORK

Deadline 23 October 2023

This is your opportunity to step up and shine a light on your work and region, obtaining valuable feedback from your peers and influencing the development of interventional cardiology.

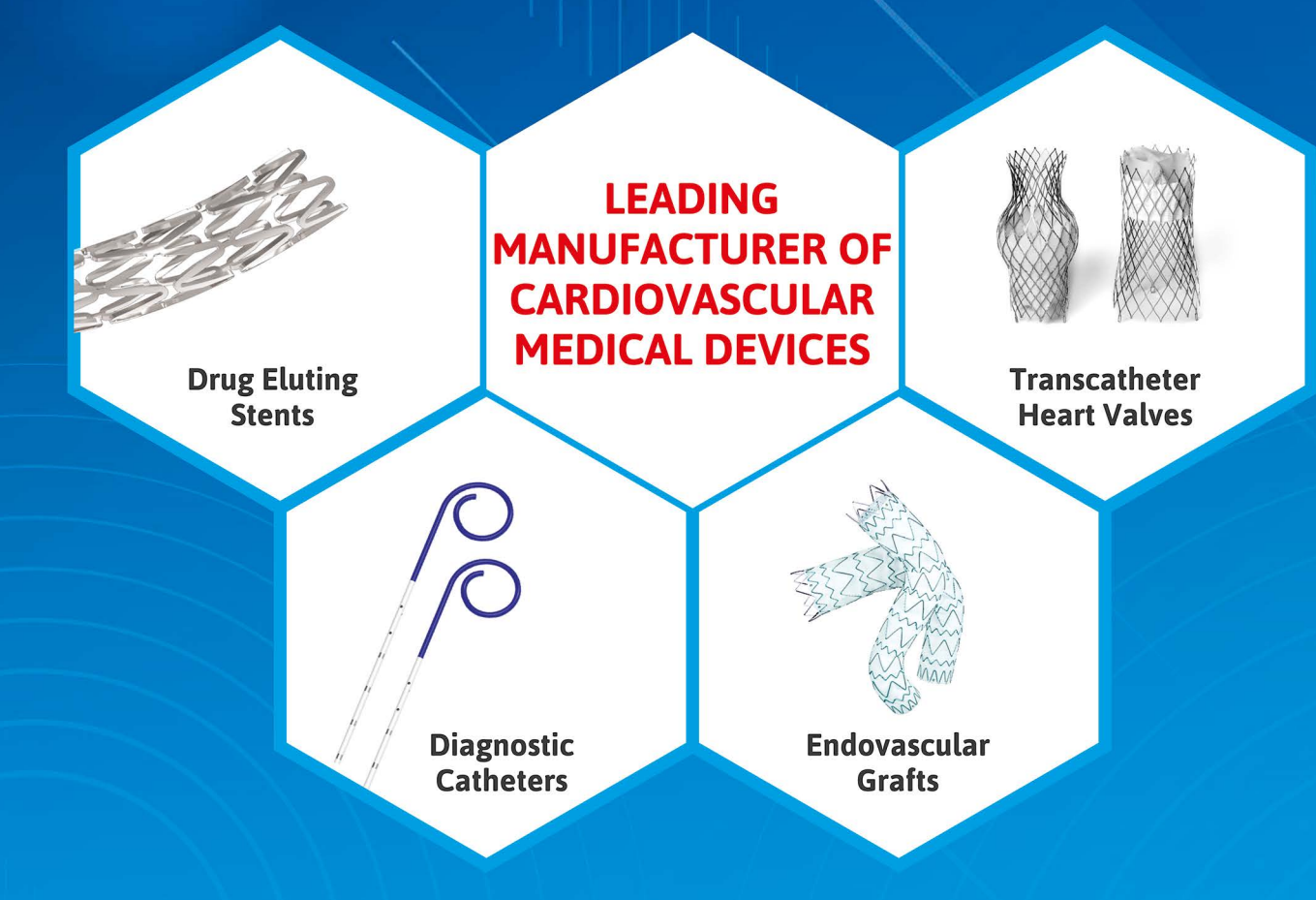






RELISYS MEDICAL DEVICES

Affordable Healthcare to all



- Fully backward integrated manufacturing facility
- •Trusted global OEM partner for end-end solutions

Relisys Medical Devices Limited

Survey No. 312, Pocharam Road, Mangalpally Village, Ibrahimpatnam Mandal, R.R. District, Hyderabad, Telangana 501510.

Medtronic

Renal denervation

is now in the ESH Guidelines



Read the guidelines

Welcome to the turning point in hypertension care

The European Society of Hypertension now includes renal denervation (RDN) as a class II recommendation that provides a safe and effective complementary hypertension treatment strategy.¹



In patients with an eGFR >40 ml/min/1.73m² who have **uncontrolled BP** despite the use of antihypertensive drug combination therapy or if drug treatment elicits serious side effects and poor quality of life.



Additional treatment option in patients with **resistant hypertension** if eGFR is >40 ml/min/1.73m²



Selection of patients should be done in a shared decision-making process



Performed in experienced centers to guarantee **appropriate selection of eligible patients** and completeness of the denervation procedure

With over 25,000 real world RDN patients and counting, Medtronic's Symplicity™ blood pressure procedure is **significant**, **safe**, **and sustained**.²⁻⁵

References:

- $1\ Journal\ of\ Hypertension (): 10.1097/HJH.0000000000003480,\ June\ 21,\ 2023.\ |\ DOI:\ 10.1097/HJH.000000000003480.$
- 2 Böhm M, Kario K, Kandzari DE, et al. Efficacy of catheter-based renal denervation in the absence of antihypertensive medications (SPYRAL HTN-OFF MED Pivotal): a multicentre, randomised, sham-controlled trial. The Lancet. 2020; Published online March 29, 2020.
- 3 Kandzari DE, Böhm M, Mahfoud F, et al. Effect of renal denervation on blood pressure in the presence of antihypertensive drugs: 6-month efficacy and safety results from the SPYRAL HTN-ON MED proof-of-concept randomised trial. The Lancet. 2018 Jun 9;391(10137):2346-2355.
- 4 Mahfoud F, Mancia G, Schmieder R, et al. Three-year safety and efficacy in the Global Symplicity Registry: Impact of antihypertensive medication burden on blood pressure reduction. Presented at PCR e-course 2020.
- 5 Mahfoud F, Kandzari DE, Kario K, et al. Long-term efficacy and safety of renal denervation in the presence of antihypertensive drugs (SPYRAL HTN-ON MED): a randomised, sham-controlled trial. The Lancet. 2022;399:1401-1410.

Disclaimer: This page may include information about products that may not be available in your region or country. Please consult the approved indications for use. Content on specific Medtronic products is not intended for users in markets that do not have authorization for use.

SEPTEMBER 2023

VOLUME 9, Issue 2

IN THIS ISSUE OF ASIAINTERVENTION

Carotid artery stenting or endarterectomy; OSA and PCI outcomes; µQFR for side branch evaluation; newgeneration BVS versus metallic DES; OCTACR in complex PCI; finding the optimal biplane view for CTO PCI; and much more...

Upendra Kaul, *Editor-in-Chief*

Dear friends,

We are delighted to extend a warm welcome to you on behalf of AsiaIntervention, the official journal of AICT-AsiaPCR, and the Interventional Cardiology Foundation of India (ISCL). We look forward to yet another captivating edition here in Singapore.

AsiaIntervention is thrilled to be onsite at AICT-AsiaPCR 2023, ensuring our active participation. At this year's Fellows Course, we will be present during a PCR clinical research session featuring esteemed speakers Vijay Kunadian and James Howard, who will discuss "Artificial intelligence in medical writing" and "Addressing the unmet needs of our patients through clinical research".

Throughout the year, AsiaIntervention has actively engaged in a handful of international congresses, including INDIA LIVE 2023 and EuroPCR 2023. While it is crucial for us to be physically present at these gatherings and connect directly with our peers, it is our relentless efforts behind the scenes that contribute significantly to our growth. Building on the success of our inclusion in PubMed Central in 2022, we are proud to announce that we also received our first SCOPUS score in 2023. This

achievement further propels us towards our goal. Moreover, we eagerly anticipate our first impact factor, with our application currently in progress. We hope to receive this prestigious recognition in 2024.

Without further ado, we are pleased to present the second volume of 2023. Thank you for your unwavering support which continues to inspire us.

This issue kicks off with coronary interventions and a review of the impact of obstructive sleep apnoea (OSA) on coronary revascularisation outcomes. The article by **Adrienne Y.H. Chew and Chi-Hang Lee** reports a high incidence of OSA in patients undergoing percutaneous coronary intervention (PCI) or coronary artery bypass graft and suggests that treating OSA could lead to improved outcomes. While routine screening may not be necessary, patients who experience excessive sleep or difficult-to-control hypertension post-revascularisation should be evaluated for OSA.

Jing Kan, Shao-Liang Chen and colleagues present a clinical research article detailing a novel method for estimating a single-plane quantitative flow reserve (μ QFR) in the side branch after stenting the main vessel. Their study identifies a μ QFR <0.80 in the side branch as a predictor of adverse outcomes, compared to a μ QFR >0.80. Antonella Tommasino, Emiliano Navarra and Emanuele Barbato provide insightful comments on the study in an accompanying editorial, highlighting its strengths and limitations.

In another research article, Rony Mathew Kadavil, Vijayakumar Subban and colleagues report on their experience with optical coherence tomography (OCT) and accompanying angiographic coregistration (ACR) in optimising the results of PCI. Their findings demonstrate a significant improvement in outcomes for nearly all patients studied, with excellent results observed at the 1-year mark. The accompanying invited editorial by Giulio Guagliumi and Dario Pellegrini offers expert insights and commentary on the subject.

A translational research article by **Qiuping Shi, Ming Chen and colleagues** presents a study comparing a three-dimensionally printed sirolimus-eluting bioresorbable vascular scaffold (BRS) to a metallic sirolimus-eluting stent (SES) in a porcine model. The authors evaluate the safety and efficacy of the BRS through periodic OCT and scanning electron microscopic evaluations, spanning 169 days. The study showcases positive remodelling of the BRS without compromising endothelialisation, demonstrating its comparability to metallic SES. **Adnan Kastrati and Masaru Seguchi** provide an editorial critique, analysing the experimental study's strengths and limitations.

In another translational research article, **Hitoshi Kamiunten** introduces a method for facilitating chronic total occlusion (CTO) angioplasty using trigonometric vector designs

to determine the optimal angulation on standard biplane fluoroscopic equipment. The article outlines the use of a calculator, using spreadsheet software, to minimise dead angles in biplane fluoroscopy, aiding in CTO angioplasty.

The valvular interventions section features an article by **Yutaka Konami**, **Junichi Yamaguchi and colleagues** discussing commissural alignment in the Evolut transcatheter aortic valve replacement procedure, comparing conventional and hat marker-guided shaft rotation methods.

This issue also hosts a variety of interventional flashlights, two related to coronary interventions and three to structural interventions. **Takashi Hiruma**, **Mitsuaki Isobe and colleagues** present a case of acute myocardial infarction complicated by a large ectasia with a heavy thrombus burden, which was successfully managed using an excimer atherectomy device. **Marina S. Guérios, Zeferino Demartini Jr and Enio E. Guérios** describe a case of myocardial ischaemia caused by two remote non-cardiac stenoses.

Kento Kito, Ken Kozuma and colleagues showcase a paracentral MitraClip implantation technique in a mitral valve with a small area due to rheumatic aetiology, whilst Hirofumi Hioki, Ken Kozuma and colleagues highlight a transcatheter valve-in-valve procedure in degenerative INSPIRIS RESILIA valves. Ramanathan Velayutham, A. Shaheer Ahmed and Saurav Banerjee explain how they interpreted a calcified figure of eight found on fluoroscopy during routine angiography.

In peripheral interventions, an informative review article delves into the long-standing controversy surrounding the treatment of significant carotid disease, comparing non-surgical stenting, surgical endarterectomy, and optimal medical treatment. **Sasko Kedev** rationalises the subject through a comprehensive review of randomised trials and guidelines. The article emphasises the advancements in stents, embolic protection devices, and technique refinements that have significantly improved the safety and durability of both procedures. While each approach may have advantages in specific situations, successful treatment of severe stenosis, both symptomatic and asymptomatic, is achievable by expert intervention.

Finally, we have an interesting exchange of letters on coronary bifurcation lesions by **Mohammad Reza Movahed and Shao-Ling Chen.**

I sincerely hope that the contents of this issue pique your interest and prove beneficial in your daily practice. As always, AsiaIntervention eagerly anticipates your valuable feedback and suggestions, to aid in enhancing the journal even further.

Wishing you a pleasant reading experience!

EDITORIALS

- **97** Sharing knowledge and defining partnerships across boundaries through AICT-AsiaPCR *Ashok Seth*
- **99** A novel quantitative flow ratio in coronary bifurcations: a simpler way to a real-time functional provisional stenting strategy *Antonella Tommasino, Emiliano Navarra, Emanuele Barbato*
- 101 Angiography coregistration: time to fight clinician inertia Giulio Guagliumi, Dario Pellegrini
- **103** New opportunities for bioresorbable scaffold technology *Adnan Kastrati, Masaru Seguchi*

CORONARY INTERVENTIONS

- **105** Obstructive sleep apnoea and coronary revascularisation outcomes *Adrienne Y.H. Chew, Chi-Hang Lee*
- 114 Clinical prognostic value of a novel quantitative flow ratio from a single projection in patients with coronary bifurcation lesions treated with the provisional approach

Jing Kan, Zhen Ge, Shaoping Nie, Xiaofei Gao, Xiaobo Li, Imad Sheiban, Jun-Jie Zhang, Shao-Liang Chen

124 Impact of real-time optical coherence tomography and angiographic coregistration on the percutaneous coronary intervention www strategy

Rony Mathew Kadavil, Jabir Abdullakutty, Tejas Patel, Sivakumar Rathnavel, Balbir Singh, Nagendra Singh Chouhan, Fazila Tun Nesa Malik, Shirish Hiremath, Sengottuvelu Gunasekaran, Samuel Mathew Kalarickal, Viveka Kumar, Vijayakumar Subban

- 133 Safety and efficacy of a novel 3D-printed bioresorbable sirolimus-eluting scaffold in a porcine model *Oiuping Shi, Bin Zhang, Xingang Wang, Jintao Fei, Oiao Qin, Bo Zheng, Ming Chen*
- A simple mathematical method to identify optimal biplane fluoroscopic angulations for chronic total occlusion percutaneous coronary intervention using CT angiography

 Hitoshi Kamiunten
- **152** Excimer laser coronary atherectomy for acute myocardial infarction with coronary artery ectasia and massive thrombosis *Takashi Hiruma, Tomofumi Tanaka, Mamoru Nanasato, Mitsuaki Isobe*
- 154 Myocardial ischaemia caused by two remote non-cardiac stenoses

WWW Marina S. Guérios, Zeferino Demartini Jr, Enio E. Guérios

INTERVENTIONS FOR VALVULAR DISEASE AND HEART FAILURE

- 156 Commissural alignment in the Evolut TAVR procedure: conventional versus hat marker-guided shaft rotation methods *Yutaka Konami, Tomohiro Sakamoto, Hiroto Suzuyama, Eiji Horio, Junichi Yamaguchi*
- 166 Paracentral MitraClip implantation technique in a mitral valve with a small area due to rheumatic change



168 Attention when performing transcatheter valve-in-valve procedures in degenerative INSPIRIS RESILIA valves: a case of www malfunction in the expansion zone

Hirofumi Hioki, Yusuke Watanabe, Akihisa Kataoka, Hideyuki Kawashima, Ken Kozuma

170 Calcification with a figure of eight appearance found in routine coronary angiography Ramanathan Velayutham, A. Shaheer Ahmed, Saurav Banerjee

PERIPHERAL INTERVENTIONS

172 Carotid artery interventions - endarterectomy versus stenting Sasko Kedev

LETTER TO THE EDITOR

180 Letter: Limitless suffixes for bifurcation classification with the Movahed coronary bifurcation lesion classification system Mohammad Reza Movahed

REPLY TO THE LETTER TO THE EDITOR

182 Reply: Limitless suffixes for bifurcation classification with the Movahed coronary bifurcation lesion classification system *Shao-Liang Chen*

www

Website exclusive contents: images and/or moving images

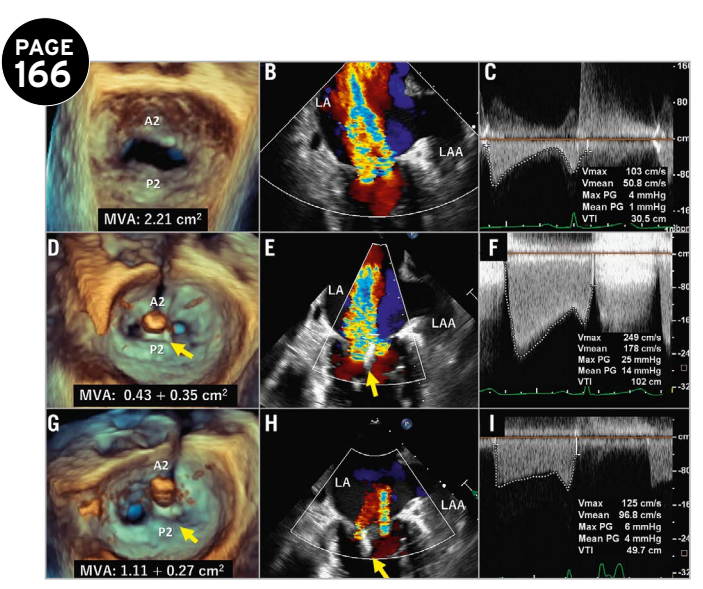


Image taken from the following paper printed in this issue:
Paracentral MitraClip implantation technique in a mitral valve with a small area due to rheumatic change
K. Kito, A. Kataoka, H. Hioki, Y. Watanabe, K. Kozuma
AsiaIntervention. 2023;9:166-7

Aims and scope

AsiaIntervention Journal is an international, English language, peer-reviewed journal whose aim is to create a forum of high-quality research and education in the field of percutaneous and surgical cardiovascular interventions.

It is released twice a year, in paper and electronic formats. AsiaIntervention is indexed in MEDLINE®/PubMed Central®.

AsiaIntervention is the official journal of the Asian-Pacific Society of Interventional Cardiology (APSIC) and the Interventional Cardiology Foundation of India (ICFI).

Advertising information

Orders and enquiries can be sent to Europa Digital & Publishing.

Orders, claims, and journal enquiries

Please contact Europa Digital & Publishing.

Copyright: © Europa Digital & Publishing. All rights reserved. The journal and the contributors are protected under copyright, and the following terms and conditions apply to their use:

Photocopying

Single copies of single articles may be made for personal use as allowed by national copyright laws. Permission from the publisher and the payment of a fee is required for all other photocopying.

Derivative works

Subscribers may reproduce tables of contents or prepare lists of articles including abstracts for internal circulation within their institutions. Permission from the publisher is required for resale or distribution outside the institution. For all other derivative works permission should be sought from the publisher.

Electronic storage or usage

Permission from the publisher is required to store or use electronically any material contained in this journal, including any article or part of an article. Please contact Europa Digital & Publishing.

Notice

No responsibility is assumed by the publisher for any injury and/ or damage to persons or property as a matter of products liability, negligence or otherwise, or from any use or operation of any methods, products, instructions or ideas contained in the material. Although all advertising material is expected to conform to ethical (medical) standards, inclusion in this publication does not constitute a guarantee or endorsement of the quality or value of such product or of the claims made of it by its manufacturer.

Disclaimer

The publishers and editors cannot be held responsible for errors or any consequences arising from the use of information contained in this journal; the views and opinions expressed do not necessarily reflect those of the publisher and editors, neither does the publication of advertisements constitute any endorsement by the publisher and editors of the products advertised.

Europa Digital & Publishing 19. allées Jean-Jaurès – BP 61508 31015 Toulouse cedex 6 - France Fax: +33 5 61 42 00 09 asiaintervention@asiaintervention.org

Author's instructions

All articles should be submitted to http://www.editorialmanager.com/aij/

A full version of the instructions can be found and downloaded on the website: www.asiaintervention.org

AsiaIntervention will consider submissions for possible publication in the following formats:

- Original research (clinical and preclinical/experimental)
- Translational research
- Expert consensus - Expert review
- Trial design
- Meta-analysis - Research correspondence
- Editorial
- Interventional flashlight
- Letter to the Editor

All submissions should be accompanied by a cover letter.

ASIAINTERVENTION Publication: 2 numéros par an Volume 9 - N°2 - Septembre 2023

Directeur de la publication:

Marc Doncieux

Responsable éditoriale:

Svlvie Lhoste

slhoste@eurointervention.org

Assistante éditoriale

Devia Bijkerk

Coordination éditoriale

Véronique Deltort Amy McDowell Sheldon Heitner Isabelle Uzielli Sonia Morcuende Jane McKellow Nikki Rubython Noëlle Wylie

Coordination digitale:

Ronnie Lassiaille Gregori Despeaux Coralie Massonnié Davy Bonnafous Florence Petit Sarah Françoise

Graphisme et mise en page:

Groupe Composer: 2, impasse du Ramier des Catalans - CS 38503 31685 Toulouse Cedex 6 - France

Editeur:

Frédéric Doncieux Président : Marc Doncieux. Principal actionnaire: FINANCIERE MF DONCIEUX; ISSN: 2426-3958 ISSN Online: 2491-0929 Dépôt légal à parution

Imprimé en Inde par Royale Press Pte Ltd Blk 1 Ang Mo Kio Industrial Park 2A #04-05 AMK Tech 1 Singapore 568049 Copyright © Europa Group 2023

Le contenu de AsiaIntervention ne peut être reproduit sans autorisation écrite de l'éditeur.

Europa Digital & Publishing est une marque commerciale d'Europa Group AsiaIntervention est édité par la Société Europa Group, SAS au capital de 1 000 000 euros, siège social : 19, allées Jean-Jaurès, 31000 Toulouse, France;

RCS Toulouse 342 066 727, APE 8230 Z.

AsiaIntervention Journal

EDITOR-IN-CHIEF

Upendra Kaul New Delhi, India

DEPUTY EDITORS

Shao-Liang Chen Nanjing, China

Surya Dharma *Jakarta, Indonesia*

Kentaro Hayashida Tokyo, Japan

Michael Kang-Yin Lee Kowloon, Hong Kong SAR, China

Huay Cheem TanSingapore, Singapore

GUEST EDITOR

Davide Capodanno Catania, Italy

ETHICS COMMITTEE

Marie-Claude Morice Massy, France

Richard NgSingapore, Singapore

ADVISORY EDITORS

Bernard Chevalier Massy, France

Jean Fajadet Toulouse, France

Run Lin Gao *Beijing, China*

- A Mitsuru Abe Alexandre Abizaid Taehoon Ahn Youngkeun Ahn Takashi Akasaka Jiro Aoki Masaki Awata
- B Vinay K. Bahl Salvatore Brugaletta Robert Byrne
- C Davide Capodanno Shaoliang Chen Donghoon Choi Hyuk Choi Seung Antonio Colombo
- D | Pim De Feyter Carlo Di Mario Gregory Ducrocq
- E | Eric Eeckhout
- F | Jean Fajadet Vasim Farooq Buntaro Fujita
- G Junbo Ge Eberhard Grube

Adnan Kastrati

Munich, Germany

Patrick W. Serruys
Galway, Ireland

Ashok Seth New Delhi, India

William Wijns Galway, Ireland

SECTION EDITORS Coronary interventions

Kirti Punamiya Mumbai, India

Goran Stankovic *Belgrade, Serbia*

Valvular interventions

Paul Chiam

Singapore, Singapore

Angus Shing Fung Chui Hong Kong SAR, China

Gunasekaran Sengottuvelu

Chennai, India

Edgar Tay

Singapore, Singapore

Khung Keong Yeo

Singapore, Singapore

Peripheral interventions

Bryan Yan

Hong Kong SAR, China

Clinical reviews

Andreas Baumbach London, United Kingdom

Intracoronary imaging

Alan Chan

Hong Kong SAR, China

Ajit Mullasari

Chennai, India

Yoshinobu Onuma

Galway, Ireland

Intracoronary physiology

Javier Escaned

Madrid, Spain

Fazila Malik

Dhaka, Bangladesh

Non-invasive imaging

Mona Bhatia New Delhi, India

Interventional pharmacology

Bashir Hanif Karachi. Pakistan

Jack Tan

Singapore, Singapore

SECTION EDITOR: STATISTICAL & META-ANALYSIS EDITORS

Sripal Bangalore New York, USA

Ganesan Karthikeyan

New Delhi, India

SENIOR EDITORIAL CONSULTANTS

Peter Barlis

Melbourne, Australia

Bernard De Bruyne

Aalst, Belgium

David Holmes

Rochester, USA

Vijay Kunadian

Newcastle, United Kingdom

Sydney Lo

Sydney, Australia

Christoph Naber

Wilhelmshaven, Germany

Duk-Woo Park

Seoul, Republic of Korea

Alexander Thomas

Coimbatore, India

Rakesh Yadav

New Delhi, India

SOCIAL MEDIA TEAM

Mirvat Alasnag

Jeddah, Saudi Arabia

International Editorial Board and Reviewers

- H Yaling Han
 Hidehiko Hara
 Ho Heo Jung
 David Hildick-Smith
 Myeong-Ki Hong
 Yong Huo
 Seung-Ho Hur
- I Javaid Iqbal Yuki Ishibashi
- J | Xiongjing Jiang Michael Joner
- K S. Mathew Kalarickal Paul H.L. Kao Adnan Kastrati Narendra Nath Khanna June-Hong Kim Kee-Sik Kim Yoshio Kobayashi Tian-Hai Koh Bon-Kwon Koo Ran Kornowski S. Radha Krishnan K. Krishna Kumar
- L | Jens Flensted Lassen | Jae-Hwan Lee | Michael K.Y. Lee

- L | Thierry Lefèvre Yves Louvard Thomas Luscher
- M Felix Mahfoud
 Jean Marco
 Atul Mathur
 Ashwin B. Mehta
 Sundeep Mishra
 Marie-Claude Morice
 Takashi Muramatsu
 Darren Mylotte
- N Toru Naganuma Yoshihisa Nakagawa Shimpei Nakatani Chang-Wook Nam Mamoru Nanasato Masahiro Natsuaki
- O Takayuki Okamura Andrew T.L. Ong Yukio Ozaki
- R | Maria Radu Lorenz Räber Sagar V. Dayasagar Rao Carlos Ruiz
- S | Manel Sabaté Naritatsu Saito

- S Shigeru Saito
 Teguh Santoso
 Ashok Seth
 Sanjeev Sharma
 Imad Sheiban
 Weifeng Shen
 Hiroki Shiomi
 Shinichi Shirai
 Horst Sievert
 Yohei Sotomi
 Bojan Stanetic
 Goran Stanković
 Giulio Stefanini
- T Tomohisa Tada Kengo Tanabe Hiroki Tateishi Tetsuya Tobaru Sanjay Tyagi
- V | Alec Vahanian Marco Valgimigli
- W Ron Waksman Wan Azman Wan Ahmad William Wijns Stephan Windecker
- Y | Kyohei Yamaji Yuejin Yan

Sharing knowledge and defining partnerships across boundaries through AICT-AsiaPCR



Ashok Seth*, FRCP, FACC, MSCAI, FAPSIC, DSc

President, Asian Pacific Society of Interventional Cardiology (APSIC)

We look forward to welcoming you all to AICT-AsiaPCR 2023, the official meeting of the Asian Pacific Society of Interventional Cardiology, being held on 21-22 September 2023 in Singapore. The preparations started well in advance, and the course directors who represent both APSIC and PCR, along with the meeting organisers, Europa Group, have spent innumerable hours brainstorming to achieve a most exciting educational programme. As the President of APSIC, I invite you all to attend and enjoy the exchange of knowledge, build camaraderie and develop academic partnerships across boundaries, and to showcase your research and innovations. It is a platform in the Asia-Pacific region for interacting with the world.

This is the first year since the COVID era began that we feel confident COVID is behind us and our lives are back to normal. This is also the first AICT-AsiaPCR in the post-COVID era without COVID restrictions. The meeting has been made compact and focused over 3 days only, with the first full day devoted to a Fellows Course (for career interventionalists). Seven to eight live cases from centres in Singapore, the UK, and India, as well as numerous sessions on "complications" in partnership with the National Societies of the Asia Pacific region, will be the highlight of the meeting, with an emphasis on learning and sharing. Please take this opportunity to share knowledge in the open spirit of friendship and camaraderie.

The APSIC continues to strengthen bonds with its member countries to consolidate its representation of interventional cardiologists in the Asia-Pacific region. Over the past year, we have inducted to the board and officially nominated representatives of 12 more national societies, namely the Afghanistan Cardiovascular Association (ACA), Cardiological Society of India (CSI), Hong Kong Society of Transcatheter Endo-Cardiovascular Therapeutics (HKSTENT), Iraqi Cardiothoracic Society (ICS), Cardiovascular Society of Mauritius (CSM), Mongolian Society of Interventional Cardiology (MSIC), Cardiac Society of Nepal (CSN), Philippine Society of Cardiovascular Catheterization and Intervention, Inc., (PSCCI), Saudi Arabian Cardiac Interventional Society (SACIS), Cardiovascular Intervention Association of Thailand (CIAT), Emirates Cardiac Society (ECS), and the Vietnam Society of Interventional Cardiology (VSIC). Thus, at this time, APSIC encompasses 29 countries across nine time zones, from New Zealand in the east to Saudi Arabia in the west. This is a great opportunity to work together on numerous combined registries to better understand the heart disease patterns in our region and to tailor treatment options to achieve the best outcomes.

Over the past year, we have worked closely with the Asia Pacific Society of Cardiology (our sister Society) to support and endorse the creation of "consensus statements" on the Management

^{*}Corresponding author: Fortis Escorts Heart Institute, Okhla Road, New Delhi 110025, India. E-mail: ashok.seth@fortishealthcare.com

of Left Main Stenosis, Transcatheter Aortic Valve Implantation, and Management of Ischaemic Cardiogenic Shock. We have also worked closely with regional societies to impart education through sessions at their national meetings, like the National Heart Association of Malaysia's MYLIVE Congress 2022, GulfPCR-GIM 2022, Taiwan Transcatheter Therapeutics (TTT 2023), Pakistan Live Interventional Cardiology (PSIC) meeting 2023, Saudi Arabian Cardiac Interventional Society annual meeting 2023, Bangladesh Society of Cardiovascular Intervention (BSCI)'s annual scientific meeting "BD INTERVENTION" 2023, Asian Pacific Society of Cardiology Congress 2023 (Singapore) and the annual meeting of the Japanese Association of Cardiovascular Intervention and Therapeutics (CVIT2023).

The creation of WIN-APSIC (Women-In-Asian Pacific Society of Interventional Cardiology), a subcouncil of APSIC¹, has stood as one of the most important initiatives of our society's contribution to defining awareness of gender diversity, not just in the understanding of cardiac disease processes and treatments, but also for professional training, participation and career advancement in interventional cardiology. In this regard, the leadership and enthusiasm of Fazila Malik (Bangladesh) and Mirvat Alasnag (Saudi Arabia) as Chair and Co-Chair, respectively, have been admirable. The council now has women interventional cardiology

representatives from 13 countries. Lim Ing Haan, the organiser of the WIN-APSIC Webinar Series, has planned a calendar of important educational webcasts every 3 months. The first of these, "Multivessel PCI in Women: Real World Challenges and How to Achieve the Best Outcomes", held on 3 May 2023, was acclaimed by all faculty and participants for the knowledge and awareness of its content. WIN-APSIC has also initiated an Asia-Pacific registry for Spontaneous Coronary Artery Dissection (SCAD) in partnership with the ongoing European Society of Cardiology (ESC) registry. Other important Asia-Pacific dedicated surveys are planned.

Let us together define a new era for interventional cardiology in the Asia-Pacific region. Let us pool our immense professional experience, our admired technical expertise, our defining techniques and technology, and our pathbreaking research and innovations. Let us inspire our younger generation of interventional cardiologists to dream and deliver the best for cardiac patients across the world.

Conflict of interest statement

A. Seth is a course director of the AICT-AsiaPCR Course.

Reference

1. Alasnag M, Malik F, Seth A. WIN-APSIC Committee: a nexus for development & inclusion. *AsiaIntervention*. 2023;9:18-9.

A novel quantitative flow ratio in coronary bifurcations: a simpler way to a real-time functional provisional stenting strategy

Antonella Tommasino¹, MD; Emiliano Navarra², MD; Emanuele Barbato^{1,3}*, MD, PhD

1. Division of Cardiology, Sant'Andrea Hospital, Rome, Italy; 2. Division of Cardiac Surgery, Sant'Andrea Hospital, Rome, Italy; 3. Department of Clinical and Molecular Medicine, Sapienza University of Rome, Rome, Italy

Percutaneous coronary interventions (PCI) in bifurcation lesions are technically challenging because of the bifurcation angle, the extent and severity of side branch (SB) disease, and dynamic changes in plaque distribution that occur during the intervention. PCI in bifurcations is often associated with suboptimal clinical outcomes as compared to PCI in non-bifurcation lesions¹. Provisional stenting of the SB is the recommended strategy for most bifurcation lesions, while an upfront two-stent strategy is reserved for bifurcation lesions with large SBs supplying significant myocardial territory². However, determining the clinical relevance of an SB has always been extremely difficult. Recently, the Bifurcation Academic Research Consortium (Bif-ARC) has proposed a standardised algorithm consisting of a simple anatomical scoring system based on angiographic estimates of the myocardial mass at risk³.

As SBs supply the myocardium less than the main branches (MBs), the functional impact of SB stenosis in terms of significant ischaemia as assessed by fractional flow reserve (FFR) is lower than a similar stenosis in an MB⁴. The use of FFR to guide PCI of bifurcation lesions has consistently shown potential benefits in optimising treatment decisions and improving clinical outcomes⁵. However, there are technical considerations and limitations, such as the "branch steal effect", the potential variations in FFR values

due to wire position, the impact of the SB size and the interactions between stenoses in the MB and SB³. All these factors can lead to an underestimation in the SB functional assessment. Furthermore, SB rewiring is not always feasible after MB stenting, depending upon the geometrical and dynamic changes that occur at the level of the bifurcation PCI. In fact, in the DKCRUSH VI trial⁶, assessing the FFR of the SB was not viable in up to 10% of cases, primarily due to the challenging rewiring required with the pressure wire. In this context, the availability of angiographic functional assessment, such as quantitative flow ratio (QFR), Murray's law-based quantitative flow ratio (mQFR), virtual FFR (vFFR), etc., could enhance the clinical adoption of functional assessment in the context of bifurcation lesions. Unlike QFR, mQFR has the additional advantage of requiring a single acquisition based on algorithms using fractal laws (i.e., Murray's law in quantitative flow ratio).

The diagnostic accuracy of a novel QFR (μ QFR) has been previously described⁷; yet, in this issue of AsiaIntervention, Kan et al⁸ significantly contribute to the available evidence by reporting on the prognostic impact of this functional analysis in bifurcations previously treated with main branch stenting where the SB is jailed. The study suggests that in a jailed SB, a μ QFR measurement can be a useful prognostic factor in patients with *de novo*

^{*}Corresponding author: Department of Clinical and Molecular Medicine, Sant'Andrea Hospital, Sapienza University of Rome, Via di Grottarossa 1035, 00189 Rome, Italy. E-mail: emanuele.barbato@uniroma1.it

true bifurcation lesions undergoing PCI, by identifying functionally relevant SBs with lower μQFR values (<0.80) that are associated with poorer outcomes. Previous PCI and SB μQFR <0.80 were found to be independent predictors of clinical endpoints.

Article, see page 114

These data are interesting and promising, yet, sobering conclusions should be drawn in consideration of the obvious limitations owing to the retrospective study design, e.g., small sample size, a potential selection bias in the group of patients with an SB µQFR < 0.80 that was older, with less complete revascularisation and/or more complex or advanced coronary artery disease. Some important variables were not considered in the analysis, like bifurcation angles, the type of stents used, whether SB treatment was driven by the functional assessment and finally, the impact of intravascular ultrasound (IVUS) guidance, which was actually used in less than 35% of the patients. Despite these limitations, the investigators should be commended for their study, which introduces a novel and easier approach to functionally significant bifurcations. Whether the real-time availability of µQFR in jailed SBs could be a reliable guide for further intervention in SBs that are functionally and prognostically significant is an interesting working hypothesis that deserves further investigation in prospective studies.

Conflict of interest statement

E. Barbato reports speaker's fees from Boston Scientific, Abbott, and Insight Lifetech. A. Tommasino and E. Navarra have no relevant conflicts of interest to declare.

References

- 1. Sawaya FJ, Lefèvre T, Chevalier B, Garot P, Hovasse T, Morice MC, Rab T, Louvard Y. Contemporary Approach to Coronary Bifurcation Lesion Treatment. *JACC Cardiovasc Interv*, 2016;9:1861-78
- 2. Burzotta F, Lassen JF, Lefèvre T, Banning AP, Chatzizisis YS, Johnson TW, Ferenc M, Rathore S, Albiero R, Pan M, Darremont O, Hildick-Smith D, Chieffo A, Zimarino M, Louvard Y, Stankovic G. Percutaneous coronary intervention for bifurcation coronary lesions: the 15th consensus document from the European Bifurcation Club. *EuroIntervention*. 2021;16:1307-17.
- 3. Lunardi M, Louvard Y, Lefèvre T, Stankovic G, Burzotta F, Kassab GS, Lassen JF, Darremont O, Garg S, Koo BK, Holm NR, Johnson TW, Pan M, Chatzizisis YS, Banning A, Chieffo A, Dudek D, Hildick-Smith D, Garot J, Henry TD, Dangas G, Stone GW, Krucoff MW, Cutlip D, Mehran R, Wijns W, Sharif F, Serruys PW, Onuma Y; Bifurcation Academic Research Consortium and European Bifurcation Club. Definitions and Standardized Endpoints for Treatment of Coronary Bifurcations. *J Am Coll Cardiol.* 2022;80:63-88.
- 4. Kim HY, Doh JH, Lim HS, Nam CW, Shin ES, Koo BK, Lee JM, Park TK, Yang JH, Song YB, Hahn JY, Choi SH, Gwon HC, Lee SH, Kim SM, Choe Y, Choi JH. Identification of Coronary Artery Side Branch Supplying Myocardial Mass That May Benefit From Revascularization. *JACC Cardiovasc Interv.* 2017;10:571-81.
- 5. Koo BK, Park KW, Kang HJ, Cho YS, Chung WY, Youn TJ, Chae IH, Choi DJ, Tahk SJ, Oh BH, Park YB, Kim HS. Physiological evaluation of the provisional side-branch intervention strategy for bifurcation lesions using fractional flow reserve. *Eur Heart J.* 2008;29:726-32.
- 6. Chen SL, Ye F, Zhang JJ, Xu T, Tian NL, Liu ZZ, Lin S, Shan SJ, Ge Z, You W, Liu YQ, Qian XS, Li F, Yang S, Kwan TW, Xu B, Stone GW. Randomized Comparison of FFR- Guided and Angiography-Guided Provisional Stenting of True Coronary Bifurcation Lesions: The DKCRUSH-VI Trial (Double Kissing Crush Versus Provisional Stenting Technique for Treatment of Coronary Bifurcation Lesions VI). *JACC Cardiovasc Interv.* 2015;8:536-46.
- 7. Tu S, Ding D, Chang Y, Li C, Wijns W, Xu B. Diagnostic accuracy of quantitative flow ratio for assessment of coronary stenosis significance from a single angiographic view: A novel method based on bifurcation fractal law. *Catheter Cardiovasc Interv.* 2021;97 Suppl 2:1040-7.
- 8. Kan J, Ge Z, Nie S, Gao X, Li X, Sheiban I, Zhang JJ, Chen SL. Clinical prognostic value of a novel quantitative flow ratio from a single projection in patients with coronary bifurcation lesions treated with the provisional approach. *AsiaIntervention*. 2023:18:114-23.

Angiography coregistration: time to fight clinician inertia



Giulio Guagliumi*, MD; Dario Pellegrini, MD

Cardiology Division, IRCCS Ospedale Galeazzi Sant'Ambrogio, Milan, Italy

Time is a constant concern. No matter how fast we move, we are always in an eternal fight against the clock. Even in our catheterisation laboratories, the timetable is witness to the daily challenge between operators and the ever-growing list of scheduled procedures.

Furthermore, procedural complexity is increasing. Nowadays, operators have a wide array of supporting tools — ranging from coronary physiology to intracoronary imaging — to quantify and characterise epicardial and microvascular disease. In an ideal world, we would use all of them to provide the best-in-class, top-notch procedural results for our patients. But, let's be honest. In the real world, this is not possible. Every device has a cost, both in terms of financial resources and time consumption, and these factors influence our selection.

In particular, time has been one of the main limitations to the diffusion of intracoronary imaging, despite the clear benefits of imaging guidance (whether it is intravascular ultrasound [IVUS] or optical coherence tomography [OCT]) both for immediate procedural results and long-term outcomes¹, especially in complex lesions.

Thus, it is mandatory that, when we decide to invest time and perform an imaging-guided procedure, we do our best to obtain the maximum amount of information from this technology and make the procedure as cost-effective as possible.

From this perspective, it is disappointing to realise that angiography coregistration (ACR) is still limited to a very small niche of centres. This technology automatically correlates each frame of an intracoronary imaging run (e.g., OCT) to a specific point of the coronary artery on angiography and provides an automated, precise and smooth transition between the two modalities. ACR can be applied to all kinds of intravascular imaging and coronary physiology, but OCT is the setting where it finds its best application, as the fast pullback of the OCT catheter prevents any real-time localisation of the OCT image during acquisition (different from IVUS, or a pressure wire pullback)².

Without ACR, operators must rely on common relevant markers (like a stent or a side branch) and perform a sort of "manual coregistration". Obviously, accuracy is limited with this method, and it may impair the advantages provided by the high spatial resolution of OCT. In particular, inaccurate stent landing and geographical miss are relevant risks when anatomical markers are not clear upon angiography. Therefore, ACR can fill a huge gap.

In this issue of AsiaIntervention, Kadavil and colleagues publish the results of the iOPTICO study³. In this all-comer registry, the

^{*}Corresponding author: Cardiology Division, IRCCS Ospedale Galeazzi Sant'Ambrogio, Via Cristina Belgioioso, 173, 20157, Milan, Italy. E-mail: guagliumig@gmail.com

investigators found that ACR-OCT guidance triggered a change in treatment strategy in 89% of procedures, compared to standard coronary angiography. The study protocol planned a stepwise approach to the procedure, with the operator being asked to provide a treatment plan after being exposed to standard angiography, OCT and ACR-OCT. Thus, the operators were also able to assess the impact of ACR implementation over plain OCT, which allowed for an additional 34% change in treatment strategy.

Article, see page 124

The obvious price to pay for using intracoronary imaging (besides the financial cost) was an increase in procedural time. Such a finding is not a surprise. The interesting point, however, is that ACR provided an additional layer of valuable information, without a significant increase in time (only +3.5 minutes compared to OCT). Considering that in normal practice ACR assessment is usually performed simultaneously with OCT (with no need for a separation of the two modalities – these were performed separately in the study for research purposes only), this may even result in a reduction of the total procedure time, as the machine dispenses with the "manual coregistration" of the operator, which otherwise costs valuable minutes. This is an affordable price to pay, considering the clear advantages in terms of reduction in complications (and related interventions), or future adverse events. Undoubtedly, a plain OCT-guided procedure may still obtain a good final result, but it may come at the price of additional stents (in case of detection of geographical miss) and a higher workload for the operator.

Nevertheless, a remark should be made about the study. Although ACR is a powerful tool, OCT should always remain the main reference. Decisions on device size, length and landing zone should be based on OCT measurements. Changing the stent length or even stent strategy, when moving from ACR to OCT, is, in our experience an uncommon practice and limited to very select cases. In these cases, the changes should probably, in part, be attributed to the judgement of the operators, who were looking for a reliable marker for stent landing on angiography. We should also avoid the risk of falling back into old habits. Angiography should bend to intracoronary imaging, not the opposite. Similarly, it seems strange that in 15% of cases, ACR made the operator decide to perform lesion preparation, instead of a direct stenting strategy decided with OCT. These decisions seem like remnants of an angiography-oriented decision-making process, which the operators were probably not entirely able to abandon. When you decide on an imaging-guided procedure, and you decide to invest time and money in it, you should follow the imaging guidance to the very end.

Indeed, this is probably the major limit of current coregistration: it is not translational. ACR data are real-time, but they refer to a specific angiography, and they do not translate to subsequent angiographic acquisitions. So, in the end, the operator will still need to perform a visual comparison between the reference view (with the OCT pullback and ACR) and the current working view. And, obviously, he will use markers with which he is familiar, a side branch, a curve, or something reliable as a marker.

The ideal development of ACR would be fusion imaging, which may be able to display the precise point-by-point intracoronary imaging findings on live angiography. This could provide an even easier, streamlined process during stent implantation. It could be useful, for example, in so-called "ostium nailing" in which precise landing of the stent, based only on angiography, is currently a matter of luck.

Future iterations of these technologies may provide significant support to all operators. Indeed, as shown by the OPTICO-Integration study⁴, refinements in treatment strategies provided by ACR compared to a previously defined strategy were independent from operator expertise. This is a crucial aspect: ACR is not merely a tutorial for beginners, who may not know how to apply imaging in the context of angiography, but a valuable tool which provides the advantage of process streamlining and improved accuracy at the same time.

So, if we want to use intracoronary imaging (and we should), we should trust the whole process. But first, we should probably fight our own inertia and eliminate old and outdated habits.

Conflict of interest statement

The authors have no conflicts of interest to declare.

References

- 1. Lee JM, Choi KH, Song YB, Lee JY, Lee SJ, Lee SY, Kim SM, Yun KH, Cho JY, Kim CJ, Ahn HS, Nam CW, Yoon HJ, Park YH, Lee WS, Jeong JO, Song PS, Doh JH, Jo SH, Yoon CH, Kang MG, Koh JS, Lee KY, Lim YH, Cho YH, Cho JM, Jang WJ, Chun KJ, Hong D, Park TK, Yang JH, Choi SH, Gwon HC, Hahn JY; RENOVATE-COMPLEX-PCI Investigators. Intravascular Imaging-Guided or Angiography-Guided Complex PCI. N Engl J Med. 2023;388:1668-79.
- 2. van der Sijde JN, Guagliumi G, Sirbu V, Shimamura K, Borghesi M, Karanasos A, Regar E. The OPTIS Integrated System: real-time, co-registration of angiography and optical coherence tomography. *EuroIntervention*. 2016;12:855-60.
- 3. Kadavil RM, Abdullakutty J, Patel T, Rathnavel S, Singh B, Chouhan NS, Malik FTN, Hiremath S, Gunasekaran S, Kalarickal SM, Kumar V, Subban V. Impact of real-time optical coherence tomography and angiographic coregistration on the percutaneous coronary intervention strategy. *AsiaIntervention*. 2023;18:124-32.
- 4. Leistner DM, Riedel M, Steinbeck L, Stähli BE, Fröhlich GM, Lauten A, Skurk C, Mochmann HC, Lübking L, Rauch-Kröhnert U, Schnabel RB, Westermann D, Blankenberg S, Landmesser U. Real-time optical coherence tomography coregistration with angiography in percutaneous coronary intervention-impact on physician decision-making: The OPTICO-integration study. *Catheter Cardiovasc Interv.* 2018;92:30-7.

New opportunities for bioresorbable scaffold technology

Adnan Kastrati^{1,2}*, MD; Masaru Seguchi^{1,3}, MD

1. Klinik für Herz- und Kreislauferkrankungen, Deutsches Herzzentrum München, Technical University Munich, Munich, Germnay 2. German Center for Cardiovascular Research (DZHK), Partner Site Munich Heart Alliance,

Munich, Germany; 3. Division of Cardiovascular Medicine, Saitama Medical Center, Jichi Medical University, Saitama, Japan

Bioresorbable scaffolds (BRS) are an attractive treatment option for coronary artery disease due to their unique property of complete degradation after implantation, potentially reducing complications associated with residual struts in the vessel wall. However, the results of clinical trials have been disappointing, demonstrating an increased risk of scaffold thrombosis and restenosis^{1,2}. Despite this setback, research and development efforts to improve the safety and efficacy of BRS continue, with a focus on several directions including strut thickness and scaffold material³. Another promising option may be to modify the strut shape to round struts, which has the potential to improve the blood flow characteristics in coronary arteries.

Three-dimensional (3D) printing technology has made remarkable progress in recent years and is widely used in the development of novel medical devices. This technology allows for flexible scaffold manufacturing, enabling the customisation of devices with varying strut thicknesses, shapes and architecture. In this issue of AsiaIntervention, Shi et al share the results of a preclinical study comparing the performance of a newly developed polymeric

sirolimus-eluting BRS (AMSorb; Beijing Advanced Medical Technologies) manufactured using 3D printing technology with a sirolimus-eluting metallic stent (SES; HELIOS [Kinhely Medical])⁴. The AMSorb scaffold has a poly-L-lactic acid (PLLA) backbone coated with a mixture of an amorphous matrix of poly (D, L-lactic acid) and sirolimus. The struts of the BRS have a circular shape with a thickness of 140 µm. The control device (an SES) was a metallic stent consisting of an 80 µm-thick cobalt-chromium alloy coated with sirolimus and polylactic-co-glycolic acid. A total of 32 BRS and 32 SES were implanted in 32 porcine coronary arteries in the present study. A comprehensive assessment, including angiography, optical coherence tomography (OCT) and histopathology, was performed to compare the performance of the study devices at 14, 28, 97, and 189 days after implantation.

Article, see page 133

Despite the quality of this study, there are some limitations. Previous experience with BRS using the same material used in this study has shown that complete polymer resorption takes >3 years. A longer follow-up and a dedicated OCT methodology would have

^{*}Corresponding author: Deutsches Herzzentrum München, Lazarettstr. 36, 80636 Munich, Germany. E-mail: kastrati@dhm.mhn.de

allowed the evaluation of this process for AMSorb. In addition, the specific advantages of the 3D printing technology and the round strut shape are best evaluated with an additional control group using conventional BRS. Furthermore, the histopathological examination did not include an evaluation of fibrin deposition in the 2 study groups. Finally, scaffold discontinuity, a potentially important correlate of late thrombosis^{5,6}, was not assessed in this study.

Overall, the present study showed satisfactory results with this novel BRS. OCT at 14 and 28 days after implantation showed significantly smaller lumen and stent areas for the AMSorb scaffold compared to the SES. However, at 97 and 189 days, no significant differences were found between the 2 devices. Quantitative coronary angiography analysis showed no significant differences in late lumen loss at any time point. Histopathological examination showed comparable levels of injury, inflammation and endothelialisation for BRS and SES. Based on these findings, the authors concluded that the safety and efficacy of this particular 3D-printed BRS in a porcine model are comparable to those observed with SES.

The absence of an Absorb (Abbott) control group in this study⁴ means that only indirect comparisons can be made. In a previous porcine model, Absorb showed a higher injury score at 12 months and more pronounced inflammation only at ≥ 6 months postimplantation compared to metallic drug-eluting stents⁷. Therefore, the lack of increased injury score and inflammation with the novel device evaluated in the present study may well be related to the shorter study period, although a positive contribution from the rounded shape of the struts is also plausible⁴.

It is well known that thicker struts increase coronary flow separation and stagnation, thereby enhancing platelet deposition and thrombin and fibrin generation⁸. However, it is very unlikely that the small difference in strut thickness between AMSorb and Absorb (<20 µm) makes a relevant difference in this regard. Previous in vitro research has shown that not only greater strut thickness but also rectangular strut geometry disturbs the local flow field creating peristrut recirculation zones with longer blood particle residence times and increased thrombus formation9. Round struts were associated with reduced recirculation zones and fibrin deposition and increased expression of protective endothelial thrombomodulin⁹. Therefore, the round struts created by the 3D printing technology may also partly explain the good results observed in the present study⁴. AMSorb was associated with a similar degree of endothelialisation to that seen in the metallic DES group⁴. Although it is possible that the strut shape and thickness of this device contributed to this result, endothelialisation was also not affected by device type (Absorb or XIENCE [Abbott]) in a previous animal study⁷.

In conclusion, the present porcine model study used a multifaceted evaluation methodology, including angiography, OCT and histopathology, and showed very encouraging results with a novel BRS based on 3D printing technology. This technology should probably be incorporated in the effort to create BRS with thinner and improved strut shapes, with greater chances of a safer and more effective device for clinical practice. However, a look at the past shows that even with the Absorb scaffold, preclinical results were encouraging enough to justify the start of clinical trials. The challenging question is which preclinical evaluation method is more likely to avoid the kind of disappointment that we have seen in clinical practice with older polymer-based and fully resorbable scaffolds. The work of Shi and colleagues⁴ has shown that this technology may have a new lease of life, provided that it is carefully evaluated and that the lessons of the past are taken into account.

Conflict of interest statement

A. Kastrati is one of the inventors of a patent application from his institution related to drug-eluting stent technology. M. Seguchi has no conflicts of interest to declare.

References

- 1. Cassese S, Byrne RA, Jüni P, Wykrzykowska JJ, Puricel S, Ndrepepa G, Schunkert H, Fusaro M, Cook S, Kimura T, Henriques JPS, Serruys PW, Windecker S, Kastrati A. Midterm clinical outcomes with everolimus-eluting bioresorbable scaffolds versus everolimus-eluting metallic stents for percutaneous coronary interventions: a meta-analysis of randomised trials. *EuroIntervention*. 2018;13:1565-73.
- 2. Cassese S, Byrne RA, Ndrepepa G, Kufner S, Wiebe J, Repp J, Schunkert H, Fusaro M, Kimura T, Kastrati A. Everolimus-eluting bioresorbable vascular scaffolds versus everolimus-eluting metallic stents: a meta-analysis of randomised controlled trials. *Lancet.* 2016;387:537-44.
- 3. Seguchi M, Aytekin A, Lenz T, Nicol P, Alvarez-Covarrubias HA, Xhepa E, Klosterman GR, Beele A, Sabic E, Utsch L, Alyaqoob A, Joner M. Challenges of the newer generation of resorbable magnesium scaffolds: Lessons from failure mechanisms of the past generation. *J Cardiol.* 2023;81:179-88.
- 4. Shi Q, Zhang B, Wang X, JFei J, Qin Q, Zheng B, Chen M. Safety and efficacy of a novel three-dimensional printed bioresorbable sirolimus-eluting scaffold in a porcine model. *AsiaIntervention*. 2023;18:133-42.
- 5. Virmani R, Jinnouchi H, Finn AV. Discontinuity: Is it a Major Cause of Scaffold Thrombosis? *J Am Coll Cardiol*. 2017;70:2345-8
- 6. Yamaji K, Ueki Y, Souteyrand G, Daemen J, Wiebe J, Nef H, Adriaenssens T, Loh JP, Lattuca B, Wykrzykowska JJ, Gomez-Lara J, Timmers L, Motreff P, Hoppmann P, Abdel-Wahab M, Byrne RA, Meincke F, Boeder N, Honton B, O'Sullivan CJ, Ielasi A, Delarche N, Christ G, Lee JKT, Lee M, Amabile N, Karagiannis A, Windecker S, Räber L. Mechanisms of Very Late Bioresorbable Scaffold Thrombosis: The INVEST Registry. *J Am Coll Cardiol.* 2017;70:2330-44.
- 7. Otsuka F, Pacheco E, Perkins LE, Lane JP, Wang Q, Kamberi M, Frie M, Wang J, Sakakura K, Yahagi K, Ladich E, Rapoza RJ, Kolodgie FD, Virmani R. Long-term safety of an everolimus-eluting bioresorbable vascular scaffold and the cobalt-chromium XIENCE V stent in a porcine coronary artery model. *Circ Cardiovasc Interv.* 2014:7:330-42.
- 8. Kolandaivelu K, Swaminathan R, Gibson WJ, Kolachalama VB, Nguyen-Ehrenreich KL, Giddings VL, Coleman L, Wong GK, Edelman ER. Stent thrombogenicity early in high-risk interventional settings is driven by stent design and deployment and protected by polymer-drug coatings. *Circulation*. 2011;123:1400-9.
- 9. Jiménez JM, Prasad V, Yu MD, Kampmeyer CP, Kaakour AH, Wang PJ, Maloney SF, Wright N, Johnston I, Jiang YZ, Davies PF. Macro- and microscale variables regulate stent haemodynamics, fibrin deposition and thrombomodulin expression. *J R Soc Interface*. 2014;11:20131079.

Obstructive sleep apnoea and coronary revascularisation outcomes



Adrienne Y.H. Chew¹, MBBS; Chi-Hang Lee^{2,3*}, MBBS, MD

1. Yong Loo Lin School of Medicine, National University of Singapore, Singapore; 2. Department of Medicine, Yong Loo Lin School of Medicine, National University of Singapore, Singapore; 3. Department of Cardiology, National University Heart Centre Singapore, Singapore

KEYWORDS

- miscellaneous
- other technique
- prior PCI

Abstract

Obstructive sleep apnoea (OSA) is a chronic sleep disorder characterised by recurrent cyclical episodes of upper airway collapse causing apnoea or hypopnoea. Despite being highly prevalent in patients with cardiovascular conditions, OSA has been a neglected component in cardiovascular practice. Fortunately, in the past few decades, increasing acknowledgement of the vulnerability of cardiac patients to OSA-related stressors and its adverse cardiovascular outcomes has made it a recognised cardiovascular risk factor in practice guidelines. Consequences of OSA include oxidative stress, endothelial dysfunction, autonomic dysfunction, and increased catecholamine release. The perturbations caused by OSA not only provide a clear mechanistic link to cardiovascular disease but also to poor outcomes after coronary revascularisation. This review article focuses on the correlation of OSA to coronary revascularisation outcomes. Our team reported that OSA is present in approximately 50% of patients undergoing coronary revascularisation. Importantly, untreated OSA was found to be an independent predictor of adverse events after both percutaneous coronary intervention and coronary artery bypass grafting. Although randomised trials did not confirm the benefits of OSA treatment in improving cardiovascular outcomes, these early trials were limited by poor treatment adherence. For now, systematic screening for OSA in patients undergoing coronary revascularisation is not indicated. Yet, with the proven benefit of OSA treatment in improving blood pressure control and quality of life, screening for and treatment of OSA is still indicated if patients have reported excessive daytime sleepiness and/or suboptimally controlled hypertension.

^{*}Corresponding author: Department of Cardiology, National University Heart Centre Singapore, 1E Kent Ridge Road, NUHS Tower Block Level 9, Singapore 119228. E-mail: mdclchr@nus.edu.sg

Abbreviations

AASM American Academy of Sleep Medicine

AHI apnoea-hypopnoea index

CABG coronary artery bypass grafting

CPAP continuous positive airway pressure

MACE major adverse cardiac eventsOSA obstructive sleep apnoea

PCI percutaneous coronary intervention

Introduction

The advent of coronary revascularisation in the early 20th century and the arduous journey of its refinement have greatly influenced and transformed the landscape of coronary artery disease management¹⁻³. This is undeniably contributed to by the concurrent deepening of our understanding of the pathophysiology of the disease and its progression. In addition to medical therapy, the two principal options for revascularisation would be surgical correction with coronary artery bypass graft (CABG) and percutaneous coronary intervention (PCI).

CABG, an open surgical procedure, aims to achieve complete revascularisation where a graft vessel is anastomosed to existing coronary vasculature, bypassing atherosclerotic occlusions that reduce luminal flow and, hence, re-establishing coronary blood flow to the myocardium. A decade and a half after the discovery of CABG, the pinnacle of revascularisation, the emergence of an alternative procedure, namely PCI, came about. In contrast to CABG, PCI is a minimally invasive procedure involving the insertion of a device percutaneously through a peripheral arterial site and threaded into the location of the stenosis or occlusion, where it is inflated. It confers different degrees of disease intervention and a myriad of choices of devices, from balloon angioplasty to bare metal stents and, most recently, the use of drug-eluting stents². While some innovative stents have been withdrawn from the market, drug-eluting stents have become the current standard of practice⁴⁻⁶. Although CABG and PCI fulfil similar roles in achieving the end result of revascularisation, both show varying efficacy in different patient groups.

Clinical outcomes of PCI and CABG in the contemporary era

Landmark randomised controlled trials and meta-analyses have established that, depending on the anatomical complexity, the extent of coronary artery lesion involvement, and pre-existing patient comorbidities, each revascularisation method has its own relative merits in providing for an individual instead of casting a blanket treatment on a patient⁷⁻⁹. It has been generally accepted, based on randomised trials, that CABG is the recognised gold standard of choice for patients with diffuse multivessel coronary artery disease and/or diabetes mellitus with a high anatomical complexity score⁷.

Revascularisation effectively addresses obstructions in the coronary vasculature that have already transpired and relieves cardiac ischaemia. However, as described above, we are beginning to recognise the importance of periprocedural patient optimisation, where addressing certain premorbid risk factors (such as hyperlipidaemia and diabetes mellitus) contributes to an improved procedural outcome¹⁰⁻¹². One such risk factor, which has not been widely researched, is obstructive sleep apnoea (OSA)^{13,14}. In the past decades, untreated OSA has been shown to be an independent predictor of adverse cardiovascular outcomes in patients undergoing coronary revascularisation.

OSA – pathophysiology, diagnosis, and prevalence

OSA is a chronic sleep disorder characterised by recurrent cyclical episodes of upper airway collapse causing cessation of breathing (apnoea) or a reduction in airflow (hypopnoea) during complete and partial obstruction, respectively¹³. This commonly presents as snoring, choking, or absence of breathing during sleep and may manifest in the form of oxygen desaturations, arousals, and fragmented sleep.

The pathophysiology of OSA is multifaceted, mainly stemming from a sleep-induced dimensional reduction of the upper airway. Pharyngeal function and patency are controlled by static and dynamic components, namely morphological skeletal and soft tissue framework, as well as the synchronised neuromuscular tone of more than 20 muscles. Craniofacial features, fatty tissue depositions, and inflammatory soft tissue oedema in the neck, which can all reduce the airway diameter, and the rostral shift of fluid to the neck during sleep are some examples of anatomical impairments. Any alterations in sleep-related physiological phenomena would result in variable pharyngeal collapsibility, causing a disruption in respiratory mechanics. A clinical measure used to quantify this would be the passive critical occlusion pressure, which is the endopharyngeal pressure associated with upper airway collapse. In addition, studies have shown that other physiological factors associated with OSA include the loop gain (ventilatory control instability) and arousal threshold (sleep-wake instability).

Statistics have shown that approximately 70% of patients have more than one non-anatomical phenotype, with each phenotype having a varying contribution to the degree and progression of the disease, giving rise to a wide potential for disease severity. Hence, qualitative phenotyping allows us to characterise the different pathophysiological traits in OSA patients and, potentially, improve the identification of more patients for diagnosis. A combination of both subjective and objective investigations is necessary for the holistic evaluation and diagnosis of patients. Subjective assessments, such as the Berlin Questionnaire and the Epworth Sleepiness Scale Questionnaire, allow clinicians to qualify self-reported nocturnal and daytime symptoms of OSA, taking into consideration individual anthropometric characteristics.

Different methods to diagnose OSA are summarised in **Table 1**; the level 1 overnight in-laboratory polysomnography, conducted and supervised by a certified sleep technologist, remains the diagnostic gold standard. During the polysomnography, the following parameters are recorded: airflow (nasal cannula and thermistor),

Table 1. American Academy of Sleep Medicine classification of sleep apnoea evaluation.

Level I. Standard polysomnography	Level II. Comprehensive portable polysomnography	Level III. Modified portable sleep apnoea testing	Level IV. Continuous (single or dual) bioparameter recording
EEG, EOG, chin EMG, ECG, airflow, respiratory effort, and oxygen saturation.	Same as for Level I except heart rate instead of ECG is acceptable.	Recording of ventilation (at least 2 channels of respiratory movement, or respiratory movement and airflow), ECG or heart rate and oxygen saturation.	Only 1 or 2 physiological variables need to be recorded.
Body position must be documented or objectively measured. Leg movement recording (EMG or motion sensor) is desirable but optional.			
Trained personnel must be in constant attendance and able to intervene.	Personnel are needed for preparation. Ability to intervene is not required for all studies.	Personnel are needed for preparation. Ability to intervene is not required for all studies.	Personnel are needed for preparation. Ability to intervene is not required for all studies.
	polysomnography EEG, EOG, chin EMG, ECG, airflow, respiratory effort, and oxygen saturation. Body position must be documented or objectively measured. Leg movement recording (EMG or motion sensor) is desirable but optional. Trained personnel must be in constant attendance and able	polysomnography EEG, EOG, chin EMG, ECG, airflow, respiratory effort, and oxygen saturation. Body position must be documented or objectively measured. Leg movement recording (EMG or motion sensor) is desirable but optional. Trained personnel must be in constant attendance and able portable polysomnography Same as for Level I except heart rate instead of ECG is acceptable. Parsonnel are needed for preparation. Ability to intervene is not required for all	polysomnographyportable polysomnographyapnoea testingEEG, EOG, chin EMG, ECG, airflow, respiratory effort, and oxygen saturation.Same as for Level I except heart rate instead of ECG is acceptable.Recording of ventilation (at least 2 channels of respiratory movement, or respiratory movement and airflow), ECG or heart rate and oxygen saturation.Body position must be documented or objectively measured. Leg movement recording (EMG or motion sensor) is desirable but optional.Trained personnel must be in constant attendance and ablePersonnel are needed for preparation. Ability to intervene is not required for all studies.

respiratory movements (respiratory inductance plethysmography), oxygen saturation (as measured by pulse oximetry), snoring episodes, electrocardiography, and body position. OSA was diagnosed on the basis of the apnoea-hypopnoea index (AHI), quantified as the total number of apnoeas or hypopnoeas recorded per hour of sleep. According to the American Academy of Sleep Medicine (AASM) guideline¹⁵, apnoea is defined as a \geq 90% decrease in airflow from baseline for at least 10 seconds, and hypopnoea is defined as a \geq 30% decrease in airflow from baseline for \geq 10 seconds, associated with either an oxygen desaturation of \geq 3% (some centres use \geq 4%) and/or arousal. Diagnosis of OSA entails the presence of daytime or nocturnal symptoms alongside an AHI \geq 5 or, in the absence of symptoms, AHI \geq 15.

There is a unanimous tacit consensus among physicians worldwide that OSA is an underdiagnosed disease entity. Exacerbating this state of the affair is the global prevalence of OSA, with an estimated 1 billion people affected and with prevalence exceeding 50% in several countries¹⁶. According to The Lancet 2019¹⁶, 936 million (95% confidence interval [CI]: 903-970) adults (men and women) aged 30-69 years old have mild to severe OSA, and 425 million (399-450) adults aged 30-69 years old have moderate to severe OSA, globally, based on AASM 2012 diagnostic criteria and the AHI threshold values of ≥ 5 events per hour and ≥ 15 events per hour, for symptomatic and non-symptomatic disease, respectively. A community-based study in Singapore¹⁷ exemplifies this, where the weighted estimates of the population prevalence of moderate to severe OSA and sleep apnoea syndrome were 30.5% and 18.1%, respectively¹⁷. Essentially, 91.0% of subjects with an AHI ≥15 events per hour were previously undiagnosed¹⁷.

It is well established that there is a strong predominance of OSA in men and obese and middle-aged patients, with additional risk factors encompassing family history, race, and ethnicity. More importantly, OSA is increasingly becoming a recognised cause of increased cardiovascular risk¹⁸. It has been surmised that this may potentially be mediated, in part, by its strong association with

cardiovascular complications such as hypertension, atrial fibrillation, coronary artery disease, congestive heart failure, stroke, diabetes, and metabolic syndrome¹⁴.

OSA - a novel cardiovascular risk factor

As detailed above, OSA is a complex and heterogeneous disease characterised by multiple underlying mechanisms. The immediate effects of repeated attempts to inspire against an obstructed upper airway include a drop in intrathoracic pressure, cortical arousal from sleep, hypoxia, and sympathetic activation. Each of these, in turn, gives rise to the adverse cardiovascular outcomes expounded below.

Exposure to prolonged negative intrathoracic pressure results in decreased left ventricular filling and increased afterload, ultimately reducing stroke volume. Furthermore, OSA causes marked, repeated BP elevation and tachycardia secondary to sympathetic nerve hyperactivity¹⁹. The sympathetic nervous system is further augmented by decreased stroke volume and the suppression of sympathetic inhibitory effects of lung stretch receptors during apnoea. Sleep arousal and respiratory events during OSA also result in peripheral vasoconstriction, the release of catecholamines and a reduction in parasympathetic modulation of the heart, resulting in elevated blood pressure (BP) during the night.

The net effect of increased left ventricular afterload, tachycardia, and BP elevation leads to myocardial oxygen supply-demand mismatch, ultimately resulting in (i) acute predisposition to cardiac ischaemia and arrhythmias and (ii) chronic predisposition to left atrial enlargement and left ventricular hypertrophy. This is aggravated by recurrent upper airway collapse which results in increased oxidative stress and reduced production of endothelium-dependent vasodilator substances²⁰, such as nitric oxide, contributing to vascular dysfunction and systemic inflammation. These processes ultimately lead to myocardial fibrosis and left ventricular diastolic dysfunction.

OSA is strongly associated with hypertension, and a doseresponse relationship exists between the severity of OSA and the degree of hypertension. In addition, OSA plays an essential role in resistant hypertension and may mediate the association with cardiovascular disease. The perturbations caused by OSA not only provide a clear mechanistic link to cardiovascular disease but also to coronary revascularisation outcomes.

OSA and coronary revascularisation outcomes OSA AND PCI

There is a lack of data from extensive cohort studies examining the prognostic significance of OSA in patients treated with PCI. In the pre-drug-eluting stent era, single-centre studies found OSA to be a predictor of restenosis and target vessel revascularisation^{21,22}. A non-randomised study suggested that patients who received treatment for OSA had reduced cardiac mortality 5 years after PCI compared with those who declined treatment²³. OSA has been linked with coronary plaque burden and an increased risk of cardiovascular disease²⁴; however, there were few studies on the prognostic effect of OSA in patients undergoing PCI before the Sleep and Stent Study (ClinicalTrials.gov: NCT02215317).

The Sleep and Stent Study is the largest multinational cohort study examining the effects of OSA on post-PCI cardiovascular outcomes to date²⁵. The Sleep and Stent Study was a prospective, multicentre study designed to assess the association between OSA and cardiovascular outcomes in patients treated with PCI. Overall, a total of 1,748 patients who had undergone a successful PCI in at least one coronary artery were enrolled in the study. The prespecified primary endpoint was a major adverse cardiac event (MACE): a composite of cardiovascular mortality, non-fatal myocardial infarction, non-fatal stroke, and unplanned revascularisation. In total, 1,311 patients completed a portable sleep study within 7 days of their PCI procedure. OSA, defined as an AHI ≥15 events per hour, was diagnosed in 45.3% of the patient cohort (n=594). Patients with OSA were older, more likely to be male, had a higher BMI, and had a higher prevalence of hypertension and diabetes mellitus than those without OSA. During the median follow-up of 1.9 years, a MACE occurred in 141 patients (3-year cumulative incidence estimate: 16.4%), including cardiovascular death in 24 patients. The incidence of MACE was higher in patients with OSA than in those without (3-year estimate: 18.9% vs 14.0%; p=0.001) (Figure 1). Cox regression analysis showed

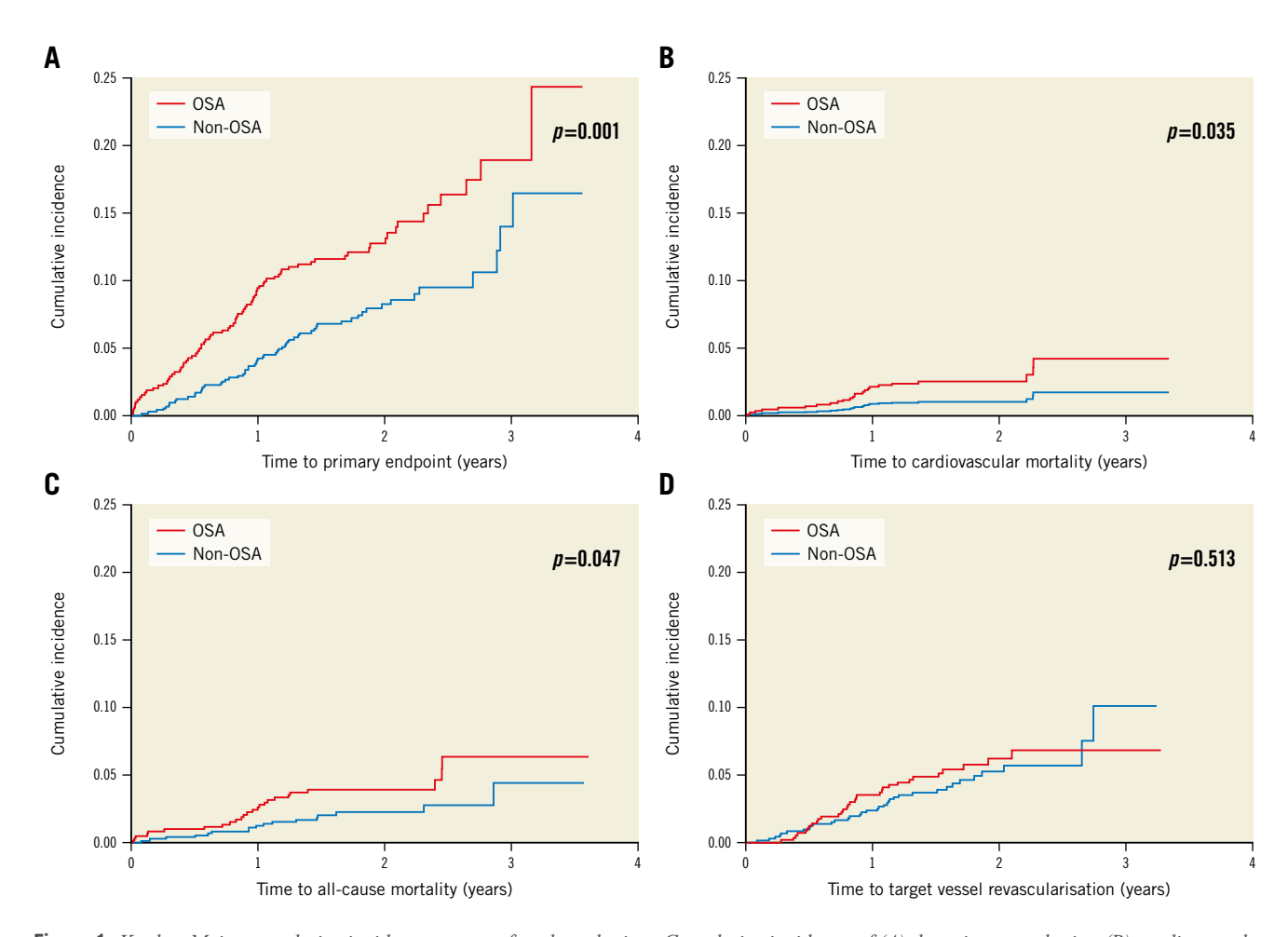


Figure 1. Kaplan-Meier cumulative incidence curves of study endpoints. Cumulative incidence of (A) the primary endpoint, (B) cardiovascular mortality, (C) all-cause mortality, and (D) target vessel revascularisation. The primary endpoint comprises cardiovascular mortality, non-fatal myocardial infarction, non-fatal stroke, and unplanned revascularisation. OSA: obstructive sleep apnoea

that OSA was an independent predictor of MACE (hazard ratio [HR] 1.57, 95% CI: 1.10-2.24; p=0.013).

OSA AND CABG

The Undiagnosed Sleep Apnea and Bypass OperaTion (SABOT) study was designed to evaluate the association between OSA and MACE in patients undergoing non-emergent CABG²⁶. Patients with multivessel coronary artery disease are often referred for CABG, and it remains unknown if OSA is a risk marker. Patients residing in Singapore and who were referred to a tertiary cardiac centre for non-emergent CABG were eligible. The recruited participants underwent an overnight sleep study using a wearable diagnostic device before undergoing CABG. Among the 1,007 patients who completed the study, OSA (defined as an AHI ≥15 events per hour) was diagnosed in 513 patients (50.9%). Over a mean followup period of 2 years, 124 patients experienced the 4-component MACE (2-year cumulative incidence estimate: 11.3%). There were a total of 33 cardiac deaths (2.5%), 42 non-fatal myocardial infarctions (3.7%), 50 non-fatal strokes (4.9%), and 36 unplanned revascularisations (3.2%). The crude incidence of MACE was higher in the OSA group than in the non-OSA group (2-year estimate: 14.7% vs 7.8%; p=0.002) (Figure 2). Similarly, the crude incidence rates of all-cause mortality, cardiovascular mortality, sudden cardiac death or resuscitated cardiac arrest, and hospitalisation for heart failure were also higher in the OSA group (Figure 3). OSA was a predictor of MACE in unadjusted Cox regression analysis (HR 1.69), and the association remained statistically significant after adjustment for the effects of confounding variables (adjusted HR 1.57).

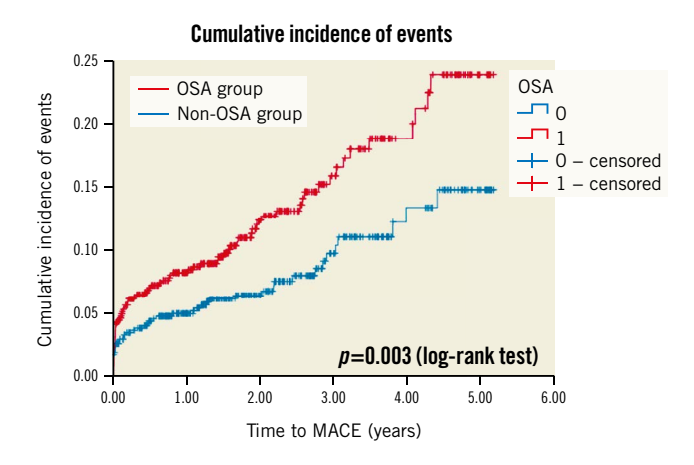


Figure 2. Cumulative incidence of the composite primary endpoint of major adverse cardiac events. Kaplan-Meier plot showing the cumulative incidence of major adverse cardiac events in patients with OSA (in red) and in patients without OSA (in blue).

MACE: major cardiac adverse events; OSA: obstructive sleep apnoea

An auxiliary study evaluated the association between OSA and total heart failure hospitalisation (HFH) after CABG. Approximately 10% of the 1,007 recruited patients had at least

one episode of HFH^{27,28}. At a mean follow-up of 3.3 years, a subgroup of 37% of patients had recurrent events that accounted for two-thirds of the total 179 HFH events. Using four robust statistical methods (Poisson, negative binomial, Andersen-Gill, and joint frailty models), we found that patients with OSA had a 1.6- to 1.8-fold increased risk of recurrent HFH, even after adjustment for differences in baseline demographic and clinical characteristics.

Treatment of OSA to improve cardiovascular outcomes

RICCADSA, SAVE, AND ISAACC

Despite ample evidence of the association between continuous positive airway pressure (CPAP) treatment and improvement in blood pressure and endothelial function^{29,30}, this is not sufficient to incorporate systematic OSA screening and treatment into the cardiovascular guidelines without supportive data from randomised clinical trials. In the past decade, three randomised controlled trials have been conducted to explore the potential benefits of CPAP in cardiovascular outcomes. These are summarised in Table 2. The first of these is the Randomized Intervention With CPAP in Coronary Artery Disease and Sleep Apnea - RICCADSA Trial³¹. In this single-centre trial, 244 patients with newly revascularised coronary artery disease and OSA (AHI ≥15 events per hour) were randomised to CPAP or usual care in a 1:1 ratio. The primary endpoint was a composite of repeat coronary revascularisation, myocardial infarction, stroke, or cardiovascular mortality. Over a median follow-up of 57 months, the incidence of the primary endpoint was 18.1% (CPAP group) versus 22.1% (usual care group) (p=0.449).

The Continuous Positive Airway Pressure Treatment of Obstructive Sleep Apnea to Prevent Cardiovascular Disease (SAVE) Study was a multicentre randomised trial and is the largest of the three listed trials³2. In contrast to most trials, where OSA was diagnosed based on the AHI, OSA was diagnosed based on an oxygen desaturation index ≥12 events per hour in the SAVE Study. Patients with stable coronary artery disease or cerebrovascular disease (n=2,717) and OSA were randomised to CPAP (n=1,346) or usual care (n=1,341). The primary outcome was a composite of death from cardiovascular causes, myocardial infarction, stroke or hospitalisation for unstable angina, and heart failure or transient ischaemic attack. Over a mean follow-up of 3.7 years, the incidence of the primary endpoint was 17.0% (CPAP group) versus 15.4% (usual care group) (p=0.34).

The CPAP in Patients With Acute Coronary Syndrome and OSA (ISAACC) Study was a multicentre randomised trial of patients with acute coronary syndrome³³. All patients underwent respiratory polygraphy during the acute phase, and patients with OSA were randomised to CPAP (n=633) or usual care (n=631). Over a median follow-up of 3.4 years, the incidence of the primary endpoint (a composite of cardiovascular death or non-fatal events [acute myocardial infarction, non-fatal stroke, hospital admission

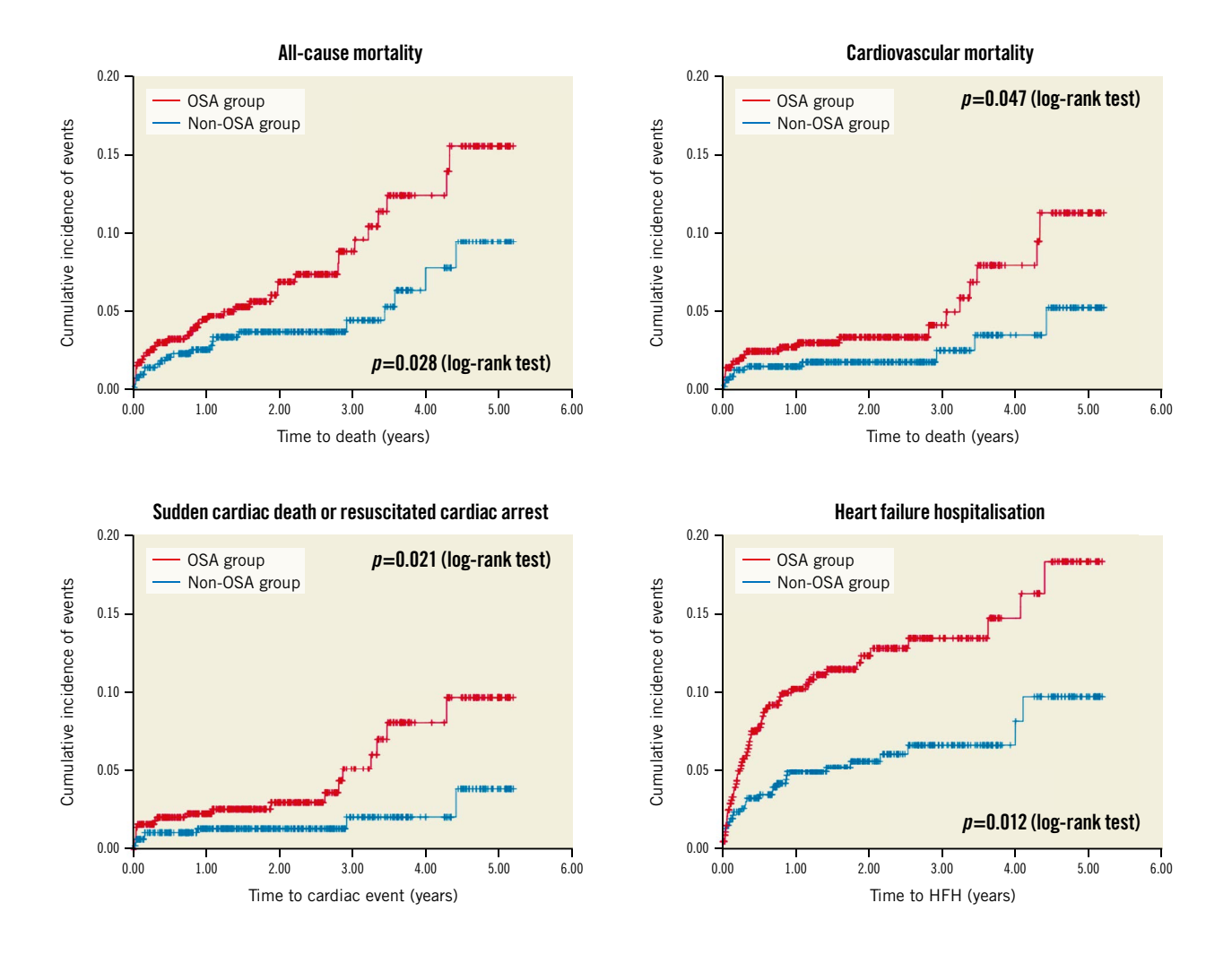


Figure 3. Cumulative incidence of secondary endpoints. Kaplan-Meier plots showing the cumulative incidences of all-cause mortality (A), cardiovascular mortality (B), sudden cardiac death or resuscitated cardiac arrest (C) and hospitalisation for heart failure (D), respectively, in patients with OSA (in red) and in patients without OSA (in blue). HFH: heart failure hospitalisation; OSA: obstructive sleep apnoea

for heart failure, and new hospitalisations for unstable angina or transient ischaemic attack]) was 16% in the CPAP group versus 17% in the usual care group (p=0.40). The major limitation of the ISAACC trial is the timing of the sleep study. A recent study has demonstrated that after acute coronary syndrome, concurrent changes occurred in the AHI, left ventricular ejection fraction, and left ventricular end-systolic volume. Of the patients diagnosed with OSA at the acute phase, resolution of OSA was seen in 48% at 6 months³⁴.

None of the three trials showed a clear benefit of OSA therapy using CPAP in improving cardiovascular outcomes. However, further data analysis revealed limitations in the design and execution of the studies. The adherence to CPAP in these trials was low. Indeed, all of these trials reported an average CPAP adherence of <4 hours per night, which is below the minimum (≥4 hours) needed to derive benefits from CPAP³⁵. Notably, these trials recruited patients who had developed cardiovascular events. Such patients differ from younger patients, whose CPAP may confer a benefit

in the primary prevention of cardiovascular disease, whereby they may be more likely to adhere to CPAP use.

LOW CPAP ADHERENCE IN CLINICAL TRIALS AND ITS IMPLICATIONS

All the research participants in the aforementioned trials presented with cardiovascular disease. These participants were unable to tolerate the CPAP over the duration of the trials to achieve clinically meaningful benefits, possibly due to excessive daytime sleepiness or drug (angiotensin-converting enzyme inhibitor)-induced airway hyperresponsiveness³6. In the RICCADSA Trial, 38% of the participants in the CPAP group stopped using the device within the first year. The adjusted on-treatment analysis showed a cardiovascular risk reduction in those who used CPAP for ≥4 versus <4 hours per night (p=0.026), suggesting that the low CPAP adherence may have contributed to the overall negative results. In the SAVE trial, despite the initial run-in period with sham CPAP achieving an average usage of 5.2 hours per

Table 2. Summary of the three randomised controlled trials on the effects of CPAP on cardiovascular events.

Trial	Single- or multicentre study	Number of patients recruited	Study period	Key inclusion criteria	Key exclusion criteria	Definition of OSA	Mean ESS* (CPAP vs usual care)	Average CPAP adherence (h/night)	Percentage of patients with CPAP adherence ≥4 h/night)
RICCADSA	Single-centre	244	2005-13	Adult patients with CAD who had undergone PCI or CABG in the previous 6 months	Patients with existing OSA, daytime sleepiness (ESS >10), and predominantly central apnoeas with Cheyne-Stokes respiration	AHI >15 events/h	NA	NA	NA
SAVE	Multicentre	2,717	2008-16	Adults between 45 and 75 years of age who had OSA and stable coronary or cerebrovascular disease	Severe daytime sleepiness (ESS >15) or were considered to have an increased risk of an accident from falling asleep, very severe hypoxaemia, or Cheyne-Stokes respiration	ODI** ≥12 events/h	7.3±3.6 vs 7.5±3.6	3.3 h/night	42%
ISAACC	Multicentre	2,551	2011-18	Aged ≥18 years, hospitalised for ACS	Previous treatment with CPAP for OSA, inability to complete questionnaires, known sleep disorder, >50% central apnoeas or the presence of Cheyne-Stokes respiration, and daytime sleepiness (ESS >10)	AHI ≥15 events/h	5.4±2.5 vs 5.3±2.5	2.8 h/night	38%

*scores range from 0 to 24, with higher scores indicating greater severity. Daytime sleepiness generally defined as ESS >10. **the number of times per hour during the oximetry recording that the blood oxygen saturation level drops by ≥4 percentage points from baseline. ACS: acute coronary syndrome; AHI: apnoea-hypopnoea index; CABG: coronary artery bypass grafting; CAD: coronary artery disease; CPAP: continuous positive airway pressure; ESS: Epworth Sleepiness Scale; ISAACC: CPAP in Patients With Acute Coronary Syndrome and OSA; NA: not available; ODI: oxygen desaturation index; OSA: obstructive sleep apnoea; PCI: percutaneous coronary intervention; RICCADSA: Randomized Intervention With CPAP in Coronary Artery Disease and Sleep Apnea; SAVE: Continuous Positive Airway Pressure Treatment of Obstructive Sleep Apnea to Prevent Cardiovascular Disease

night, CPAP usage declined over the first year to 3.5 ± 2.4 hours per night and was only 3.3 ± 2.3 hours per night at the final follow-up. Moreover, only 42% of participants in the CPAP group achieved the conventional criteria for good adherence (≥4 hours per night). The propensity score-matched analyses showed that the patients adhering to CPAP therapy had a lower risk of stroke (p=0.05) and the composite endpoint of cerebral events (p=0.02) than those in the usual care group. Similarly, adherence to CPAP was extremely low in the ISAACC Study. Indeed, 1 year after starting CPAP, the average adherence was only 2.8 ± 2.6 hours per night, with only 36% of the patients in the CPAP group achieving ≥4 hours per night. A propensity score analysis comparing patients who achieved "good adherence" with those receiving usual care showed an HR of 0.80, favouring the CPAP group³⁷.

It has long been recognised that some patients diagnosed with OSA are not receptive to CPAP, despite it being a guideline-mandated first-line treatment for OSA that improves snoring and daytime sleepiness. Using recent data from 789,260 patients initiated on CPAP in the US Centers for Medicare & Medicaid Services database, the overall adherence rate (≥4 hours of use on 70% of nights over a consecutive 30-day period) in the first 90 days was only 72.6%³⁸.

Despite the introduction and testing of many interventional measures, these interventions have had limited success, and this

treatment modality continues to be plagued by a lack of adherence. Indeed, overall non-adherence remains consistent at 30%-40%, especially in health systems where the cost of CPAP is not reimbursable^{39,40}.

Conclusions

OSA is a prevalent, chronic sleep disorder that affects a patient's quality of life. In the past decades, there has been emerging evidence that OSA is an independent predictor of adverse cardiovascular outcomes in patients undergoing coronary revascularisation. Affected individuals had a 50% higher risk of experiencing adverse events if the OSA was untreated. CPAP, with positive airway pressure applied through a nasal or oronasal interface to splint the upper airway open, is the mainstay of therapy for OSA. CPAP is effective in alleviating OSA-associated sleepiness. Moreover, epidemiological data have demonstrated that patients with OSA who use CPAP have a lower risk of fatal and non-fatal cardiovascular events than non-users. Similarly, randomised trials have shown the benefits of CPAP in improving systolic blood pressure, inflammation, and endothelial function. However, due to poor CPAP adherence, randomised controlled trials have failed to verify the benefits of CPAP in reducing cardiovascular events. For now, systematic screening for OSA in patients undergoing coronary revascularisation is not indicated. Although, screening for and treatment of OSA is still

indicated if the patients have reported excessive daytime sleepiness and/or suboptimally controlled hypertension.

Funding

This study was supported by the Clinician Scientist Award (Senior Investigator category) from the National Medical Research Council (Singapore).

Conflict of interest statement

The authors have no conflicts of interest to declare.

References

- 1. Writing Committee Members; Lawton JS, Tamis-Holland JE, Bangalore S, Bates ER, Beckie TM, Bischoff JM, Bittl JA, Cohen MG, DiMaio JM, Don CW, Fremes SE, Gaudino MF, Goldberger ZD, Grant MC, Jaswal JB, Kurlansky PA, Mehran R, Metkus TS Jr, Nnacheta LC, Rao SV, Sellke FW, Sharma G, Yong CM, Zwischenberger BA. 2021 ACC/AHA/SCAI Guideline for Coronary Artery Revascularization: Executive Summary: A Report of the American College of Cardiology/American Heart Association Joint Committee on Clinical Practice Guidelines. *J Am Coll Cardiol*. 2022;79:197-215.
- 2. Stefanini GG, Holmes DR Jr. Drug-eluting coronary-artery stents. *N Engl J Med*. 2013;368:254-65.
- 3. Head SJ, Milojevic M, Taggart DP, Puskas JD. Current Practice of State-of-the-Art Surgical Coronary Revascularization. *Circulation*. 2017;136:1331-45.
- 4. Byrne RA, Stone GW, Ormiston J, Kastrati A. Coronary balloon angioplasty, stents, and scaffolds. *Lancet*. 2017;390:781-92.
- Feng SS, Zeng W, Teng Lim Y, Zhao L, Yin Win K, Oakley R, Hin Teoh S, Hang Lee RC, Pan S. Vitamin E TPGS-emulsified poly(lactic-co-glycolic acid) nanoparticles for cardiovascular restenosis treatment. *Nanomedicine (Lond)*. 2007;2:333-44.
- 6. Lee CH, Lim J, Low A, Zhang XL, Kyaing TT, Chan MY, Wong HB, Lim YT, Tan HC. Sirolimus-eluting, bioabsorbable polymer-coated constant stent (Cura) in acute ST-elevation myocardial infarction: a clinical and angiographic study (CURAMI Registry). *J Invasive Cardiol*. 2007;19:182-5.
- 7. Serruys PW, Morice MC, Kappetein AP, Colombo A, Holmes DR, Mack MJ, Ståhle E, Feldman TE, van den Brand M, Bass EJ, Van Dyck N, Leadley K, Dawkins KD, Mohr FW; SYNTAX Investigators. Percutaneous coronary intervention versus coronary-artery bypass grafting for severe coronary artery disease. *N Engl J Med.* 2009;360:961-72.
- 8. Bangalore S, Guo Y, Samadashvili Z, Blecker S, Xu J, Hannan EL. Everolimuseluting stents or bypass surgery for multivessel coronary disease. *N Engl J Med*. 2015;372:1213-22.
- 9. Fearon WF, Zimmermann FM, De Bruyne B, Piroth Z, van Straten AHM, Szekely L, Davidavičius G, Kalinauskas G, Mansour S, Kharbanda R, Östlund-Papadogeorgos N, Aminian A, Oldroyd KG, Al-Attar N, Jagic N, Dambrink JE, Kala P, Angerås O, MacCarthy P, Wendler O, Casselman F, Witt N, Mavromatis K, Miner SES, Sarma J, Engstrøm T, Christiansen EH, Tonino PAL, Reardon MJ, Lu D, Ding VY, Kobayashi Y, Hlatky MA, Mahaffey KW, Desai M, Woo YJ, Yeung AC, Pijls NHJ; FAME 3 Investigators. Fractional Flow Reserve-Guided PCI as Compared with Coronary Bypass Surgery. N Engl J Med. 2022;386:128-37.
- 10. Lee CH, de Feyter P, Serruys PW, Saia F, Lemos PA, Goedhart D, Soares PR, Umans VA, Ciccone M, Cortellaro M. Beneficial effects of fluvastatin following percutaneous coronary intervention in patients with unstable and stable angina: results from the Lescol intervention prevention study (LIPS). *Heart*. 2004;90:1156-61.
- 11. Nusca A, Piccirillo F, Bernardini F, De Filippis A, Coletti F, Mangiacapra F, Ricottini E, Melfi R, Gallo P, Cammalleri V, Napoli N, Ussia GP, Grigioni F. Glycaemic Control in Patients Undergoing Percutaneous Coronary Intervention: What Is the Role for the Novel Antidiabetic Agents? A Comprehensive Review of Basic Science and Clinical Data. *Int J Mol Sci.* 2022;23:7261.
- 12. Wilson S, Mone P, Kansakar U, Jankauskas SS, Donkor K, Adebayo A, Varzideh F, Eacobacci M, Gambardella J, Lombardi A, Santulli G. Diabetes and restenosis. *Cardiovasc Diabetol.* 2022;21:23.
- 13. Javaheri S, Barbe F, Campos-Rodriguez F, Dempsey JA, Khayat R, Javaheri S, Malhotra A, Martinez-Garcia MA, Mehra R, Pack AI, Polotsky VY, Redline S, Somers VK. Sleep Apnea: Types, Mechanisms, and Clinical Cardiovascular Consequences. *J Am Coll Cardiol*. 2017;69:841-58.
- 14. Yeghiazarians Y, Jneid H, Tietjens JR, Redline S, Brown DL, El-Sherif N, Mehra R, Bozkurt B, Ndumele CE, Somers VK. Obstructive Sleep Apnea and Cardiovascular

- Disease: A Scientific Statement From the American Heart Association. *Circulation*. 2021:144:e56-67
- 15. Berry RB, Brooks R, Gamaldo C, Harding SM, Lloyd RM, Quan SF, Troester MT, Vaughn BV. AASM Scoring Manual Updates for 2017 (Version 2.4). *J Clin Sleep Med.* 2017:13:665-6.
- 16. Benjafield AV, Ayas NT, Eastwood PR, Heinzer R, Ip MSM, Morrell MJ, Nunez CM, Patel SR, Penzel T, Pépin JL, Peppard PE, Sinha S, Tufik S, Valentine K, Malhotra A. Estimation of the global prevalence and burden of obstructive sleep apnoea: a literature-based analysis. *Lancet Respir Med.* 2019;7:687-98.
- 17. Tan A, Cheung YY, Yin J, Lim WY, Tan LW, Lee CH. Prevalence of sleep-disordered breathing in a multiethnic Asian population in Singapore: A community-based study. *Respirology*. 2016;21:943-50.
- 18. Cheung YY, Tai BC, Loo G, Khoo SM, Cheong KY, Barbe F, Lee CH. Screening for Obstructive Sleep Apnea in the Assessment of Coronary Risk. *Am J Cardiol*. 2017:119:996-1002.
- 19. Fletcher EC. The relationship between systemic hypertension and obstructive sleep apnea: facts and theory. *Am J Med.* 1995;98:118-28.
- 20. Gjørup PH, Sadauskiene L, Wessels J, Nyvad O, Strunge B, Pedersen EB. Abnormally increased endothelin-1 in plasma during the night in obstructive sleep apnea: relation to blood pressure and severity of disease. *Am J Hypertens*. 2007;20: 44-52
- 21. Steiner S, Schueller PO, Hennersdorf MG, Behrendt D, Strauer BE. Impact of obstructive sleep apnea on the occurrence of restenosis after elective percutaneous coronary intervention in ischemic heart disease. *Respir Res.* 2008;9:50.
- 22. Yumino D, Tsurumi Y, Takagi A, Suzuki K, Kasanuki H. Impact of obstructive sleep apnea on clinical and angiographic outcomes following percutaneous coronary intervention in patients with acute coronary syndrome. *Am J Cardiol.* 2007;99:26-30.
- 23. Cassar A, Morgenthaler TI, Lennon RJ, Rihal CS, Lerman A. Treatment of obstructive sleep apnea is associated with decreased cardiac death after percutaneous coronary intervention. *J Am Coll Cardiol*. 2007;50:1310-4.
- 24. Tan A, Hau W, Ho HH, Ghaem Maralani H, Loo G, Khoo SM, Tai BC, Richards AM, Ong P. Lee CH. OSA and coronary plaque characteristics. *Chest.* 2014:145:322-30.
- 25. Lee CH, Sethi R, Li R, Ho HH, Hein T, Jim MH, Loo G, Koo CY, Gao XF, Chandra S, Yang XX, Furlan SF, Ge Z, Mundhekar A, Zhang WW, Uchôa CH, Kharwar RB, Chan PF, Chen SL, Chan MY, Richards AM, Tan HC, Ong TH, Roldan G, Tai BC, Drager LF, Zhang JJ. Obstructive Sleep Apnea and Cardiovascular Events After Percutaneous Coronary Intervention. *Circulation*. 2016:133:2008-17.
- 26. Koo CY, Aung AT, Chen Z, Kristanto W, Sim HW, Tam WW, Gochuico CF, Tan KA, Kang GS, Sorokin V, Ong PJL, Kojodjojo P, Richards AM, Tan HC, Kofidis T, Lee CH. Sleep apnoea and cardiovascular outcomes after coronary artery bypass grafting. *Heart*. 2020;106:1495-502.
- 27. Zhao LP, Kofidis T, Chan SP, Ong TH, Yeo TC, Tan HC, Lee CH. Sleep apnoea and unscheduled re-admission in patients undergoing coronary artery bypass surgery. *Atherosclerosis*. 2015;242:128-34.
- 28. Teo YH, Tam WW, Koo CY, Aung AT, Sia CH, Wong RCC, Kong W, Poh KK, Kofidis T, Kojodjojo P, Lee CH. Sleep apnea and recurrent heart failure hospitalizations after coronary artery bypass grafting. *J Clin Sleep Med.* 2021;17:2399-407.
- 29. Drager LF, Bortolotto LA, Figueiredo AC, Krieger EM, Lorenzi-Filho G. Effects of continuous positive airway pressure on early signs of atherosclerosis in obstructive sleep apnea. *Am J Respir Crit Care Med.* 2007;176:706-12.
- 30. Montesi SB, Edwards BA, Malhotra A, Bakker JP. The effect of continuous positive airway pressure treatment on blood pressure: a systematic review and meta-analysis of randomized controlled trials. *J Clin Sleep Med.* 2012;08:587-96.
- 31. Peker Y, Glantz H, Eulenburg C, Wegscheider K, Herlitz J, Thunström E. Effect of Positive Airway Pressure on Cardiovascular Outcomes in Coronary Artery Disease Patients with Nonsleepy Obstructive Sleep Apnea. *Am J Respir Crit Care Med.* 2016; 194:613-20.
- 32. McEvoy RD, Antic NA, Heeley E, Luo Y, Ou Q, Zhang X, Mediano O, Chen R, Drager LF, Liu Z, Chen G, Du B, McArdle N, Mukherjee S, Tripathi M, Billot L, Li Q, Lorenzi-Filho G, Barbe F, Redline S, Wang J, Arima H, Neal B, White DP, Grunstein RR, Zhong N, Anderson CS; SAVE Investigators and Coordinators. CPAP for Prevention of Cardiovascular Events in Obstructive Sleep Apnea. *N Engl J Med.* 2016;375:919-31.
- 33. Sánchez-de-la-Torre M, Sánchez-de-la-Torre A, Bertran S, Abad J, Duran-Cantolla J, Cabriada V, Mediano O, Masdeu MJ, Alonso ML, Masa JF, Barceló A, de la Peña M, Mayos M, Coloma R, Montserrat JM, Chiner E, Perelló S, Rubinós G, Mínguez O, Pascual L, Cortijo A, Martínez D, Aldomà A, Dalmases M, McEvoy RD, Barbé F; Spanish Sleep Network. Effect of obstructive sleep apnoea and its treatment with continuous positive airway pressure on the prevalence of cardiovascular events in patients with acute coronary syndrome (ISAACC study): a randomised controlled trial. *Lancet Respir Med.* 2020;8:359-67.

- 34. Tan LL, Ting J, Balakrishnan I, Seneviratna A, Gong L, Chan MY, Tai ES, Richards AM, Tai BC, Ling LH, Lee CH. Sleep Apnea Evolution and Left Ventricular Recovery After Percutaneous Coronary Intervention for Myocardial Infarction. *J Clin Sleep Med.* 2018;14:1773-81.
- 35. Weaver TE, Maislin G, Dinges DF, Bloxham T, George CF, Greenberg H, Kader G, Mahowald M, Younger J, Pack AI. Relationship between hours of CPAP use and achieving normal levels of sleepiness and daily functioning. *Sleep.* 2007;30:711-9.
- 36. Ou YH, Thant AT, Lee CH. Sudden deterioration of CPAP adherence after myocardial infarction in a Chinese patient: potential effect of ACEI-induced airway hyperresponsiveness. *J Clin Sleep Med.* 2022;18:1463-5.
- 37. Dissanayake HU, Colpani JT, Sutherland K, Loke W, Mohammadieh A, Ou YH, de Chazal P, Cistulli PA, Lee CH. Obstructive sleep apnea therapy for cardiovascular risk reduction-Time for a rethink? *Clin Cardiol*. 2021;44:1729-38.
- 38. Patel SR, Bakker JP, Stitt CJ, Aloia MS, Nouraie SM. Age and sex disparities in adherence to CPAP. Chest. 2021;159:382-9.
- 39. Rotenberg BW, Murariu D, Pang KP. Trends in CPAP adherence over twenty years of data collection: a flattened curve. *J Otolaryngol Head Neck Surg.* 2016;45:43.
- 40. Tan B, Tan A, Chan YH, Mok Y, Wong HS, Hsu PP. Adherence to Continuous Positive Airway Pressure therapy in Singaporean patients with Obstructive Sleep Apnea. *Am J Otolaryngol.* 2018;39:501-6.

Clinical prognostic value of a novel quantitative flow ratio from a single projection in patients with coronary bifurcation lesions treated with the provisional approach



Jing Kan¹, MPH; Zhen Ge¹, MD; Shaoping Nie², MD; Xiaofei Gao¹, MD; Xiaobo Li¹, MD; Imad Sheiban³, MD; Jun-Jie Zhang¹, MD; Shao-Liang Chen¹*, MD

1. Division of Cardiology, Nanjing First Hospital, Nanjing Medical University, Nanjing, People's Republic of China; 2. Beijing Anzhen Hospital, Capital Medical University, Beijing, People's Republic of China; 3. Division of Cardiology, Pederzoli Hospital-Peschiera del Garda, Verona, Italy

J. Kan and Z. Ge contributed equally to this work.

This paper also includes supplementary data published online at: https://www.asiaintervention.org/doi/10.4244/AIJ-D-22-00045

KEYWORDS

- bifurcation
- drug-eluting stent
- other imaging modalities

Abstract

Background: A novel quantitative flow ratio (μ QFR) for bifurcated coronary vessels, derived from a single projection, has been recently reported. Provisional stenting is effective for most bifurcation lesions. However, the clinical value of the side branch (SB) μ QFR in patients with coronary bifurcation lesions undergoing provisional stenting remains unclear.

Aims: This study aims to determine the clinical predictive value of the SB μ QFR after provisional stenting in patients with coronary bifurcation lesions.

Methods: Between June 2015 and May 2018, 288 patients with true coronary bifurcation lesions who underwent a provisional approach without SB treatment (including predilation, kissing balloon inflation or stenting) were classified by an SB μ QFR <0.8 (n=65) and \geq 0.8 (n=223) groups. The primary endpoint was the three-year composite of target vessel failure (TVF), including cardiac death, target vessel myocardial infarction (TVMI), and revascularisation (TVR).

Results: Three years after the procedures, there were 43 (14.9%) TVFs, with 19 (29.2%) in the SB μ QFR <0.8 and 24 (10.8%) in the SB μ QFR ≥0.8 groups (adjusted hazard ratio [HR] 2.45, 95% confidence interval [CI] 1.39-5.54; p=0.003), mainly driven by increased TVMI (16.9% vs 5.4%, adjusted HR 3.29, 95% CI: 1.15-6.09; p=0.030) and TVR (15.4% vs 2.2%, adjusted HR 6.39, 95% CI: 2.04-13.48; p=0.007). Baseline diameter stenosis at the ostial SB and SB lesion length were the two predictors of an SB μ QFR <0.8 immediately after stenting the main vessel, whereas previous percutaneous coronary intervention and an SB μ QFR <0.8 were the two independent factors of 3-year TVF.

Conclusions: An SB μ QFR <0.8 immediately after the provisional approach is strongly associated with clinical events. Further randomised studies with large patient populations are warranted.

^{*}Corresponding author: Nanjing First Hospital, Nanjing Medical University, 140 Hanzhong Rd, Gulou, Nanjing, Jiangsu, Nanjing 210029, People's Republic of China. E-mail: chmengx@hotmail.com

Abbreviations

KBI kissing balloon inflation

LAD left anterior descending coronary artery

LCx left circumflex coronary artery

MI myocardial infarction

MV main vessel

PCI percutaneous coronary intervention

μQFR novel quantitative flow ratio

SB side branch
ST stent thrombosis
TVF target vessel failure

Introduction

Coronary artery bifurcation is anatomically complicated; stenting coronary bifurcation lesions yields suboptimal clinical results, including frequent stent thrombosis (ST) and unplanned repeat revascularisations, compared to non-bifurcation lesions¹. While the main vessel (MV) lesion is the primary determinant of clinical outcome, in this modern era of percutaneous coronary intervention (PCI) using drug-eluting stents (DES), when and how to treat side branch (SB) lesions are still key questions². This is largely because of the dissociation between anatomical severity and functional significance^{3,4}. The DKCRUSH VI study⁵ is the only randomised study analysing the differences in clinical outcome between fractional flow reserve (FFR)-guided and angiography-guided stenting of bifurcation lesions. The study failed to show a clinical benefit of FFR guidance, except for a lower requirement for SB stenting. One reason for this may be the high rate (9%) of failure to access the SB using rigid pressure wires after stenting the MV. Thus, angiography-derived quantitative flow ratio (QFR), without the administration of adenosine or the use of costly and less manageable pressure wires, is becoming a point of interest⁶.

Several studies have analysed the diagnostic performance of the QFR in comparison with pressure wire-measured FFR⁶⁻¹³ and revealed that the QFR showed good agreement, diagnostic accuracy, and predictive value compared with FFR8,10,12, except for borderline FFR zones with acute myocardial infarction (AMI)11. However, the first-generation software for calculating QFR requires two angiographic projections with angles 25° apart and does not apply to SB QFR measurements. The accuracy of an MV µQFR measurement from a single angiographic projection has recently been demonstrated to have as good a diagnostic performance as FFR¹⁴ among patients in the FAVOR II China study¹⁵. In this study, however, the agreement between SB µQFR and FFR was not reported. Furthermore, the predictive value of SB μQFR immediately after provisional stenting (the predominant stenting technique for uncomplicated bifurcation lesions) for short- and long-term clinical outcomes is unclear. Accordingly, this study aims to identify the prevalence of SB μQFR <0.8 after stenting the MV without SB treatment (including predilation, kissing balloon inflation or SB stenting) and the association of SB μQFR with clinical events during 3 years of follow-up.

Editorial, see page 99

Methods

PATIENT POPULATION

Patients presenting with *de novo* coronary bifurcation lesions intended for PCI at participating centres, between June 2015 and May 2018, were evaluated for an intention-to-treat analysis in the study. Patients were included if they had only one bifurcation lesion treated with provisional stenting (MV stenting with a jailed wire in the SB), were >18 years old, presented with silent ischaemia, stable or unstable angina, or myocardial infarction (MI) >24 hours prior to treatment. For study inclusion, all bifurcation lesions were Medina 1, 1, 1 or 0, 1, 1 with a reference vessel diameter (RVD) in the SB \geq 2.5 mm by visual estimation. Patients who had participated in other clinical trials were excluded from this analysis.

PROVISIONAL STENTING PROCEDURE

The provisional stenting technique has been described previously^{2,5,16,17}. The MV and SB were wired. Predilating the SB was not encouraged. A stent with a stent/artery ratio of 1.1:1 was implanted in the MV, then the proximal optimisation technique (POT) using non-compliant balloons (1:1 of balloon/stent ratio, >18 atm) was performed. After MV stenting, ballooning or stenting the SB was performed, if the SB Thrombolysis in Myocardial Infarction (TIMI) flow was <3. Patients who had undergone SB treatment (predilation, kissing balloon inflation or stenting) before SB μ QFR measurement were excluded from this analysis.

MEASUREMENT OF µQFR

The measurements of µOFR for the MV and all SBs have been described elsewhere 14. The μQFR was computed using a prototype software (AngioPlus Core, Pulse Medical Imaging Technology) by three experienced technicians who were blinded to the objectives of this study. The computation included 1) delineation of the interrogated epicardial coronary artery during contrast injection and calculation of contrast flow velocity based on the centreline length divided by the contrast dye filling time; 2) selection of the analysis frame with sharp lumen contour at the stenotic segment as the key frame; 3) delineation of the lumen contour of the interrogated vessel and its SBs with diameters of ≥1.0 mm on the key frame; 4) reconstruction of the reference diameter function with the step-down size across bifurcations; 5) modelling of hyperaemic flow velocity based on the contrast flow velocity and calculation of pressure drop based on fluid dynamics equations, assuming a blood density of 1,060 kg/m³ and viscosity of 0.0035 kg/(m.s).

INTRA- AND INTEROBSERVER ANALYSIS

To analyse intraobserver variability in μQFR measurements, 30 randomly selected vessels were analysed simultaneously by three well-trained technicians who were blinded to the study objectives. For interobserver variability analysis, 20 vessels were randomly selected and reanalysed by the same technician and a second technician 1 week later. The μQFR of the MV and SB

were calculated at baseline and immediately after stenting the MV and POT.

MEDICATION AND FOLLOW-UP

Procedural anticoagulation was achieved with unfractionated heparin. All patients were treated with aspirin preprocedure and received a 300 mg loading dose of clopidogrel if not on chronic dual antiplatelet therapy. After the intervention, all patients received 100 mg/day of aspirin indefinitely and clopidogrel 75 mg/day for at least 12 months. Additional medications for secondary prevention, including statins, β -blockers and angiotensin-converting enzyme inhibitors, were prescribed according to current guidelines. Clinical follow-up was done through office visits or telephone interviews at 1, 6, 12, 24, and 36 months.

ENDPOINTS AND DEFINITIONS

The primary endpoint was target vessel failure (TVF) at 3-year follow-up, defined as the composite of cardiac death, target vessel MI (TVMI), or clinically driven target vessel revascularisation (TVR). Death from cardiac causes was defined as any death without a clear non-cardiac cause. Protocol-defined periprocedural MI (within 48 hours) was defined as a creatine kinase myocardial band (CK-MB) $>10\times$ the upper reference limit (URL) of the assay, or >5× URL plus either i) new pathological Q waves in ≥2 contiguous leads or new left bundle branch block (LBBB); ii) angiographically documented graft or coronary artery occlusion or new severe stenosis with thrombosis; iii) imaging evidence of new loss of viable myocardium; or iv) new regional wall motion abnormality. Spontaneous MI (after 48 hours) was defined as a clinical syndrome of MI with CK-MB or troponin >1× the URL and new ST-segment elevation or depression, or any of the findings described above. All MIs were considered TVMI unless there was clear evidence that they were attributable to a non-target vessel16,17. Clinically driven TVR was defined as angina or ischaemia attributable to the target vessel requiring repeat PCI or coronary artery bypass graft. Secondary endpoints included cardiac death, TVMI, clinically driven target lesion revascularisation (TLR), and all-cause death. Definite or probable ST, according to the Academic Research Consortium, 18 was the major safety endpoint. All events were adjudicated by a central committee using original source documents blinded to treatment. The functionally complete revascularisation was defined by a post-PCI µQFR >0.80 in all treated vessels.

STATISTICAL ANALYSIS

Patients were assigned to the SB μ QFR <0.8 and SB μ QFR \geq 0.8 groups immediately after MV stenting with final POT.

Baseline characteristics are reported as counts and percentages or as mean±standard deviation (SD). The chi-squared or Fisher's exact tests were used to compare categorical variables. The Student's t-test or Wilcoxon rank-sum scores for non-normally distributed data were used to compare continuous variables. Time-to-first event curves were generated using Kaplan-Meier analysis and compared

using the log-rank test. Landmark analysis was used to determine the difference in TVF within 30 days, from 31 days to 1 year, and from 1 to 3 years between the two groups. Cox regression analysis was used to compare the differences in the primary endpoints and to identify the predictors of 3-year TVF and SB μ QFR <0.8 after stenting the MV with POT, with outputs of hazard ratios (HR), 95% confidence intervals (CI), and p-values. Baseline variables with a p-value <0.05 between the groups were used for an adjusted analysis of endpoints. All statistical tests were two-sided, and a p-value of <0.05 was considered statistically significant. All analyses were performed with Stata v12.0 (StataCorp).

Results

PATIENT POPULATION

Between June 2015 and May 2018, 1,113 patients with true bifurcation lesions were screened (**Figure 1**). Of them, 825 patients were excluded: chronic total occlusions (CTOs) in 89 patients (60 CTOs in the MV, 16 in the SB, and 12 in both the MV and the SB); a two-stent approach in 9 patients; poor imaging quality in 192 patients; and 535 undergoing SB treatment (including predilation or kissing balloon inflation or stenting). Finally, 288 patients were included in this study. Immediately after the PCI procedures, 65 (22.6%) patients had an SB μ QFR <0.8 and 223 (77.4%) patients had an SB μ QFR \geq 0.8.

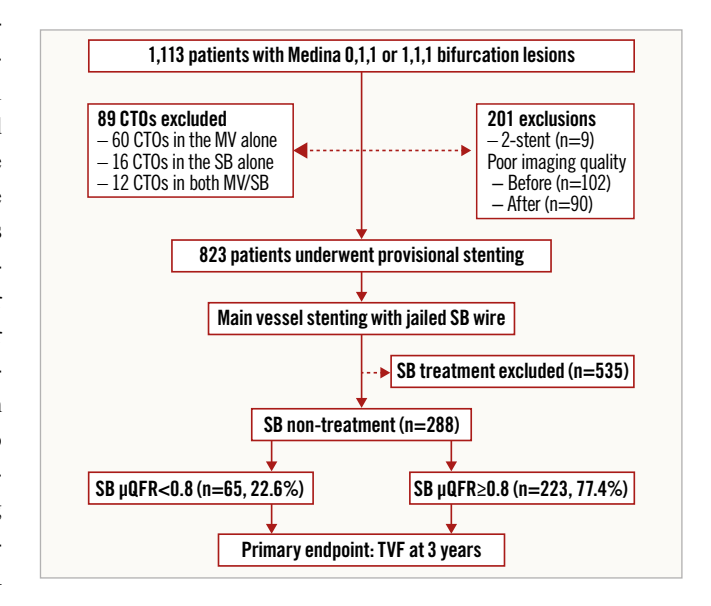


Figure 1. Study flowchart. Of 288 patients with true coronary bifurcation lesions after stenting the main vessel (MV) without side branch (SB) treatment (including predilation, or kissing balloon inflation or stenting), 65 patients had an SB quantitative flow ratio (μ QFR) of <0.8 and 223 patients had an SB μ QFR \geq 0.8. CTO: chronic total occlusion; TVF: target vessel failure

BASELINE CLINICAL CHARACTERISTICS

Patients in the SB μ QFR <0.8 group were older (66.4 \pm 10.0 years vs 64.4 \pm 9.9 years; p=0.017) and had more frequent previous PCI

(32.3% vs 13.0%; p=0.001), compared to patients in the SB μ QFR \geq 0.8 group (**Table 1**).

LESION AND PROCEDURAL CHARACTERISTICS

The lesion length in the MV was 37.5 ± 12.4 mm in the SB μ QFR <0.8 group (**Table 2**), significantly longer than the 34.9 ± 17.4 mm in the SB μ QFR \geq 0.8 group (p=0.022). Baseline diameter stenosis at the ostial SB (59.9% vs 52.0%; p=0.072) and SB lesion length (14.5 \pm 7.1 vs 13.4 \pm 9.2; p=0.382) were comparable between the two groups. More lesions needed to be treated (2.23 \pm 0.86 vs 1.92 \pm 0.82; p<0.001) in the SB μ QFR <0.8 group, resulting in a higher rate of staged procedures (40.0% vs 26.0%; p=0.043) and fewer complete revascularisations (40.0% vs 63.7%; p=0.001). Most procedures were performed using the

Table 1. Baseline characteristics of patients.

		SB μQFR <0.8 (n=65)	SB μQFR ≥0.8 (n=223)	<i>p</i> -value
Age, years	Age, years		64.4±9.9	0.017
Male, n (%)		51 (78.5)	165 (74.0)	0.518
Body mass inde	ex, kg/m²	24.6±3.1	24.6±2.9	0.629
Body surface a	rea, m²	1.86±0.16	1.86±0.17	0.888
Hypertension, n	ı (%)	44 (67.7)	144 (64.6)	0.767
Diabetes, n (%))	23 (35.4)	69 (30.9)	0.546
Hyperlipidaemi	a, n (%)	34 (52.3)	107 (48.0)	0.575
Previous MI, n ((%)	10 (15.4)	30 (13.5)	0.686
Previous PCI, n	(%)	21 (32.3)	29 (13.0)	0.001
Previous CABG,	n (%)	0	2 (0.9)	1.000
Renal dysfunction, n (%)		4 (6.2)	8 (3.6)	0.478
Current smoker	Current smoker, n (%)		41 (18.4)	0.592
Family history, n (%)		2 (3.1)	11 (4.9)	0.739
GI bleeding, n ((%)	2 (3.1)	5 (2.2)	0.658
Stroke, n (%)		7 (10.8)	24 (10.8)	1.000
Peripheral arte	ry disease, n (%)	1 (1.5)	17 (7.6)	0.085
Heart failure, n	Heart failure, n (%)		18 (12.6)	1.000
LVEF, %		59.4±8.4	60.8±7.5	0.583
Heart rate, bpm	Heart rate, bpm		74.1±11.1	0.695
Systolic blood p	oressure, mmHg	135.9±17.9	131.8±17.3	0.300
Diastolic blood	pressure, mmHg	77.9±10.2	78.6±10.5	0.909
Clinical	Silent ischaemia	3 (4.6)	11 (4.9)	1.000
presentation, n (%)	Stable angina	13 (20.0)	42 (18.8)	0.858
	Unstable angina	34 (52.3)	122 (54.7)	0.778
	AMI >24 h	15 (23.1)	48 (21.5)	0.865
	STEMI	6 (9.2)	25 (11.2)	0.821
	NSTEMI	9 (13.8)	23 (10.3)	0.500

Data are mean \pm standard deviation or n (%). AMI: acute myocardial infarction; CABG: coronary artery bypass graft; GI: gastrointestinal; LVEF: left ventricular ejection fraction; MI: myocardial infarction; NSTEMI: non-ST-elevation myocardial infarction; PCI: percutaneous coronary intervention; μ QFR: novel quantitative flow ratio; SB: side branch; STEMI: ST-segment elevation myocardial infarction

transradial approach. Intravscular ultrasound guidance was used in fewer than 30% of patients.

DYNAMIC CHANGE OF µQFR

The inter- and intraobserver variances were less than 5%.

At baseline, the absolute value of μQFR in the SB μQFR <0.8 group was lower than that in the SB $\mu QFR \ge 0.8$ group (0.61±0.19 vs 0.71±0.22; p=0.001) **(Table 3)**, and the percentage of patients with an SB $\mu QFR < 0.8$ was 90.8% (n=59), significantly different from the 59.2% (n=132) in the SB $\mu QFR \ge 0.8$ group (p<0.001). However, the percentage of patients with a baseline MV $\mu QFR < 0.8$ did not differ significantly between the two groups.

After stenting the MV and POT, the μ QFR in the MV increased to 0.93±0.07 in the SB μ QFR \geq 0.8 group, compared to 0.91±0.09 (p=0.008) in the SB μ QFR <0.8 group, resulting in a higher rate of μ QFR <0.89 in the SB μ QFR <0.8 group (23.1% vs 12.6%; p=0.047).

For the SB, immediately after stenting the MV and POT, a more profound increase of μ QFR in the SB was measured in the SB μ QFR \geq 0.8 group (0.20±0.22), compared to 0.03±0.21 in the SB μ QFR <0.8 group (p<0.001). Baseline diameter stenosis at the ostial SB (odds ratio [OR] 9.55, 95% CI: 1.51-15.92; p=0.023) and SB lesion length (OR 5.433, 95% CI: 1.201-10.93; p<0.001) were the two predictors of a μ QFR <0.8 in the SB immediately after stenting the MV.

PRIMARY AND SECONDARY ENDPOINTS

At 30 days, the rate of endpoints was comparable between the two groups after adjusted analysis (**Table 4**). Within one-year after stenting, the incidence of TVMI and TVR in the SB μ QFR <0.8 group were 15.4% and 12.3%, respectively, significantly different to the 4.9% and 1.3% in the SB μ QFR \geq 0.8 group, by either unadjusted or adjusted analyses.

At 3-year follow-up, TVF was reported in 43 (20.0%) patients overall, with 29.2% of patients in the SB μ QFR <0.8 group and 10.8% in the SB μ QFR \geq 0.8 group (adjusted HR 2.45, 95% CI: 1.30-5.53; p=0.003) experiencing TVF, largely driven by increased rates of TVMI (16.9% vs 5.4%, adjusted HR 3.29, 95% CI: 1.15-6.09; p=0.030) and TVR (15.4% vs 2.2%, adjusted HR 6.39, 95% CI: 2.04-13.48; p=0.007) (Table 4, Figure 2). Landmark analysis between the two groups (Figure 3) showed a significant difference in TVF within 30 days and at one year but not between one and three years.

By multivariate analysis, previous PCI (OR 4.81, 95% CI: 1.07-21.69; p=0.041) and an SB μ QFR <0.8 (OR 6.88, 95% CI: 2.09-22.64; p=0.002) were the two independent factors of 3-year TVF.

CORRELATION OF SB μQFR <0.8 WITH SB TIMI FLOW AND TVF

Immediately after the procedures, SB TIMI flow grade <3 was seen in 18 (6.3%) patients, with 15 (23.1%) in the SB μ QFR <0.8 group and 3 (1.3%) in the SB μ QFR \geq 0.8 group (p<0.001)

Table 2. Lesions and procedural characteristics.

		SB µQFR <0.8 (n=65)	SB μQFR ≥0.8 (n=223)	<i>p</i> -value
No. of diseased vessels	Single-vessel disease, n (%)	12 (18.5)	61 (27.4)	0.194
	Two-vessel disease, n (%)	29 (44.6)	103 (46.2)	0.888
	Three-vessel disease, n (%)	24 (36.9)	59 (26.5)	0.120
	LM bifurcation lesions, n (%)	20 (30.8)	79 (35.4)	0.554
Moderate-severe calcification	Main vessel, n (%)	20 (30.8)	68 (30.5)	1.000
	Side branch, n (%)	9 (13.8)	19 (8.5)	0.234
Thrombus-containing lesion	Main vessel, n (%)	2 (3.1)	8 (3.6)	1.000
	Side branch, n (%)	1 (1.5)	0	0.226
TIMI flow grade 3 prior to procedure	Main vessel, n (%)	59 (90.8)	200 (89.7)	0.823
	Side branch, n (%)	62 (95.4)	213 (95.5)	0.334
Lesion length	Main vessel, mm	37.5±12.4	34.9±17.4	0.022
	Side branch, mm	14.5±7.1	13.4±9.2	0.382
Diameter stenosis	Main vessel, %	54.3±14.0	52.2±17.8	0.243
	Side branch, %	59.9±13.9	52.0±19.2	0.072
No. of lesions, n		2.34±0.87	2.14±0.91	< 0.001
No. of treated lesions, n		2.23±0.86	1.92±0.82	<0.001
Transradial access, n (%)		50 (76.9)	187 (83.9)	0.201
IVUS guidance, n (%)		18 (27.7)	66 (29.6)	0.877
IABP, n (%)		0	1 (0.4)	1.000
MV TIMI flow grade 3 post-procedure, n (%)		64 (98.5)	222 (99.6)	0.862
SB TIMI flow grade 3 post-procedure, n (%)		50 (76.9)	220 (98.7)	<0.001
Staged PCI, n (%)		26 (40.0)	58 (26.0)	0.043
Complete revascularisation, n (%)		26 (40.0)	142 (63.7)	0.001

Data are mean±standard deviation or n (%). IABP: intra-aortic balloon pumping; IVUS: intravascular ultrasound; LM: left main; MV: main vessel; PCI: percutaneous coronary intervention; µQFR: novel quantitative flow ratio; SB: side branch; TIMI: Thrombolysis in Myocardial Infarction

Table 3. Dynamic change of quantitative flow ratio.

		SB μQFR <0.8 (n=65)	SB μQFR ≥0.8 (n=223)	<i>p</i> -value	
Target vessel,	LAD-LCx	16 (24.6)	65 (29.1)		
n (%)	LAD-diagonal	36 (55.4)	128 (57.4)		
	LCx-obtuse marginal	11 (16.9)	21 (9.4)	0.386	
	Distal RCA	2 (3.1)	9 (4.0)		
Main vessel μQFR	Baseline	0.61±0.22	0.61±0.24	0.046	
	<0.8, n (%)	46 (70.8)	167 (74.9)	0.523	
	Post-procedure	0.91±0.09	0.93±0.07	0.008	
	<0.89, n (%)	15 (23.1)	28 (12.6)	0.047	
Side branch µQFR	Baseline	0.61±0.19	0.71±0.22	0.001	
	<0.8, n (%)	59 (90.8)	132 (59.2)	<0.001	
	Post-procedure	0.64±0.14	0.91±0.06	<0.001	
	ΔμQFR	0.03±0.21	0.20±0.22	<0.001	

Data are mean±standard deviation or n (%). LAD: left anterior descending artery; LCx: left circumflex; MV: main vessel; µQFR: novel quantitative flow ratio; RCA: right coronary artery; SB: side branch

(Table 2). Of patients with SB TIMI flow grade <3, >33.0% of patients suffered 3-year TVF **(Figure 4)**, with no significant difference between the SB μ QFR <0.8 and \geq 0.8 groups. Notably, of 270 patients with TIMI flow grade 3, the rate of 3-year TVF was 28.0% (14/50) in patients with an SB μ QFR <0.8 and 10.5% (23/220) in patients with an SB μ QFR \geq 0.8 (p=0.003) **(Figure 3)**.

Discussion

To the best of our knowledge, this is the first study to report the clinical predictive value of the μQFR from a single projection in patients with true coronary artery bifurcation lesions treated with the provisional approach. We successfully measured the μQFR in the MV and SB in 82.7% of patients and found that 1) baseline diameter stenosis at the ostial SB and SB lesion length are predictors of an SB μQFR <0.8 immediately after stenting the MV; 2) a post-procedural SB μQFR <0.8 is strongly associated with TVMI, TVR, and subsequent TVF, within one year of the procedure; 3) previous PCI and an SB μQFR <0.8 predict the occurrence of three-year TVF.

Table 4. Primary and secondary endpoints.

	SB µQFR <0.8	SB µQFR ≥0.8	Unadjusted analy	sis	Adjusted analys	is
	(n=65)	(n=223)	HR (95% CI)	<i>p</i> -value	HR (95% CI)	<i>p</i> -value
At 30 days	'					
TVF	9 (13.8)	13 (5.8)	2.59 (1.06-6.38)	0.038	2.44 (0.67-5.25)	0.162
Cardiac death	0	3 (1.3)	_	0.997	-	0.944
TVMI	8 (12.3)	11 (4.9)	2.71 (1.04-7.04)	0.041	2.57 (0.56-6.89)	0.227
PMI	8 (12.3)	10 (4.5)	2.99 (1.13-7.92)	0.028	2.73 (0.79-6.61)	0.091
TVR	1 (1.5)	0	-	0.995	-	0.994
ST	0	2 (0.9)	_	0.997	-	0.994
At 1 year						
TVF	16 (24.6)	15 (6.7)	4.53 (2.09-9.78)	<0.001	4.02 (1.77-6.83)	0.004
Cardiac death	1 (1.5)	3 (1.3)	1.15 (0.12-11.21)	0.907	1.02 (0.10-1.12)	0.638
TVMI	10 (15.4)	11 (4.9)	3.50 (1.42-8.67)	0.007	3.35 (1.03-7.33)	0.045
TVR	8 (12.3)	3 (1.3)	10.29 (2.65-40.04)	0.001	7.95 (1.13-35.98)	0.037
ST	0	3 (1.3)	_	0.997	-	0.995
Any death	2 (3.1)	5 (2.2)	1.38 (0.26-7.31)	0.702	1.26 (0.21-5.45)	0.608
At 3 years						
TVF	19 (29.2)	24 (10.8)	3.43 (1.73-6.77)	<0.001	2.45 (1.39-5.54)	0.003
Cardiac death	4 (6.2)	4 (1.8)	3.59 (0.87-14.77)	0.077	1.02 (0.09-3.20)	0.987
TVMI	11 (16.9)	12 (5.4)	3.58 (1.49-8.56)	0.004	3.29 (1.15-6.09)	0.030
TVR	10 (15.4)	5 (2.2)	7.93 (2.60-24.14)	<0.001	6.39 (2.04-13.48)	0.007
ST	2 (3.1)	4 (1.8)	1.74 (0.31-9.71)	0.529	1.48 (0.26-4.23)	0.390
Any death	6 (9.2)	13 (5.8)	1.64 (0.59-4.51)	0.335	1.58 (0.46-4.01)	0.995

Data are n(%). Parameters for adjusted analysis included age, history of percutaneous coronary intervention, peripheral artery disease, renal dysfunction, heart failure, triple-vessel disease, lesion length in the main vessel and side branch, baseline diameter stenosis at the ostial side branch, number of lesions, number of treated lesions, staged percutaneous coronary intervention, final two-stent techniques, and complete revascularisation.

CI: confidence interval; HR: hazard ratio; MI: myocardial infarction; PMI: periprocedural myocardial infarction; µQFR: novel quantitative flow ratio; SB: side branch; ST: stent thrombosis; TVF: target vessel failure; TVMI: target vessel myocardial infarction; TVR: target vessel revascularisation

The measurement of the µQFR has the advantage of not requiring the administration of adenosine (which may induce some side effects, i.e., dyspnoea and bradyarrhythmia) or the use of a costly pressure wire, and subsequently shortens the measuring time (usually 1-2 min)⁶. Since μQFR measurements rely largely on the identification of arterial boundaries from angiography, the reproducibility of µQFR is a major issue. Kornowski et al⁷ reported that a high degree of concordance was found between two measurements of QFR performed by two different operators (interclass correlation coefficient of 0.97; p<0.001), which is consistent with our results. Since angiographic quality is the determinant of a successfully measured QFR⁷⁻¹⁸, the failure of measurements varied from 5.9% 10 to 16%, similar to our findings. The common feature of these lesions is slow flow, with a QFR >0.80 due to no significant stenosis, but a TIMI flow grade \leq 3. It is important to note that the μ QFR only assesses the presence of ischaemia caused by lesions in the epicardial coronary vessels, so coronary microvascular lesions may present with a normal QFR but slow blood flow. Recently, a metaanalysis¹⁹ of 16 studies demonstrated that 18% of evaluated vessels could not be analysed. Obviously, prospective analysis will promote the successful measurement of QFR given that the quality of angiography meets the requirements¹⁹. Diagnostic performance of the QFR is another concern. Results from the WIFI II Study¹⁰ showed that the overall sensitivity, specificity, and positive and negative predictive values of the QFR in a single vessel were 77%, 86%, 75%, and 87%, respectively. The sensitivity and specificity of the QFR increased to 86.5% and 88.9%, respectively, in the FAVOR II China study¹², in line with a recent pooled analysis¹⁹. However, the accuracy of the SB μ QFR was not analysed because of a lack of wirebased FFR in the SB.

Coronary bifurcation lesions account for 20-25% of treated lesions^{1,2}. Although a 3D model of a bifurcated vessel for QFR measurement was introduced in 2015²⁰, successful measurement of the µQFR in both the MV and SB using a single projection was only reported more recently¹⁴ in 330 vessels in the FAVOR II China study ¹⁵. The vessel-based analysis demonstrated that not only had the sensitivity remained stable, but the specificity had increased from 89% ¹⁹ to 96.2%¹⁴. Contrary to the FAVOR II China study¹⁵, our study included all bifurcation lesions needing treatment and reported a much lower baseline µQFR for both the MV and SB. Another

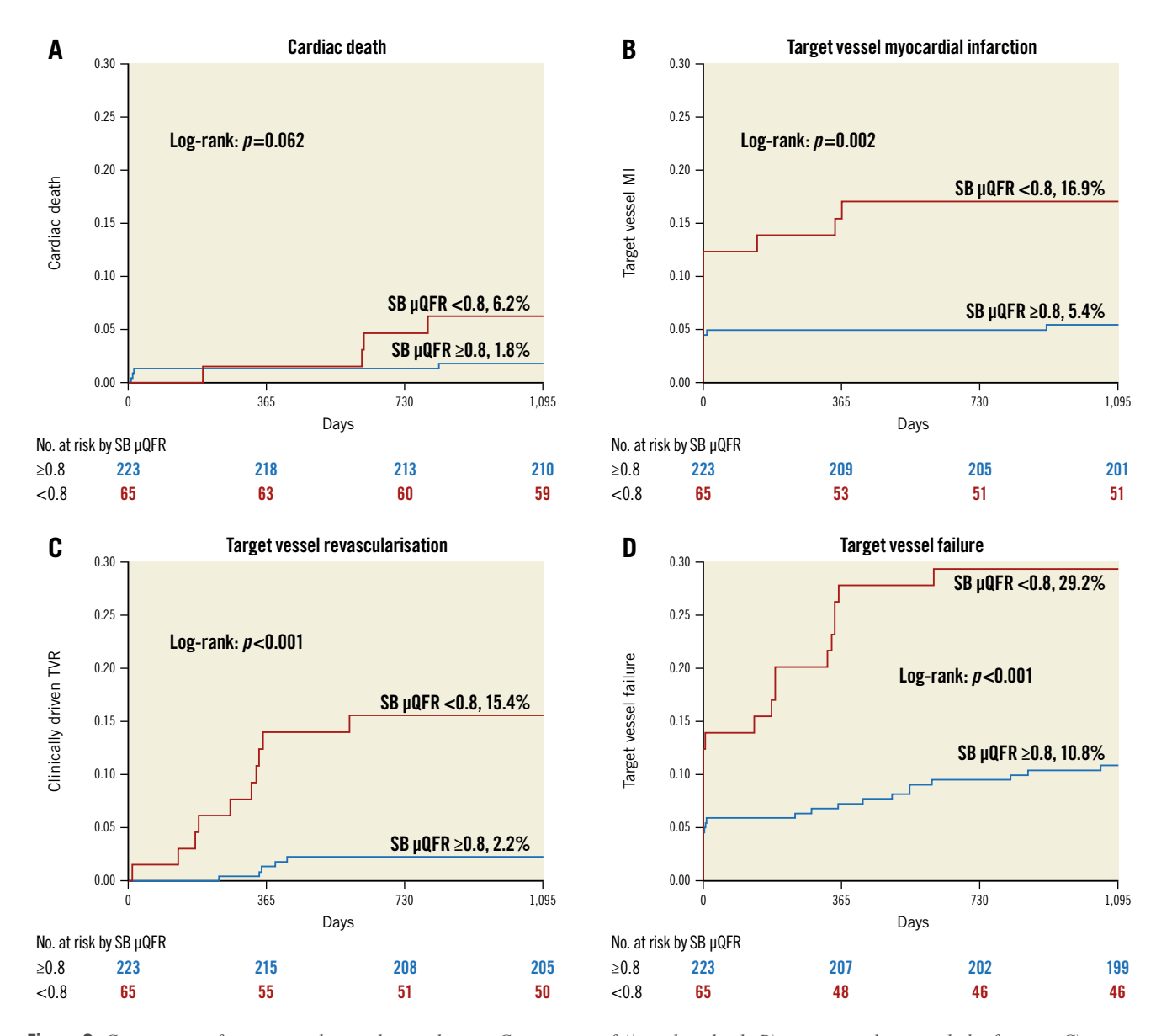


Figure 2. Comparison of primary and secondary endpoints. Comparison of A) cardiac death, B) target vessel myocardial infarction, C) target vessel revascularisation, and D) target vessel failure between patients with a quantitative flow ratio in the SB (SB μ QFR) <0.8 and \geq 0.8. μ QFR: novel quantitative flow ratio; SB: side branch

important finding was the MV μ QFR <0.89 after the stenting procedure, which was found in 124 (15.1%) patients, similar to the 13% of 123 vessels with suboptimal results from the HAWKEYE study. Using wire-based FFR after stenting the MV, an SB FFR <0.75 was seen in 26% of 110 patients with bifurcation lesions²¹, similar to the 22.6% in our study, using a cut-off of 0.8 for the μ QFR.

Post-stenting wire-based FFR was the major predictor of clinical events after bifurcation stenting $^{4,21\text{-}24}$. Unfortunately, while QFR has generally been accepted to be an alternative to functional parameters for ischaemia, there is no study systematically analysing the association of SB μQFR after the provisional approach with clinical outcomes. At 30 days after the procedure in our study, the differences in TVF and TVMI (driven by periprocedural MI) between the SB μQFR <0.8 and \geq 0.8 groups by unadjusted analysis became non-significant after the adjusted

analysis. However, the significant differences in TVMI, TVR, and TVF were sustained through three years of follow-up by either unadjusted or adjusted analyses (**Table 4**). Furthermore, landmark analysis failed to show the difference in TVF from one year to three years between the two groups. Consequently, the more solid correlation of an SB μ QFR <0.8 with the occurrence of TVMI, TVR, and TVF within one year has emerged, as most TVFs took place within one year.

The next concern is how to predict QFR in SBs after stenting the MV. The reasons for a reduced FFR post-stenting are multifactorial and include the presence of a muscle bridge, distal lesions, spasm, and microcirculatory dysfunction. In this study, age and SB lesion length were predictors of an SB μ QFR <0.8 after the MV intervention. As a result, measurement of the μ QFR in the SB after stenting the MV should be recommended, particularly

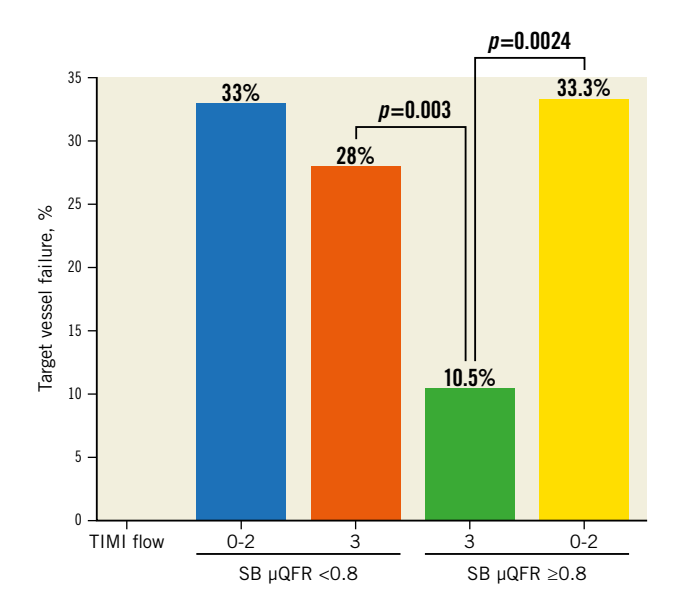


Figure 3. Correlation of SB μ QFR with TIMI flow and TVF. SB: side branch; TIMI: Thrombolysis in Myocardial Infarction; TVF: target vessel failure; μ QFR: novel quantitative flow ratio

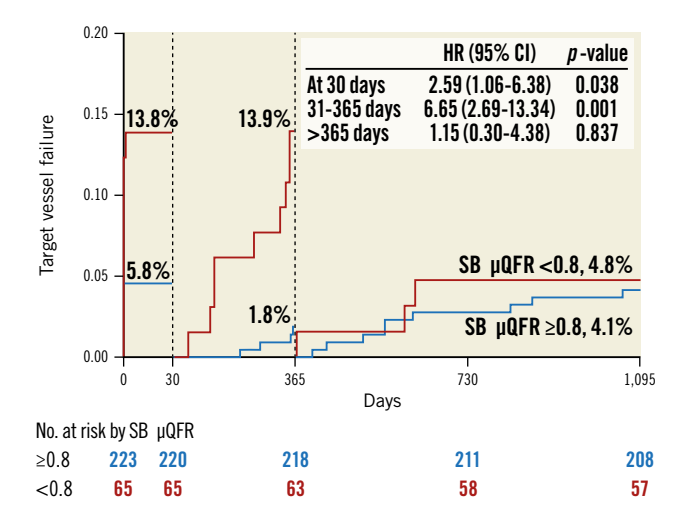


Figure 4. Landmark analysis of target vessel failure. Landmark analysis showed a significant difference in target vessel failure at 30 days and between 31 and 365 days, but not between 366 days and 3 years, for patients with an SB μ QFR < 0.8 and an SB μ QFR \geq 0.8. CI: confidence interval; HR: hazard ratio; SB: side branch; μ QFR: novel quantitative flow ratio

for bifurcation lesions with long lesion lengths in the SB. We also found that previous PCI and an SB μ QFR <0.8 were the two independent factors for TVF at three-year follow-up. The important role of SB lesion length has been clearly studied in the DEFINITION study²⁵, in which a lesion length \geq 10 mm in the SB was the major criterion for defining complex bifurcation lesions. The recently published DEFINITION II trial² further confirmed the superiority of the systematic two-stent approach to the provisional approach for bifurcation lesions with complex coronary bifurcation lesions. Another striking finding was that an SB μ QFR

<0.8 was not rare (6.3%) among patients with SB TIMI flow grade 3; however, the underlying mechanisms may be correlated with microcirculatory dysfunction. Altogether, routine measurement of the μ QFR in the SB after stenting the MV should be performed, particularly for lesions with a long lesion length in the SB.

Limitations

This study has several limitations. First, the coronary angiographies in the study were obtained without adherence to a dedicated QFR acquisition protocol; therefore, the OFR could not be analysed in 17.3% of the lesions, which hampered a per-patient and intention-totreat analysis. The relatively high exclusion rate shows, in our opinion, that the quality of the image matters and supports the theory that there are optimal postures to expose lesions and improve measurement accuracy. Second, only patients with bifurcation lesions treated with the provisional approach were selected, which constituted a selection bias and did not allow for calculation of the real rate of SB μQFR <0.8 after both two- and one-stent techniques; however, this study aimed to analyse the impact of the SB µQFR on clinical outcomes for bifurcation lesions treated with provisional stenting only. Third, intravascular imaging was used in fewer than 35% of lesions. This may have increased the number of µQFR <0.89 in the MV and the likelihood of µOFR <0.8 in the SB. Therefore, translating our data into clinical practice should be done very cautiously. Fourth, as a post hoc analysis of µQFR measurements, patients with a reduced SB µQFR could not be randomly studied. Finally, the SB µQFR was not compared with pressure wire-based FFR. It is known that not only SB stenosis but also bifurcation angles and the amount of myocardium subtended contribute to FFR values in the SB. Therefore. further elaboration on the potential impact of these factors on the SB μOFR would be of interest. But our finding has linked the SB μOFR to clinical outcomes, which means the SB µQFR is clinically relevant. Altogether, further study is required to analyse the accuracy of the SB µQFR and to compare the treatment effects of two-stent vs one-stent techniques for an SB μQFR <0.8 after stenting the MV.

Conclusions

The μQFR can be reliably measured in most patients with coronary bifurcation lesions. An SB μQFR <0.8 is strongly correlated with clinical events.

Impact on daily practice

In coronary bifurcations, the novel μQFR derived from a single angiographic projection has an acceptable performance as compared to wire-based FFR. However, the relationship between the side branch (SB) μQFR and clinical outcomes after provisional stenting is unclear. In this study, we found a strong correlation between an SB μQFR <0.8 and target vessel failure within one year of MV stenting procedures. SB lesion length plays an important role in predicting the SB μQFR and clinical events after stenting the MV. The μQFR should be routinely measured and used to guide the necessity of SB treatment.

Acknowledgements

We deeply acknowledge Dr Bao-Xiang Duan (Chair) as the director of the independent committee. We thank Ms Ling Lin and Ms Hai-Mei Xu for their contributions to the completion of this study. Moreover, we appreciate Ms Lingling Liu, Ms Rong-Fang Wang, Ms Wen Teng, and Ms Yingying Zhao for remote monitoring and data collection throughout the study. We also appreciate the support of the Cooperative Innovational Center of Nanjing Medical University throughout the study.

Funding

The trial was funded by a grant from the National Science Foundation of China (Funding no.: NSFC 91639303, NSFC 81770441), Jiangsu Provincial Special Program of Medical Science, and jointly supported by the Nanjing Municipal Medical Development Project.

Conflict of interest statement

The authors have no conflicts of interest to declare.

References

- 1. Raphael CE, O'Kane PD. Contemporary approaches to bifurcation stenting. *JRSM Cardiovasc Dis.* 2021:10:2048004021992190.
- 2. Zhang JJ, Ye F, Xu K, Kan J, Tao L, Santoso T, Munawar M, Tresukosol D, Li L, Sheiban I, Li F, Tian NL, Rodríguez AE, Paiboon C, Lavarra F, Lu S, Vichairuangthum K, Zeng H, Chen L, Zhang R, Ding S, Gao F, Jin Z, Hong L, Ma L, Wen S, Wu X, Yang S, Yin WH, Zhang J, Wang Y, Zheng Y, Zhou L, Zhou L, Zhu Y, Xu T, Wang X, Qu H, Tian Y, Lin S, Liu L, Lu Q, Li Q, Li B, Jiang Q, Han L, Gan G, Yu M, Pan D, Shang Z, Zhao Y, Liu Z, Yuan Y, Chen C, Stone GW, Han Y, Chen SL. Multicentre, randomized comparison of two-stent and provisional stenting techniques in patients with complex coronary bifurcation lesions: the DEFINITION II trial. *Eur Heart J.* 2020;41: 2523-36.
- 3. Pijls NH, Fearon WF, Tonino PA, Siebert U, Ikeno F, Bornschein B, van't Veer M, Klauss V, Manoharan G, Engstrøm T, Oldroyd KG, Ver Lee PN, MacCarthy PA, De Bruyne B; FAME Study Investigators. Fractional flow reserve versus angiography for guiding percutaneous coronary intervention in patients with multivessel coronary artery disease: 2-year follow-up of the FAME (Fractional Flow Reserve Versus Angiography for Multivessel Evaluation) study. *J Am Coll Cardiol*. 2010;56: 177-84.
- 4. Lee JM, Hwang D, Choi KH, Lee HJ, Song YB, Cho YK, Nam CW, Hahn JY, Shin ES, Doh JH, Hoshino M, Hamaya R, Kanaji Y, Murai T, Zhang JJ, Ye F, Li X, Ge Z, Chen SL, Kakuta T, Koo BK. Prognostic Impact of Residual Anatomic Disease Burden After Functionally Complete Revascularization. *Circ Cardiovasc Interv.* 2020;13:e009232.
- 5. Chen SL, Ye F, Zhang JJ, Xu T, Tian NL, Liu ZZ, Lin S, Shan SJ, Ge Z, You W, Liu YQ, Qian XS, Li F, Yang S, Kwan TW, Xu B, Stone GW. Randomized Comparison of FFR-Guided and Angiography-Guided Provisional Stenting of True Coronary Bifurcation Lesions: The DKCRUSH-VI Trial (Double Kissing Crush Versus Provisional Stenting Technique for Treatment of Coronary Bifurcation Lesions VI). *JACC Cardiovasc Interv.* 2015;8:536-46.
- 6. Tu S, Barbato E, Köszegi Z, Yang J, Sun Z, Holm NR, Tar B, Li Y, Rusinaru D, Wijns W, Reiber JH. Fractional flow reserve calculation from 3-Dimensional quantitative coronary angiography and TIMI frame count: A fast computer model to quantify the functional significance of moderately obstructed coronary arteries. *JACC Cardiovasc Interv.* 2014;7:768-77.
- 7. Kornowski R, Lavi I, Pellicano M, Xaplanteris P, Vaknin-Assa H, Assali A, Valtzer O, Lotringer Y, De Bruyne B. Fractional Flow Reserve Derived From Routine Coronary Angiograms. *J Am Coll Cardiol*. 2016;68:2235-7.
- 8. Tu S, Westra J, Yang J, von Birgelen C, Ferrara A, Pellicano M, Nef H, Tebaldi M, Murasato Y, Lansky A, Barbato E, van der Heijden LC, Reiber JHC, Holm NR, Wijns W; FAVOR Pilot Trial Study Group. Diagnostic Accuracy of Fast Computational Approaches to Derive Fractional Flow Reserve From Diagnostic Coronary Angiography: The International Multicenter FAVOR Pilot Study. *JACC Cardiovasc Interv.* 2016;9:2024-35.

- 9. Biscaglia S, Tebaldi M, Brugaletta S, Cerrato E, Erriquez A, Passarini G, Ielasi A, Spitaleri G, Di Girolamo D, Mezzapelle G, Geraci S, Manfrini M, Pavasini R, Barbato E, Campo G. Prognostic Value of QFR Measured Immediately After Successful Stent Implantation: The International Multicenter Prospective HAWKEYE Study. *JACC Cardiovasc Interv.* 2019;12:2079-88.
- 10. Westra J, Tu S, Winther S, Nissen L, Vestergaard MB, Andersen BK, Holck EN, Fox Maule C, Johansen JK, Andreasen LN, Simonsen JK, Zhang Y, Kristensen SD, Maeng M, Kaltoft A, Terkelsen CJ, Krusell LR, Jakobsen L, Reiber JHC, Lassen JF, Bøttcher M, Bøtker HE, Christiansen EH, Holm NR. Evaluation of Coronary Artery Stenosis by Quantitative Flow Ratio During Invasive Coronary Angiography: The WIFI II study (Wire-Free Functional Imaging II). *Circ Cardiovasc Imaging*. 2018;11:e007107.
- 11. Lee KY, Hwang BH, Kim MJ, Choo EH, Choi IJ, Kim CJ, Lee SW, Lee JM, Kim MJ, Jeon DS, Chung WS, Youn HJ, Kim KJ, Yoon MH, Chang K. Influence of lesion and disease subsets on the diagnostic performance of the quantitative flow ratio in real-world patients. *Sci Rep.* 2021;11:2995.
- 12. Westra J, Andersen BK, Campo G, Matsuo H, Koltowski L, Eftekhari A, Liu T, Di Serafino L, Di Girolamo D, Escaned J, Nef H, Naber C, Barbierato M, Tu S, Neghabat O, Madsen M, Tebaldi M, Tanigaki T, Kochman J, Somi S, Esposito G, Mercone G, Mejia-Renteria H, Ronco F, Bøtker HE, Wijns W, Christiansen EH, Holm NR. Diagnostic Performance of In-Procedure Angiography-Derived Quantitative Flow Reserve Compared to Pressure-Derived Fractional Flow Reserve: The FAVOR II Europe-Japan Study. *J Am Heart Assoc.* 2018;7:e009603.
- 13. Asano T, Katagiri Y, Chang CC, Kogame N, Chichareon P, Takahashi K, Modolo R, Tenekecioglu E, Collet C, Jonker H, Appleby C, Zaman A, van Mieghem N, Uren N, Zueco J, Piek JJ, Reiber JHC, Farooq V, Escaned J, Banning AP, Serruys PW, Onuma Y. Angiography-Derived Fractional Flow Reserve in the SYNTAX II Trial: Feasibility, Diagnostic Performance of Quantitative Flow Ratio and Clinical Prognostic Value of Functional SYNTAX Score Derived From Quantitative Flow Ratio in Patients With 3-Vessel Disease. *JACC Cardiovasc Interv.* 2019:12:259-70.
- 14. Tu S, Ding D, Chang Y, Li C, Wijns W, Xu B. Diagnostic accuracy of quantitative flow ratio for assessment of coronary stenosis significance from a single angiographic view: A novel method based on bifurcation fractal law. *Catheter Cardiovasc Interv.* 2021:97:1040-7.
- 15. Xu B, Tu S, Qiao S, Qu X, Chen Y, Yang J, Guo L, Sun Z, Li Z, Tian F, Fang W, Chen J, Li W, Guan C, Holm NR, Wijns W, Hu S. Diagnostic Accuracy of Angiography-Based Quantitative Flow Ratio Measurements for Online Assessment of Coronary Stenosis. *J Am Coll Cardiol.* 2017;70:3077-87.
- 16. Chen SL, Santoso T, Zhang JJ, Ye F, Xu YW, Fu Q, Kan J, Paiboon C, Zhou Y, Ding SQ, Kwan TW. A randomized clinical study comparing double kissing crush with provisional stenting for treatment of coronary bifurcation lesions: results from the DKCRUSH-II (Double Kissing Crush versus Provisional Stenting Technique for Treatment of Coronary Bifurcation Lesions) trial. *J Am Coll Cardiol*. 2011;57: 914-20
- 17. Chen SL, Zhang JJ, Han Y, Kan J, Chen L, Qiu C, Jiang T, Tao L, Zeng H, Li L, Xia Y, Gao C, Santoso T, Paiboon C, Wang Y, Kwan TW, Ye F, Tian N, Liu Z, Lin S, Lu C, Wen S, Hong L, Zhang Q, Sheiban I, Xu Y, Wang L, Rab TS, Li Z, Cheng G, Cui L, Leon MB, Stone GW. Double Kissing Crush Versus Provisional Stenting for Left Main Distal Bifurcation Lesions: DKCRUSH-V Randomized Trial. *J Am Coll Cardiol.* 2017;70:2605-17.
- 18. Mauri L, Hsieh WH, Massaro JM, Ho KK, D'Agostino R, Cutlip DE. Stent thrombosis in randomized clinical trials of drug-eluting stents. *N Engl J Med.* 2007;356: 1020–9
- 19. Cortés C, Carrasco-Moraleja M, Aparisi A, Rodriguez-Gabella T, Campo A, Gutiérrez H, Julca F, Gómez I, San Román JA, Amat-Santos IJ. Quantitative flow ratio-Meta-analysis and systematic review. *Catheter Cardiovasc Interv.* 2021;97: 807-14
- 20. Tu S, Echavarria-Pinto M, von Birgelen C, Holm NR, Pyxaras SA, Kumsars I, Lam MK, Valkenburg I, Toth GG, Li Y, Escaned J, Wijns W, Reiber JH. Fractional flow reserve and coronary bifurcation anatomy: a novel quantitative model to assess and report the stenosis severity of bifurcation lesions. *JACC Cardiovasc Interv.* 2015:8:564-74.
- 21. Koo BK, Park KW, Kang HJ, Cho YS, Chung WY, Youn TJ, Chae IH, Choi DJ, Tahk SJ, Oh BH, Park YB, Kim HS. Physiological evaluation of the provisional side-branch intervention strategy for bifurcation lesions using fractional flow reserve. *Eur Heart J.* 2008;29:726-32.
- 22. Li SJ, Ge Z, Kan J, Zhang JJ, Ye F, Kwan TW, Santoso T, Yang S, Sheiban I, Qian XS, Tian NL, Rab TS, Tao L, Chen SL. Cutoff Value and Long-Term Prediction of Clinical Events by FFR Measured Immediately After Implantation of a Drug-Eluting Stent in Patients with Coronary Artery Disease: 1- to 3-Year Results From the DKCRUSH VII Registry Study. *JACC Cardiovasc Interv.* 2017;10:986-95.

- 23. Koo BK, Waseda K, Kang HJ, Kim HS, Nam CW, Hur SH, Kim JS, Choi D, Jang Y, Hahn JY, Gwon HC, Yoon MH, Tahk SJ, Chung WY, Cho YS, Choi DJ, Hasegawa T, Kataoka T, Oh SJ, Honda Y, Fitzgerald PJ, Fearon WF. Anatomic and functional evaluation of bifurcation lesions undergoing percutaneous coronary intervention. *Circ Cardiovasc Interv.* 2010;3:113-9.
- 24. Kumsars I, Narbute I, Thuesen L, Niemelä M, Steigen TK, Kervinen K, Sondore D, Holm NR, Lassen JF, Christiansen EH, Maeng M, Jegere S, Juhnevica D, Erglis A; Nordic-Baltic PCI study group. Nordic-Baltic PCI study group. SB fractional flow reserve measurements after main vessel stenting: a Nordic-Baltic Bifurcation Study III substudy. *EuroIntervention*. 2012;7:1155-61.
- 25. Chen SL, Sheiban I, Xu B, Jepson N, Paiboon C, Zhang JJ, Ye F, Sansoto T, Kwan TW, Lee M, Han YL, Lv SZ, Wen SY, Zhang Q, Wang HC, Jiang TM, Wang Y, Chen LL, Tian NL, Cao F, Qiu CG, Zhang YJ, Leon MB. Impact of the complexity of bifurcation lesions treated with drug-eluting stents: the DEFINITION study

(Definitions and impact of complEx biFurcation lesIons on clinical outcomes after percutaNeous coronary IntervenTIOn using drug-eluting steNts). *JACC Cardiovasc Interv.* 2014;7:1266-76.

Supplementary data

Supplementary Table 1. Excluded cases.

The supplementary data are published online at: https://www.asiaintervention.org/doi/10.4244/AIJ-D-22-00045



Impact of real-time optical coherence tomography and angiographic coregistration on the percutaneous coronary intervention strategy



Rony Mathew Kadavil^{1*}, MD, DM, DNB; Jabir Abdullakutty¹, MD, DM; Tejas Patel², MD, DM; Sivakumar Rathnavel³, MD, DNB; Balbir Singh⁴, MD, DM; Nagendra Singh Chouhan⁴, MD, DNB; Fazila Tun Nesa Malik⁵, MBBS, FCPS(BD), MRCP (UK); Shirish Hiremath⁶, MD, DM; Sengottuvelu Gunasekaran⁷, MD, DM, DNB; Samuel Mathew Kalarickal⁸, MD, DM; Viyeka Kumar⁹, MD, DM; Vijayakumar Subban¹⁰, MD, DM, FNB

1. Lisie Heart Institute, Lisie Hospital, Ernakulum, India; 2. APEX Heart Institute, Ahmedabad, India; 3. Department of Cardiology, Meenakshi Mission Hospital and Research Centre, Madurai, India; 4. Department of Interventional Cardiology, Medanta-Heart Institute, New Delhi, India; 5. Department of Cardiology, National Heart Foundation Hospital & Research Institute, Dhaka, Bangladesh; 6. Department of Cardiology, Ruby Hall Clinic, Pune, India; 7. Department of Cardiology, Apollo Hospitals, Chennai, India; 8. Department of Cardiology, Lilavati Hospital & Research Centre, Mumbai, India; 9. Department of Cardiology, Max Super Speciality Hospital, Saket, India; 10. Indian Cardiology Research Foundation Core Lab, Chennai, India

This paper also includes supplementary data published online at: https://www.asiaintervention.org/doi/10.4244/AIJ-D-22-00064

KEYWORDS

- ACS/NSTE-ACS
- optical coherence tomography
- other imaging modalities

Abstract

Background: The use of optical coherence tomography (OCT) with angiographic coregistration (ACR) during percutaneous coronary intervention (PCI) for procedural decision-making is evolving; however, large-scale data in real-world practice are lacking.

Aims: Our study aims to evaluate the real-time impact of OCT-ACR on clinician decision-making during PCI

Methods: Patients with angiographic diameter stenosis >70% in at least one native coronary artery were enrolled in the study. The pre- and post-PCI procedural strategies were prospectively assessed after angiography, OCT, and ACR.

Results: A total of 500 patients were enrolled in the study between November 2018 and March 2020. Among these, data related to 472 patients with 483 lesions were considered for analysis. Preprocedural OCT resulted in a change in PCI strategy in 80% of lesions: lesion preparation (25%), stent length (53%), stent diameter (36%), and device landing zone (61%). ACR additionally impacted the treatment strategy in 34% of lesions. Postprocedural OCT demonstrated underexpansion (15%), malapposition (14%), and tissue/thrombus prolapse (7%), thereby requiring further interventions in 30% of lesions. No further change in strategy was observed with subsequent postprocedural ACR. Angiographic and procedural success was achieved in 100% of patients, and the overall incidence of major adverse cardiovascular events at 1 year was 0.85%.

Conclusions: The outcomes reflect the real-time impact of OCT-ACR on the overall procedural strategy in patients undergoing PCI. ACR had a significant impact on the treatment strategy and was associated with better clinical outcomes at 1 year after index PCI. OCT-ACR has become a practical tool for improving outcomes in patients with complex lesions.

^{*}Corresponding author: Head of Department, Cardiology, Lisie Heart Institute, Lisie Hospital Rd, North Kaloor, Kaloor, Kochi 682018, Kerala, India. E-mail: drronymathew@yahoo.com

Abbreviations

ACR angiographic coregistration AHA American Heart Association CA

coronary angiography

MACE major adverse cardiovascular events OCT optical coherence tomography PCI percutaneous coronary intervention TLR target lesion revascularisation

TIMI Thrombolysis in Myocardial Infarction

Introduction

Coronary angiography (CA) is routinely used to assess the extent and degree of coronary artery disease (CAD) and guide percutaneous coronary intervention (PCI). However, CA only provides a twodimensional luminogram and has inherent limitations in evaluating the vessel wall pathology and lumen stenosis¹, which makes it inadequate for strategising PCI procedures with precision. A growing body of evidence suggests that intracoronary imaging, especially intravascular ultrasound (IVUS) and optical coherence tomography (OCT), is superior to CA in guiding PCI²⁻⁴. Three-dimensional OCT imaging, with its higher spatial resolution, provides unique insights into plaque morphology and procedure-related complications and is more valuable in managing complex lesion subsets, such as acute coronary syndrome (ACS), bifurcation, and calcified lesions⁴⁻⁶.

Angiographic coregistration (ACR; the OPTIS integrated system [OPTISi; Abbott]) is a new technology that facilitates real-time coregistration of OCT images with the angiogram in the catheterisation laboratory7. This enables a matched side-by-side view of OCT and angiography, eliminates the need for the currently used stand-alone, mobile OCT carts, and provides accurate OCT measurements, which might improve short- and long-term clinical outcomes post-PCI^{7,8}. The OPTISi system is being increasingly used in busy catheterisation laboratories in South Asia. However, clinical outcomes in such settings are sparsely reported. The present study evaluated the impact of real-time OCT and ACR on physician decision-making in a real-world scenario. The outcomes of the study could further help PCI optimisation in South Asia.

Editorial, see page 101

Methods

STUDY DESIGN AND POPULATION

This was a multicentre, prospective, investigator-initiated, non-randomised, observational study conducted between November 2018 and March 2020 across nine centres in South Asia. Consecutive patients scheduled for OCT-guided PCI who met the inclusion criteria and were willing to participate in the study were enrolled. The detailed protocol and patient flow are provided in Supplementary Appendix 1 and Supplementary Figure 1, respectively. The study enrolled adults (aged ≥18 years) with angiographic diameter stenosis >70% in at least one native coronary artery. Patients with extreme angulation (>90°) or excessive vessel tortuosity, renal insufficiency (estimated glomerular filtration rate <50 mL/min/1.73 m²) or any other severe medical condition interfering with patients' safety or study results, contraindications to dual antiplatelet therapy up to 1 year, and life expectancy of less than 1 year were excluded from the study.

PROCEDURES

The study was initiated after obtaining ethical committee approvals at the respective institutes. Angiographic lesion complexity was classified according to the American Heart Association (AHA) consensus statement. The patients underwent conventional angiography followed by preprocedural OCT imaging and ACR. All study procedures were carried out using intracoronary OCT imaging by clinicians experienced in PCI. OCT was performed with a Dragonfly OPTIS imaging catheter (Abbott). The OCT catheter was introduced using a standard 0.014 inch guidewire, and image acquisition was done after the administration of intracoronary nitrates (100 µg). Blood was cleared from the vessel by injecting contrast medium, either manually or using an automated power injector. OCT was performed at a frame rate of 180 frames/second and with a frame density of 5 frames/mm. Real-time ACR (semiautomatic) was performed with the OPTIS integrated system to coregister the angiogram recorded during the OCT pullback with the OCT image⁷. The pre- and post-PCI procedural strategies were prospectively assessed following angiography, OCT and ACR. The interventional strategy, defined by the clinician, was recorded by an independent research assistant in real time following (a) CA, (b) OCT imaging and (c) ACR. As the OCT console is usually equipped to provide the ACR details after performing OCT, the investigator was blinded to the ACR details until the OCT-only-based strategy had been documented. The following preprocedural variables were collected as a part of the clinician's interventional strategy: need for predilatation, intended need for lesion debulking by means of scoring/cutting balloons and rotablation, vessel reference diameter, intended stent length and diameter, device landing zone, and stenting strategy (i.e., 1- vs 2-stent strategy). After documentation of the preprocedural variables, PCI was performed by the clinician according to standard techniques and current guidelines. Post-PCI OCT imaging was performed with ACR.

The need for further optimisation was based on the following variables: stent underexpansion, malapposition, geographic miss, edge dissection, and tissue prolapse. All the angiographic and OCT images were independently reviewed at the designated core lab (Indian Cardiology Research Foundation). During the study, the core lab trained all sites on image capturing, the transfer of images for assessment and also provided real-time feedback to sites. Data related to study enrolment and follow-up are summarised in Figure 1A and **Figure 1B**. Overall, 28 patients were excluded because of inadequate OCT image quality for analysis. All enrolled patients were followed up, either telephonically or clinically, at 6 months and 1 year. Details about the patient's well-being and any hospitalisation/revascularisation after the initial PCI were recorded at follow-up.

ENDPOINTS

The primary endpoint was a change in the procedural strategy pre- and post-PCI with ACR. Pre-PCI strategy change involved

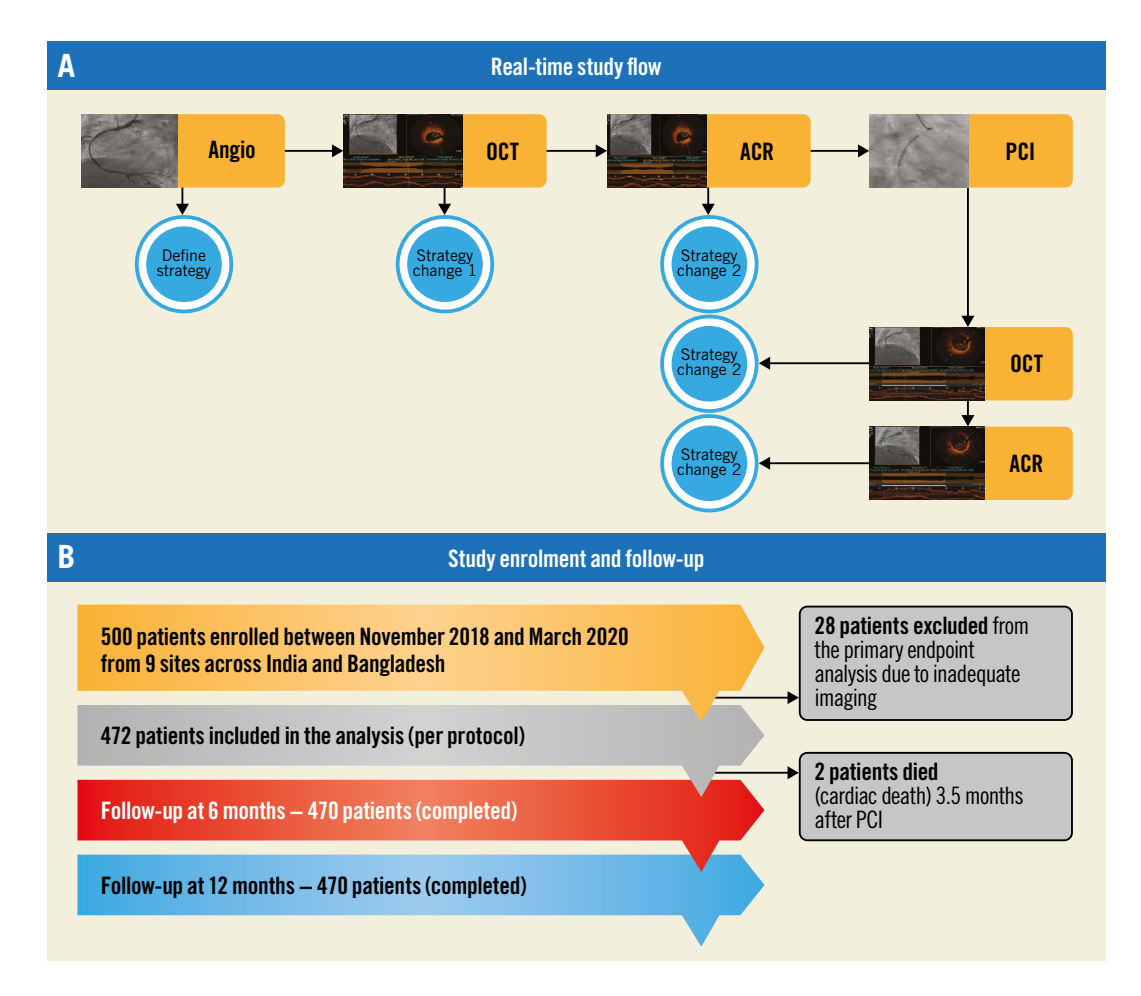


Figure 1. Study flow, enrolment and follow-up. A) Study flowchart. B) Study enrolment and follow-up. ACR: angiographic coregistration; OCT: optical coherence tomography; PCI: percutaneous coronary intervention

the need to change the intended stent length and size, stenting strategy, and/or intended device landing zone. Post-PCI strategy change involved the need for additional interventional procedures for PCI optimisation after identification of stent underexpansion, malapposition, geographic miss, edge dissections and/or tissue prolapse.

The secondary endpoints included (a) procedural outcomes with ACR-guided PCI in the entire study population; (b) the rate of major adverse cardiovascular events (MACE; composite of cardiac death, myocardial infarction [MI], and target lesion revascularisation [TLR]) at 6 months and 1 year with ACR-guided PCI; (c) total change in the procedural strategy pre-PCI with OCT imaging versus angiography; and (d) time to conduct OCT and ACR (pre- and post-PCI) and contrast volume used.

DEFINITIONS

Optimal stent expansion was defined as a minimum stent area >80% of the average reference lumen area. Significant stent malapposition was defined as a strut-to-vessel wall distance of $\geq\!400~\mu m$ extending for $\geq\!1$ mm (measured from the endoluminal strut surface to the lumen contour)¹. Significant edge dissection was defined as a flap meeting either one or more of the following

criteria: involving >60° of the vessel circumference, >2 mm in longitudinal extension, and the involvement of media or deeper layers¹. Significant tissue protrusion was defined as intrastent tissue protrusion/thrombus reducing the residual lumen area to <4 mm² or a reduction in the flow area of >20%9. Angiographic success was defined as <30% residual stenosis and Thrombolysis in Myocardial Infarction (TIMI) grade 3 flow. Procedural success was defined as angiographic success without major procedural or in-hospital complications (death, MI, emergent bypass surgery, or repeat PCI). All these events were adjudicated by the institutional review board.

STATISTICAL ANALYSES

No formal sample size was calculated as it was a single-arm, observational study. All the categorical variables are presented as numbers and percentages and continuous data as mean and standard deviation (SD).

Results

BASELINE CHARACTERISTICS

Between November 2018 and March 2020, a total of 500 patients with 511 lesions underwent PCI with OCT assessment. Of them,

472 patients (483 lesions), who had all parameters related to OCT data, were considered for the final analysis. The mean age of the study population (n=472) was 57.8±10.4 years, and 16.6% were females. The major coronary risk factors were systemic hypertension (58%) and diabetes mellitus (52%). About two-thirds of patients presented with ACS. Baseline clinical characteristics are summarised in **Table 1**.

Table 1. Baseline characteristics.

Demographics	Patients (n=472)
Age, years (mean±SD)	57.8±10.49
Female	78 (16.6)
Male	394 (83.4)
Medical history	
DM	245 (52.1)
Dyslipidaemia	55 (11.7)
Hypertension	274 (58.1)
FH CAD	108 (22.9)
Previous PCI	83 (17.6)
Previous CABG	22 (4.7)
Previous MI	33 (7.0)
HF	10 (2.1)
Smoking	42 (9.0)
Alcohol	36 (7.4)
Renal disease	7 (1.5)
Bronchial asthma	8 (1.7)
Indication for PCI	
Unstable angina	117 (24.8)
Recent STEMI	95 (20.0)
Stable angina	83 (17.6)
NSTEMI	76 (16.1)
Asymptomatic positive stress test	37 (7.4)
Others	64 (13.7)

All data are presented as n (%) unless otherwise indicated. CABG: coronary artery bypass grafting; CAD: coronary artery disease; DM: diabetes mellitus; FH: familial hypercholesterolaemia; HF: heart failure; MI: myocardial infarction; NSTEMI: non-ST-segment elevation myocardial infarction; PCI: percutaneous coronary intervention; SD: standard deviation; STEMI: ST-segment elevation myocardial infarction

LESION CHARACTERISTICS AND PROCEDURAL DETAILS

Table 2 summarises the baseline vessel/lesion characteristics and procedural details. The majority of the lesions were found in the left anterior descending coronary artery (62%). In terms of lesion characteristics, bifurcation lesions were the most common (14.3%), whereas moderate or severe calcification was observed in 11.6% of lesions. About 87% of lesions were classified as type B and type C lesions (American College of Cardiology/AHA classification).

PRE-PCI STRATEGY CHANGE

Preprocedural OCT resulted in a change in PCI strategy in 80% of lesions, which included the need for lesion preparation (25%)

Table 2. Lesion characteristics and procedural details.

	onaraotoriotico ana	procedurar as					
ι	esion characteristic	s (n=483 lesio	ns)				
Vessels treated	LAD	300	(62.1)				
	RCA	111	(22.7)				
	LCx	43	(8.9)				
	LM	25	(5.2)				
	RI	4 (0.8)					
Lesion	Ostial lesion	54	(11.2)				
characteristics	Thrombus	33	(6.8)				
	СТО	6	(1.2)				
	Bifurcation lesion	69	(14.3)				
	Calcification	232	2 (48)				
	Mild	171	(35.4)				
	Moderate	34 (7.0)					
	Severe	27 (5.6)					
Lesion length, mm	(mean±SD)	25.5±12.0					
Long lesions (>20	mm)	288 (60.0)					
Preprocedure diam (mean±SD)	eter stenosis, %	85.0±8.1					
ACC/AHA	A	62 (12.8)					
classification	B1	191	(39.5)				
	B2	108	(22.4)				
	С	122	(25.3)				
TIMI flow	1	34	(7.0)				
	2	186	(38.5)				
	3	263 (54.5)					
Time taken for (OCT and ACR	Preprocedure	Post-procedure				
OCT image acquis	ition, mins (mean±SD)	6.6±4.0	10.7±1.1				
Assessment of OC	T, mins (mean±SD)	3.6±2.2	8.3±1.1				
Assessment of ACI	R, mins (mean±SD)	3.9±2.3	7.3±0.9				

All data are presented as n (%) unless otherwise indicated. ACC/AHA: American College of Cardiology/American Heart Association; ACR: angiography coregistration; CTO: chronic total occlusion; LAD: left anterior descending artery; LCx: left circumflex; LM: left main; OCT: optimal coherence tomography; RCA: right coronary artery; RI: ramus intermedius; SD: standard deviation; TIMI: Thrombolysis in Myocardial Infarction

and change in stent length (53%), stent diameter (36%), stenting strategy (3%) and device landing zone (61%). The subsequent use of ACR further altered the treatment strategy in 34% of lesions, which included the need for lesion preparation (15%) and change in stent length (10%), stent diameter (5%) and device landing zone (16%) (Figure 2A, Figure 2B). Overall, preprocedural ACR with OCT resulted in a strategy change in 86% of lesions. The mean (±SD) stent lengths as assessed by CA, OCT and ACR were 29.6 ± 12.2 mm, 32.5 ± 13.3 mm and 33.0 ± 13.4 mm, respectively. The mean (±SD) stent diameters as assessed by CA, OCT and ACR were 2.95±0.43 mm, 3.00±0.45 mm and 3.00±0.45 mm, respectively. The differences in the mean stent length were statistically significant when CA versus OCT (p<0.0001), CA versus ACR (p<0.0001) and OCT versus ACR (p=0.0006) were compared. The differences in the mean stent diameter were statistically significant when CA versus OCT (p=0.0004) and CA versus ACR (p=0.0003) were compared.

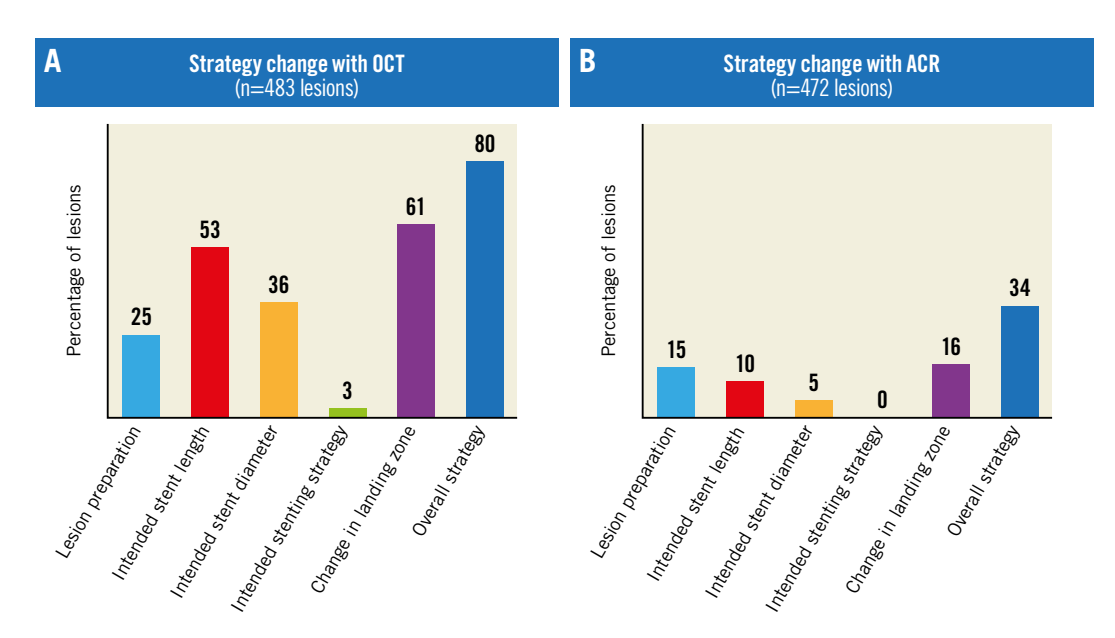


Figure 2. Strategy changes with OCT and ACR. A) Change in strategy with OCT (n=483 lesions). B) Change in strategy with ACR (n=472 lesions). ACR: angiographic coregistration; OCT: optical coherence tomography

Further, the need for debulking was evident in a higher number of cases following OCT-ACR (8.5%) compared to CA (5.4%). An overall strategy change was noted in 17 (3.5%) cases following OCT-ACR; debulking was carried out by means of scoring/cutting and/or rotablation in these cases.

POST-PCI STRATEGY CHANGE

Postprocedural OCT demonstrated edge dissections (3%), underexpansion (15%), malapposition (14%), and tissue/thrombus prolapse (7%), which required additional interventions (ballooning/stenting) in 30% of lesions (**Figure 3**). The addition of ACR to OCT did not result in any further strategy change post-PCI. Thus, postprocedural ACR with OCT resulted in an overall strategy change in 30% of lesions.

OVERALL STRATEGY CHANGE

Pre- and postprocedural ACR with OCT was associated with an overall strategy change in 89% of the lesions (Central illustration).

SECONDARY OUTCOMES

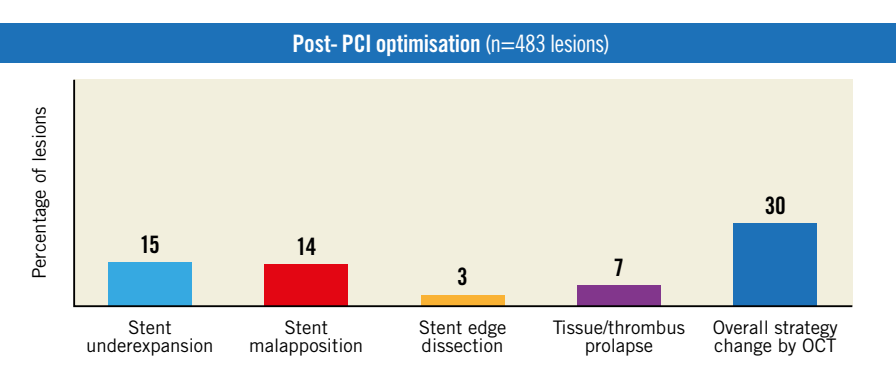
Angiographic and procedural success was achieved in 100% of patients. One-year follow-up data for 470 patients were available. The incidence of MACE at 1 year was 0.85% (including cardiac death in two patients [0.4%], MI in one patient [0.2%], and TLR in one patient [0.2%]). The adverse events that resulted in hospitalisation are provided in **Supplementary Table 1**. The total amount of contrast used for the procedure was 210.0±106.6 mL, which included 41.6±20.1 mL for OCT and ACR. The time taken for OCT and ACR is summarised in **Table 2**.

Discussion

Detailed characterisation of the lesion morphology and accurate vessel sizing with OCT can improve procedural outcomes. While pre-PCI OCT can guide the procedural strategy, post-PCI OCT assists in detecting suboptimal stent deployment, which may not be detected by angiography⁹. ACR along with OCT can further improve PCI outcomes, and the feasibility of coregistration of OCT with angiography during PCI has been established in earlier studies^{7,8}.

The OPTICO-Integration study was one of the first studies in the South East Asia region that evaluated OCT guidance with real-time ACR in a cohort of 50 patients and reported that OCT plus ACR improves PCI results. Notably, preprocedural OCT imaging altered the PCI strategy in 71% of lesions in the OPTICO-Integration study. Moreover, the use of ACR led to changes in PCI strategy in 40.7% of lesions¹⁰. The current multicentre, prospective iOPTICO study was performed in a similar real-world setting with a larger sample size (500 patients). Pre-PCI OCT was associated with a change in PCI strategy in 80% of lesions, and the addition of real-time ACR to OCT led to a strategy change in 34% of lesions. Optimisation was required in 30% of lesions when OCT was performed post-PCI.

The use of ACR facilitates the localisation of OCT morphology accurately on the angiogram monitor. This, in turn, enables precise identification of the landing zones when there are no angiographic markers, such as side branches, especially when the disease is diffuse, in which case landing zones with lipid-rich plaque and fibrous plaque appear similar on the angiogram. A previous study has shown a significant reduction in edge restenosis when appropriate landing zones were identified with OCT¹¹. In particular, stent length and stent diameter can be more accurately assessed with OCT and ACR compared to CA. A significant difference was noted in the current study when the stent length and diameter values assessed with CA were compared with OCT and ACR. Accordingly, accurate identification of the landing zone following



The addition of ACR to OCT did not result in any further strategy change post-PCI.

Figure 3. Post-PCI strategy change (OCT; n=483 lesions). ACR: angiographic coregistration; OCT: optical coherence tomography; PCI: percutaneous coronary intervention

ACR in the current study led to a strategy change in over 50% of lesions, including a change in the stent length and stent diameter and further lesion preparation.

OCT after PCI also helps to identify markers of suboptimal stent deployment that are not apparent on the angiogram. In the CLI-OPCI study¹², OCT helped detect edge dissection, lumen narrowing, stent malapposition, stent underexpansion and thrombi, which could not be detected in the angio group in 34.7% of cases. Similarly, in the ILUMIEN II trial¹³, edge dissection, malapposition and underexpansion were observed post-PCI, which led to further optimisation in 25% of patients. According to the ILUMIEN III: OPTIMIZE PCI study¹⁴, better resolution of OCT helped detect more stent malapposition and edge dissections, compared to IVUS or angiography. Similarly, the DOCTORS¹⁵ and OCTACS¹⁶ trials also reported a higher incidence of post-stent optimisation procedures, such as post-dilatation and additional stent implantations with OCT-guided PCI versus angiography-guided PCI. In the OPTICO-Integration study¹⁰, postprocedural OCT led to PCI optimisation in 52% of cases, which predominantly included stent malapposition and stent underexpansion. Similarly, in the present study, post-PCI optimisation was required in 30% of lesions, owing to stent malapposition, underexpansion, edge dissection and tissue prolapse.

In the OPTICO-Integration study¹⁰, postprocedural ACR did not have any further impact on the PCI strategy. Similarly, in the present study, the addition of ACR to OCT did not yield any additional changes in the post-PCI strategy. The presence of a stent with apposition and expansion indicators from the OCT pullback itself serves as a roadmap for the physician; hence, ACR did not likely influence post-PCI optimisation.

New insights from the LightLab initiative were presented recently. According to the outcomes reported, CA guidance was associated with inaccurate stent diameter assessment in 38% of the lesions (https://www.cardiovascular.abbott/content/dam/bss/divisionalsites/cv/pdf/reports/Abbott-LightLab-ePCR-Presentation. pdf. [Last accessed 04 March 2023]).

Lesion characteristics in the current study were similar to those reported in the LightLab initiative, with the majority of the lesions noted in the left anterior descending artery. The cumulative impact of OCT in the LightLab initative was a change in PCI strategy in 88% of lesions, which was similar to the strategy change observed in the present study. Further, while pre-PCI OCT led to a strategy change in 83% of lesions, post-PCI OCT resulted in a PCI strategy change in 31% of lesions in the LightLab study (https://www.cardiovascular.abbott/content/dam/bss/divisionalsites/cv/pdf/reports/Abbott-LightLab-ePCR-Presentation.pdf. [Last accessed 04 March 2023]). The corresponding figures in the present study were also similar (86% and 30%, respectively).

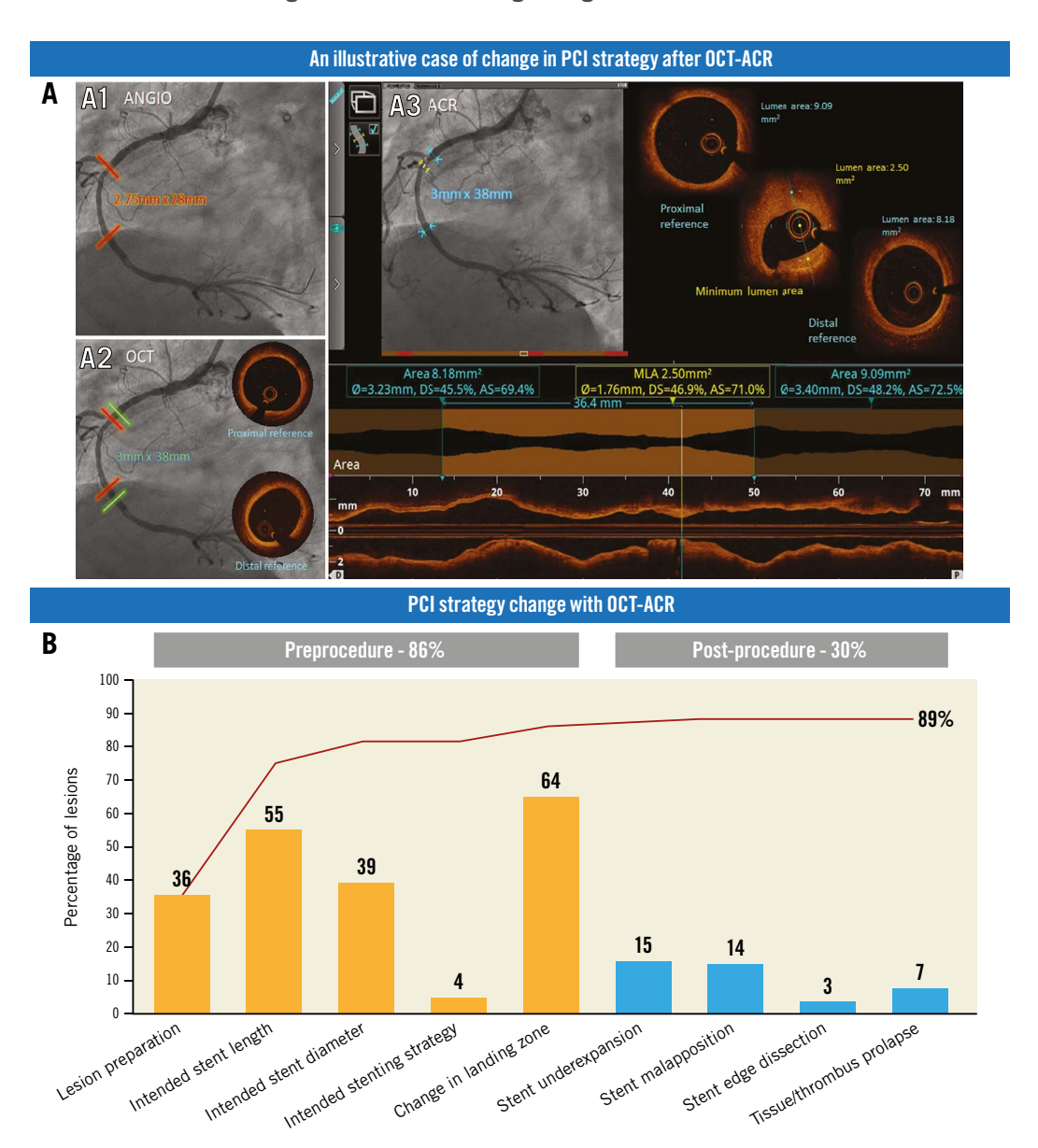
The average time taken in the present study for OCT imaging was 29 minutes, which was considerably lower compared to contemporary studies, such as the DOCTORS Study (56 mins)¹⁷ and the OPTICO-integration II Study (40 mins)¹⁸. The total amount of contrast used (210.0±106.6 mL) was comparable to amount used in the OPTICO-integration II Study (200 mL)¹⁸ and the DOCTORS Study (190 mL)¹⁷.

PCI optimisation following the use of OCT improves clinical outcomes in patients undergoing PCI19,20. In the Pan-London PCI cohort study, OCT-guided PCI was associated with better procedural success rates and reduced in-hospital MACE, which translated into a reduction in mortality at 4.8-year follow-up¹⁹. Moreover, mortality was significantly lower in the CA plus OCTguided group versus the CA group (hazard ratio [HR] 0.39, 95% confidence interval [CI]: 0.21-0.77; p=0.0008) and similar to the CA plus IVUS-guided group (HR 0.88, 95% CI: 0.61-1.38; p=0.43)¹⁹. The CLI-OPCI registry also observed an 8.3% reduction in the composite of cardiac death, MI, or repeat revascularisation at 1 year when OCT guidance was used for PCI²⁰. In the present study, 100% procedural and angiographic success was achieved with no in-hospital MACE. Further, the procedural strategy with OCT- and ACR-guided PCI translated into better clinical outcomes at 12 months, with the overall incidence of MACE being <1%.

The outcomes related to the use of drug-eluting stents (DES) in the present study can be compared with those of two real-world studies, involving patients with complex lesions, conducted in India and the USA (XIENCE V [XV] India²¹ and XV USA²²).

AsiaIntervention

CENTRAL ILLUSTRATION OCT-ACR guided decision-making during PCI.



A) An illustrative case of change in PCI strategy after OCT-ACR. A1, A2, and A3 show stent length, diameter and landing zone based on angiogram, OCT and OCT-ACR, respectively. B) PCI strategy change with OCT-ACR. ACR: angiographic coregistration; OCT: optical coherence tomography; PCI: percutaneous coronary intervention

The placement of DES in these two studies was based on findings noted on CA. The XV India and XV USA studies reported a 1-year MACE rate of 5% and 6.9%, respectively, following DES implantation. Notably, the rates of death and TLR were significantly lower in the present study compared to the XV USA study (p=0.0401 and p<0.0001, respectively), and the incidence of MI was significantly lower in the present study compared to both the XV USA and XV India studies (p=0.0421 and p<0.0001, respectively) (Figure 4)^{21,22}. The low incidence of MACE seen in the current study could be attributed to the use of OCT and ACR, which resulted in stent optimisation and, consequently, better 1-year outcomes.

Notably, the use of ACR with OCT is currently not limited to clinical research and is being increasingly preferred as an option in the busy catheterisation laboratories (despite the additional time required) owing to improved MACE rates. The current study reflects the actual benefits noted in a real-world scenario, especially in patients with complex lesions. The improved outcomes noted in the study may be attributed to better characterisation of the lesion morphology, accurate vessel sizing, and optimal strategy change following pre- and postprocedural OCT with ACR (including change in the stent length and stent diameter and additional lesion preparation).

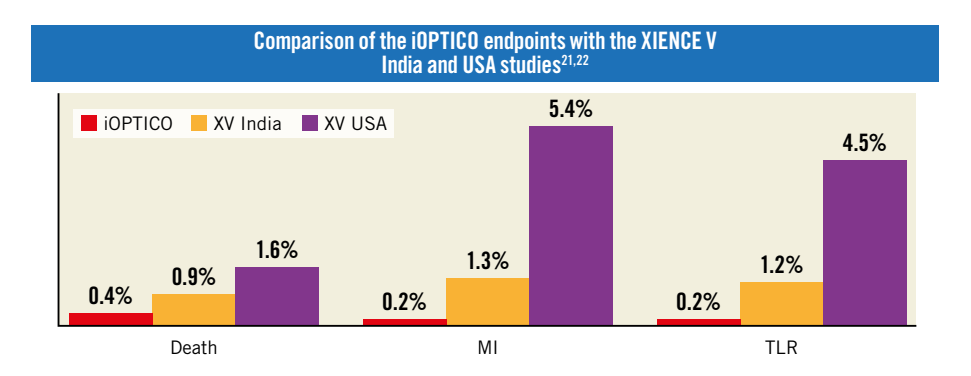


Figure 4. Comparison of the iOPTICO endpoints with the XV India and XV USA studies. MI: myocardial infarction; TLR: target lesion revascularisation

Limitations

The present study is limited by its observational and non-randomised design. There is a possibility of "operator bias" as the operators were not blinded to the study. Nevertheless, the iOP-TICO study reiterates the findings reported in other studies, albeit in a real-world scenario with a larger sample size. OCT with ACR was associated with a higher percentage of change in PCI strategy compared to earlier studies, suggesting a potential improvement in the technology. Notably, the overall incidence of MACE was <1%, which supports the belief that better procedural strategy with OCT-and ACR-guided PCI translates into improved clinical outcomes.

Conclusions

The study reflects the real-time benefits of ACR with OCT in patients undergoing PCI. The use of OCT resulted in a significant change in the overall preprocedural strategy, while real-time ACR had an additional significant impact on the treatment strategy with good long-term outcomes at 1 year after the index PCI.

Impact on daily practice

Intracoronary imaging with OCT ushers in a precision era of PCI planning and optimisation by providing enhanced visualisation and high-resolution imaging of the coronary artery. The current iOPTICO study hypothesised that the utility of OCT along with ACR will considerably impact the clinician's decision-making and overall procedural strategy compared to angiography. Preprocedural OCT resulted in a change in PCI strategy in 80% of lesions, with an additional change in treatment strategy in 34% of lesions when ACR was used. Post-PCI, OCT helped identify a need for further PCI optimisation in 30% of lesions. The impact of OCT imaging on decision-making is pronounced, being additionally and incrementally beneficial when performed preprocedurally with ACR. Post-PCI, identifying the need for additional intervention with OCT helps in optimising stent implantation. Taken together, this results in better clinical outcomes at 1 year; hence, OCT with ACR may play an important role in decisionmaking during coronary interventions and may translate into best clinical practices, especially in complex coronary lesions.

Acknowledgements

The authors would like to thank all the study staff (co-investigators and research coordinators) for their support in executing the study, St. Jude Medical India Pvt. Ltd. (now Abbott) for the research grant, and BioQuest Solutions Pvt. Ltd. for supporting the execution of the study.

Funding

The study was funded by St. Jude Medical India Pvt. Ltd. (now Abbott). The funding agency had no role in the study design, execution, analysis, or interpretation of results.

Conflict of interest statement

The authors have no conflicts of interest to declare.

References

- 1. Räber L, Mintz GS, Koskinas KC, Johnson TW, Holm NR, Onuma Y, Radu MD, Joner M, Yu B, Jia H, Meneveau N, de la Torre Hernandez JM, Escaned J, Hill J, Prati F, Colombo A, di Mario C, Regar E, Capodanno D, Wijns W, Byrne RA, Guagliumi G; ESC Scientific Document Group. Clinical use of intracoronary imaging. Part 1: guidance and optimization of coronary interventions. An expert consensus document of the European Association of Percutaneous Cardiovascular Interventions. *Eur Heart J.* 2018;39:3281-300.
- 2. Buccheri S, Franchina G, Romano S, Puglisi S, Venuti G, D'Arrigo P, Francaviglia B, Scalia M, Condorelli A, Barbanti M, Capranzano P, Tamburino C, Capodanno D. Clinical Outcomes Following Intravascular Imaging-Guided Versus Coronary Angiography-Guided Percutaneous Coronary Intervention With Stent Implantation: A Systematic Review and Bayesian Network Meta-Analysis of 31 Studies and 17,882 Patients. JACC Cardiovasc Interv. 2017;10:2488-98.
- 3. Kuku KO, Ekanem E, Azizi V, Melaku G, Bui A, Meirovich YF, Dheendsa A, Beyene S, Hideo-Kajita A, Lipinski MJ, Waksman R, Garcia-Garcia HM. Optical coherence tomography-guided percutaneous coronary intervention compared with other imaging guidance: a meta-analysis. *Int J Cardiovasc Imaging*. 2018;34:503-13.
- 4. Prati F, Guagliumi G, Mintz GS, Costa M, Regar E, Akasaka T, Barlis P, Tearney GJ, Jang IK, Arbustini E, Bezerra HG, Ozaki Y, Bruining N, Dudek D, Radu M, Erglis A, Motreff P, Alfonso F, Toutouzas K, Gonzalo N, Tamburino C, Adriaenssens T, Pinto F, Serruys PW, Di Mario C; Expert's OCT Review Document. Expert review document part 2: methodology, terminology and clinical applications of optical coherence tomography for the assessment of interventional procedures. *Eur Heart J.* 2012;33: 2513-20.
- 5. Mintz GS, Guagliumi G. Intravascular imaging in coronary artery disease. *Lancet*. 2017;390:793-809.
- 6. Prati F, Regar E, Mintz GS, Arbustini E, Di Mario C, Jang IK, Akasaka T, Costa M, Guagliumi G, Grube E, Ozaki Y, Pinto F, Serruys PW; Expert's OCT Review Document. Expert review document on methodology, terminology, and clinical applications of optical coherence tomography: physical principles, methodology of image acquisition, and clinical application for assessment of coronary arteries and atherosclerosis. *Eur Heart J.* 2010;31:401-15.

- 7. van der Sijde JN, Guagliumi G, Sirbu V, Shimamura K, Borghesi M, Karanasos A, Regar E. The OPTIS Integrated System: real-time, co-registration of angiography and optical coherence tomography. *EuroIntervention*. 2016;12:855-60.
- 8. Camacho Freire SJ, León Jiménez J, Gómez Menchero AE, Roa Garrido J, Cardenal Piris R, Díaz Fernández JF. Utility of 3D-OCT Imaging With Angiographic Co-Registration in Acute Coronary Syndrome With Normal or Near-Normal Coronary Arteries. *J Invasive Cardiol.* 2017;29:E84-5.
- 9. Wijns W, Shite J, Jones MR, Lee SW, Price MJ, Fabbiocchi F, Barbato E, Akasaka T, Bezerra H, Holmes D. Optical coherence tomography imaging during percutaneous coronary intervention impacts physician decision-making: ILUMIEN I study. *Eur Heart J.* 2015;36:3346-55.
- 10. Leistner DM, Riedel M, Steinbeck L, Stähli BE, Fröhlich GM, Lauten A, Skurk C, Mochmann HC, Lübking L, Rauch-Kröhnert U, Schnabel RB, Westermann D, Blankenberg S, Landmesser U. Real-time optical coherence tomography coregistration with angiography in percutaneous coronary intervention-impact on physician decision-making: The OPTICO-integration study. *Catheter Cardiovasc Interv.* 2018;92:30-7.
- 11. Ino Y, Kubo T, Matsuo Y, Yamaguchi T, Shiono Y, Shimamura K, Katayama Y, Nakamura T, Aoki H, Taruya A, Nishiguchi T, Satogami K, Yamano T, Kameyama T, Orii M, Ota S, Kuroi A, Kitabata H, Tanaka A, Hozumi T, Akasaka T. Optical Coherence Tomography Predictors for Edge Restenosis After Everolimus-Eluting Stent Implantation. *Circ Cardiovasc Interv.* 2016;9:e004231.
- 12. Prati F, Di Vito L, Biondi-Zoccai G, Occhipinti M, La Manna A, Tamburino C, Burzotta F, Trani C, Porto I, Ramazzotti V, Imola F, Manzoli A, Materia L, Cremonesi A, Albertucci M. Angiography alone versus angiography plus optical coherence tomography to guide decision-making during percutaneous coronary intervention: the Centro per la Lotta contro l'Infarto-Optimisation of Percutaneous Coronary Intervention (CLI-OPCI) study. *EuroIntervention*. 2012;8:823-9.
- 13. Maehara A, Ben-Yehuda O, Ali Z, Wijns W, Bezerra HG, Shite J, Généreux P, Nichols M, Jenkins P, Witzenbichler B, Mintz GS, Stone GW. Comparison of Stent Expansion Guided by Optical Coherence Tomography Versus Intravascular Ultrasound: The ILUMIEN II Study (Observational Study of Optical Coherence Tomography [OCT] in Patients Undergoing Fractional Flow Reserve [FFR] and Percutaneous Coronary Intervention). *JACC Cardiovasc Interv.* 2015;8:1704-14.
- 14. Ali ZA, Maehara A, Généreux P, Shlofmitz RA, Fabbiocchi F, Nazif TM, Guagliumi G, Meraj PM, Alfonso F, Samady H, Akasaka T, Carlson EB, Leesar MA, Matsumura M, Ozan MO, Mintz GS, Ben-Yehuda O, Stone GW; ILUMIEN III: OPTIMIZE PCI Investigators. Optical coherence tomography compared with intravascular ultrasound and with angiography to guide coronary stent implantation (ILUMIEN III: OPTIMIZE PCI): a randomised controlled trial. *Lancet*. 2016;388:2618-28.
- 15. Hebsgaard L, Nielsen TM, Tu S, Krusell LR, Maeng M, Veien KT, Raungaard B, Terkelsen CJ, Kaltoft A, Reiber JH, Lassen JF, Christiansen EH, Holm NR. Co-registration of optical coherence tomography and X-ray angiography in percutaneous coronary intervention. the Does Optical Coherence Tomography Optimize Revascularization (DOCTOR) fusion study. *Int J Cardiol*. 2015;182:272-8
- 16. Antonsen L, Thayssen P, Maehara A, Hansen HS, Junker A, Veien KT, Hansen KN, Hougaard M, Mintz GS, Jensen LO. Optical Coherence Tomography Guided Percutaneous Coronary Intervention With Nobori Stent Implantation in Patients With

- Non-ST-Segment-Elevation Myocardial Infarction (OCTACS) Trial: Difference in Strut Coverage and Dynamic Malapposition Patterns at 6 Months. *Circ Cardiovasc Interv.* 2015:8:e002446.
- 17. Meneveau N, Souteyrand G, Motreff P, Caussin C, Amabile N, Ohlmann P, Morel O, Lefrançois Y, Descotes-Genon V, Silvain J, Braik N, Chopard R, Chatot M, Ecarnot F, Tauzin H, Van Belle E, Belle L, Schiele F. Optical Coherence Tomography to Optimize Results of Percutaneous Coronary Intervention in Patients with Non-ST-Elevation Acute Coronary Syndrome: Results of the Multicenter, Randomized DOCTORS Study (Does Optical Coherence Tomography Optimize Results of Stenting). Circulation. 2016;134:906-17.
- 18. Schneider VS, Böhm F, Blum K, Riedel M, Abdelwahed YS, Klotsche J, Steiner JK, Heuberger A, Skurk C, Mochmann HC, Lauten A, Fröhlich G, Rauch-Kröhnert U, Haghikia A, Sinning D, Stähli BE, Landmesser U, Leistner DM. Impact of real-time angiographic co-registered optical coherence tomography on percutaneous coronary intervention: the OPTICO-integration II trial. *Clin Res Cardiol.* 2021;110:249-57.
- 19. Jones DA, Rathod KS, Koganti S, Hamshere S, Astroulakis Z, Lim P, Sirker A, O'Mahony C, Jain AK, Knight CJ, Dalby MC, Malik IS, Mathur A, Rakhit R, Lockie T, Redwood S, MacCarthy PA, Desilva R, Weerackody R, Wragg A, Smith EJ, Bourantas CV. Angiography Alone Versus Angiography Plus Optical Coherence Tomography to Guide Percutaneous Coronary Intervention: Outcomes From the Pan-London PCI Cohort. *JACC Cardiovasc Interv.* 2018;11:1313-21.
- 20. Prati F, Romagnoli E, Burzotta F, Limbruno U, Gatto L, La Manna A, Versaci F, Marco V, Di Vito L, Imola F, Paoletti G, Trani C, Tamburino C, Tavazzi L, Mintz GS. Clinical Impact of OCT Findings During PCI: The CLI-OPCI II Study. *JACC Cardiovasc Imaging*. 2015;8:1297-305.
- 21. Seth A, Patel TM, Stuteville M, Kumar R, Mullasari AS, Kaul U, Mathew R, Sreenivas Kumar A, Ying SW, Sudhir K. Three-year data from the XIENCE V INDIA study: safety and efficacy of XIENCE V in 1000 real world Indian patients. *Indian Heart J.* 2014;66:302-8.
- 22. Krucoff MW, Rutledge DR, Gruberg L, Jonnavithula L, Katopodis JN, Lombardi W, Mao VW, Sharma SK, Simonton CA, Tamboli HP, Wang J, Wilburn O, Zhao W, Sudhir K, Hermiller JB. A new era of prospective real-world safety evaluation primary report of XIENCE V USA (XIENCE V Everolimus Eluting Coronary Stent System condition-of-approval post-market study). *JACC Cardiovasc Interv.* 2011;4: 1298-309.

Supplementary data

Supplementary Appendix 1. Protocol information. Supplementary Table 1. Serious adverse events. Supplementary Figure 1. Study flowchart.

The supplementary data are published online at: https://www.asiaintervention.org/doi/10.4244/AIJ-D-22-00064



Safety and efficacy of a novel 3D-printed bioresorbable sirolimus-eluting scaffold in a porcine model



Qiuping Shi¹, MD; Bin Zhang¹, PhD, MD; Xingang Wang¹, MD; Jintao Fei¹, MD; Qiao Qin¹, MD; Bo Zheng^{1,2}*, MD; Ming Chen¹, MD

1. Department of Cardiology, Peking University First Hospital, Beijing, People's Republic of China; 2. Institute of Cardiovascular Disease, Peking University First Hospital, Beijing, People's Republic of China

Q. Shi and B. Zhang contributed equally to this manuscript.

KEYWORDS

- bioresorbable scaffolds
- drug-eluting stent
- optical coherence tomography
- QCA

Abstract

Background: The effect of 3D-printed bioresorbable vascular scaffolds (BRS) in coronary heart disease has not been clarified.

Aims: We aimed to compare the safety and efficacy of 3D-printed BRS with that of metallic sirolimus-eluting stents (SES).

Methods: Thirty-two BRS and 32 SES were implanted into 64 porcine coronary arteries. Quantitative coronary angiography (QCA) and optical coherence tomography (OCT) were performed at 14, 28, 97, and 189 days post-implantation. Scanning electron microscopy (SEM) and histopathological analyses were performed at each assessment.

Results: All stents/scaffolds were successfully implanted. All animals survived for the duration of the study. QCA showed the two devices had a similar stent/scaffold-to-artery ratio and acute percent recoil. OCT showed the lumen area (LA) and scaffold/stent area (SA) of the BRS were significantly smaller than those of the SES at 14 and 28 days post-implantation (14-day LA: BRS vs SES 4.52±0.41 mm² vs 5.69±1.11 mm²; p=0.03; 14-day SA: BRS vs SES 4.99±0.45 mm² vs 6.11±1.06 mm²; p=0.03; 28-day LA: BRS vs SES 2.93±1.03 mm² vs 4.82±0.74 mm²; p=0.003; 28-day SA: BRS vs SES 3.86±0.98 mm² vs 5.75±0.71 mm²; p=0.03). Both the LA and SA of the BRS increased over time and were similar to those of the SES at the 97-day and 189-day assessments. SEM and histomorphological analyses showed no significant between-group differences in endothelialisation at each assessment.

Conclusions: The novel 3D-printed BRS showed safety and efficacy similar to that of SES in a porcine model. The BRS also showed a long-term positive remodelling effect.

^{*}Corresponding author: Department of Cardiology, Institute of Cardiovascular Disease, Peking University First Hospital, No.8 Xishiku Str, Xicheng District, Beijing 100034, People's Republic of China. E-mail: zhengbopatrick@163.com

Abbreviations

3D three-dimensional

BRS bioresorbable vascular scaffold

CHD coronary heart diseaseDES drug-eluting stent

LA lumen area

MLD minimal lumen diameter

NA neointimal area

OCT optical coherence tomography
 PCI percutaneous coronary intervention
 QCA quantitative coronary angiography

SA scaffold/stent area

SEM scanning electron microscopy

ses sirolimus-eluting stentstent thrombosis

Introduction

The development of percutaneous coronary intervention (PCI) has improved the prognosis of patients with coronary heart disease (CHD). However, a permanent metallic implant may contribute to late/very-late stent thrombosis (ST). A bioresorbable vascular scaffold (BRS) has potential advantages over traditional metallic drug-eluting stents (DES), including removal of the rigid caging in the stented vessel and restoring the vessel to a physiological state^{1,2}. Owing to its potential biodegradability, a BRS can theoretically reduce late/very-late ST3. However, recent studies have revealed an increased incidence of ST and in-stent restenosis following implantation of BRS^{4,5}. There are several possible mechanical causes of ST, including malapposition, incomplete coverage of lesions, device-vessel mismatch, stent fracture, late stent discontinuity, stent overlap, uncovered struts, and neoatherosclerosis6. Procedural and lesion characteristics are crucial factors, and most of the above-mentioned factors are also possibly related to the scaffold design.

To compensate for the reduced radial strength of non-metallic struts, a BRS requires an appropriate strut thickness. However, thicker struts impede the healing process and increase the risk of malapposition because of factors such as fracture or breaks in the integrity of the BRS as a result of the absorption of the scaffold. Furthermore, the rectangular-shaped struts most often used in the current BRS may affect the local haemodynamic microenvironment in treated vessels and increase the risk of ST8. Therefore, there is a need for a re-engineering of the scaffold, including consideration of the type of polymer, the geometric shape and thickness of the strut, and vessel wall coverage.

As is well-known, depending on the characteristics of coronary artery anatomy, tapered coronary artery lesions are often encountered in clinical practice⁹ and subsequent stent edge dissection is a predictor of an adverse clinical outcome^{10,11}. Due to differences in materials, the current BRS devices cannot be overexpanded in the same way as metal stents and may have an increased risk of proximal malapposition, distal dissection, and haematoma when used in vessels that are obviously tapered. Using 3D printing technology

combined with angiographic image processing, reconstruction, and an innovative fabrication strategy, personalised stents can be produced, thus allowing the production of stents that are more suitable for these lesions. The aim of this preclinical study was to evaluate the safety and efficacy of a novel 3D-printed bioresorbable sirolimus-eluting scaffold with circular-shaped struts and a nanoparticle coating with a fixed size in a normal porcine coronary artery.

Editorial, see page 103

Methods

STUDY SCAFFOLDS

The BRS used in this study was the AMSorb (Beijing Advanced Medical Technologies) and the metallic SES used was the HELIOS (Kinhely Medical). The BRS is a 3D-printed balloon-expandable coronary scaffold, which consists of a polymer backbone of novel poly-L-lactic acid (PLLA) coated with a thin layer of a 1:1 mixture of an amorphous matrix of poly(D,L-lactic acid) and $100~\mu g/cm^2$ of the antiproliferative drug sirolimus. The struts have a cross-sectional circular shape with a thickness of $140~\mu m$ (Figure 1, Table 1). The SES consists of an L605 cobalt chromium alloy platform with a thickness of $80~\mu m$ coated with a layer of sirolimus ($135~\mu g/cm^2$) with poly(lactic-co-glycolic acid) (PLGA). The scaffold/stent size was fixed for the purposes of this study at 3 mm in diameter and 12 mm in length for both the BRS and SES.

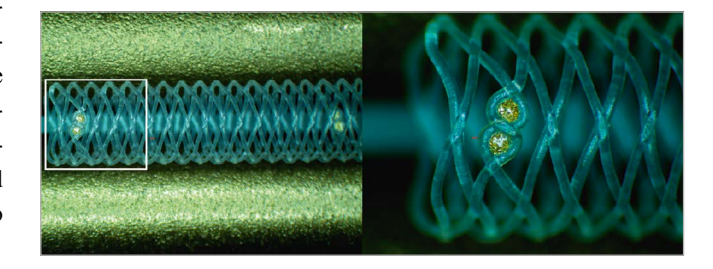


Figure 1. Configuration and structure of the AMSorb scaffold.

ANIMALS

The study protocol was approved by the Institutional Animal Care and Use Committee of Peking University First Hospital (reference number J201612) and conducted in accordance with the National Institutes of Health Guide for the Care and Use of Laboratory Animals. Pigs of either sex (weight: 25-40 kg; age: 6-8 months) were sourced from the China Agricultural University and fed a standard laboratory chow diet without added lipids.

EXPERIMENT GROUPS AND PROCEDURE

All animals received pretreatment with 300 mg of aspirin and 75 mg of clopidogrel one day prior to the implantation of the allocated device. Aspirin 100 mg/day and clopidogrel 75 mg/day were administered through to the time each animal was euthanised. A BRS or SES was implanted into either the left anterior descending artery, left circumflex artery, or right coronary artery in

Table 1. Different scaffold of Absorb BRS and AMSorb.

Device	Shape	Backbone Coating Drug		Drug	Dose	Strut thickness					
Absorb BRS	BRS Rounded rectangle		PDLLA	Everolimus	100 μg/cm ²	157 μm					
AMSorb Ellipse PLLA PDLLA Sirolimus 100 µg/cm² 140 µm											
BRS: bioresorbable	BRS: bioresorbable vascular scaffold; PLLA: poly-L-lactic acid; PDLLA: poly(D,L-lactide)										

a randomised manner, so that two types of devices were implanted in two different coronary arteries in each animal **(Table 2)**. The stent/scaffold-to-artery ratio was limited to 1.1-1.2:1 according to the quantitative coronary angiography (QCA) analysis. The method used to induce anaesthesia and the SES implantation procedure have been described previously¹². The BRS needed to be in contact with blood for more than 90 seconds before delivery to the target coronary segment and then inflated at a steady rate over 10 seconds until it expanded to its maximum diameter. The expansion pressure (generally 8-10 atm) was then maintained for up to 30 seconds. Angiography was repeated after implantation to confirm that no obvious dissection or thrombosis had occurred.

EVALUATION BY QUANTITATIVE CORONARY ANGIOGRAPHY

QCA was performed in eight animals at 14, 28, 97, and 189 days after implantation using CAAS 5.9 OCA software (Pie Medical Imaging). In each vessel, the stent/scaffold segment and the peristent/scaffold segment (defined as 5 mm proximal and distal to the stent/scaffold edge) were evaluated post-implantation and at each assessment time. The evaluations were performed independently by two cardiovascular experts (XG. Wang and B. Zhang). A third investigator (B. Zheng) checked their results. The following OCA parameters were measured: minimal lumen diameter (MLD) immediately after implantation, reference vessel diameter, MLD at the various assessment times, percentage diameter stenosis, and late lumen loss (defined as the difference between the MLD post-implantation and the MLD at the assessments post-implantation). We also evaluated acute recoil, which was defined as the difference between the mean diameter of the inflated balloon (X) and the mean lumen diameter of the stent immediately after deflation of the balloon (Y). Acute percent recoil was defined as (X-Y)/X and expressed as a percentage13.

OPTICAL COHERENCE TOMOGRAPHY IMAGING AND EVALUATION

Optical coherence tomography (OCT) was performed at each assessment using a C7XR Dragonfly imaging system (Abbott) with a pullback speed of 2.5 cm/s (n=8 in each group). The OCT

measurements were repeated offline using the LightLab Imaging workstation (Abbott). The OCT evaluations were performed independently by two cardiovascular experts (XG. Wang and B. Zhang). A third investigator (B. Zheng) checked their results. Contiguous cross-sections were analysed at 1 mm longitudinal intervals within the treated segment and at 5 mm proximal and distal to the stent/scaffold edges to measure the proximal and distal reference vessel areas (RVA). The RVA, lumen area (LA), stent/scaffold area (SA), neointimal area (NA), and percentage area of stenosis were calculated according to the methods used in previous studies¹⁴.

STENT/SCAFFOLD HARVEST AND EVALUATION OF HISTOLOGY AND MORPHOLOGY

Eight animals were euthanised after the imaging examination at each assessment time. Their hearts were removed and perfused with heparinised saline for 30 minutes at a pressure of 100 mmHg (1 mmHg=0.0133 kPa).

For histological and morphological evaluation, the stent/scaffold vessel segment was separated rapidly, fixed in 10% formal-dehyde solution, and stained with haematoxylin and eosin for histopathological analysis. The following parameters were investigated according to published methods^{15,16}: LA, internal elastic lamina area (IELA), NA (IELA – LA), and percent area of stenosis (IELA – LA/LA×100%) with morphological analysis of injury, inflammation, and endothelialisation.

For scanning electron microscopy (SEM), the stented vessel segments were separated, cut along the longitudinal axis, and fixed with 3% buffered glutaraldehyde and 1% buffered osmium tetroxide (n=2 for SES, n=2 for BRS). The samples were then dehydrated in a series of ethanol baths (50%, 75% and 100%), dried in liquid CO₂ in a critical point dryer (72.8 atm, 31°C), and sputter-coated for 3 min at 15 mA with gold. SEM images (H-450; Hitachi) were acquired at low magnification (×18) to evaluate the overall neointimal coverage of the stents and at various high magnifications to identify the composition of the tissue covering the surfaces of the stents. Endothelial cells were identified as sheets of closely connected monolayer cells with a spindle or polygonal shape.

Table 2. Distribution of stents in the coronary arteries at the four assessment times.

	14 days			28 days			97 days			189 days		
	LAD	LCx	RCA	LAD	LCx	RCA	LAD	LCx	RCA	LAD	LCx	RCA
BRS	5	3	0	7	1	0	8	0	0	4	3	1
SES	3	5	0	1	4	3	0	8	0	4	3	1

BRS: bioresorbable sirolimus-eluting scaffold (AMSorb); LAD: left anterior descending artery; LCx: left circumflex artery; RCA: right coronary artery; SES: metallic sirolimus-eluting stent

STATISTICAL ANALYSIS

Continuous values that were distributed normally are expressed as the mean±standard deviation. Categorical data are expressed as the percentage. *n* represents the number of stents of each type. The independent two-sample t-test was used to detect betweengroup differences. All statistical analyses of numerical data were performed using SPSS Statistics 24.0 (IBM). A p-value <0.05 was considered statistically significant.

Results

A total of 64 stents/scaffolds (BRS n=32, SES n=32) were successfully implanted in the coronary arteries of 32 pigs. All animals survived for the planned study duration without any complications (angiographic stent thrombosis, migration, or fragmentation).

QUANTITATIVE CORONARY ANGIOGRAPHY ANALYSIS

The results of the QCA analysis at baseline and parameters associated with acute recoil are presented in **Table 3**. There was no difference in the diameter of the reference vessel between the BRS and the SES (2.82±0.32 mm vs 2.76±0.28 mm; p=0.44)

at baseline. The stent-to-artery ratio for the BRS was similar to that for the SES (1.03 ± 0.10 vs 1.07 ± 0.10 ; p=0.13). The acute absolute recoil was similar in both groups (0.07 ± 0.21 mm vs 0.08 ± 0.17 mm; p=0.98), as was the acute percent recoil ($2.50\pm7.33\%$ vs $2.44\pm5.78\%$; p=0.97). The results for MLD immediately after the procedure, MLD at the various assessment times, late lumen loss, and percent diameter of stenosis are presented in **Table 4**. The MLD was significantly smaller for the BRS than for the SES at day 14 (1.90 ± 0.30 mm vs 2.38 ± 0.33 mm; p=0.01) but not at any other assessment time. The late lumen loss and percent diameter of stenosis were comparable between the two groups at each assessment time. The greatest late lumen loss with the BRS was 0.89 ± 0.40 mm at 28 days and with the SES was 0.80 ± 0.31 mm at 97 days.

ANALYSIS BY OPTICAL COHERENCE TOMOGRAPHY

OCT examination was performed successfully for all of the study devices (**Table 5**). The appearance of the struts at each OCT examination is shown in **Figure 2**. All struts had a preserved box-like appearance with no ST, malapposition, dissection, or tissue

Table 3. QCA analysis at baseline and parameters associated with acute recoil.

Parameter	BRS (n=32)	SES (n=32)	<i>p</i> -value
Reference vessel diameter (mm)	2.82±0.32	2.76±0.28	0.44
Stent-to-artery ratio	1.03±0.10	1.07±0.10	0.13
Mean diameter of inflated balloon (X, mm)	2.87±0.13	2.93±0.18	0.15
Mean diameter of stent immediately after balloon inflation (Y, mm)	2.79±0.22	2.85±0.20	0.29
Acute absolute recoil (X-Y, mm)	0.07±0.21	0.08±0.17	0.98
Acute percent recoil ([X-Y]/X, %)	2.50±7.33	2.44±5.78	0.97
BRS: bioresorbable sirolimus-eluting scaffold (AMSorb); QCA: quantitative coronar	y angiography; SES: metall	ic sirolimus-eluting stent	

Table 4. QCA analysis of late lumen loss and percentage diameter of stenosis.

IMLD (mm)	FU-MLD (mm)	LLL (mm)	%DS (%)
2.37±0.11	1.90±0.30	0.47±0.31	19.88±13.36
2.62±0.16	2.38±0.33	0.25±0.28	9.33±10.59
0.002*	0.01*	0.15	0.10
IMLD (mm) FU-MLD (mm)		LLL (mm)	%DS (%)
2.67±0.28	1.78±0.29	0.89±0.40	32.62±13.26
2.66±0.20	2.17±0.45	0.49±0.39	18.54±14.89
0.94	0.08	0.08	0.09
IMLD (mm)	FU-MLD (mm)	LLL (mm)	%DS (%)
2.57±0.18	1.99±0.20	0.58±0.17	22.56±6.51
2.66±0.25	1.85±0.36	0.80±0.31	30.31±11.87
0.44	0.37	0.10	0.13
IMLD (mm)	FU-MLD (mm)	LLL (mm)	%DS (%)
2.66±0.16	2.17±0.47	0.49±0.51	17.89±18.75
2.72±0.19	2.05±0.25	0.67±0.13	24.91±4.37
0.52	0.51	0.35	0.33
	2.37±0.11 2.62±0.16 0.002* IMLD (mm) 2.67±0.28 2.66±0.20 0.94 IMLD (mm) 2.57±0.18 2.66±0.25 0.44 IMLD (mm) 2.66±0.16 2.72±0.19	2.37±0.11 1.90±0.30 2.62±0.16 2.38±0.33 0.002* 0.01* IMLD (mm) 2.67±0.28 1.78±0.29 2.66±0.20 2.17±0.45 0.94 0.08 IMLD (mm) FU-MLD (mm) 2.57±0.18 1.99±0.20 2.66±0.25 1.85±0.36 0.44 0.37 IMLD (mm) FU-MLD (mm) 2.66±0.16 2.17±0.47 2.72±0.19 2.05±0.25	2.37±0.11 1.90±0.30 0.47±0.31 2.62±0.16 2.38±0.33 0.25±0.28 0.002* 0.01* 0.15 IMLD (mm) LLL (mm) 2.67±0.28 1.78±0.29 0.89±0.40 2.66±0.20 2.17±0.45 0.49±0.39 0.94 0.08 0.08 IMLD (mm) FU-MLD (mm) LLL (mm) 2.57±0.18 1.99±0.20 0.58±0.17 2.66±0.25 1.85±0.36 0.80±0.31 0.44 0.37 0.10 IMLD (mm) FU-MLD (mm) LLL (mm) 2.66±0.16 2.17±0.47 0.49±0.51 2.72±0.19 2.05±0.25 0.67±0.13

^{*}Statistically significant difference. FU-MLD: MLD at the various assessment times; IMLD: minimal lumen diameter immediately after implantation; LLL: late lumen loss; %DS: percentage of diameter stenosis

Table 5. OCT analysis at each assessment of the BRS and SES.

	BRS	SES		
14 days	n=8	n=8	<i>p</i> -value	
RVA (mm ²)	5.72±1.30	5.62±1.14	0.88	
LA (mm²)	4.52±0.41	5.69±1.11	0.03*	
SA (mm²)	4.99±0.45	6.11±1.06	0.03*	
NA (mm²)	0.46±0.10	0.43±0.16	0.58	
%AS	9.35±1.65	7.28±3.30	0.14	
28 days	n=8	n=8	<i>p</i> -value	
RVA (mm²)	6.06±1.03	5.15±0.7	0.10	
LA (mm²)	2.93±1.03	4.82±0.74	0.003*	
SA (mm²)	3.86±0.98	5.75±0.71	0.002*	
NA (mm²)	0.93±0.39	0.92±0.25	0.98	
%AS	25.43±13.21	16.50±4.68	0.15	
97 days	n=8	n=8	<i>p</i> -value	
RVA (mm²)	5.92±0.35	5.62±0.59	0.27	
LA (mm²)	3.90±0.60	3.63±1.08	0.57	
SA (mm²)	5.33±0.83	5.30±0.78	0.93	
NA (mm²)	1.44±0.69	1.67±0.64	0.53	
%AS	26.95±9.50	32.43±13.30	0.39	
189 days	n=8	n=8	<i>p</i> -value	
RVA (mm²)	6.65±0.68	6.21±1.36	0.46	
LA (mm²)	4.31±1.06	3.78±0.54	0.32	
SA (mm²)	5.89±1.22	5.54±0.66	0.58	
NA (mm²)	1.58±0.40	1.78±0.56	0.49	
%AS	27.22±6.10	31.72±8.07	0.28	

*Statistically significant difference. %AS: percentage area of stenosis; BRS: bioresorbable sirolimus-eluting scaffold (AMSorb); LA: lumen area; NA: neointimal area; RVA: reference vessel area; SA: stent area; SES: metallic sirolimus-eluting stent

prolapse in either group. The RVA was similar between the two groups at all assessment times. The LA of the BRS was significantly smaller than that of the SES at 14 days ($4.52\pm0.41~\text{mm}^2$ vs $5.69\pm1.11~\text{mm}^2$; p=0.03) and 28 days ($2.93\pm1.03~\text{mm}^2$ vs $4.82\pm0.74~\text{mm}^2$; p=0.003). The SA showed a pattern similar to that of the LA. The SA of the BRS was significantly smaller than that of the SES at 14 days ($4.99\pm0.45~\text{mm}^2$ vs $6.11\pm1.06~\text{mm}^2$; p=0.03) and 28 days ($3.86\pm0.98~\text{mm}^2$ vs $5.75\pm0.71~\text{mm}^2$; p=0.002). The LA and SA of the BRS were numerically larger than those of the SES at 97 days and 189 days, but the differences were not statistically significant (**Figure 3**). There was no significant difference in NA or the percent area of stenosis between the BRS and SES at any assessment time.

HISTOPATHOLOGICAL AND HISTOMORPHOLOGICAL ANALYSES

The histopathological findings under light microscopy at each assessment time are shown in **Figure 4** (low magnification, 20×) and **Figure 5** (high magnification, 200×). At each assessment, all BRS and SES devices were structurally intact and all stent/scaffold beam surfaces were covered with endothelial cells. No thrombus formation was observed in either group. The results of the morphological analyses are shown in **Table 6**. There were no statistically significant between-group differences in LA, IELA, NA, or percentage area of stenosis at any assessment time. There were also no significant differences in the injury, inflammation, or endothelialisation scores between the two groups at any assessment (**Table 7**). The endothelialisation scores were similar between the two groups and showed complete re-endothelialisation at 97 days and 189 days, which is consistent with the findings on SEM (**Figure 6**, **Figure 7**).

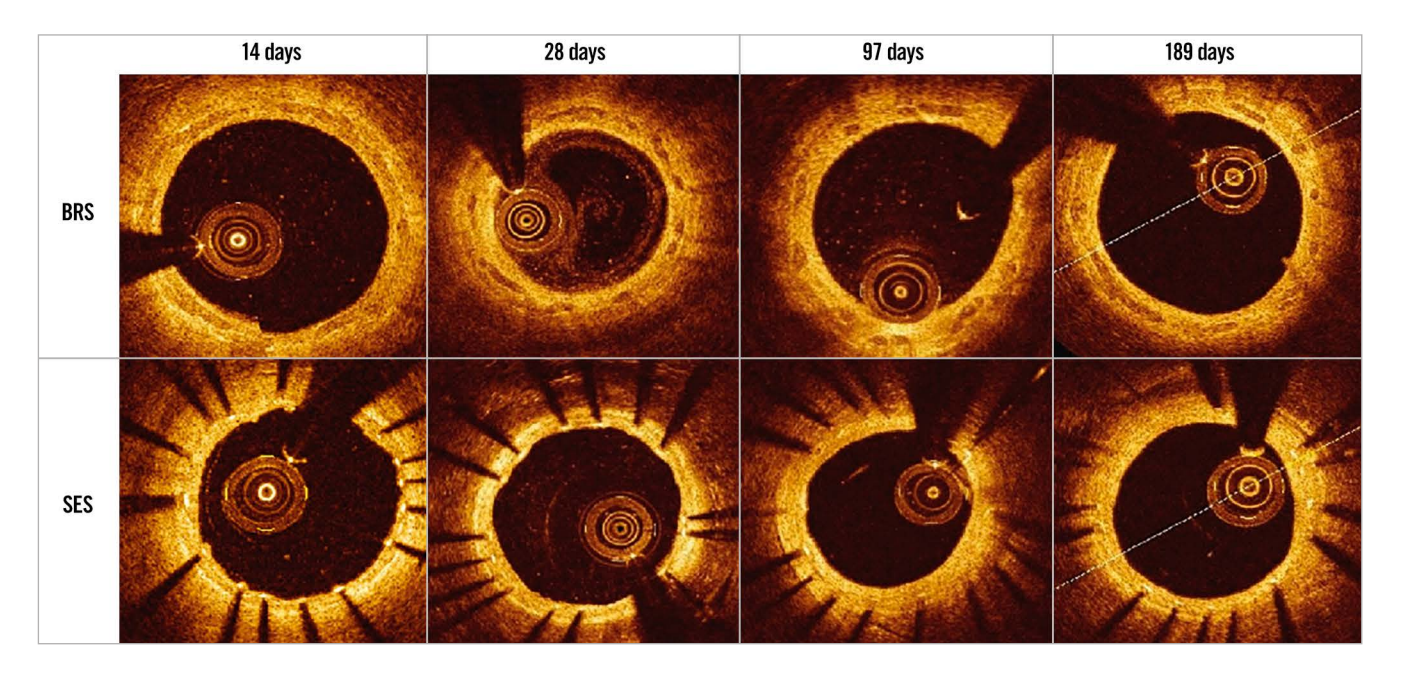


Figure 2. Performance of the BRS and SES at each optical coherence tomography assessment. BRS: bioresorbable sirolimus-eluting scaffold (AMSorb); SES: metallic sirolimus-eluting stent

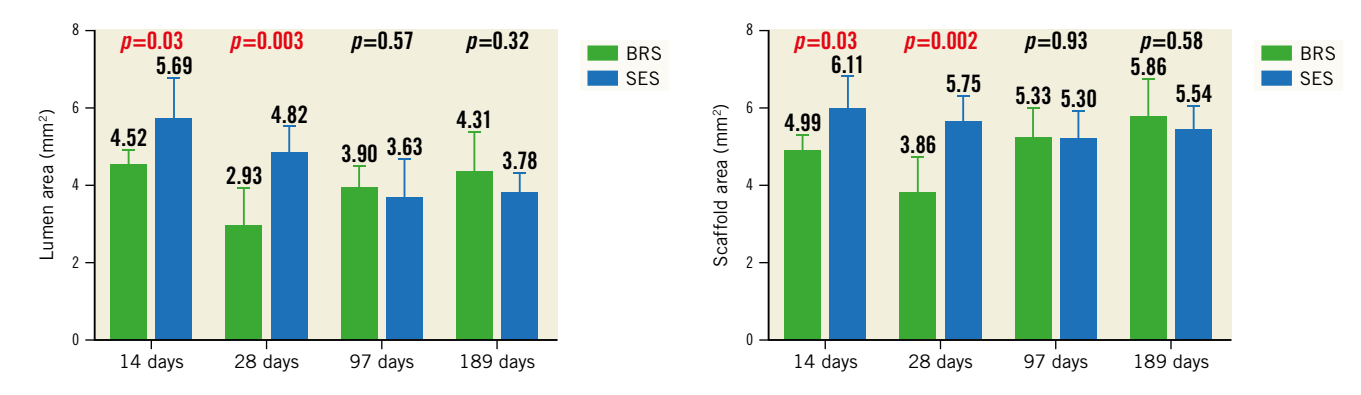


Figure 3. Lumen area and scaffold/stent area of the BRS and SES at each assessment time. BRS: bioresorbable sirolimus-eluting scaffold (AMSorb); SES: metallic sirolimus-eluting stent

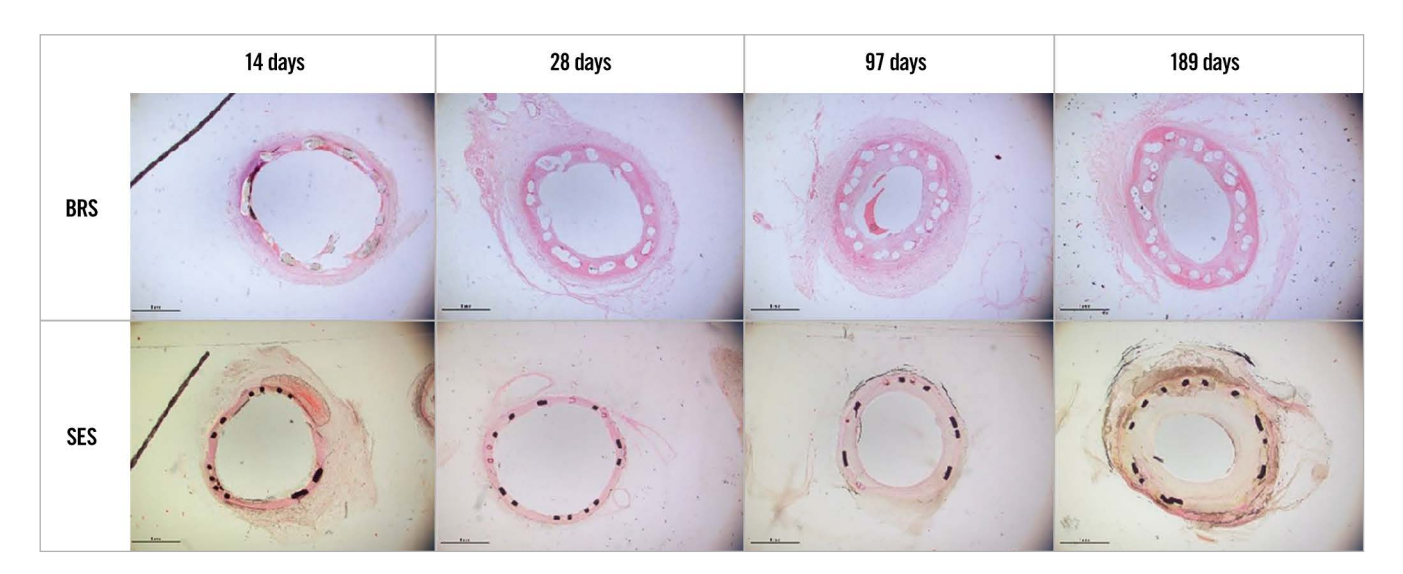


Figure 4. Histopathological findings for the BRS and SES at each assessment time (low magnification). BRS: bioresorbable sirolimus-eluting scaffold (AMSorb); SES: metallic sirolimus-eluting stent

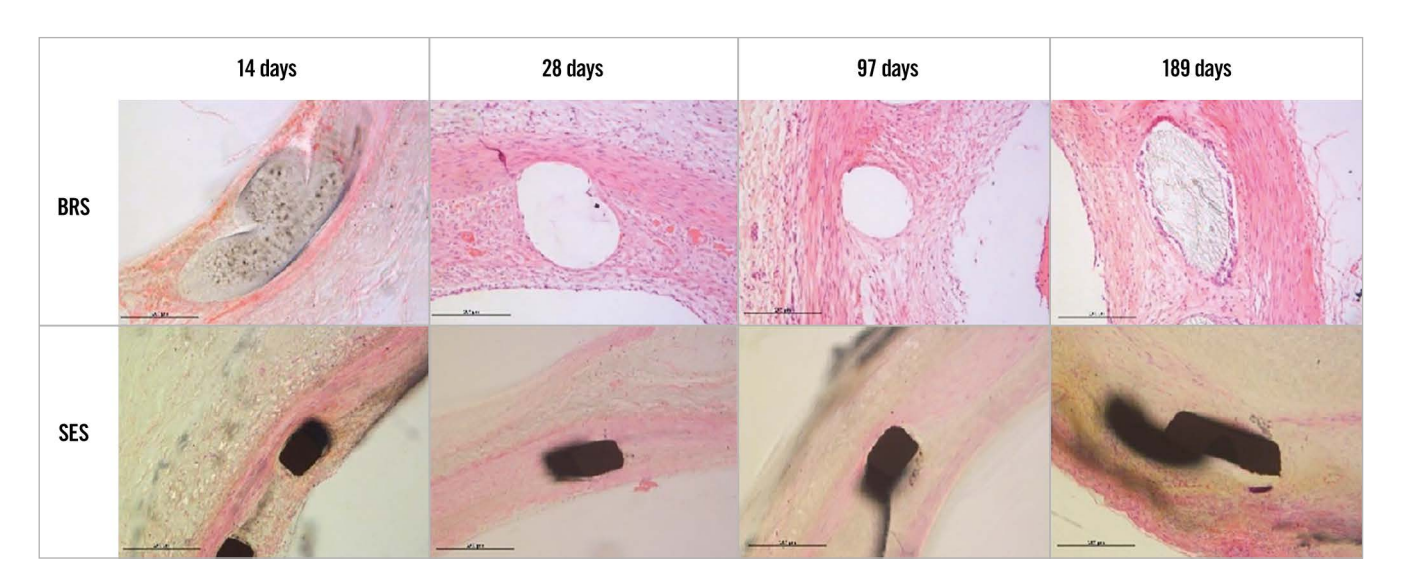


Figure 5. Histopathological findings for the BRS and SES at each assessment time (high magnification). BRS: bioresorbable sirolimus-eluting scaffold (AMSorb); SES: metallic sirolimus-eluting stent

Table 6. Histomorphometric parameters for BRS and SES at each assessment time.

	14 (days	28 (days	97 (days	189	days	
	BRS n=6	SES n=6	BRS n=6	SES n=6	BRS n=6	SES n=6	BRS n=6	SES n=6	
LA (mm ²)	4.16±1.16	4.24±1.56	2.04±1.27	3.18±1.17	1.49±0.61	2.29±1.27	1.96±0.96	2.78±0.92	
<i>p</i> -value	0.92		0.14		0.	0.19		0.17	
IELA (mm²)	4.77±1.20	5.28±1.31	3.58±1.39	4.91±1.07	5.16±2.77	5.31±0.90	4.99±1.35	6.50±1.82	
<i>p</i> -value	0.	50	0.09		0.90		0.13		
NA (mm²)	0.61±0.20	1.04±0.85	1.54±0.28	1.73±1.22	3.67±3.29	3.02±1.27	3.03±1.83	3.73±2.36	
<i>p</i> -value	0.	28	0.73		0.66		0.58		
%AS	13.52±6.02	20.03±15.79	49.09±21.72	34.72±20.44	62.80±20.05	57.26±23.07	57.64±19.49	53.58±20.45	
<i>p</i> -value	0.	37	0.27		0.	67	0.73		
, ,	,	s; BRS: bioresorb lic sirolimus-eluti		iting scaffold (AM	Sorb); LA: lumen	area; IELA: inter	nal elastic lamina	area;	

Table 7. Pathological scores for BRS and SES at each assessment time.

	14 (days	28 (days	97 (lays	189 days		
	BRS n=6	SES n=6	BRS n=6	SES n=6	BRS n=6	SES n=6	BRS n=6	SES n=6	
Inflammation score	0.33±0.52	0.33±0.52 0.00±0.00		0.50±0.55		1.17±1.17	1.50±1.05	1.17±1.17	
<i>p</i> -value	0.18		0.08		0.64		0.62		
Injury score	0.33±0.52	0.17±0.41	0.33±0.52	0.00±0.00	1.00±1.10	1.00±1.10	0.67±0.82	0.33±0.52	
<i>p</i> -value	0.9	55	0.18		1.0	00	0.42		
Endothelialisation score	2.17±0.98	2.50±0.84	2.83±0.41	3.00±0.00	3.00±0.00	3.00±0.00	3.00±0.00	3.00±0.00	
<i>p</i> -value	0.9	54	0.36		-		-		
BRS: bioresorbable	sirolimus-eluting	g scaffold (AMSo	rb); SES: metalli	c sirolimus-elutin	g stent				

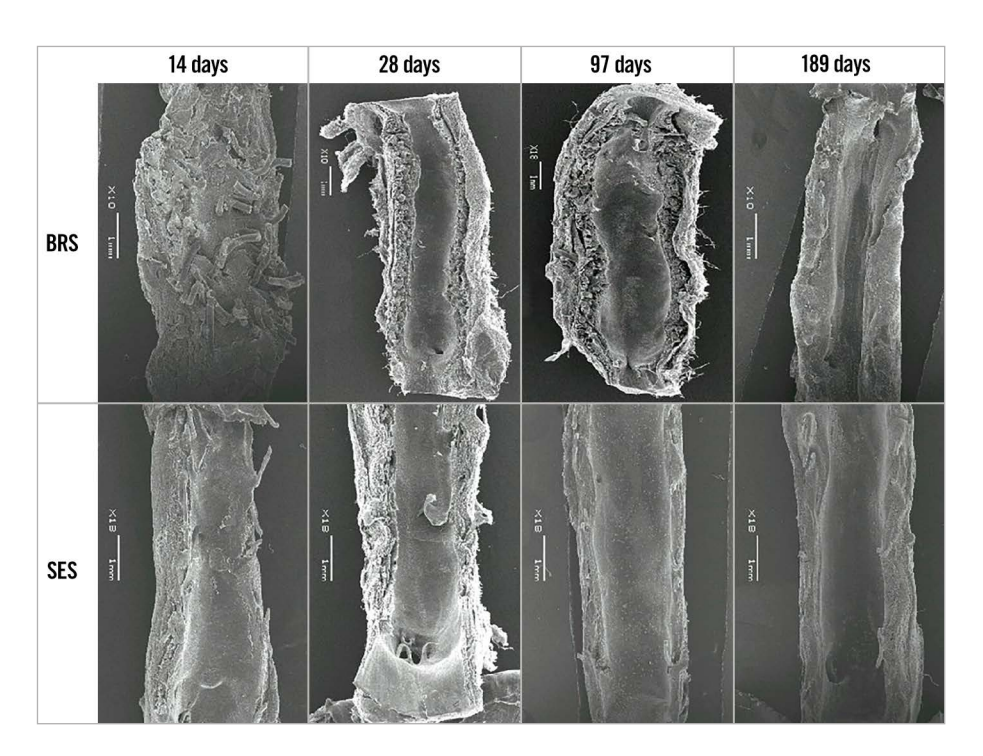


Figure 6. Findings on scanning electron microscopy for the BRS and SES at each assessment time (low magnification). BRS: bioresorbable sirolimus-eluting scaffold (AMSorb); SES: metallic sirolimus-eluting stent

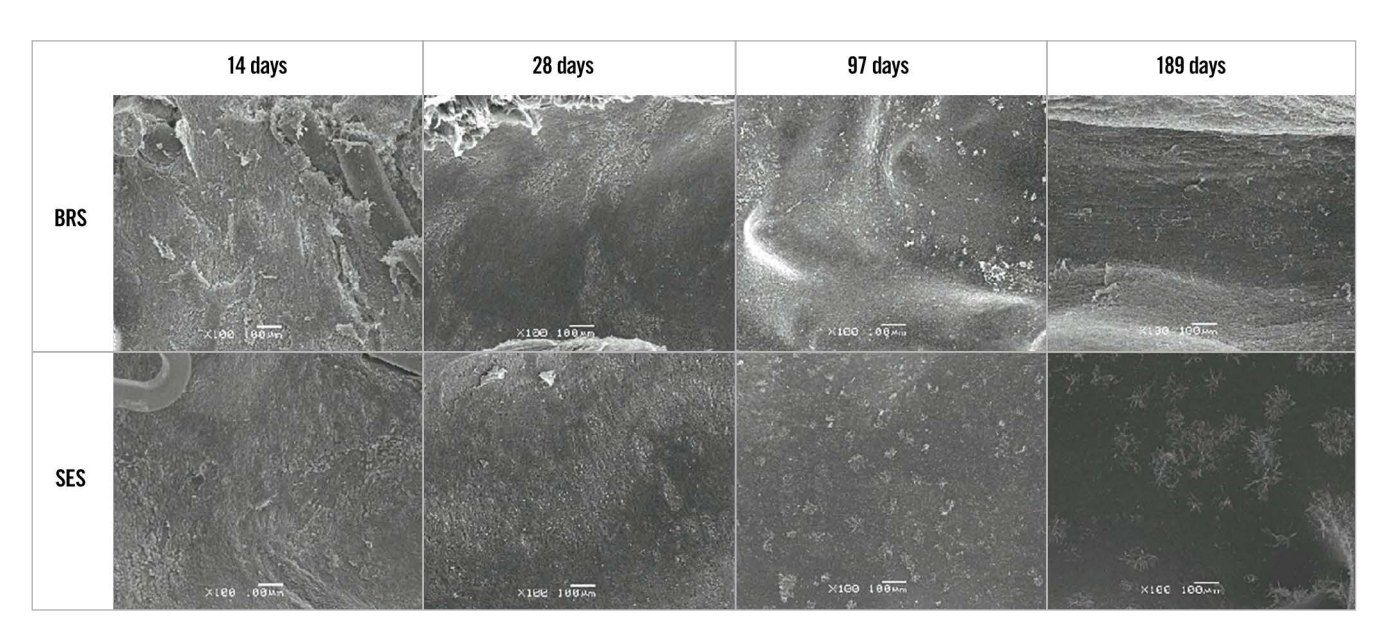


Figure 7. Findings on scanning electron microscopy for the BRS and SES at each assessment time (high magnification). BRS: bioresorbable sirolimus-eluting scaffold (AMSorb); SES: metallic sirolimus-eluting stent

Discussion

3D printing technology is gradually being applied in several fields of medicine, including fabrication of medical devices, advanced visualisation, diagnosis planning, and simulation of surgical procedures¹⁷. However, few systematic long-term studies have demonstrated the feasibility of 3D-printed scaffolds for CHD in vivo¹⁸. This preclinical study further validated the safety of a fully degradable sirolimus-eluting 3D-printed scaffold by implanting it into normal coronary arteries in a porcine model. All animals survived for the entire duration of the study without stent thrombosis, migration, or fragmentation, confirming that the safety of the BRS is comparable with that of the SES. Previous studies have demonstrated the good biocompatibility of the PLLA bioabsorbable vascular stent (BVS)19,20. In our histopathological analysis, there were no or few aggregations of inflammatory cells in the BRS-stented arterial wall tissue, which suggests that this stent has favourable biocompatibility. Moreover, it was noted to be inert and non-thrombogenic at the 189-day assessment. In terms of inflammation scores, the BRS seems to be better than BVS in previous studies¹⁵. The circular shape and smaller thickness of the BRS may be one of the reasons for less inflammation, and the unstable injury score may be another confounding factor. A healthy, intact, and functioning endothelial layer controls thrombosis and thrombolysis, interactions between platelets and leukocytes, and the release of vasodilating (e.g., nitric oxide) and vasoconstricting (e.g., endothelin-1) substances, as well as regulating vascular tone and growth²¹. Early re-endothelialisation would be helpful for suppressing neointimal hyperplasia, preventing restenosis, and reducing complications of ST22. Our OCT and SEM analyses showed that the BRS scaffolds had a good degree of endothelial cell coverage at each assessment time. Pathological analysis showed that the endothelialisation scores were similar for the two

stents; the BRS achieved early re-endothelialisation within 28 days and complete endothelialisation at 97 days, suggesting that, unlike the SES, the BRS does not delay the re-endothelialisation process. Two-stage degradation and the vascular characteristics of the novel 3D-printed scaffold may demonstrate the potential of this device to promote endothelial function²³.

A bioabsorbable PLLA stent has several advantages due to its good biocompatibility and ability to be moulded into scaffolds of different shapes^{19,20}. However, there is still a concern about the acute stent recoil and radial strength of the scaffold because it has material and structural characteristics that are different from those of the metallic stent. In the ABSORB and SPIRIT trials, the mean acute recoil of the bioabsorbable everolimus-eluting coronary scaffold (Absorb BVS 1.0, Abbott; 6.85±6.96%) was slightly higher than that of the metallic everolimus-eluting stent (XIENCE V, Abbott; 4.27±7.08%)²⁴, and the improved Absorb BVS revision 1.1 had an acute recoil similar to that of the Absorb BVS revision 1.0¹³. In the present study, both the BRS and SES had similar acute recoil $(2.50\pm7.33\% \text{ vs } 2.44\pm5.78\%; p=0.97)$, which suggests that, like the commercially available SES, the BRS could provide sufficient radial strength to support a vessel wall in the acute phase. OCT analysis showed that the LA and SA of the stents in the BRS group were significantly smaller than those in the SES group at the 14-day and 28-day assessments but that there was no significant between-group difference in the NA. Therefore, consideration should be given to the possibility of late recoil with the BRS caused by a decrease in radial strength. However, at the 97-day and 189-day assessments, both OCT and the histopathological examination showed that the BRS scaffold beam remained intact. There was no significant betweengroup difference in the LA or SA, and even the above-mentioned parameters in the BRS group surpassed those in the SES group,

suggesting that the novel 3D-printed absorbable scaffold can provide enough support to resist elastic recoil and restrict neointimal proliferation in porcine coronary arteries for at least 6 months. This novel scaffold has a unique closed-loop unit structure with a spiral arrangement and is circular in cross-section, which is conducive to attachment to the inner wall of a blood vessel and reducing the effect on local blood flow⁸. Therefore, in theory, the novel scaffold could provide a better local haemodynamic microenvironment in treated vessels, thereby reducing the risk of ST. Furthermore, the novel nanoparticle coating on the scaffold effectively inhibits proliferation of smooth muscle cells in vitro²⁵. This could be the reason for its good flexural properties, radial support force, and limited neointimal proliferation. However, the lack of immediate baseline OCT data in this study meant that it was not possible to analyse the late stent recoil, and this will be the subject of a future study.

An earlier study of the Absorb BVS in a porcine coronary model²⁶ showed late lumen gain with an increase in the LA of the BVS from 2.87±1.28 mm² at 28 days to 5.13±0.84 mm² at 2 years and 6.85±1.25 mm² at 4 years. Serial assessment of this BVS in patients showed a similar tendency, with further intravascular ultrasound examination suggesting that reduction of plaque led to late lumen enlargement rather than positive vessel remodelling²⁷. An earlier preclinical study demonstrated that this late lumen gain might be coupled with positive remodelling of the scaffold-treated segment²⁸. In our study, late lumen enlargement and SA enlargement of the BRS were similarly documented by OCT. Analysis of the mean LA on OCT showed a significant increase from 2.93±1.03 mm² at 28 days to 4.31±1.06 mm² at 189 days and an increase in SA from 3.86±0.98 mm² at 28 days to 5.89±1.22 mm² at 189 days. However, the OCT was performed in different animals at each time point in this study; therefore, the late lumen enlargement might be a pseudomorph. Therefore, continuous intravascular imaging, such as continuous OCT or intravascular ultrasound follow-up studies, should be considered to validate this phenomenon. In addition, we will make more efforts to characterise the change in tissue composition during biodegradation by histopathology on the neointimal tissue around the struts in the long-term evaluation, per the European Society of Cardiology/European Association of Percutaneous Cardiovascular Interventions Task Force's executive summary on bioresorbable scaffolds²⁹.

Finally, the scaffold was manufactured by 3D printing technology and can be tailor-made for specific coronary lesions, to help prevent device-vessel mismatch and associated malapposition, and avoid incomplete coverage of lesions, stent overlap, and uncovered struts. Considering that this study primarily explored the safety of this novel scaffold in porcine coronary arteries, this potential advantage should be investigated in further preclinical and clinical studies.

Limitations

This study had some limitations. First, it was performed in healthy animals with no atherosclerotic lesions in the coronary arteries. Therefore, it could not reflect complex clinical scenarios. Moreover, the possibility that growth of the animals during the study contributed to positive vessel remodelling cannot be excluded. Second, different animal cohorts were examined at the different assessment times without the benefit of serial observations in the same animals. The late scaffold discontinuity and late recoil of BRS were two important influencing factors in determining late outcomes. A serial intravascular imaging study in the same vessels and long-term histopathological analysis would be needed to observe dynamic evolution. Third, we used only one size of stent and did not tailor the stent to fit the vessel in each animal. Therefore, this study did not fully reflect the characteristics of 3D printing technology, and further research is needed to explore personalised percutaneous coronary intervention based on intravascular imaging and 3D printing technology.

Conclusions

This novel 3D-printed BRS showed safety and efficacy similar to that of an SES in a porcine model and had a long-term positive remodelling effect. Our preliminary findings for this novel stent warrant further clinical evaluation in patients with coronary artery disease.

Impact on daily practice

This preclinical study validated the safety and efficacy of a fully degradable sirolimus-eluting 3D-printed scaffold by implanting it into normal coronary arteries in a porcine model. The scaffold could be tailor-made for specific coronary lesions, which could help to prevent device-vessel mismatch and associated malapposition, and avoid incomplete coverage of lesions, stent overlap, and uncovered struts. Ultimately it may reduce clinical events and improve patient outcomes.

Acknowledgements

The authors thank all personnel who contributed to the animal experiments.

Funding

This work was supported by the National Key R&D Program of China (No. 2016YFC1102205) and the National Natural Science Funds of China (No. 81800312).

Conflict of interest statement

The authors have no conflicts of interest to declare.

References

- Ormiston JA, Serruys PW. Bioabsorbable coronary stents. Circ Cardiovasc Interv. 2009;2:255-60
- 2. Serruys PW, Garcia-Garcia HM, Onuma Y. From metallic cages to transient bioresorbable scaffolds: change in paradigm of coronary revascularization in the upcoming decade? *Eur Heart J.* 2012;33:16-25b.
- Garcia-Garcia HM, Serruys PW, Campos CM, Muramatsu T, Nakatani S, Zhang YJ, Onuma Y, Stone GW. Assessing bioresorbable coronary devices: methods and parameters. *JACC Cardiovasc Imaging*. 2014;7:1130-48.

- 4. Kereiakes DJ, Ellis SG, Metzger C, Caputo RP, Rizik DG, Teirstein PS, Litt MR, Kini A, Kabour A, Marx SO, Popma JJ, McGreevy R, Zhang Z, Simonton C, Stone GW; ABSORB III Investigators. 3-Year Clinical Outcomes With Everolimus-Eluting Bioresorbable Coronary Scaffolds: The ABSORB III Trial. *J Am Coll Cardiol*. 2017:70:2852-62.
- 5. Elias J, van Dongen IM, Kraak RP, Tijssen RYG, Claessen BEPM, Tijssen JGP, de Winter RJ, Piek JJ, Wykrzykowska JJ, Henriques JPS. Mid-term and long-term safety and efficacy of bioresorbable vascular scaffolds versus metallic everolimus-eluting stents in coronary artery disease: A weighted meta-analysis of seven randomised controlled trials including 5577 patients. *Neth Heart J.* 2017;25:429-38.
- 6. Sotomi Y, Suwannasom P, Serruys PW, Onuma Y. Possible mechanical causes of scaffold thrombosis: insights from case reports with intracoronary imaging. *EuroIntervention*. 2017;12:1747-56.
- Jinnouchi H, Torii S, Sakamoto A, Kolodgie FD, Virmani R, Finn AV. Fully bioresorbable vascular scaffolds: lessons learned and future directions. *Nat Rev Cardiol*. 2019:16:286-304.
- 8. Tenekecioglu E, Torii R, Bourantas C, Sotomi Y, Cavalcante R, Zeng Y, Collet C, Crake T, Suwannasom P, Onuma Y, Serruys PW. Difference in haemodynamic microenvironment in vessels scaffolded with Absorb BVS and Mirage BRMS: insights from a preclinical endothelial shear stress study. *EuroIntervention*. 2017;13:1327-35.
- 9. Zhang LR, Xu DS, Liu XC, Wu XS, Ying YN, Dong Z, Sun FW, Yang PP, Li X. [Coronary artery lumen diameter and bifurcation angle derived from CT coronary angiographic image in healthy people] [Article in Chinese]. *Zhonghua Xin Xue Guan Bing Za Zhi*. 2011;39:1117-23.
- 10. Jinnouchi H, Sakakura K, Yanase T, Ugata Y, Tsukui T, Taniguchi Y, Yamamoto K, Seguchi M, Wada H, Fujita H. Impact of stent edge dissection detected by optical coherence tomography after current-generation drug-eluting stent implantation. *PLoS One.* 2021;16:e0259693.
- 11. Kobayashi N, Mintz GS, Witzenbichler B, Metzger DC, Rinaldi MJ, Duffy PL, Weisz G, Stuckey TD, Brodie BR, Parvataneni R, Kirtane AJ, Stone GW, Maehara A. Prevalence, Features, and Prognostic Importance of Edge Dissection After Drug-Eluting Stent Implantation: An ADAPT-DES Intravascular Ultrasound Substudy. *Circ Cardiovasc Interv.* 2016;9:e003553.
- 12. Zhang B, Chen M, Zheng B, Wang XG, Wang XT, Fan YY, Huo Y. A novel high nitrogen nickel-free coronary stents system: evaluation in a porcine model. *Biomed Environ Sci.* 2014;27:289-94.
- 13. Onuma Y, Serruys PW, Gomez J, de Bruyne B, Dudek D, Thuesen L, Smits P, Chevalier B, McClean D, Koolen J, Windecker S, Whitbourn R, Meredith I, Garcia-Garcia H, Ormiston JA; ABSORB Cohort A and B investigators. Comparison of in vivo acute stent recoil between the bioresorbable everolimus-eluting coronary scaffolds (revision 1.0 and 1.1) and the metallic everolimus-eluting stent. *Catheter Cardiovasc Interv.* 2011;78:3-12.
- 14. Tearney GJ, Regar E, Akasaka T, Adriaenssens T, Barlis P, Bezerra HG, Bouma B, Bruining N, Cho JM, Chowdhary S, Costa MA, de Silva R, Dijkstra J, Di Mario C, Dudek D, Falk E, Feldman MD, Fitzgerald P, Garcia-Garcia HM, Gonzalo N, Granada JF, Guagliumi G, Holm NR, Honda Y, Ikeno F, Kawasaki M, Kochman J, Koltowski L, Kubo T, Kume T, Kyono H, Lam CC, Lamouche G, Lee DP, Leon MB, Maehara A, Manfrini O, Mintz GS, Mizuno K, Morel MA, Nadkarni S, Okura H, Otake H, Pietrasik A, Prati F, Råber L, Radu MD, Rieber J, Riga M, Rollins A, Rosenberg M, Sirbu V, Serruys PW, Shimada K, Shinke T, Shite J, Siegel E, Sonoda S, Suter M, Takarada S, Tanaka A, Terashima M, Thim T, Uemura S, Ughi GJ, van Beusekom HM, van der Steen AF, van Es GA, van Soest G, Virmani R, Waxman S, Weissman NJ, Weisz G; International Working Group for Intravascular Optical Coherence Tomography (IWG-IVOCT). Consensus standards for acquisition, measurement, and reporting of intravascular optical coherence tomography standardization and Validation. *J Am Coll Cardiol.* 2012;59:1058-72.
- 15. Otsuka F, Pacheco E, Perkins LE, Lane JP, Wang Q, Kamberi M, Frie M, Wang J, Sakakura K, Yahagi K, Ladich E, Rapoza RJ, Kolodgie FD, Virmani R. Long-term

- safety of an everolimus-eluting bioresorbable vascular scaffold and the cobalt-chromium XIENCE V stent in a porcine coronary artery model. *Circ Cardiovasc Interv.* 2014:7:330-42.
- 16. Schwartz RS, Huber KC, Murphy JG, Edwards WD, Camrud AR, Vlietstra RE, Holmes DR. Restenosis and the proportional neointimal response to coronary artery injury: results in a porcine model. *J Am Coll Cardiol*. 1992;19:267-74.
- 17. Khalaj R, Tabriz AG, Okereke MI, Douroumis D. 3D printing advances in the development of stents. *Int J Pharm.* 2021;609:121153.
- 18. Sang Jin Lee, Ha Hyeon Jo, Kyung Seob Lim, Dohyung Lim, Soojin Lee, Jun Hee Lee, Wan Doo Kim, Myung Ho Jeong, Joong Yeon Lim, Il Keun Kwon, Youngmee Jung, Jun-Kyu Park, Su A Park. Heparin coating on 3D printed poly (I-lactic acid) biodegradable cardiovascular stent via mild surface modification approach for coronary artery implantation. *Chem Engineering J.* 2019;378:122116.
- 19. Lincoff AM, Furst JG, Ellis SG, Tuch RJ, Topol EJ. Sustained local delivery of dexamethasone by a novel intravascular eluting stent to prevent restenosis in the porcine coronary injury model. *J Am Coll Cardiol*. 1997;29:808-16.
- 20. Yamawaki T, Shimokawa H, Kozai T, Miyata K, Higo T, Tanaka E, Egashira K, Shiraishi T, Tamai H, Igaki K, Takeshita A. Intramural delivery of a specific tyrosine kinase inhibitor with biodegradable stent suppresses the restenotic changes of the coronary artery in pigs in vivo. *J Am Coll Cardiol*. 1998;32:780-6.
- 21. Moncada S, Palmer RM, Higgs EA. Nitric oxide: physiology, pathophysiology, and pharmacology. *Pharmacol Rev.* 1991;43:109-42.
- 22. Yamamoto T, Shibata R, Ishii M, Kanemura N, Kito T, Suzuki H, Miyake H, Maeda K, Tanigawa T, Ouchi N, Murohara T. Therapeutic reendothelialization by induced pluripotent stem cells after vascular injury-brief report. *Arterioscler Thromb Vasc Biol.* 2013;33:2218-21.
- 23. Yin T, Du R, Wang Y, Huang J, Ge S, Huang Y, Tan Y, Liu Q, Chen Z, Feng H, Du J, Wang Y, Wang G. Two-stage degradation and novel functional endothelium characteristics of a 3-D printed bioresorbable scaffold. *Bioact Mater*. 2021;10:378-96.
- 24. Tanimoto S, Serruys PW, Thuesen L, Dudek D, de Bruyne B, Chevalier B, Ormiston JA. Comparison of in vivo acute stent recoil between the bioabsorbable everolimus-eluting coronary stent and the everolimus-eluting cobalt chromium coronary stent: insights from the ABSORB and SPIRIT trials. *Catheter Cardiovasc Interv.* 2007;70:515-23.
- 25. Zhao J, Mo Z, Guo F, Shi D, Han QQ, Liu Q. Drug loaded nanoparticle coating on totally bioresorbable PLLA stents to prevent in-stent restenosis. *J Biomed Mater Res B Appl Biomater*: 2018;106:88-95.
- 26. Onuma Y, Serruys PW, Perkins LE, Okamura T, Gonzalo N, García-García HM, Regar E, Kamberi M, Powers JC, Rapoza R, van Beusekom H, van der Giessen W, Virmani R. Intracoronary optical coherence tomography and histology at 1 month and 2, 3, and 4 years after implantation of everolimus-eluting bioresorbable vascular scaffolds in a porcine coronary artery model: an attempt to decipher the human optical coherence tomography images in the ABSORB trial. *Circulation*. 2010;122: 2288-300.
- 27. Serruys PW, Ormiston JA, Onuma Y, Regar E, Gonzalo N, Garcia-Garcia HM, Nieman K, Bruining N, Dorange C, Miquel-Hébert K, Veldhof S, Webster M, Thuesen L, Dudek D. A bioabsorbable everolimus-eluting coronary stent system (ABSORB): 2-year outcomes and results from multiple imaging methods. *Lancet*. 2009;373:897-910.
- 28. Strandberg E, Zeltinger J, Schulz DG, Kaluza GL. Late positive remodeling and late lumen gain contribute to vascular restoration by a non-drug eluting bioresorbable scaffold: a four-year intravascular ultrasound study in normal porcine coronary arteries. *Circ Cardiovasc Interv.* 2012;5:39-46.
- 29. Byrne RA, Stefanini GG, Capodanno D, Onuma Y, Baumbach A, Escaned J, Haude M, James S, Joner M, Jüni P, Kastrati A, Oktay S, Wijns W, Serruys PW, Windecker S. Report of an ESC-EAPCI Task Force on the evaluation and use of bioresorbable scaffolds for percutaneous coronary intervention: executive summary. *Eur Heart J.* 2018;39:1591-601.

A simple mathematical method to identify optimal biplane fluoroscopic angulations for chronic total occlusion percutaneous coronary intervention using CT angiography



Hitoshi Kamiunten*, MD

Division of Cardiology, Kitsuki City Yamaga Hospital, Kitsuki City, Japan

This paper also includes supplementary data published online at: https://www.asiaintervention.org/doi/10.4244/AIJ-D-22-00084

KEYWORDS

- chronic coronary total occlusion
- miscellaneous
- MSCT

Abstract

Background: The concept of three-dimensional (3D) wiring for chronic total occlusion (CTO) percutaneous coronary intervention (PCI) is now widely accepted among coronary interventionalists. The 3 axes, i.e., the 2 X-ray beams and the CTO segment, should intersect with each other at as close to a right angle as possible. However, how to specify optimal fluoroscopic angulations for a given CTO segment has not been well established.

Aims: We aimed to develop a simple and practical method to identify optimal fluoroscopic angulations for CTO PCI.

Methods: A CTO vector can be derived from slab maximum intensity projection (MIP) images of coronary computed tomography (CT) angiography. Using trigonometric functions, the inner product of vectors and the equation of a plane, we calculated 2 fluoroscopic vectors perpendicular to each other and to the CTO vector.

Results: We applied this method to a patient with mid-left circumflex CTO and translated the resulting fluoroscopic vectors into optimal fluoroscopic angulations. To facilitate its use, we developed a calculator using spreadsheet software that can output optimal fluoroscopic angulations within a practical range by inputting the x, y, and z components of the CTO vector. This approach also helps to minimise dead angles in biplane fluoroscopy.

Conclusions: This method has the potential to make CTO PCI safer and easier, without requiring dedicated equipment or software. Its effectiveness should be validated in clinical practice.

^{*}Corresponding author: Division of Cardiology, Kitsuki City Yamaga Hospital, 1612-1, Yamaga-machi Noharu, Kitsuki City, Japan. E-mail: hitoshi.kamiunten@gmail.com

Abbreviations

CCTA coronary CT angiography
CT computed tomography
CTO chronic total occlusion
LAO left anterior oblique

MIP maximum intensity projection
PCI percutaneous coronary intervention

RAO right anterior oblique3D three-dimensional

Introduction

The concept of three-dimensional (3D) wiring is widely accepted among coronary interventionalists, especially among those who are enthusiastic about chronic total occlusion (CTO) percutaneous coronary intervention (PCI)¹⁻³. Generally, during PCI it is important to view the target lesion from multiple directions without foreshortening. For 3D wiring, it is even more crucial to see the CTO segment from the correct angle, and, in addition, from 2 directions perpendicular to each other^{2,3} (Figure 1A). However, how to find the optimal fluoroscopic angulations for a given CTO segment has not been well established. The CT TrueView (Philips) is a software product which can display the optimal rotation and angulation of a C-arm of a designated coronary segment⁴. However, the software is not widely available because it is attached to Allura (Philips), a fluoroscopic system that only provides a single fluoroscopic plane angulation. We present a simple and practical

approach for determining the optimal biplane fluoroscopic angulations. Our method utilises coronary computed tomography (CT) angiography (CCTA) and basic mathematical principles, without the need for specialised equipment or software.

Methods

Assuming a CTO segment to be a vector (CTO vector), optimal fluoroscopic lines should lie on the plane which is perpendicular to the vector (fluoroscopic plane) (Figure 1B). Fluoroscopic lines are depicted as vectors (fluoroscopic vectors). The objective of this article is to present a method for determining a CTO vector and, subsequently, identifying the fluoroscopic vectors. These vectors are then translated into a combination of optimal right and left fluoroscopic angulations. To achieve this goal, we will employ basic mathematical concepts such as trigonometric functions, inner products of vectors, and equations of a plane, in addition to maximum intensity projection (MIP) images of coronary CT angiography.

This study was exempt from the requirements of the Institutional Review Board at Kitsuki City Yamaga Hospital because it contains no patient-identifiable information.

BASICS OF TRIGONOMETRIC FUNCTIONS AND EQUATION OF A PLANE

For two vectors making an angle θ , the formula of the inner product describes the relationship between the inner product, their lengths, and the angle between them (Figure 2A).

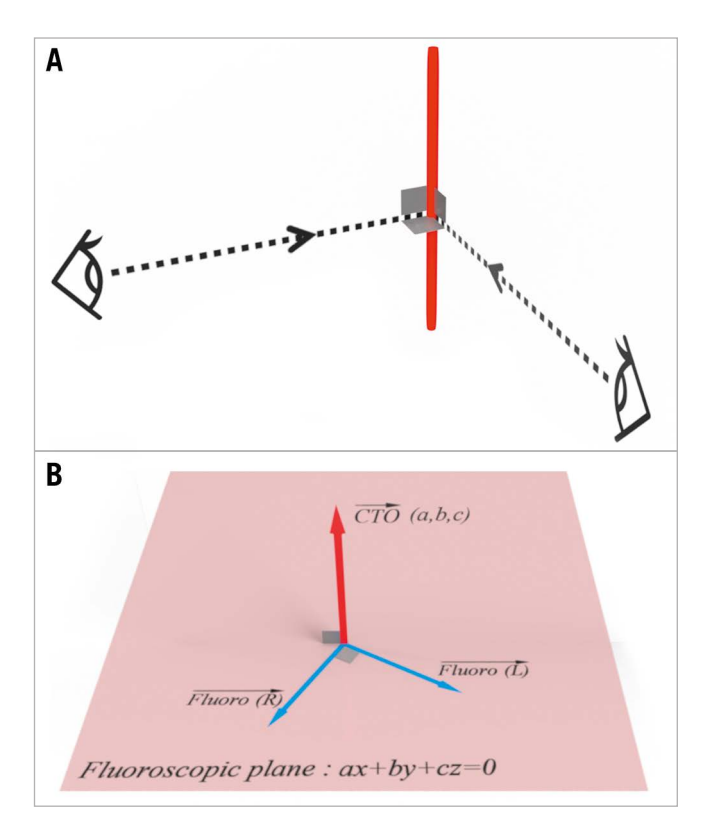


Figure 1. Triaxial orthogonality and the application of the equation of a plane. A) Viewing the CTO segment without foreshortening from 2 directions perpendicular to each other. B) Optimal fluoroscopic lines lie on the fluoroscopic plane. Red bold axis: CTO segment; red bold arrow: CTO vector; Fluoro (R): right fluoroscopic vector; Fluoro (L): left fluoroscopic vector. CTO: chronic total occlusion

A
$$\vec{A} (a, b, c)$$

$$\vec{B} = al + bm + cn = |\vec{A}| |\vec{B}| \cos \theta$$

$$= \sqrt{a^2 + b^2 + c^2} \sqrt{l^2 + m^2 + n^2} \cos \theta$$
B
$$\vec{A} (a, b, c)$$

$$\vec{A} \cdot \vec{B} = al + bm + cn = |\vec{A}| |\vec{B}| \cos \theta = 0$$

$$\vec{B} (l, m, n)$$

Figure 2. Inner product of vectors. Inner product of vectors (A) and a specific case of 2 vectors making a right angle (B)

In the specific case where the 2 vectors make a right angle, the inner product equals zero, as the cosine of 90 degrees is 0 (Figure 2B).

In the application on a plane, the relationship between a vector (a, b, c) perpendicular to a plane and an arbitrary position vector (x, y, z) on this plane is represented as ax + by + cz = 0 (equation of a plane) (Figure 1B). The vector (a, b, c) is referred to as the normal vector of the plane. Assuming the normal vector to be a CTO vector, the fluoroscopic vectors, shown here as Fluoro (R) and Fluoro (L), would be located on this plane.

DERIVATION OF CTO VECTOR

In a virtual XYZ space overlaid on a patient's body, we set reference X-, Y-, Z-axes and reference coronal, sagittal and transverse planes (**Figure 3**). The CTO vector is represented by a bold red arrow, with its x, y, and z components depicted as fine red lines.

Transverse plane

Bagittal plane

Coronal plane

Coronal plane

Figure 3. CTO vector in a virtual XYZ space. The CTO vector is shown as a red bold arrow, its x, y and z components as red fine lines, and its projection vector onto the reference planes as red dotted arrows. The CTO vector is noted as the simplest trigonometric functions. CTO: chronic total occlusion

Drawing its projection vectors onto the reference planes (red dotted arrows) and measuring the angle with the reference axis, the CTO vector can be expressed using trigonometric functions. In this paper, vectors are represented by the simplest trigonometric functions, as only the direction of the vector is relevant for the purposes of this study and not its magnitude.

Results

We will apply this to a patient with a mid-left circumflex (LCx) CTO (Figure 4), using the image viewer to display 3 of the basic cross-sections of a CCTA (Figure 5A). With the universally prevalent image viewers, you can set the thickness of slab MIP. Apply a 9 mm thick slab, in this case on the coronal plane, and search for an adequate slab that contains the whole length of the CTO. For this case, calcifications at the origin, middle, and end of the CTO help us orient the location of the CTO (Figure 5B). These allow us to draw the projection line of the CTO onto the coronal plane, and the angle with the Y-axis measures 23.6 degrees. Similarly, by applying a 8 mm thick slab, drawing the projection line onto the sagittal plane and measuring the angle with the Y-axis, we derived 25.6 degrees (Figure 5C). Using trigonometric functions, the CTO vector in the left anterior oblique (LAO) cranial direction was

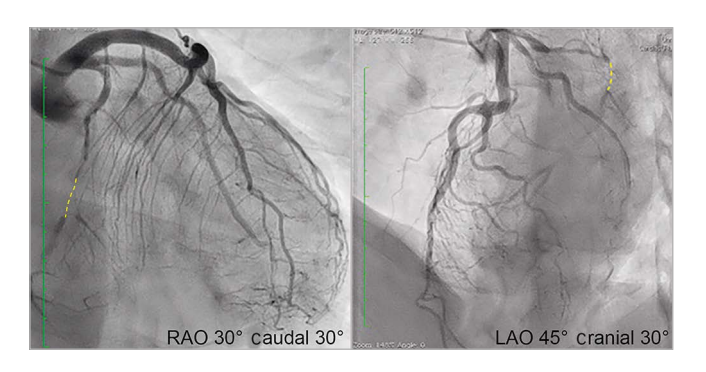


Figure 4. A case of mid-LCx CTO. Yellow dotted lines represent the CTO segment of the mid-LCx. CTO: chronic total occlusion; LCx: left circumflex

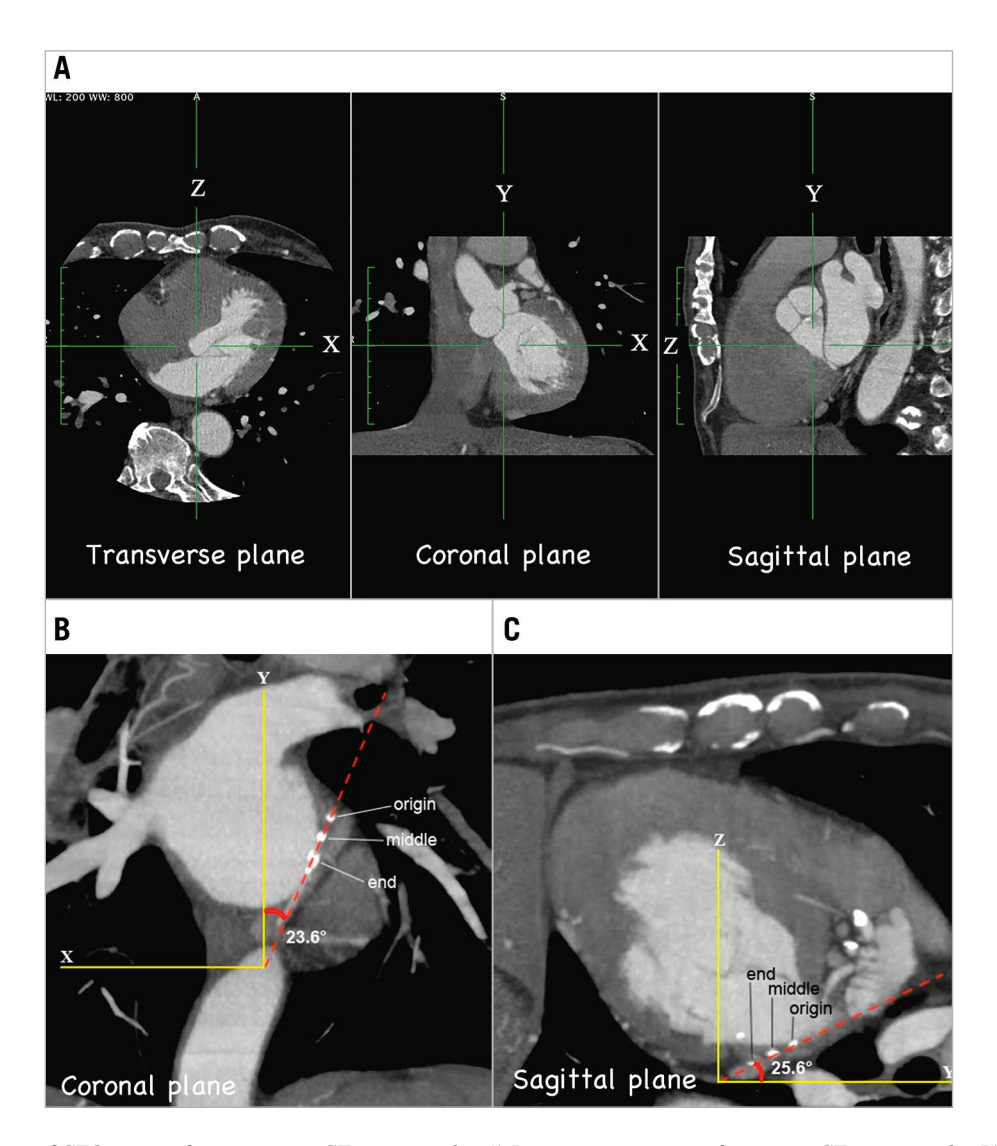


Figure 5. Derivation of CTO vectors from coronary CT angiography. A) Basic cross-sections of coronary CT angiography. B) Slab MIP image on coronal plane. A 9 mm-thick slab allows the operator to draw the projection line of the whole length of the CTO onto the coronal plane (red dotted line) and to measure the angle with the Y-axis. C) A slab MIP image on the sagittal plane. An 8 mm-thick slab is applied to draw the projection line onto the sagittal plane (red dotted line) and to measure the angle with the Y-axis. CT: computed tomography; CTO: chronic total occlusion; MIP: maximum intensity projection

determined as (0.437, 1.000, 0.479) (Figure 6A, Supplementary Figure 1).

The thickness of the slab required to project the entire length of the CTO segment onto the coronal and sagittal planes is denoted as t1 and t2, respectively.

DERIVATION OF FLUOROSCOPIC VECTORS AND ANGULATIONS

Using the equation of a plane, a plane perpendicular to the CTO vector is represented as:

0.437x + y + 0.479z = 0 (equation of a fluoroscopic plane)

Both the right and left fluoroscopic vectors lie on it (Figure 6B). There are numerous possibilities, so from a viewpoint of practical utility, we set the right anterior oblique (RAO) angle at 30 degrees for the right fluoroscopic vector. Here, we examined how to create

fluoroscopic angulations, such as LAO 45° caudal 30°, which involves a series of rotations performed by the C-arm⁵. The C-arm first rotates clockwise on the transverse plane by 45 degrees (Figure 7A) and then rotates caudally by 30 degrees on the left 45-degree plane (Figure 7B). Note that for any vector on the left 45-degree plane, regardless of its cranial or caudal angulation, the ratio of its x and z components is always 1:1. When RAO 30° is applied, similarly the x and z components of the right fluoroscopic vector are automatically set as -1 and $\sqrt{3}$, respectively. By assigning these values to the equation of the fluoroscopic plane, the y component can be calculated, and the right fluoroscopic vector was determined, as shown in **Supplementary Figure 2**, and **Figure 8A**.

Next, the method for converting a vector into a fluoroscopic angulation is described (Figure 8A). Calculating the angle between

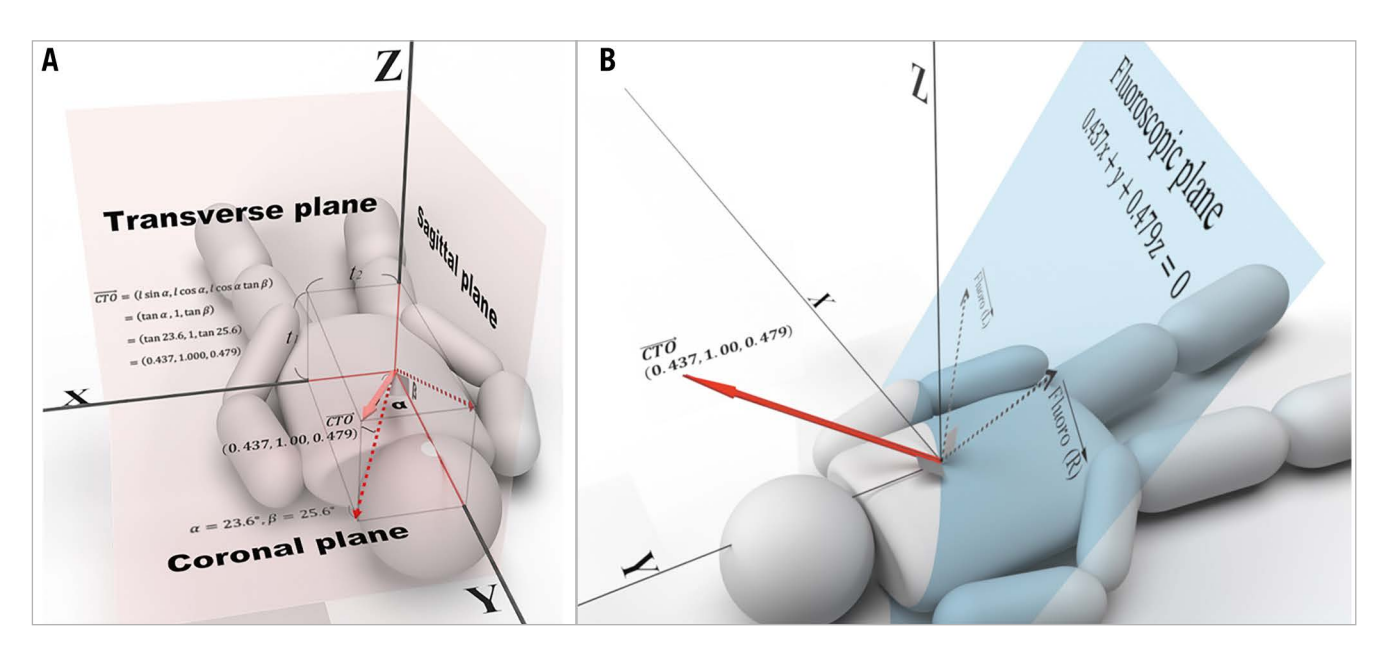


Figure 6. Determination of the CTO vector of the mid-LCx and derivation of the fluoroscopic plane. A) Determination of the CTO vector from angles measured in Figure 5 and trigonometric functions. t1 is the thickness of slab needed for the projection of the whole length of the CTO onto the coronal plane; t2 is the thickness of slab needed for the projection of the whole length of the CTO onto the sagittal plane. B) The fluoroscopic plane is depicted in the virtual XYZ space along with the CTO vector (red bold arrow) as its normal vector. The combination of optimal fluoroscopic vectors lie on this plane (black dotted arrows, Fluoro [R]: right fluoroscopic vector and Fluoro [L]: left fluoroscopic vector). CTO: chronic total occlusion, LCx: left circumflex artery

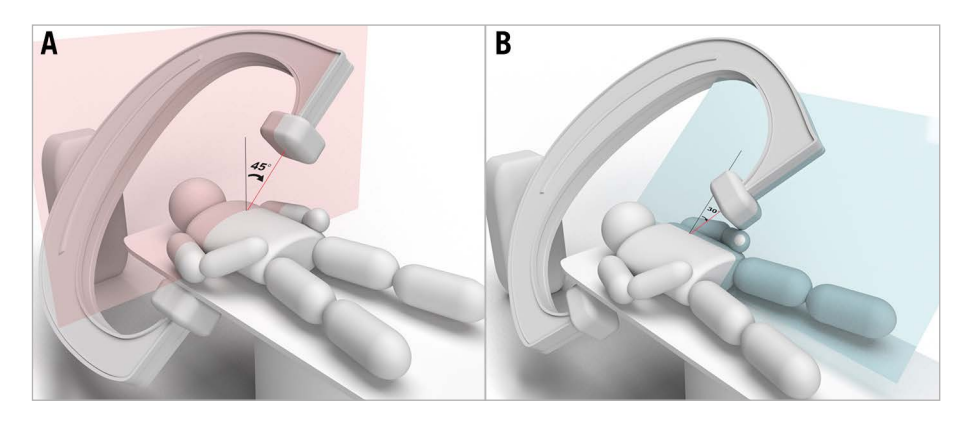


Figure 7. How to create LAO 45° caudal 30°. A) Clockwise rotation of the C-arm on the transverse plane by 45 degrees, followed by (B) rotating caudally on the left 45-degree plane by 30 degrees. LAO: left anterior oblique

the right fluoroscopic vector (the blue solid vector) and its projection vector onto the transverse plane (the blue dotted vector) according to the formula for an inner product, the angle is 11.1 degrees (**Figure 8B**). The right fluoroscopic angulation is finally determined as (RAO 30° caudal 11°).

Because the CTO, the right and left fluoroscopic vectors are orthogonal to each other, the left fluoroscopic vector is calculated as (2.32, -1.49, 1.00) by solving the system of the equations in **Supplementary Figure 3**.

As mentioned for the right fluoroscopic vector, the LAO angle is determined by the x and z components of the fluoroscopic vector. That is, the angle giving a tangent of 2.32/1.00 is 66.7 degrees **(Figure 8B)**. The angle between the left fluoroscopic vector and

its projection onto the transverse plane (2.32, 0, 1.00), according to the formula of inner product, is determined to be 30.6 degrees. Now we have identified one of the combinations of optimal fluoroscopic angulations: (RAO 30° caudal 11°) and (LAO 67° caudal 31°).

APPLICATION TO ANOTHER CTO CASE

Another case of PCI for mid-circumflex CTO, in which this method was actually applied, is shown. Using slab MIP of CCTA and the calculator, the combination of practical optimal fluoroscopic angulations was calculated as (RAO 45° cranial 8°) and (LAO 46° cranial 8°) (Supplementary Figure 4, Supplementary Figure 5, Supplementary Table 1). We started the procedure with a bilateral

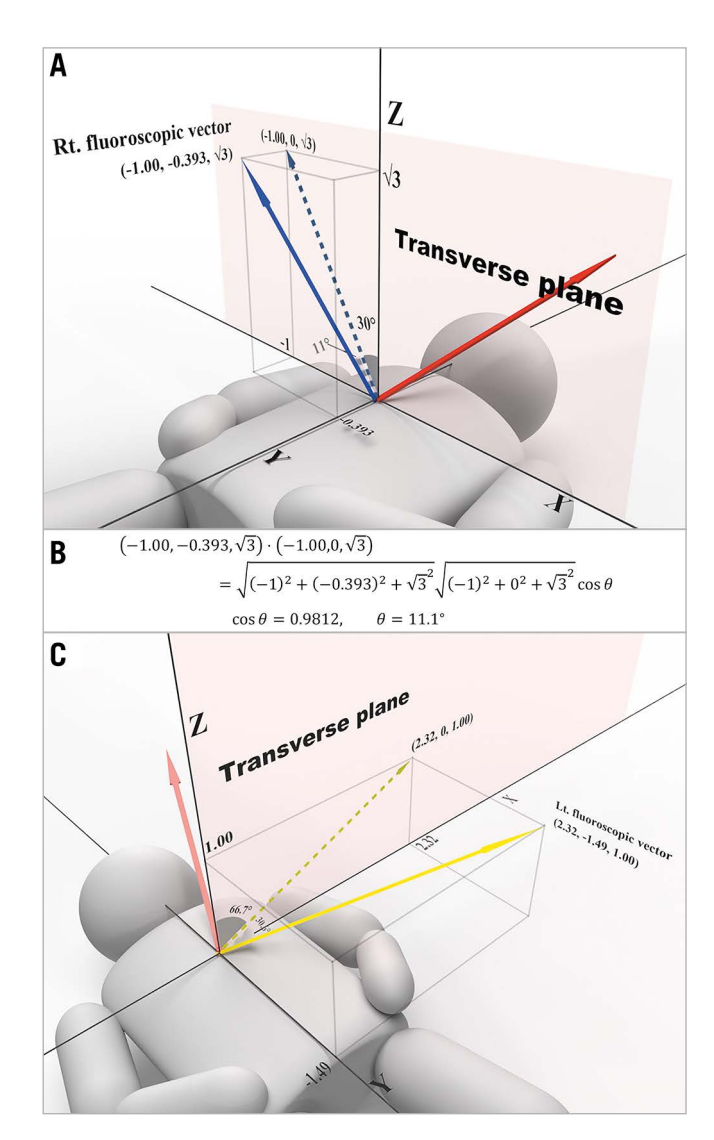


Figure 8. Right and left fluoroscopic vectors and angulations.

A) Right fluoroscopic vector and angulation. The caudal angulation is the angle between the right fluoroscopic vector (blue solid arrow) and its projection vector onto the transverse plane (blue dotted arrow). B) The caudal angulation can be calculated from the formula of the inner product. C) Left fluoroscopic vector and angulation. The left fluoroscopic angulation can be derived just as in the right fluoroscopic angulation. Note that the LAO angle is determined only by the x and z components of the fluoroscopic vector. Red bold arrow: CTO vector; yellow solid arrow: left fluoroscopic vector; yellow dotted arrow: projection vector onto the transverse plane of the left fluoroscopic vector. CTO: chronic total occlusion, LAO: left anterior oblique

approach. Bilateral tip injection allowed good visualisation of the CTO at LAO 46° cranial 8° but the visualisation at RAO 45° cranial 8° was poor because of the overlap of the guide and prosthesis (**Supplementary Figure 6**). In order to avoid these obstacles, alternative angulations (RAO 11° cranial 23°) were adopted for the right fluoroscopic angulation (**Supplementary Figure 7**). We used another calculator here (**Supplementary Table 2**), by which the angle between the 2 vectors and the shortening rate can be

obtained. By entering the CTO vector in advance and entering (RAO 11° cranial 23°) in the fluoroscopic angle cell, the angle of 56.5 degrees is derived. Since 1 – sin 56.5° is equal to 0.166, the shortening rate of the lesion when this fluoroscopic angulation is adopted is 16.6%. Of course, for the ideal fluoroscopic angulation, this angle would be 90 degrees, so the foreshortening would be 0%. The second row of the table shows the angle between the 2 adopted fluoroscopic vectors. This calculator can be used in the cath lab during the procedure. For the right fluoroscopic angulation, an alternative was used to proceed with the procedure, a tapered guidewire passed antegradely through the lesion (Supplementary Figure 8), and finally, a drug-eluting stent was implanted (Supplementary Figure 9).

DEVELOPMENT OF THE CALCULATOR

Because calculating complex formulas at each CTO vector requires so much energy, we developed a calculator using spreadsheet software (Table 1). Assigning the x, y and z components of a CTO vector, the answers for designated RAO angles can be calculated automatically. It will display combinations of the right and left fluoroscopic angulations in 5-degree increments in the range from RAO 0 to 60 degrees for practical use. Recalculations are done to confirm if these complex calculations are true: the inner product of any 2 of the 3 vectors should equal 0 and there should be no discrepancy between fluoroscopic vectors derived from a CTO vector and those inversely translated from fluoroscopic angulations (independently calculated from the original formulas) (Table 2).

Discussion

Minimising shortening is crucial not only for CTO but also for any target lesion. When biplane fluoroscopy, which provides orthogonal views as shown in Figure 1A, is available, the guidewire tip behaviour can be accurately visualised, potentially enhancing procedural success and safety. However, identifying optimal biplane fluoroscopic angulations is challenging. Here, we propose a method based on the equation of a plane. By adopting the CTO vector as the plane's normal vector, the fluoroscopic lines will lie on this plane. We further utilised CCTA's slab MIP images to vectorise the CTO lesion, which can be achieved using standard image viewers without specialised software. With the use of trigonometric functions and inner product formulas, fluoroscopic vectors can be translated into multiple optimal fluoroscopic angulations. It is important to note that due to different reference planes and axes for each CTO lesion, careful attention must be paid to the CTO vector's direction while calculating the components to avoid disorientation.

Images of CCTA are reconstructed from the data acquired mainly during end systole or mid-diastole⁶⁻⁹. In case of excessive excursion during the cardiac cycle, as is often seen in the midportion of right coronary arteries, optimal fluoroscopic angulations in other cardiac phases might differ significantly from what we propose here. Nonetheless, the cardiac motion is minimal, and accordingly, it is easy to observe a guidewire during these periods.

Table 1. Calculator for right and left fluoroscopic angulations.

RAO	RAO CTO vector			Right fluoroscopic vector			Left fluoroscopic vector			Right fluoroscopic angulation		Left fluoroscopic angulation	
	Х	у	Z	Х	у	Z	Х	у	Z	RAO	Cranial	LAO	Cranial
R0	0.437	1.000	0.479	0.000	-0.479	1.000	-5.874	2.087	1.000	0.0°	-25.6°	-80.3°	19.3°
R5	0.437	1.000	0.479	-0.087	-0.439	0.996	-11.521	4.554	1.000	5.0°	-23.7°	-85.0°	21.5°
R10	0.437	1.000	0.479	-0.174	-0.396	0.985	1,805.611	-789.331	1.000	10.0°	-21.6°	90.0°	-23.6°
R15	0.437	1.000	0.479	-0.259	-0.350	0.966	10.690	-5.150	1.000	15.0°	-19.3°	84.7°	-25.6°
R20	0.437	1.000	0.479	-0.342	-0.301	0.940	5.146	-2.727	1.000	20.0°	-16.7°	79.0°	-27.5°
R25	0.437	1.000	0.479	-0.423	-0.250	0.906	3.272	-1.908	1.000	25.0°	-14.0°	73.0°	-29.2°
R30	0.437	1.000	0.479	-0.500	-0.196	0.866	2.318	-1.492	1.000	30.0°	-11.1°	66.7°	-30.6°
R35	0.437	1.000	0.479	-0.574	-0.142	0.819	1.734	-1.237	1.000	35.0°	-8.1°	60.0°	-31.7°
R40	0.437	1.000	0.479	-0.643	-0.086	0.766	1.334	-1.062	1.000	40.0°	-4.9°	53.1°	-32.5°
R45	0.437	1.000	0.479	-0.707	-0.030	0.707	1.039	-0.933	1.000	45.0°	-1.7°	46.1°	-32.9°
R50	0.437	1.000	0.479	-0.766	0.027	0.643	0.810	-0.833	1.000	50.0°	1.5°	39.0°	-32.9°
R55	0.437	1.000	0.479	-0.819	0.083	0.574	0.624	-0.752	1.000	55.0°	4.7°	32.0°	-32.5°
R60	0.437	1.000	0.479	-0.866	0.139	0.500	0.468	-0.683	1.000	60.0°	7.9°	25.1°	-31.8°

Assigning the x, y and z components of a CTO vector (boxes with yellow figures), fluoroscopic vectors and fluoroscopic angulations for a designated RAO angle are automatically calculated. R0~60 represent RAO angles. Negative values in cranial boxes demonstrate "caudal" angles. LAO: left anterior oblique; RAO: right anterior oblique

Thus, it is reasonable to employ images from CCTA to derive optimal fluoroscopic angulations. PCI operators need to be aware of the timing of acquisition shown on the summary of the relevant coronary CT angiography.

Although it is possible to calculate optimal fluoroscopic angulations for any CTO vectors, they sometimes do not work in practice. For example, in case of a CTO vector parallel to the Z (anteroposterior)-axis, fluoroscopic beams lie on the coronal plane, which would not be clinically applicable because of the inability to set the X-ray tube and the detector in place or an unacceptable increase in X-ray dose (Figure 9). In such cases or the actual application to PCI mentioned above, the calculator shown in **Supplementary Table 2** can be used to find the angle between the adopted "realistic" fluoroscopic vector and the CTO segment as well as the shortening rate. In this way, even if the ideal fluoroscopic angulations (where the 3 vectors are orthogonal) cannot be used, it is important to proceed with the procedure while being conscious of how obliquely the lesion is viewed and how much the lesion is shortened.

The spreadsheet software developed in this study is capable of displaying optimal fluoroscopic angulations by inputting the x, y and z components of a CTO vector. However, when the CTO vector has a y component of 0 (lying on the transverse plane), the software fails to output the correct solution due to a denominator of 0 in the formula. In such cases, assigning a very small value to the y component could yield a nearly correct solution.

This method is not applicable to bent sections, including the acute margin of the right coronary arteries. However, the optimal fluoroscopic angulations for the proximal and distal straight-line portions adjacent to bent sections, if any, can be separately calculated.

Although the methodology is relatively straightforward and does not necessitate any specialised tools or applications, the derivation

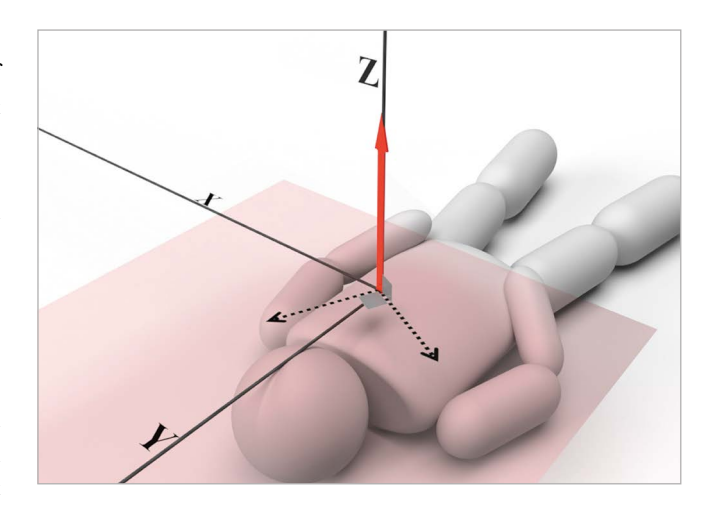


Figure 9. CTO vector parallel to the Z-axis. It is virtually impossible to continue a PCI procedure with a fluoroscopic vector on the coronal plane. Red bold arrow: CTO vector; black dotted arrows: fluoroscopic vectors. CTO: chronic total occlusion; PCI: percutaneous coronary intervention

of the CTO vector from the slab MIP may be deemed complex. To streamline this aspect, the development of an application capable of automatically computing the optimal angles by drawing CTO lines on the angiographic view of CCTA or coronary angiography would be highly advantageous. Such a tool would simplify the process and render it more accessible to a wider range of PCI operators, ultimately contributing to the advancement of the field.

Even when using biplane fluoroscopy, there may still be areas where the guidewire appears to be inside the vessel despite actually deviating outside (dead angle; blue dotted areas in **Figure 10A**). This dead angle is minimised when sin θ equals 1, which occurs when the 2 fluoroscopic lines are orthogonal to each other (**Figure 10B**).

Table 2. Recalculation table.

					F	Recalculation						
							Re	calculation				
	oroscopic Ilation	Left fluoroscopic angulation		Inner product of 2 of the 3 vectors			Right f	luoroscopic	vector	Left fluoroscopic vector		
RAO	Cranial	LAO	Cranial	CTO & Fluoro (R)	CTO & Fluoro (L)	Fluoro (R) & Fluoro (L)	Х	у	Z	х	у	Z
0.0°	-25.6°	-80.3°	19.3°	0.00	0.00	0.00	0.000	-0.479	1.000	-5.874	2.087	1.000
5.0°	-23.7°	-85.0°	21.5°	0.00	0.00	0.00	-0.087	-0.439	0.996	-11.521	4.554	1.000
10.0°	-21.6°	90.0°	-23.6°	0.00	0.00	0.00	-0.174	-0.396	0.985	1,805.611	-789.331	1.000
15.0°	-19.3°	84.7°	-25.6°	0.00	0.00	0.00	-0.259	-0.350	0.966	10.690	-5.150	1.000
20.0°	-16.7°	79.0°	-27.5°	0.00	0.00	0.00	-0.342	-0.301	0.940	5.146	-2.727	1.000
25.0°	-14.0°	73.0°	-29.2°	0.00	0.00	0.00	-0.423	-0.250	0.906	3.272	-1.908	1.000
30.0°	-11.1°	66.7°	-30.6°	0.00	0.00	0.00	-0.500	-0.196	0.866	2.318	-1.492	1.000
35.0°	-8.1°	60.0°	-31.7°	0.00	0.00	0.00	-0.574	-0.142	0.819	1.734	-1.237	1.000
40.0°	-4.9°	53.1°	-32.5°	0.00	0.00	0.00	-0.643	-0.086	0.766	1.334	-1.062	1.000
45.0°	-1.7°	46.1°	-32.9°	0.00	0.00	0.00	-0.707	-0.030	0.707	1.039	-0.933	1.000
50.0°	1.5°	39.0°	-32.9°	0.00	0.00	0.00	-0.766	0.027	0.643	0.810	-0.833	1.000
55.0°	4.7°	32.0°	-32.5°	0.00	0.00	0.00	-0.819	0.083	0.574	0.624	-0.752	1.000
60.0°	7.9°	25.1°	-31.8°	0.00	0.00	0.00	-0.866	0.139	0.500	0.468	-0.683	1.000

Right and left fluoroscopic vectors demonstrate right and left fluoroscopic vectors calculated inversely from the fluoroscopic angulations and independently of the original formulas. CTO: chronic total occlusion vector; Fluoro (L): left fluoroscopic vector; Fluoro (R): right fluoroscopic vector; LAO: left anterior oblique; RAO: right anterior oblique

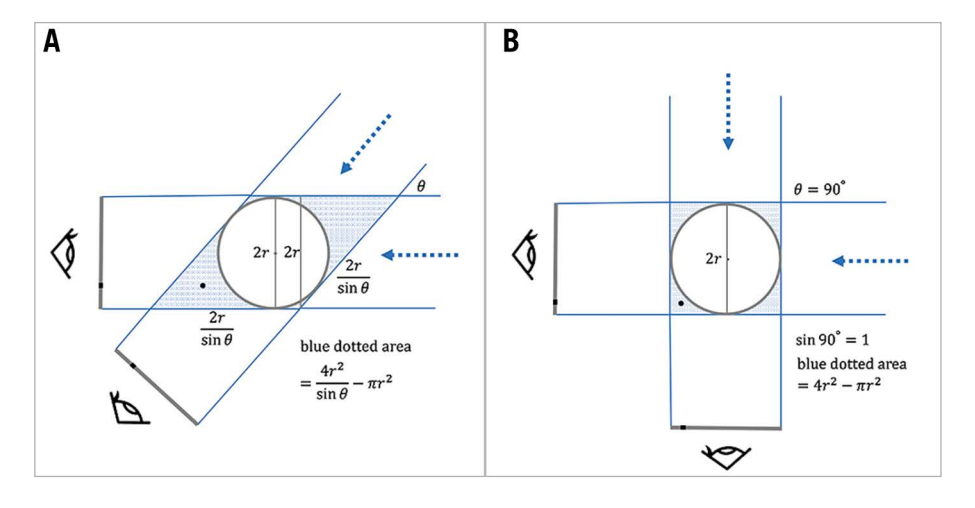


Figure 10. Dead angle with biplane fluoroscopy. A black circlet demonstrates a guidewire deviating outside the vessel. The blue dotted area demonstrates a dead angle of biplane fluoroscopy (A). It will be minimised when the fluoroscopic lines are orthogonal to each other (B).

Therefore, by minimising the dead angle that cannot be completely resolved even with biplane fluoroscopy, this method may reduce the risk of vessel perforation and improve the safety of CTO PCI.

Limitations

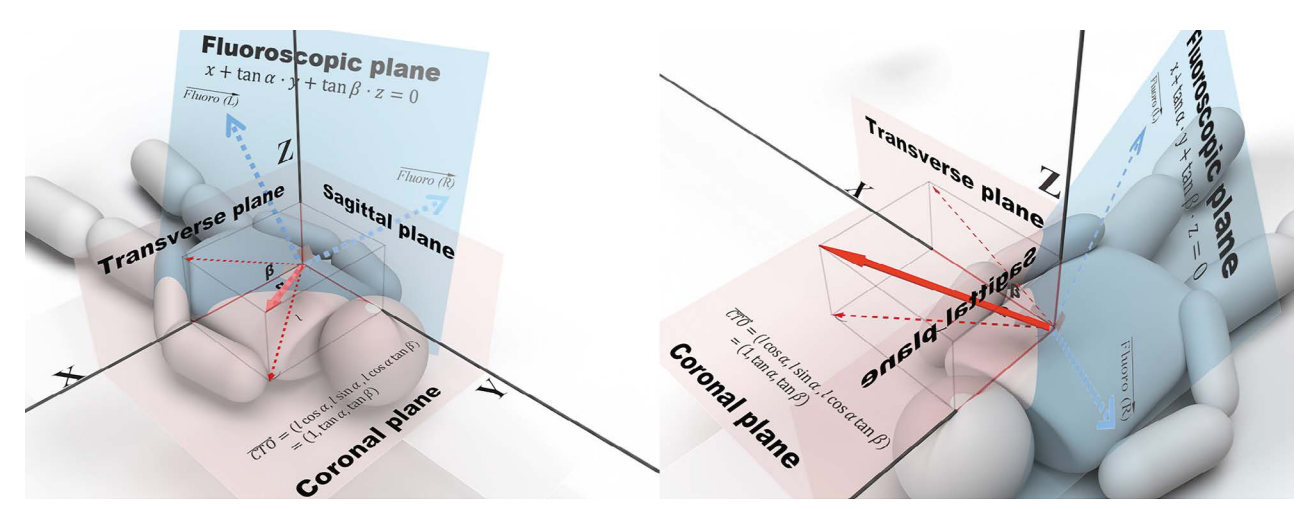
At present, this method remains theoretical and has not yet been tested in practice. Its efficacy should be evaluated in future research, taking into account the success rate of the procedure, the time required to perform it, the amount of dye and X-ray exposure, and the comfort level of the operators.

Conclusions

In this study, we present a simple approach for identifying optimal fluoroscopic angulations for CTO PCI utilising slab MIP images of CCTA and basic mathematical concepts, without specialised equipment or software. Specifically, we describe a process whereby a CTO segment can be vectorised, as outlined in the **Central illustration**. This approach has the potential to enhance the safety of CTO PCI by reducing dead angles in biplane fluoroscopy. Future research may be warranted to further investigate the effectiveness of this method.

AsiaIntervention

CENTRAL ILLUSTRATION CTO vector, fluoroscopic plane and fluoroscopic vectors.



Conceptual images at a glance. After vectorising a CTO segment using slab MIP images of CCTA and trigonometric functions, fluoroscopic vectors are calculated from the equation of a plane. They are finally translated into a combination of optimal fluoroscopic angulations. To allow readers to better understand, 2 different perspectives are shown. Note that the CTO vector and the 2 fluoroscopic vectors are orthogonal to each other. Fluoro (R): right fluoroscopic vector; Fluoro (L): left fluoroscopic vector. CCTA: coronary computed tomography angiography; CTO: chronic total occlusion; MIP: maximum intensity projection

Impact on daily practice

The proposed method detailed in this study provides precise fluoroscopic angulations that are based on the exact direction of a CTO segment, rather than relying on the subjective feelings or experiences of operators. Even if the calculated optimal angulations are not employed, operators can still appreciate the difference between the correct answer and what they observe.

Conflict of interest statement

The author has no conflicts of interest to declare.

References

- 1. Tanaka T, Okamura A, Iwakura K, Iwamoto M, Nagai H, Yamasaki T, Sumiyoshi A, Tanaka K, Inoue K, Koyama Y, Masuyama T, Ishihara M, Fujii K. Efficacy and Feasibility of the 3-Dimensional Wiring Technique for Chronic Total Occlusion Percutaneous Coronary Intervention: First Report of Outcomes of the 3-Dimensional Wiring Technique. *JACC Cardiovasc Interv.* 2019;12:545-55.
- 2. Okamura A, Iwakura K, Mutsumi I, Nagai H, Sumiyoshi A, Tanaka K, Tanaka T, Inoue K, Koyama Y, Fujii K. Tip Detection Method Using the New IVUS Facilitates the 3-Dimensional Wiring Technique for CTO Intervention. *JACC Cardiovasc Interv.* 2020;13:74-82.
- Okamura A, Iwakura K, Nagai H, Kawamura K, Yamasaki T, Fujii K. Chronic total occlusion treated with coronary intervention by three-dimensional guidewire manipulation: an experimental study and clinical experience. *Cardiovasc Interv Ther.* 2016; 31:238-44
- 4. Instructions for Use. Philips CT TrueView Release 2.0. https://www.documents.philips.com/doclib/enc/11690822/452296299191_LR.pdf. Date last accessed: 16 June 2023.
- 5. Taylor KW, McLoughlin MJ, Aldridge HE. Specification of angulated projections in coronary arteriography. *Cathet Cardiovasc Diagn*. 1977;3:367-74.
- 6. Vembar M, Garcia MJ, Heuscher DJ, Haberl R, Matthews D, Böhme GE, Greenberg NL. A dynamic approach to identifying desired physiological phases for cardiac imaging using multislice spiral CT. *Med Phys.* 2003;30:1683-93

- 7. Achenbach S, Ropers D, Holle J, Muschiol G, Daniel WG, Mashage W. In-plane coronary arterial motion velocity: measurement with electron-beam CT. *Radiology*. 2000:216:457-63.
- 8. Herzog C, Arning-Erb M, Zangos S, Eichler K, Hammerstingl R, Dogan S, Ackermann H, Vogal TJ. Multi-detector row CT coronary angiography: influence of reconstruction technique and heart rate on image quality. *Radiology*. 2006;238:75-86.
- 9. Achenbach S, Manolopoulos M, Schuhbäck A, Ropers D, Rixe J, Schneider C, Krombach GA, Uder M, Hamm C, Daniel WG, Lell M. Influence of heart rate and phase of the cardiac cycle on the occurrence of motion artifact in dual-source CT angiography of the coronary arteries. *J Cardiovasc Comput Tomogr.* 2012;6:91-8.

Supplementary data

Supplementary Table 1. Biplane optimal fluoroscopic angulations. **Supplementary Table 2.** Angle between 2 vectors and shortening rate.

Supplementary Figure 1. CTO vector represented by trigonometric functions.

Supplementary Figure 2. The right fluoroscopic vector.

Supplementary Figure 3. The left fluoroscopic vector.

Supplementary Figure 4. Slab MIP of mid-circumflex CTO.

Supplementary Figure 5. CTO vector and fluoroscopic plane.

Supplementary Figure 6. Combination of optimal fluoroscopic angulations.

Supplementary Figure 7. "Realistic" alternative fluoroscopic angulation.

Supplementary Figure 8. Fluoroscopic images from a PCI procedure.

Supplementary Figure 9. Final images of CTO PCI.

The supplementary data are published online at: https://www.asiaintervention.org/doi/10.4244/AIJ-D-22-00084



Excimer laser coronary atherectomy for acute myocardial infarction with coronary artery ectasia and massive thrombosis



Takashi Hiruma^{1,2*}, MD; Tomofumi Tanaka¹, PhD; Mamoru Nanasato¹, PhD; Mitsuaki Isobe¹, PhD

1. Department of Cardiology, Sakakibara Heart Institute, Tokyo, Japan; 2. Department of Cardiovascular Medicine, Graduate School of Medicine, The University of Tokyo, Tokyo, Japan

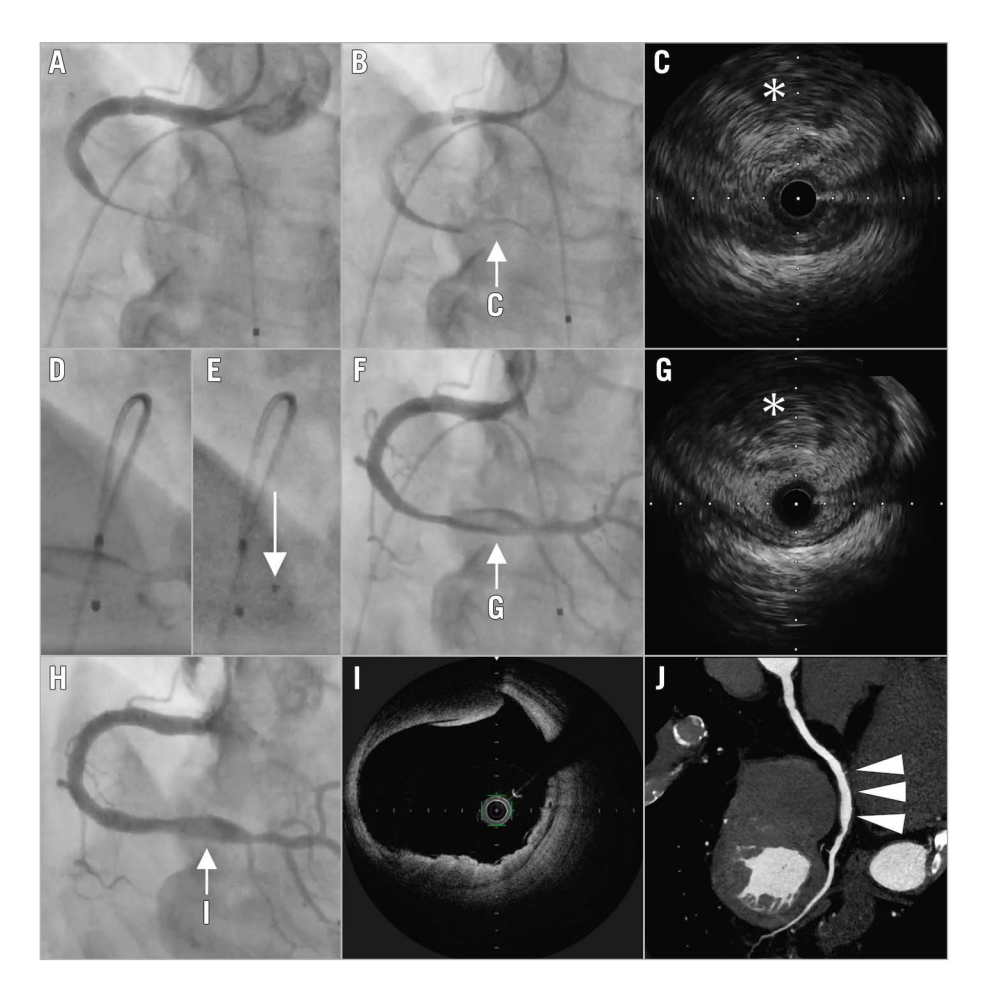


Figure 1. Excimer laser coronary atherectomy for acute myocardial infarction with coronary artery ectasia and massive thrombus. A) The initial coronary angiography (CAG) of the right coronary artery (RCA) showing total occlusion of the distal RCA (left anterior oblique cranial view). B) CAG after thrombus aspiration, showing grade 1 TIMI flow. C) Intravascular ultrasound (IVUS) depicting a massive thrombus (white asterisk). D, E) Angiography during excimer laser coronary atherectomy (ELCA; white arrow, left anterior oblique view). F) CAG after ELCA, showing grade 3 TIMI flow. G) IVUS after ELCA presented a reduction of the thrombus (white asterisk). H) CAG performed on day 6, showing almost complete disappearance of the thrombus. I) Optical frequency domain imaging demonstrating a slight mural thrombus. J) Multimodality computed tomography follow-up at the 2-year mark, showing no thrombus at the ectatic coronary artery (white arrowheads). TIMI: Thrombolysis in Myocardial Infarction

^{*}Corresponding author: Department of Cardiology, Sakakibara Heart Institute, 3-16-1 Asahi-cho, Fuchu, Tokyo 183-0003, Japan. E-mail: thiruma@shi.heart.or.jp

Percutaneous coronary intervention (PCI) for acute myocardial infarction (AMI) with coronary artery ectasia and massive thrombus remains technically challenging because standard techniques using balloon angioplasty and stenting are unsuitable for such lesions.

A 73-year-old male patient with diabetes and dyslipidaemia was referred to our hospital with a complaint of persistent chest pain. The initial electrocardiogram showed ST-segment elevation in the II, III and aVF leads. The patient was diagnosed with inferior AMI. An emergency coronary angiography (CAG) revealed that the distal right coronary artery (RCA) was completely occluded with a massive thrombus (Figure 1A). Multiple rounds of thrombus aspiration were performed, but few fibrin thrombi were removed, and Thrombolysis in Myocardial Infarction (TIMI) flow remained grade 1 (Figure 1B). Intravascular ultrasound (IVUS) revealed a markedly positive remodelled ectatic vessel exceeding 8.0 mm, filled with a massive thrombus (Figure 1C). We inserted an intraaortic balloon pump because the patient developed cardiogenic shock, and attempted to reduce the thrombus using excimer laser coronary atherectomy (ELCA). A 1.4 mm concentric-type laser catheter was passed through the lesion and pulled back at a speed of 1.0 mm/s with an additional injection of saline (initial fluency of 40 mJ/m², repetition rate of 25 Hz) (Figure 1D, Figure 1E). After the third round at the initial setting, the fluency and repetition rate subsequently increased to 60 mJ/m² and 40 Hz, respectively. While the floating thrombus remained at the ectatic lesion, TIMI flow grade 3 was achieved (Figure 1F). Additionally, IVUS showed a reduced thrombus (Figure 1G). We finalised the procedure after considering the risk of distal embolism and slow flow/no-reflow phenomenon that could be caused by additional balloon angioplasty or stenting. The patient was treated with 100 mg aspirin and 3.75 mg prasugrel daily and unfractionated heparin (target activated clotting time of 250-300 seconds) for 3 days. Subsequently, the medication was altered to 3.75 mg prasugrel and 10 mg apixaban. A CAG performed on day 6 showed the near disappearance of the thrombus (Figure 1H), and optical frequency domain imaging revealed a slight mural thrombus (Figure 11). No evident plaque ruptures were observed. At two years, multimodality computed tomography follow-up showed no thrombus (Figure 1J), and the patient was free of cardiovascular events.

Coronary artery ectasia is a strong and independent predictor of the no-reflow phenomenon after primary PCI for AMI1. ELCA is a revascularisation therapy based on the effect of a catheterguided pulsed ultraviolet excimer laser light, which vaporises the thrombus by emitting photomechanical, photochemical, and photothermal energy². In addition, exposure to the excimer laser suppresses platelet aggregation and reduces platelet force development capability, which is referred to as the "stunned platelet phenomenon"3. The standard strategy combines ELCA with adjunctive balloon angioplasty or stenting⁴. In patients with AMI, using ELCA before stenting improves procedural success and reduces in-hospital cardiovascular events⁵. Although there are limited data on ELCA use during primary PCI, our case suggests that ELCA is feasible for emergent revascularisation in ectatic coronary artery disease with a massive thrombus and favourable midterm durability.

Acknowledgements

The authors wish to thank all the members of the catheterisation room of the Sakakibara Heart Institute.

Conflict of interest statement

M. Nanasato has received a lecture fee from Boston Scientific Japan. The other authors have no conflicts of interest to declare.

References

- 1. Schram HCF, Hemradj VV, Hermanides RS, Kedhi E, Ottervanger JP; Zwolle Myocardial Infarction Study Group. Coronary artery ectasia, an independent predictor of no-reflow after primary PCI for ST-elevation myocardial infarction. *Int J Cardiol.* 2018;265:12-7.
- 2. Topaz O. Plaque removal and thrombus dissolution with the photoacoustic energy of pulsed-wave lasers-biotissue interactions and their clinical manifestations. *Cardiology*. 1996;87:384-91.
- 3. Topaz O, Minisi AJ, Bernardo NL, McPherson RA, Martin E, Carr SL, Carr ME Jr. Alterations of platelet aggregation kinetics with ultraviolet laser emission: the "stunned platelet" phenomenon. *Thromb Haemost.* 2001;86:1087-93.
- 4. Nishino M, Mori N, Takiuchi S, Shishikura D, Doi N, Kataoka T, Ishihara T, Kinoshita N; ULTRAMAN Registry investigators. Indications and outcomes of excimer laser coronary atherectomy: efficacy and safety for thrombotic lesions-The ULTRAMAN registry. *J Cardiol.* 2017;69:314-9.
- 5. Shishikura D, Otsuji S, Takiuchi S, Fukumoto A, Asano K, Ikushima M, Yasuda T, Hasegawa K, Kashiyama T, Yabuki M, Hanafusa T, Higashino Y. Vaporizing thrombus with excimer laser before coronary stenting improves myocardial reperfusion in acute coronary syndrome. *Circ J.* 2013;77:1445-52.

Myocardial ischaemia caused by two remote non-cardiac stenoses



Marina S. Guérios¹, MB; Zeferino Demartini Jr², MD; Enio E. Guérios^{3*}, MD, PhD

1. Universidade Positivo, Curitiba, Brazil; 2. Interventional Neuroradiology Department, Hospital de Clínicas da Universidade Federal do Paraná, Curitiba, Brazil; 3. Interventional Cardiology Department, Hospital de

Clínicas da Universidade Federal do Paraná, Curitiba, Brazil

This paper also includes supplementary data published online at: https://www.asiaintervention.org/doi/10.4244/AIJ-D-23-00011

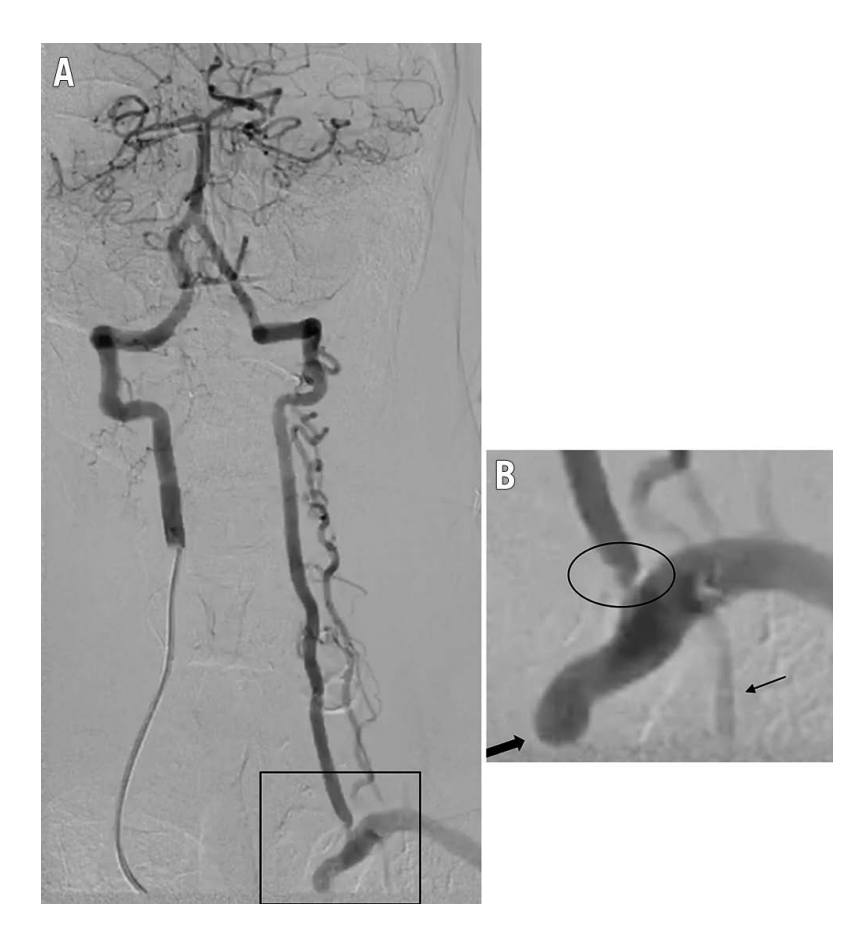


Figure 1. Right vertebral artery angiography. A) Contrast injection in the right vertebral artery shows retrograde flow of left vertebral artery supplying the left subclavian artery and left internal mammary artery (LIMA). B) Magnification depicts the left subclavian artery ostial occlusion (thick arrow), LIMA (thin arrow) and ostial left vertebral artery stenosis (circle).

^{*}Corresponding author: Interventional Cardiology Dept., Hospital de Clínicas da UFPR, Rua General Carneiro 181-Alto da Glória, Curitiba, Brazil. E-mail: enioeguerios@gmail.com

Coronary angiography was indicated for a 66-year-old female patient with a history of diabetes mellitus, dyslipidaemia and hypertension who underwent myocardial revascularisation in 2014 (left internal mammary artery [LIMA] to left anterior descending artery [LAD] and saphenous vein grafts [SVGs] to the right coronary artery [RCA] and the first obtuse marginal branch [OM]). She complained of progressive chest pain and effort dyspnoea. Her stress test was positive, and her myocardial scintigraphy showed anteroseptal ischaemia.

Angiography, performed using right femoral artery access, demonstrated chronic occlusion of the distal left main (Moving image 1), patency of both SVGs (Moving image 2, Moving image 3), no collateral vessels to the LAD and normal left ventricular (LV) function. An aortogram showed a calcified ostial occlusion of the left subclavian artery (LSA) (Moving image 4). Considering that LV function was normal and that there were no collaterals to the LAD, the LIMA-to-LAD was considered to be patent. However, since the LSA was chronically occluded proximally, with no visible collateralisation, LIMA flow could only come from the vertebral system. Hence, an angiography of the right vertebral artery (VA) was performed. It demonstrated a widely patent vessel that provided a good retrograde flow to the left VA, which had a 90% ostial stenosis (Moving image 5, Figure 1). A later Doppler ultrasound examination performed on the ward confirmed inverted flow in the left vertebral artery, compatible with subclavian steal physiology. Selective LIMA-to-LAD angiography performed by left radial artery access showed a good functioning graft, with no significant stenoses in either vessels (Moving image 6).

Although a percutaneous recanalisation of the chronically occluded LSA would naturally be the first therapeutic choice for a case like this, this procedure was considered very challenging in this specific patient, as there was no proximal tapered stump, and the occluded segment (as demonstrated by the angiography done by left radial access) was long and calcified. Angioplasty of the

ostial left VA could also potentially alleviate myocardial ischaemia, but it would probably lead to subclavian steal symptoms. Therefore, a left common carotid-to-LSA bypass was proposed as a therapeutic strategy. However, despite a full explanation of the clinical picture, the patient declined any further invasive procedure.

Patients with subclavian steal syndrome are frequently asymptomatic¹. Cardiac ischaemia, however, may occur in patients revascularised with mammary artery grafts while using their ipsilateral arm. In this case, the concomitant left ostial VA stenosis prevented subclavian steal symptoms but impaired flow to the LSA and LIMA, leading to myocardial ischaemia. The case of this patient underscores the need to look for symptoms of vertebrobasilar insufficiency and for interarm blood pressure differences in patients with myocardial ischaemia after surgical revascularisation that used one or both internal mammary arteries.

Conflict of interest statement

The authors have no conflicts of interest to declare.

References

1. Kargiotis O, Siahos S, Safouris A, Feleskouras A, Magoufis G, Tsivgoulis G. Subclavian Steal Syndrome with or without Arterial Stenosis: A Review. *J Neuroimaging*. 2016;26:473-80.

Supplementary data

Moving image 1. Left main coronary artery angiography.

Moving image 2. Saphenous vein graft to right coronary artery.

Moving image 3. Saphenous vein graft to obtuse marginal branch.

Moving image 4. Aortography.

Moving image 5. Right vertebral artery angiography.

Moving image 6. Left internal mammary artery angiography.

The supplementary data are published online at: https://www.asiaintervention.org/doi/10.4244/AIJ-D-23-00011



Commissural alignment in the Evolut TAVR procedure: conventional versus hat marker-guided shaft rotation methods



Yutaka Konami^{1,2*}, MD; Tomohiro Sakamoto¹, MD, PhD; Hiroto Suzuyama¹, MD; Eiji Horio¹, MD; Junichi Yamaguchi², MD, PhD

- 1. Division of Cardiology, Cardiovascular Center, Saiseikai Kumamoto Hospital, Kumamoto, Japan;
- 2. Department of Cardiology, Tokyo Women's Medical University, Shinjuku, Tokyo, Japan

KEYWORDS

- aortic stenosis
- coronary artery disease
- TAVR

Abstract

Background: Coronary cannulation after TAVR is sometimes difficult due to an overlap between native and neo-commissures, especially in Evolut devices with a supra-annular position. The Evolut C-tab corresponds to a neo-commissure, and the hat marker is in a fixed position. Therefore, the orientation of the hat marker can be adjusted to minimise overlaps.

Aims: We investigated whether the HAt marker-guided SHaft rotation method (HASH, stylised as the #rotation method) is effective in facilitating coronary artery access after transcatheter aortic valve replacement (TAVR) with an Evolut system.

Methods: We retrospectively analysed 95 patients who underwent electrocardiogram-gated cardiac computed tomography after TAVR. In the #rotation method, the hat marker of the delivery catheter was adjusted to face the greater curvature of the descending thoracic aorta in the left anterior oblique view. Its orientation was maintained while the system passed through the aortic arch.

Results: In total, 60 and 35 patients underwent TAVR with the #rotation and non-#rotation methods, respectively. A $\pm 15^{\circ}$ angle between the native and neo-commissures was more frequent in the #rotation group (p=0.001). Favourable angles and appropriate frame orientation for access to the left coronary artery were significantly more frequent in the #rotation group than in the non-#rotation group (p<0.001 and p=0.001). Although the #rotation method showed a higher rate of favourable angles and frames in the right coronary artery, statistically significant differences were not found.

Conclusions: The #rotation method is useful for improving commissural post alignment in TAVR with Evolut devices, especially in the ostium of the left coronary artery.

^{*}Corresponding author: Division of Cardiology, Cardiovascular Center, Saiseikai Kumamoto Hospital, 5-3-1 Chikami, Minami-ku, Kumamoto, 861-4193, Japan. E-mail: u.godwave@gmail.com

Abbreviations

#rotation method HAt marker-guided SHaft (HASH) rotation

method

CT computed tomography
LCA left coronary artery
LCC left coronary cusp

PCI percutaneous coronary intervention

RCA right coronary artery right coronary cusp

RLCC right/left coronary cusp commissure
TAVR transcatheter aortic valve replacement

THV transcatheter heart valve

Introduction

Transcatheter aortic valve replacement (TAVR) is widely accepted as a definitive therapeutic option for patients with severe aortic stenosis, and its effectiveness has been demonstrated in several randomised trials¹⁻⁶. In recent years, TAVR has demonstrated comparable results to surgical aortic valve replacement, even in surgical low-risk patients^{7,8}. As a result, the indications for TAVR have expanded to patients with longer life expectancy.

A relatively large number of patients with aortic stenosis have concomitant coronary artery disease⁹. In previous large trials, patients with aortic stenosis complicated by coronary artery disease comprised 15-81% of the study population¹⁻⁸. This variation may have been due to differences in the average age of participants. Since coronary artery disease is a progressive disease, the likelihood of developing it increases with age. As the indications for TAVR gradually shift towards younger patients, the need for post-TAVR percutaneous coronary intervention (PCI) will inevitably increase, even if there is no coronary lesion requiring intervention at the time of TAVR.

Following surgical aortic valve replacement, cannulation of the coronary arteries is relatively straightforward because the bioprosthetic valve is implanted to align the neo-commissure with the native commissures. However, it is not always possible to completely align a transcatheter heart valve (THV) with the native commissures in a TAVR procedure. Therefore, the THV neo-commissure is sometimes positioned to face the ostium of the coronary artery¹⁰. A prosthesis in the Evolut (Medtronic) series can be placed in a unique supra-annular position, which may further complicate the process of engaging a catheter in cases where the THV neo-commissure faces the coronary artery¹¹.

Aligning the THV neo-commissure with the native commissure can facilitate coronary access after TAVR, especially when using Evolut devices. Therefore, we investigated whether it is possible to implant an Evolut device in a manner that allows access to the coronary artery after TAVR. To do this, we adjusted the direction of the delivery catheter, taking into account the structural characteristics of the Evolut device.

Methods

STUDY POPULATION

In this study, we enrolled patients with severe aortic stenosis who had undergone TAVR with an Evolut device at the Cardiovascular

Center of Saiseikai Kumamoto Hospital between March 2019 and April 2022 and who had postoperative electrocardiogram-gated contrast-enhanced cardiac computed tomography (CT) imaging. During the first half of the study period, TAVR was performed using the conventional technique, in which the delivery catheter was advanced normally into the body to the aortic position. All of these patients underwent contrast-enhanced CT at the time of their outpatient visit, unless they met the exclusion criteria. In the latter half, all patients underwent TAVR with adjustment of the delivery catheter direction. Any patients who did not meet the exclusion criteria underwent contrast-enhanced CT during hospitalisation. We excluded the following cases from analysis: 1) TAVR performed with approaches other than the transfemoral approach; 2) TAVR for failed surgical bioprostheses; 3) TAVR for a bicuspid aortic valve; 4) an estimated glomerular filtration rate <30 ml/ min/1.73 m² (increased risk of worsening renal function due to the use of contrast media); 5) lack of patient consent for the use of contrast media (Figure 1).

INTENTIONAL DELIVERY FOR COMMISSURAL ALIGNMENT

The method used to orient the hat marker and place it at the aortic valve was called the HAt marker-guided SHaft (HASH) rotation method (stylised as the #rotation method in this study) (Figure 2). When the delivery system was initially inserted into the body, the flush port was oriented at 3 o'clock. Next, we used the left anterior oblique view to check whether the hat marker was facing the side of the greater curvature of the descending thoracic aorta. If not, the shaft of the delivery system was rotated so that the hat marker faced the side of the greater curvature. This orientation of the hat marker was maintained while the delivery system was passed through the aortic arch to just above the aortic valve. Thereafter, the angle of the fluoroscopy system was changed to the cusp-overlap view of the right and left coronary cusps (RCC/LCC). The THV was implanted after confirming that the hat marker was positioned centre front on the fluoroscopic display. Even though the hat marker was displaced from the centre front position in this location in the aortic valve, rotation of the delivery system in this position was not performed because of concerns about the potential risk of access route injury. We also did not pull the delivery system back to the descending aorta, because we thought it would increase the risk of cerebral infarction. The non-#rotation method in this study was the conventional technique, in which the flush port orientation was at 12 o'clock at insertion and the orientation of the hat marker was unknown after insertion.

ELECTROCARDIOGRAM-GATED CARDIAC CT IMAGES

Electrocardiogram-gated cardiac CT was performed with a collimation of 320x0.5 mm. The range of tube current values was automatically set for each patient under model-based iterative reconstruction conditions, and the tube potential was fixed at 100 kV. Images were reconstructed in 0.5 mm thick slices at 0.5 mm intervals with no overlap. Iterative reconstruction was performed with RR intervals of 10% ranging from 0% to 90%. CT images

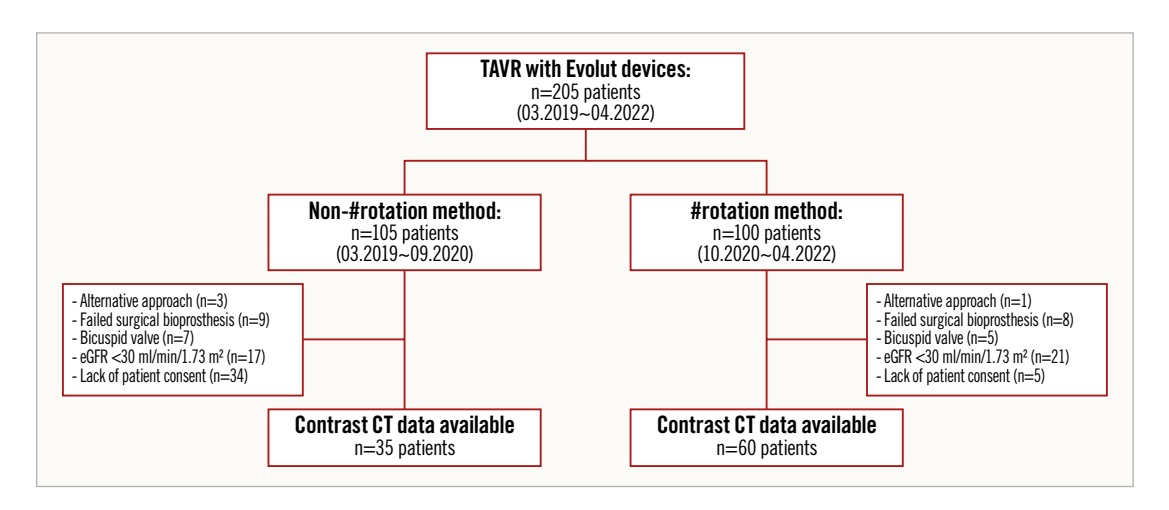


Figure 1. Patient flow diagram and study design. #rotation method: HAt marker-guided Shaft (HASH) rotation method; CT: computed tomography; eGFR: estimated glomerular filtration rate; TAVR: transcatheter aortic valve replacement

were reconstructed using the 3mensio Valves software (version 9.1; Pie Medical Imaging) and analysed in our dedicated core laboratory. The relationships between the THV neo-commissure and the coronary artery (right: RCA; left: LCA) ostia were evaluated with end-diastolic CT data. First, 3 orthogonal planes were used for multiplanar reconstruction to create a centreline orthogonal to the THV and to locate each THV neo-commissure. The inflow level of each THV was checked, and the distance between the THV inflow and the inferior border of each ostium of the coronary

artery was measured. The angle between the native right/left coronary cusp (RLCC) commissure and the C-tab commissure was also evaluated (Figure 3).

STUDY ENDPOINTS

The primary endpoint of this study was to orient the THV frames such that they faced the LCA/RCA ostium to a degree that allowed coronary access after TAVR. As a secondary endpoint, we evaluated whether the angle between the C-tab commissure and the

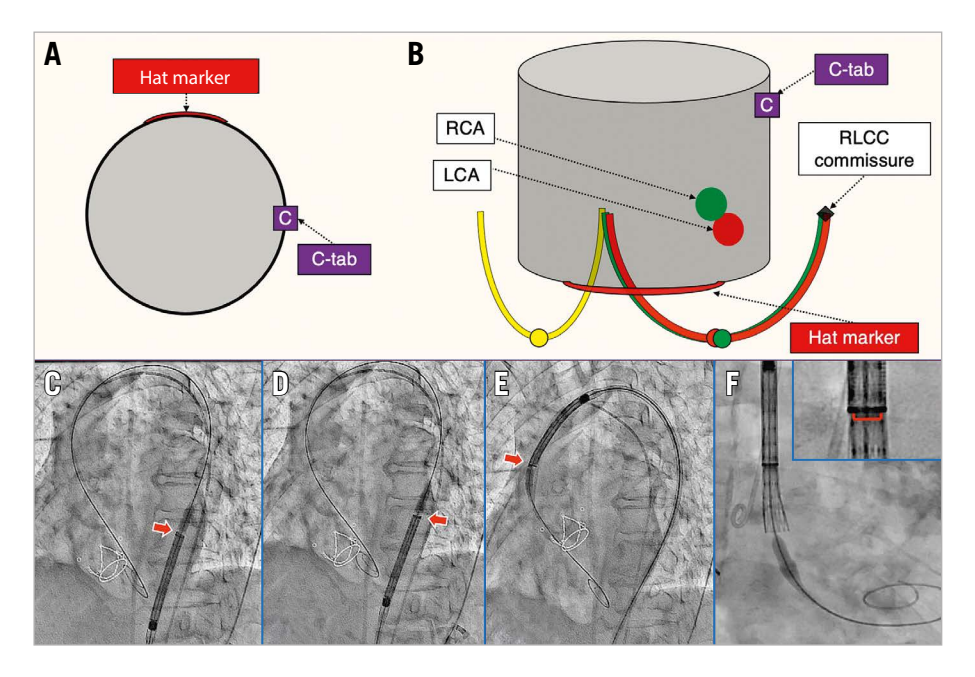


Figure 2. The #rotation method. A) Positional relationship between the hat marker and the C-tab of the THV. B) The aortic valve viewed from the angle of overlap between the RCC (green curve) and LCC (red curve). When the hat marker is located in the centre front position, the C-tab is located near the native RLCC commissure. C,D) The hat marker (red arrow) should face the greater curvature of the descending thoracic aorta. Otherwise, the shaft of the delivery catheter should be rotated. E) If the hat marker passes through the aortic arch facing the greater curvature, it is positioned centre front (red arrow) at the position of the aortic valve (F). #rotation method: HAt marker-guided SHaft (HASH) rotation method; LCA: left coronary artery; LCC: left coronary cusp; RCA: right coronary artery; RCC: right coronary cusp; RLCC: right/left coronary cusp; THV: transcatheter heart valve

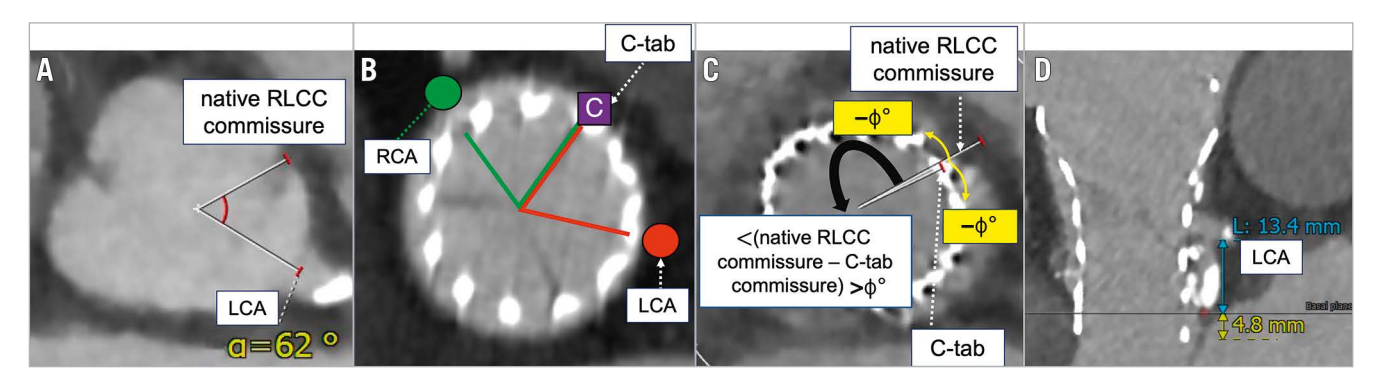


Figure 3. Examples of cardiac computed tomography measurements. Angles between (A) the native RLCC commissure and the LCA; B) the C-tab commissure and the RCA or LCA; and (C) the C-tab commissure and the native RLCC commissure. When the native RLCC commissure is oriented clockwise or counterclockwise relative to the C-tab, the angle is indicated with a positive or negative value, respectively. D) The distance between the THV inflow and the inferior border of the LCA ostium (total length of the blue and yellow lines). LCA: left coronary artery; LCC: left coronary cusp; RCA: right coronary artery; RCC: right/left coronary cusp; THV: transcatheter heart valve

LCA/RCA ostium was suitable for coronary access after TAVR. In Evolut devices, the structure of the prosthetic valve varies according to its size. Therefore, favourable angles (relative to the C-tab commissure) for coronary access were defined as 24-96° for the 23 mm valves and 36-84° for valves sized 26, 29, and 34 mm. These estimates accounted for the fact that angles that overlap with the commissural triangles of the THV should be avoided. In this study, we used THV frames without a commissural triangle or skirt.

ETHICAL STATEMENT

The study was conducted according to the principles of the Declaration of Helsinki, and the protocol was approved by the institutional review board or ethics committee of each participating centre. All participating patients gave written/oral consent.

STATISTICAL ANALYSIS

Continuous variables were denoted as the mean±standard deviation (SD) or median (interquartile range [IQR]), as appropriate. Categorical variables were reported as numbers and percentages. Continuous variables were compared using the Student's t-test or Wilcoxon signed-rank sum test, depending on the distribution of the variables. Categorical variables were compared using either the chi-squared test or Fisher's exact test, depending on the frequencies in the contingency table. The JMP Pro software (version 16; SAS Institute) was used for all statistical analyses. A 2-sided p-value<0.05 was considered to indicate statistical significance.

Results

Data were analysed from a total of 95 patients, including 35 who underwent TAVR with other methods (the non-#rotation group) and 60 who underwent TAVR with the #rotation method. The overall mean age was 84.6 years, and 66.3% of the participants were women, with no significant differences between the 2 groups (Table 1). There were no between-group differences in

renal function or history of coronary artery disease. Preoperative transthoracic echocardiography showed that the severity of aortic stenosis was similar across groups.

There were no between-group differences in the size of the THV, fluoroscopy time, or the percentage of patients who underwent TAVR using an in-line sheath (**Table 2**). In the #rotation method group, 42 patients (70.0%) did not require manual rotation of the delivery catheter to properly orient the hat marker, and 18 patients (30.0%) required manual rotation. Among cases that required rotation, no case presented any difficulty in maintaining the orientation of the hat marker while the delivery system was passed through the aortic arch. The #rotation method did not increase the risk of vascular complications or postoperative cerebral infarction. On the other hand, in the non-#rotation group, only 23 out of 35 patients had a fluoroscopic record that could confirm the orientation of the hat marker as it passed through the aortic arch. Among them, the hat marker faced the greater curvature in 47.8% (11/23 patients).

In the preoperative electrocardiogram-gated cardiac CT, the angles between the native RLCC commissure and the respective coronary artery were 62.5±10.1° (LCA) and 77.0±14.2° (RCA) (**Table 3**). The height of the coronary artery from the basal annular plane was 12.7±2.5 mm (for the LCA) and 16.0±2.6 mm (for the RCA). There were no significant differences in these anatomical characteristics between the non-#rotation and #rotation groups.

We also compared postoperative electrocardiogram-gated cardiac CT imaging data between the groups (**Table 3**). The mean angles between the native RLCC and C-tab commissures were not significantly different between groups (non-#rotation: -8.0° ; #rotation: 3.0° ; p=0.79). However, the C-tab commissure was placed within $\pm 30^{\circ}$ of the native RLCC commissure more frequently in the #rotation group than in the non-#rotation group (#rotation: 53 patients, 88.3%; non-#rotation: 13 patients, 42.9%; p<0.001). Similar results were noted when the angle was limited to $\pm 15^{\circ}$ (#rotation: 34 patients, 56.7%; non-#rotation: 7 patients,

Table 1. Baseline clinical and echocardiographic characteristics of patients.

	AII (n=95)	#rotation method (n=60)	Non-#rotation method (n=35)	<i>p</i> -value (#rotation method vs non-#rotation method)
Age, years	84.6±5.1	84.8±5.5	84.2±4.4	0.578
Female	63 (66.3)	37 (61.7)	25 (71.4)	0.378
BMI, kg/m ²	22.9±3.2	22.5±2.7	23.5±3.9	0.147
STS score, %	5.2±2.6	5.2±2.6	5.2±2.7	0.93
eGFR, ml/min/1.73 m ²	53.9±15.6	52.3±16.3	56.7±14.0	0.181
BNP, pg/dl	157.0 [55.9, 291.8]	172.0 [54.9, 372.7]	122.9 [57.1, 220.9]	0.241
Coronary artery disease	23 (24.2)	17 (28.3)	6 (17.1)	0.321
Atrial fibrillation	18 (18.9)	13 (21.7)	5 (14.3)	0.429
Prior permanent pacemaker	8 (8.4)	7 (11.7)	1 (2.9)	0.251
LVEF, %	64.0 [59.5, 68.0]	63.0 [55.8, 66.0]	66.0 [64.0, 69.5]	0.004
Peak aortic velocity, m/s	4.6±0.6	4.6±0.7	4.6±0.5	0.992
Aortic valve area, cm ²	0.67±0.16	0.66±0.17	0.67±0.13	0.759

Values are n (%), mean±SD, or median [interquartile range]. #rotation method: HAt marker-guided SHaft (HASH) rotation method; BMI: body mass index; BNP: brain natriuretic peptide; eGFR: estimated glomerular filtration rate; LVEF: left ventricular ejection fraction; SD: standard deviation; STS: Society of Thoracic Surgeons

22.9%; p=0.001). This indicated that C-tab commissures placed with the #rotation method were more closely aligned with the native RLCC commissures (Figure 4).

The angle between the C-tab commissure and the LCA was significantly smaller in the #rotation group than in the non-#rotation group (#rotation: $67.1\pm20.9^{\circ}$; non-#rotation: $90.2\pm30.1^{\circ}$; p<0.001). However, there was no between-group difference in the angle of the C-tab commissure relative to the RCA (#rotation: $76.5\pm23.0^{\circ}$; non-#rotation: $81.9\pm33.5^{\circ}$; p=0.348). Favourable angles for post-TAVR access to the LCA were significantly more frequent in the #rotation group (#rotation: 55 patients, 91.7° ; non-#rotation: 19 patients, 62.9° ; p=0.001). For access to the RCA, there was no significant between-group difference in the frequency of

favourable angles (#rotation: 50 patients, 83.3%; non-#rotation: 24 patients, 68.6%; p=0.125) (**Figure 5**).

The distance between the THV inflow and the inferior border of each ostium of the coronary artery was not significantly different between groups in either the LCA or the RCA. To visualise the positional relationship between the THV and the coronary artery, we generated a scatter plot with the angle between the C-tab commissure and the coronary artery on the horizontal axis and the distance between the THV inflow and the inferior border of the ostium of the coronary artery on the vertical axis (**Figure 6**). The sample size in the group with the 23 mm prosthetic valve was too low for statistical comparisons. Therefore, we compared the data among patients who had received the 26, 29, and 34 mm

Table 2. Procedural characteristics.

Procedural characteristics					
		All (n=95)	#rotation method (n=60)	Non-#rotation method (n=35)	<i>p</i> -value (#rotation method vs non-#rotation method)
mm	23	5 (5.3)	3 (5.0)	2 (5.7)	0.406
	26	52 (54.7)	31 (51.7)	21 (60.0)	
	29	33 (34.7)	21 (35.0)	12 (34.3)	
	34	5 (5.3)	5 (8.3)	0 (0)	
Contrast dye,	ml	62.5 [59.0, 85.0]	57.0 [47.0, 78.5]	70.0 [57.0, 101.0]	0.004
Fluoroscopy t	ime, min	24.8 [19.9, 28.8]	24.8 [21.1, 29.3]	24.9 [18.4, 27.7]	0.391
In-line sheath	1	85 (89.5)	55 (91.7)	30 (85.7)	0.49
Rotation of d	elivery system	18 (18.9)	18 (30.0)	0 (0)	< 0.001
Complication	S	18 (18.9)	8 (13.3)	10 (28.6)	0.102
Vascular com	plications	8 (8.4)	2 (3.3)	6 (17.1)	0.048
Cerebral infar	rction	3 (3.2)	3 (5.0)	0 (0)	0.295
New pacemaker implantation 8 (8.4)		8 (8.4)	4 (6.7)	4 (11.4)	0.461

Values are n (%), mean±SD, or median [interquartile range]. #rotation method: HAt marker-guided SHaft (HASH) rotation method; SD: standard deviation; THV: transcatheter heart valve

Table 3. Baseline and post-TAVR findings on multislice computed tomography.

-				
	AII (n=95)	#rotation method (n=60)	Non-#rotation method (n=35)	<i>p</i> -value (#rotation method vs non-#rotation method)
Baseline MSCT				
Area, mm ²	400±65	410±68	377±53	0.027
Perimeter, mm	72.2±5.7	73.1±6.1	70.4±4.6	0.046
LCA height, mm	12.7±2.5	12.9±2.5	12.1±2.2	0.133
RCA height, mm	16.0±2.6	16.3±2.6	15.3±2.6	0.092
<(native RLCC commissure - LCA), °	62.5±10.1	62.8±10.4	62.0±9.5	0.728
<(native RLCC commissure - RCA), $^{\circ}$	77.0±14.2	78.6±13.0	73.7±16.2	0.13
Post-TAVR MSCT				
THV inflow to LCA ostium	18.1±3.8	18.4±4.0	17.7±3.3	0.4
THV inflow to RCA ostium	19.2±4.1	19.5±3.7	18.6±4.8	0.333
<(C-tab commissure - LCA), °	75.6±27.0	67.1±20.9	90.2±30.1	< 0.001
<(C-tab commissure - RCA), °	78.5±27.3	76.5±23.0	81.9±33.5	0.348
<(C-tab commissure - native RLCC commissure), °	3.0 [-23.0, 16.0]	3.0 [-16.0, 14.0]	-8.0 [-31.0, 64.5]	0.796

Values are n (%), mean±SD, or median [interquartile range]. #rotation method: HAt marker-guided SHaft (HASH) rotation method; LCA: left coronary artery; MSCT: multislice computed tomography; RCA: right coronary artery; RLCC: right/left coronary cusp; SD: standard deviation; TAVR: transcatheter aortic valve replacement: THV: transcatheter heart valve

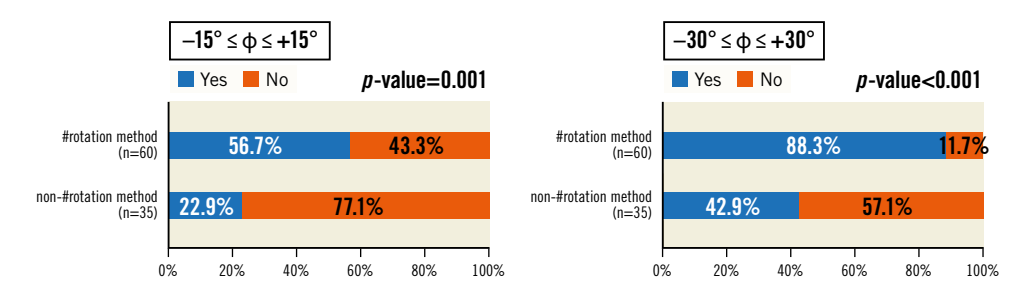


Figure 4. Angles between the native RLCC commissure and C-tab commissure (φ). The percentage of patients in whom the C-tab commissure is placed at $\pm 15^{\circ}$ relative to the native RLCC commissure is significantly higher in the #rotation group (56.7%) than in the non-#rotation group (22.9%). The percentage in the #rotation group is even higher (88.3%) when the permitted angle is increased to $\pm 30^{\circ}$. #rotation method: HAt marker-guided SHaft (HASH) rotation method; RLCC: right/left coronary cusp

prosthetic valves. The orientation of the THV frame facilitated post-TAVR access to the LCA more frequently in the #rotation group (#rotation: 52 patients, 91.2%; non-#rotation: 21 patients, 63.6%; p=0.001). However, the #rotation method did not provide such an advantage in the RCA (#rotation: 47 patients, 82.4%; non-#rotation: 24 patients, 72.4%; p=0.34).

Discussion

We investigated whether an Evolut THV can be oriented in a way that facilitates coronary access after TAVR. To achieve this, we adjusted the orientation of the hat marker on the delivery system when positioning it at the aortic valve. The main results of this study are summarised below.

- Compared with non-#rotation methods, the #rotation method allowed us to place the C-tab commissure closer to the native RLCC commissure.
- 2. The LCA ostium did not face the commissural triangle of the THV and was positioned at a more favourable angle for

- coronary artery access in the #rotation group than in the non-#rotation group. In contrast, there was no significant betweengroup difference in the angle in the RCA.
- 3. When distances between the THV inflow and the coronary artery ostia were considered in addition to the orientation of the THV, the #rotation group had a higher probability of favourable frame alignment for post-TAVR access to the LCA than the non-#rotation group.

As the indications for TAVR expand to include low-risk and younger patients, the number of patients who require post-TAVR PCI is expected to increase. Although there are limited data regarding the incidence of coronary events after TAVR, acute coronary syndrome after TAVR is known to result in high mortality¹². Several factors complicate post-TAVR coronary access, including device-related and procedural factors (such as the orientation of the commissural tab, height of the sealing skirt, and depth of the valve implant) and the patient's anatomy¹³. The orientation of the THV is particularly important for coronary access when using

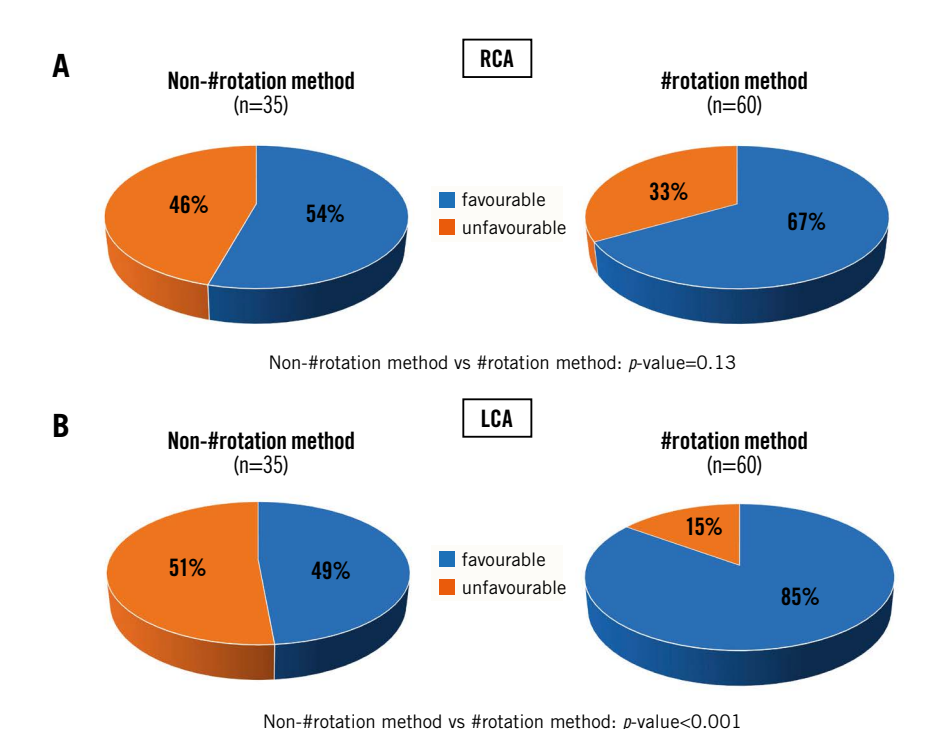


Figure 5. Incidence of favourable angles for post-TAVR coronary access. A) The percentage of patients with a favourable angle between the C-tab commissure and the ostium of the RCA is higher in the #rotation group, but the difference is not significantly significant. B) This difference is statistically significant in the LCA. #rotation method: HAt marker-guided SHaft (HASH) rotation method LCA: left coronary artery; RCA: right coronary artery; TAVR: transcatheter aortic valve replacement

Evolut prosthetic valves, as these have a taller frame than other devices¹⁴.

Coronary access after THV implantation is a major concern after TAVR and has been the subject of many studies^{10,13-17}. Aligning the THV neo-commissure with the native commissure can greatly facilitate coronary access after TAVR¹⁸. In Evolut valves, the C-tab paddle is located at a 90° angle clockwise from the hat marker on the delivery catheter¹⁹. Since the C-tab paddle coincides with one of the THV neo-commissures, adjusting the hat marker to the proper orientation can enable the proper deployment of the C-tab commissure. Normally, when the hat marker passes through the aortic arch facing the greater curvature of the descending thoracic aorta in the left anterior oblique view, it is also at the centre front in the RCC/LCC cusp-overlap view. In these cases, the native RLCC commissure is located at the left edge of the fluoroscopic display in the RCC/LCC cusp-overlap view. The hat marker being in the centre front indicates that the C-tab commissure is close to the native RLCC commissure.

Tang et al have recommended that the delivery system be inserted with the flush port oriented towards the 3 o'clock position, and the hat marker be tracked to see whether it faces the greater curvature in the aortic arch and is positioned in the centre front of the aortic valve position or not¹⁷. Compared with the conventional method, this method has a higher probability of implanting the prosthetic valve in the preferred orientation. However, it

is not clear how often the hat marker did not face the greater curvature and whether they rotated the delivery system that way. The vascular tortuosity in the iliac artery and abdominal aorta has an impact on the direction of the hat marker at the aortic arch. Indeed, approximately 30% of the cases in this study required rotation of the delivery system, even though the flush port was inserted in the 3 o'clock position.

Bieliauskas et al reported that adjusting the orientation of the THV based on the fluoroscopic marker on the delivery catheter is useful for neo-commissural alignment²⁰. Our present study differs from this view in two respects. First, the authors evaluated the angle deviations between the native aortic valve commissures and the THV neo-commissures, whereas we examined the angle between the C-tab commissure and the LCA or RCA. Second, they rotated the delivery catheter at the level of the aortic valve, whereas we rotated it at the level of the descending thoracic aorta. The Evolut delivery system has 2 shaft spines that face each other. Therefore, adjusting the orientation of the hat marker after crossing the aortic arch is difficult in terms of operability and is not recommended because of the risk of vascular injury and damage to the delivery catheter²¹. Therefore, if the orientation of the delivery system needs to be adjusted, this should be done before it passes through the aortic arch. Our results suggest that adjustment at the level of the descending thoracic aorta is appropriate.

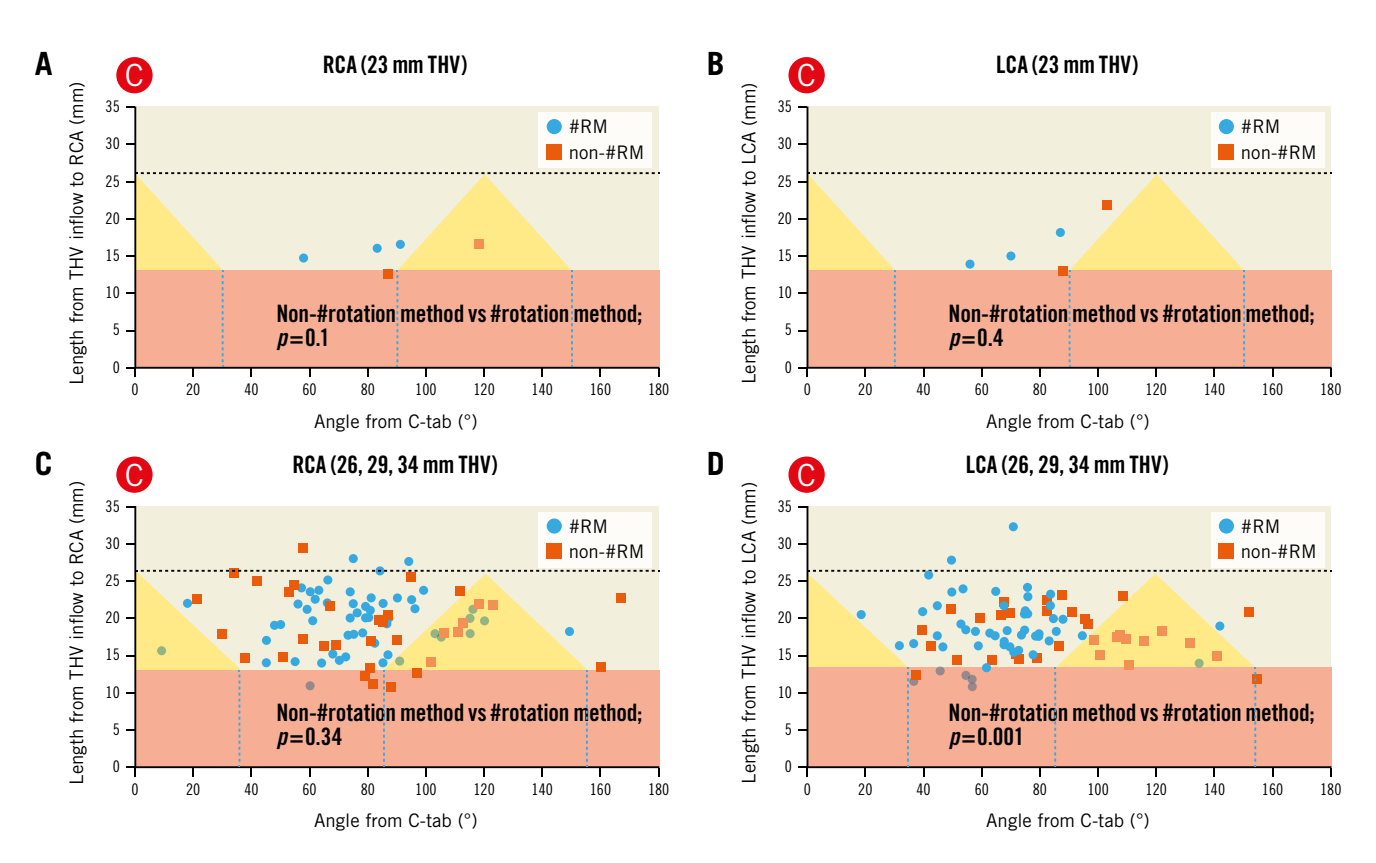


Figure 6. Favourable orientation of THV cells for post-TAVR coronary access. A, B) The x-axes show the angle between the C-tab commissure and the ostium of the coronary artery. The y-axes show the distance between the THV inflow and the ostium of the coronary artery. The pink and yellow areas correspond to the skirt and commissural triangle, respectively. The blue circles and orange squares represent the ostium of the coronary artery in the #rotation and non-#rotation groups, respectively. THVs with a size of 23 mm were excluded from analysis due to a low sample size. C) There is no between-group difference for THVs ≥26 mm with regard to coronary access to the RCA. D) The #rotation method is superior for coronary access to the LCA. #rotation method: HAt marker-guided SHaft (HASH) rotation method; LCA: left coronary artery; RCA: right coronary artery; RM: rotation method; TAVR: transcatheter aortic valve replacement; THV: transcatheter heart valve

In TAVR with Evolut devices, THV positions which are unfavourable for future coronary access are more common in the LCA than in the RCA¹⁰. In general, the LCA is a more important myocardial perfusion territory than the RCA. As such, ensuring access to the LCA is essential for long-term prognosis after TAVR. The present study shows that the LCA is located approximately 60° clockwise from the native RLCC commissure. Therefore, placing the C-tab commissure closer to the native RLCC commissure can reduce the risk of the LCA ostium facing the commissural triangle of the THV. Moreover, the LCA tends to be closer to the basal annular plane than the RCA. Considering the presence of the sealing skirt, it is important to have a preoperative plan that adjusts the orientation of the THV in the #rotation method and also places it at a depth that takes into account the height of the coronary artery.

Previous studies have also reported that the success rate of post-TAVR coronary angiography is lower for the RCA than for the LCA²². Unfortunately, the #rotation method failed to demonstrate superiority over the conventional method in facilitating access to the RCA after TAVR. This may be because, compared

with the LCA, the RCA is oriented at a larger angle (~80° clockwise) relative to the native RLCC commissure. This makes the RCA more susceptible to the effects of misalignment between the C-tab commissure and the native RLCC commissure. If the C-tab commissure could be aligned with the RCA-LCA-centred line instead of the native RLCC commissure, it would be more favourable for access to both coronary arteries. However, it is technically difficult to align with the RCA-LCA-centred line at present. Furthermore, it is generally known that the RCA ostium is more eccentric than the LCA ostium²³. Additionally, in this study, the angle from the native RLCC to the RCA ostium had a greater variation than the angle to the LCA ostium, which may also have contributed to the lower percentage of cases where access to the RCA was maintained. However, it was still possible to obtain a favourable orientation for coronary access in 83.3% of participants in this study, and this percentage is relatively acceptable. To increase the success rate of access to the RCA, devices need to evolve so that the orientation of the C-tab commissure more accurately matches that of the native RLCC commissure.

Limitations

This study has some limitations. First, this was a single-centre, retrospective, observational study, and the possibility of patient selection bias is undeniable. However, consecutive patients were enrolled with the same criteria for both groups, and the results of the non-#rotation group were comparable to previous studies. Second, the orientation of the delivery catheter in the #rotation method was not adjusted in the aortic valve position but in the descending aorta. Therefore, there was some deviation from the ideal orientation at the position of the aortic valve. Moreover, the position of the hat marker might deviate from the centre front at the aortic valve position due to too much torque during the passage through the aortic arch. Future improvements in devices may allow us to safely change the orientation of the THV at the level of the aortic valve. Third, we evaluated the ease of coronary access from the direction of the implanted prosthetic valve but did not attempt to engage the catheter in the coronary arteries. The ease of coronary access is also related to anatomical factors, such as the width of the sinus of Valsalva, length and calcification of the valve leaflet, and other device-related factors (such as the frame of the prosthetic valve).

Conclusions

The #rotation method allowed the C-tab commissure of Evolut to be positioned near the native RLCC commissure. This significantly improved the probability of achieving a favourable THV orientation for postoperative coronary access, especially for the LCA.

Impact on daily practice

Close alignment between the transcatheter heart valve (THV) neo-commissure and native commissure reduces the risk of overlap between the coronary artery and the THV neo-commissure. The hat marker of the delivery catheter and the C-tab of the THV are in a fixed position, and the C-tab coincides with the THV neo-commissure. By adjusting the orientation of the hat marker on the fluoroscopic display, it may be possible to implant the Evolut so that the C-tab commissure is adjacent to the native commissure.

Acknowledgements

The authors thank Dr Eiji Taguchi, Dr Toshiharu Sassa, Dr Ichiro Ideta, Dr Tomoko Nakayama, Dr Masahiro Yamada and Dr Youko Horibata for useful discussions; the Heart Team of the Saiseikai Kumamoto Hospital Cardiovascular Center for years of collaboration and advice; and Ms Naoko Takahashi (Saiseikai Kumamoto Hospital) for her statistical assistance.

Conflict of interest statement

T. Sakamoto is a clinical proctor of the Evolut TAVR system. The other authors have no conflicts of interest to declare.

References

- 1. Smith CR, Leon MB, Mack MJ, Miller DC, Moses JW, Svensson LG, Tuzcu EM, Webb JG, Fontana GP, Makkar RR, Williams M, Dewey T, Kapadia S, Babaliaros V, Thourani VH, Corso P, Pichard AD, Bavaria JE, Herrmann HC, Akin JJ, Anderson WN, Wang D, Pocock SJ; PARTNER Trial Investigators. Transcatheter versus surgical aortic-valve replacement in high-risk patients. *N Engl J Med.* 2011;364:2187-98.
- 2. Adams DH, Popma JJ, Reardon MJ, Yakubov SJ, Coselli JS, Deeb GM, Gleason TG, Buchbinder M, Hermiller J Jr, Kleiman NS, Chetcuti S, Heiser J, Merhi W, Zorn G, Tadros P, Robinson N, Petrossian G, Hughes GC, Harrison JK, Conte J, Maini B, Mumtaz M, Chenoweth S, Oh JK; U.S. CoreValve Clinical Investigators. Transcatheter aortic-valve replacement with a self-expanding prosthesis. *N Engl J Med.* 2014;370: 1790-8
- 3. Leon MB, Smith CR, Mack M, Miller DC, Moses JW, Svensson LG, Tuzcu EM, Webb JG, Fontana GP, Makkar RR, Brown DL, Block PC, Guyton RA, Pichard AD, Bavaria JE, Herrmann HC, Douglas PS, Petersen JL, Akin JJ, Anderson WN, Wang D, Pocock S; PARTNER Trial Investigators. Transcatheter aortic-valve implantation for aortic stenosis in patients who cannot undergo surgery. *N Engl J Med.* 2010;363: 1597-607
- 4. Popma JJ, Adams DH, Reardon MJ, Yakubov SJ, Kleiman NS, Heimansohn D, Hermiller J Jr, Hughes GC, Harrison JK, Coselli J, Diez J, Kafi A, Schreiber T, Gleason TG, Conte J, Buchbinder M, Deeb GM, Carabello B, Serruys PW, Chenoweth S, Oh JK; CoreValve United States Clinical Investigators. Transcatheter aortic valve replacement using a self-expanding bioprosthesis in patients with severe aortic stenosis at extreme risk for surgery. *J Am Coll Cardiol.* 2014;63:1972-81.
- 5. Leon MB, Smith CR, Mack MJ, Makkar RR, Svensson LG, Kodali SK, Thourani VH, Tuzcu EM, Miller DC, Herrmann HC, Doshi D, Cohen DJ, Pichard AD, Kapadia S, Dewey T, Babaliaros V, Szeto WY, Williams MR, Kereiakes D, Zajarias A, Greason KL, Whisenant BK, Hodson RW, Moses JW, Trento A, Brown DL, Fearon WF, Pibarot P, Hahn RT, Jaber WA, Anderson WN, Alu MC, Webb JG; PARTNER 2 Investigators. Transcatheter or Surgical Aortic-Valve Replacement in Intermediate-Risk Patients. N Engl J Med. 2016;374:1609-20.
- 6. Reardon MJ, Van Mieghem NM, Popma JJ, Kleiman NS, Søndergaard L, Mumtaz M, Adams DH, Deeb GM, Maini B, Gada H, Chetcuti S, Gleason T, Heiser J, Lange R, Merhi W, Oh JK, Olsen PS, Piazza N, Williams M, Windecker S, Yakubov SJ, Grube E, Makkar R, Lee JS, Conte J, Vang E, Nguyen H, Chang Y, Mugglin AS, Serruys PW, Kappetein AP; SURTAVI Investigators. Surgical or Transcatheter Aortic-Valve Replacement in Intermediate-Risk Patients. *N Engl J Med.* 2017;376:1321-31.
- 7. Mack MJ, Leon MB, Thourani VH, Makkar R, Kodali SK, Russo M, Kapadia SR, Malaisrie SC, Cohen DJ, Pibarot P, Leipsic J, Hahn RT, Blanke P, Williams MR, McCabe JM, Brown DL, Babaliaros V, Goldman S, Szeto WY, Genereux P, Pershad A, Pocock SJ, Alu MC, Webb JG, Smith CR; PARTNER 3 Investigators. Transcatheter Aortic-Valve Replacement with a Balloon-Expandable Valve in Low-Risk Patients. *N Engl J Med.* 2019;380:1695-705.
- 8. Popma JJ, Deeb GM, Yakubov SJ, Mumtaz M, Gada H, O'Hair D, Bajwa T, Heiser JC, Merhi W, Kleiman NS, Askew J, Sorajja P, Rovin J, Chetcuti SJ, Adams DH, Teirstein PS, Zorn GL 3rd, Forrest JK, Tchétché D, Resar J, Walton A, Piazza N, Ramlawi B, Robinson N, Petrossian G, Gleason TG, Oh JK, Boulware MJ, Qiao H, Mugglin AS, Reardon MJ; Evolut Low Risk Trial Investigators. Transcatheter Aortic-Valve Replacement with a Self-Expanding Valve in Low-Risk Patients. N Engl J Med. 2019;380:1706-15.
- 9. Walther T, Hamm CW, Schuler G, Berkowitsch A, Kötting J, Mangner N, Mudra H, Beckmann A, Cremer J, Welz A, Lange R, Kuck KH, Mohr FW, Möllmann H; GARY Executive Board. Perioperative Results and Complications in 15,964 Transcatheter Aortic Valve Replacements: Prospective Data From the GARY Registry. *J Am Coll Cardiol.* 2015;65:2173-80.
- 10. Ochiai T, Chakravarty T, Yoon SH, Kaewkes D, Flint N, Patel V, Mahani S, Tiwana R, Sekhon N, Nakamura M, Cheng W, Makkar R. Coronary Access After TAVR. *JACC Cardiovasc Interv.* 2020;13:693-705.
- 11. Boukantar M, Gallet R, Mouillet G, Belarbi A, Rubimbura V, Ternacle J, Dubois-Rande JL, Teiger E. Coronary Procedures After TAVI With the Self-Expanding Aortic Bioprosthesis Medtronic CoreValveTM, Not an Easy Matter. *J Interv Cardiol*. 2017;30: 56-62.
- 12. Vilalta V, Asmarats L, Ferreira-Neto AN, Maes F, de Freitas Campos Guimarães L, Couture T, Paradis JM, Mohammadi S, Dumont E, Kalavrouziotis D, Delarochellière R, Rodés-Cabau J. Incidence, Clinical Characteristics, and Impact of Acute Coronary Syndrome Following Transcatheter Aortic Valve Replacement. *JACC Cardiovasc Interv.* 2018;11:2523-33.
- 13. Tang GHL, Zaid S, Ahmad H, Undemir C, Lansman SL. Transcatheter Valve Neo-Commissural Overlap With Coronary Orifices After Transcatheter Aortic Valve Replacement. *Circ Cardiovasc Interv.* 2018;11:e007263.
- 14. Yudi MB, Sharma SK, Tang GHL, Kini A. Coronary Angiography And Percutaneous Coronary Intervention After Transcatheter Aortic Valve Replacement. *J Am Coll Cardiol.* 2018;71:1360-78.

- 15. Hirose S, Enta Y, Ishii K, Inoue A, Nakashima M, Nomura T, Saigan M, Tada N. En face view of the transcatheter heart valve from deep right-anterior-oblique cranial position for coronary access after transcatheter aortic valve implantation: a case series. *Eur Heart J Case Rep.* 2022;6:ytac059.
- 16. Redondo A, Baladrón Zorita C, Tchétché D, Santos-Martinez S, Delgado-Arana JR, Barrero A, Gutiérrez H, Serrador Frutos A, Ybarra Falcón C, Gómez MG, Carrasco Moraleja M, Sevilla T, Sanchez Lite I, Sanz E, San Román JA, Amat-Santos IJ. Commissural Versus Coronary Optimized Alignment During Transcatheter Aortic Valve Replacement. *JACC Cardiovasc Interv.* 2022;15:135-46.
- 17. Tang GHL, Sengupta A, Alexis SL, Zaid S, Leipsic JA, Blanke P, Grubb KJ, Gada H, Yakubov SJ, Rogers T, Lerakis S, Khera S, Adams DH, Sharma SK, Kini A, Reardon MJ. Conventional versus modified delivery system technique in commissural alignment from the Evolut low-risk CT substudy. *Catheter Cardiovasc Interv.* 2022:99:924-31.
- 18. Fuchs A, Kofoed KF, Yoon SH, Schaffner Y, Bieliauskas G, Thyregod HG, Makkar R, Søndergaard L, De Backer O, Bapat V. Commissural Alignment of Bioprosthetic Aortic Valve and Native Aortic Valve Following Surgical and Transcatheter Aortic Valve Replacement and its Impact on Valvular Function and Coronary Filling. *JACC Cardiovasc Interv.* 2018;11:1733-43.
- 19. Tang GHL, Zaid S, Fuchs A, Yamabe T, Yazdchi F, Gupta E, Ahmad H, Kofoed KF, Goldberg JB, Undemir C, Kaple RK, Shah PB, Kaneko T, Lansman SL, Khera S,

- Kovacic JC, Dangas GD, Lerakis S, Sharma SK, Kini A, Adams DH, Khalique OK, Hahn RT, Søndergaard L, George I, Kodali SK, De Backer O, Leon MB, Bapat VN. Alignment of Transcatheter Aortic-Valve Neo-Commissures (ALIGN TAVR): Impact on Final Valve Orientation and Coronary Artery Overlap. *JACC Cardiovasc Interv.* 2020;13:1030-42.
- 20. Bieliauskas G, Wong I, Bajoras V, Wang X, Kofoed KF, De Backer O, Søndergaard L. Patient-Specific Implantation Technique to Obtain Neo-Commissural Alignment With Self-Expanding Transcatheter Aortic Valves. *JACC Cardiovasc Interv.* 2021;14:2097-108.
- 21. Piayda K, Scharlau J, Hellhammer K, Zeus T. Delivery Catheter Capsule Demolition During the Deployment of a Medtronic CoreValve Evolut R. *JACC Cardiovasc Interv.* 2020;13:e79-80.
- 22. Tanaka A, Jabbour RJ, Testa L, Agnifili M, Ettori F, Fiorina C, Adamo M, Bruschi G, Giannini C, Petronio AS, Barbanti M, Tamburino C, De Felice F, Reimers B, Poli A, Colombo A, Latib A. Incidence, Technical Safety, and Feasibility of Coronary Angiography and Intervention Following Self-expanding Transcatheter Aortic Valve Replacement. *Cardiovasc Revasc Med.* 2019;20:371-5.
- 23. Wang X, De Backer O, Bieliauskas G, Wong I, Bajoras V, Xiong TY, Zhang Y, Kofoed KF, Chen M, Sondergaard L. Cusp Symmetry and Coronary Ostial Eccentricity and its Impact on Coronary Access Following TAVR. *JACC Cardiovasc Interv.* 2022;15:123-34.

Paracentral MitraClip implantation technique in a mitral valve with a small area due to rheumatic change



Kento Kito, MD; Akihisa Kataoka*, MD, PhD; Hirofumi Hioki, MD, PhD; Yusuke Watanabe, MD, PhD; Ken Kozuma, MD, PhD

Department of Medicine, Teikyo University School of Medicine, Tokyo, Japan

This paper also includes supplementary data published online at: https://www.asiaintervention.org/doi/10.4244/AIJ-D-22-00063

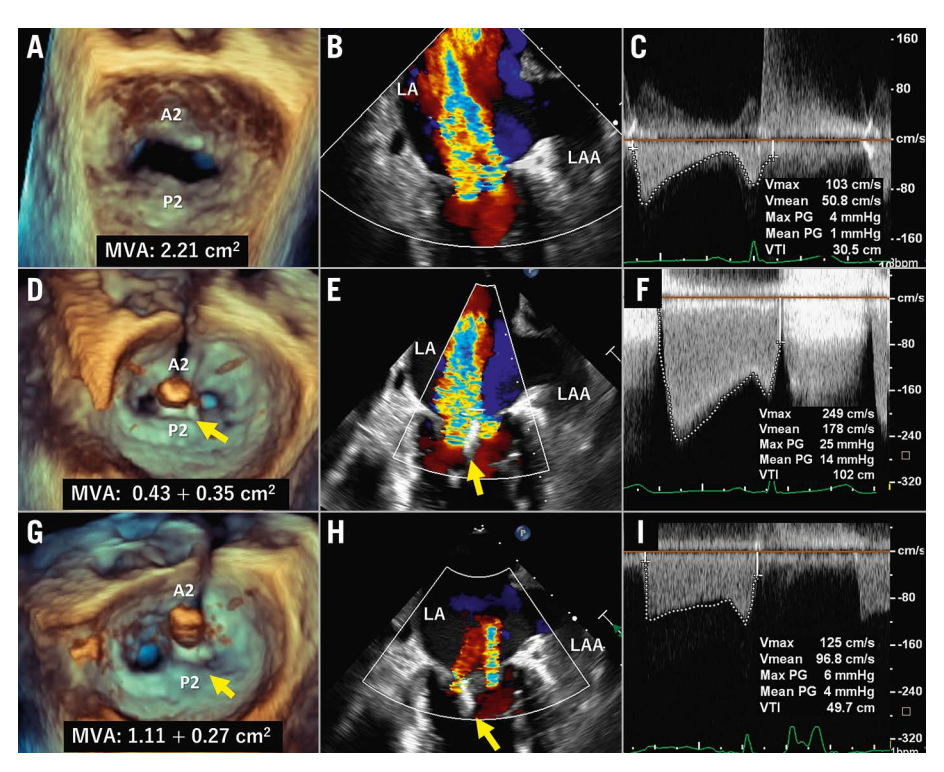


Figure 1. Transoesophageal echocardiography images at screening and during the procedure. En face commissure, and mitral valve pressure gradient images, at screening (A-C) and during the procedure after the central (D-F) and paracentral full grasping (G-I). Yellow arrows indicate the MitraClip. LA: left atrium; LAA: left atrial appendage; MVA: mitral valve area

^{*}Corresponding author: Department of Medicine, Teikyo University School of Medicine, 2-11-1 Kaga Itabashi-Ku, Tokyo, 173-8606 Japan. E-mail: kataoaki@sd5.so-net.ne.jp

An 85-year-old woman was referred to our hospital with severely symptomatic mitral regurgitation (MR). Transoesophageal echocardiography (TOE) showed a small mitral valve (MV) area (MVA) (2.21 cm² on three-dimensional multiplanar reconstruction); mean MV pressure gradient (MVPG) of 1 mmHg, with restricted anterior mitral leaflet (AML) motion due to rheumatic changes, and MR jet from the A2/P2 region (Figure 1A-Figure 1C, Moving image 1, Moving image 2). Despite the rheumatic MV anatomy, our Heart Team offered transcatheter edge-to-edge repair because of the patient's frailty and high surgical risk.

The procedure was performed on day 6 after admission. The MitraClip G4 NT (Abbott) was selected, and full grasping of the A2/P2 central region demonstrated worsened MR with unacceptably elevated MVPG (14 mmHg) and reduced MVA (0.43+0.35 cm²) (Figure 1D-Figure 1F, Moving image 3, Moving image 4). The target region was changed to the medial area of A2/P2, and full grasping showed a significant reduction of MR from 4+ to 2+, with acceptable MVPG (4 mmHg) and MVA (1.11+0.27 cm²) (Figure 1G-Figure 1I, Moving image 5, Moving image 6). The MitraClip was finally implanted without any complications. Thereafter, the patient was discharged on postoperative day 6 with reduced dyspnoea. One month after the procedure, the transthoracic echocardiography showed no evidence of MV damage, and the MR was reduced to 1+ with mildly elevated MVMG (8 mmHg). The patient was in a good condition and had no heart failure exacerbations during the 6-month follow-up.

Although the latest generation of MitraClip G4 NT was used in this case, it made no difference to the treatment quality because the clip size was the same as that of former generations. Central MitraClip implantation in the A2/P2 region is favoured over the paracentral position to prevent clinically relevant mitral stenosis¹. As the AML is longest in the centre, implantation here yields lower valve tension and greater stability. However, owing to the reduced AML flexibility in rheumatic MVs, central implantation may unacceptably increase the MV tension, resulting in failed MR reduction and elevated MVPG due to significant residual MR, together with smaller neo-MVA. In contrast, A2/P2 paracentral implantation may stabilise the leaflet coaptation without excessively increasing the valve tension and MVPG, as it preserves the lateral AML motion. This technique provides a larger MVA and more MR reduction than central implantation. While a rheumatic

MV anatomy is generally considered a relative contraindication, the paracentral implantation technique may be useful to avoid clinically significant mitral stenosis when a MitraClip is necessary.

Conflict of interest statement

A. Kataoka and Y. Watanabe received remuneration from Abbott Medical Japan as proctors for MitraClip. The other authors have no conflicts of interest to declare.

References

 Kassar M, Praz F, Hunziker L, Pilgrim T, Windecker S, Seiler C, Brugger N. Anatomical and Technical Predictors of Three-Dimensional Mitral Valve Area Reduction After Transcatheter Edge-To-Edge Repair. J Am Soc Echocardiogr. 2022;35:96-104.

Supplementary data

Moving image 1. 3D-TOE video of the *en face* view before the procedure shows a small mitral valve area (2.21 cm² measured by 3D-MPR) and restrictive mitral valve leaflet motion. (corresponds to **Figure 1A**).

Moving image 2. 2D-TOE colour video of the commissure view before the procedure shows severe MR jet from A2/P2 region (corresponds to **Figure 1B**).

Moving image 3. 3D-TOE video of the *en face* view after full grasping of the MitraClip NT to the A2/P2 central region shows strikingly decreased mitral valve area (0.43+0.26 cm² measured by 3D-MPR) (corresponds to **Figure 1D**).

Moving image 4. 2D-TOE colour video of the commissure view after full grasping of the MitraClip NT to the A2/P2 central region shows severe split MR jets (corresponds to **Figure 1E**).

Moving image 5. 3D-TOE video of the *en face* view after full grasping of the MitraClip NT to the A2/P2 medial region (paracentral) shows greater mitral valve area (1.11+0.27 cm² measured by 3D-MPR) than that of the A2/P2 central region grasping (corresponds to **Figure 1G**).

Moving image 6. 2D-TOE colour video of the commissure view after full grasping of the MitraClip NT to the A2/P2 medial region shows decreased MR jets from 4+ to 2+ (corresponds to **Figure 1H**).

The supplementary data are published online at: https://www.asiaintervention.org/doi/10.4244/AIJ-D-22-00063



Attention when performing transcatheter valve-in-valve procedures in degenerative INSPIRIS RESILIA valves: a case of malfunction in the expansion zone



Hirofumi Hioki*, MD, PhD; Yusuke Watanabe, MD, PhD; Akihisa Kataoka, MD, PhD; Hideyuki Kawashima, MD, PhD; Ken Kozuma, MD, PhD

Division of Cardiology, Department of Internal Medicine, Teikyo University Hospital, Tokyo, Japan

This paper also includes supplementary data published online at: https://www.asiaintervention.org/doi/10.4244/AIJ-D-22-00079

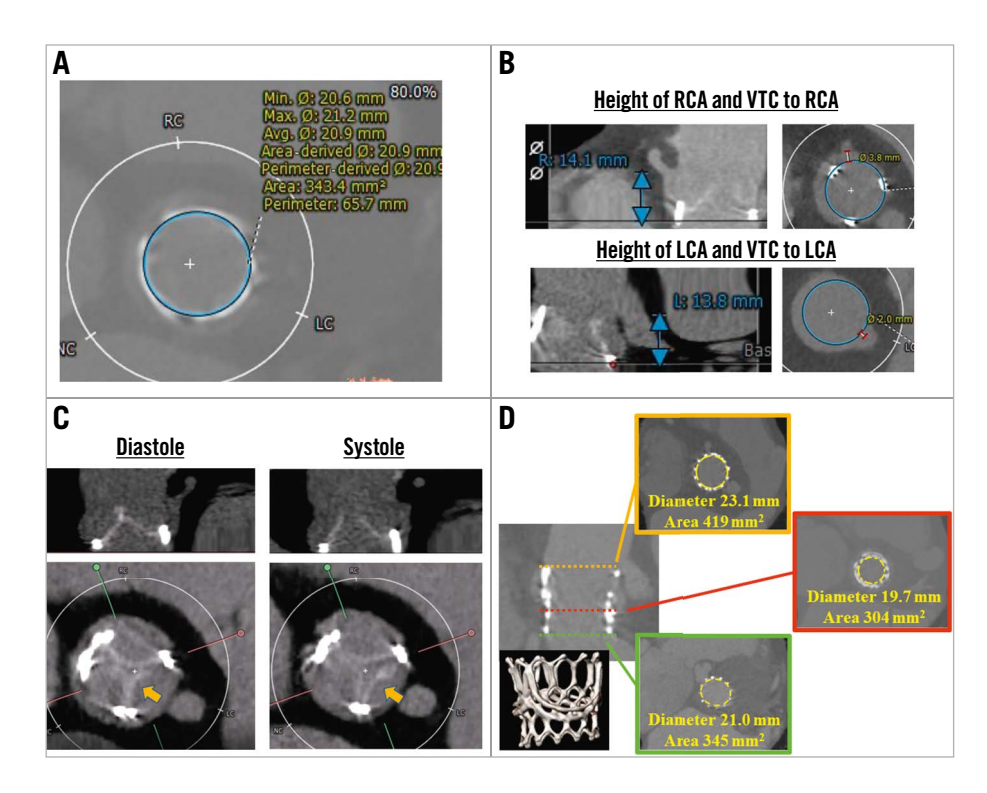


Figure 1. Computed tomographic images before and after transcatheter valve-in-valve procedure. A) Area and perimeter of the INSPIRIS RESILIA 23 mm valve. B) Coronary height and virtual transcatheter heart valve to coronary artery distance. C) Leaflet calcification on INSPIRIS RESILIA valve. The only leaflet located in native left coronary cusp opened during systolic phase (arrow). D) Postprocedural computed tomographic image demonstrating a funnel-shaped appearance of the SAPIEN 3 26 mm without frame expansion of the INSPIRIS RESILIA valve. LCA: left coronary artery; RCA: right coronary artery; VTC: valve-to-coronary distance

^{*}Corresponding author: Division of Cardiology, Department of Internal Medicine, Teikyo University Hospital, 2-11-1 Kaga, Itabashi-ku, Tokyo 173-0003, Japan. E-mail: hioki.teikyo@gmail.com

Transcatheter valve-in-valve (ViV) procedures have become an effective option for failed surgical bioprosthesis implantation in order to avoid a second surgical valve replacement¹. As ViV treatment becomes more common because of degenerative surgical valves, patients and doctors are increasingly choosing tissue valves as the first valve in aortic valve replacement. The INSPIRIS RESILIA aortic valve (Edwards Lifesciences) is the latest tissue valve with a novel technology of a valve frame that can expand to accomodate future ViV procedures. However, no published data on the performance of this expansion technology in ViV treatment are available. Here, we report a case of ViV treatment for a failed INSPIRIS RESILIA valve with insights from the postpreedural computed tomographic findings.

An 81-year-old female was admitted to undergo transcatheter valve-in-valve treatment for a calcified INSPIRIS RESILIA 23 mm valve, resulting in severe aortic stenosis with a peak velocity of 4.26 m/s and a mean pressure gradient of 43 mmHg. She had undergone surgical aortic valve replacement using a Perceval (LivaNova) valve, size M, 2 years earlier. She subsequently had another surgical aortic valve replacement due to infective endocarditis, and a 23 mm INSPIRIS RESILIA valve was implanted, concomitant with a Bentall procedure, 1 year and 4 months after the SAVR with the Perceval valve. Preprocedural computed tomography (CT) demonstrated that the area of the 23 mm INSPIRIS RESILIA was 343 mm² (perimeter 65.7 mm) (Figure 1A) and showed leaflet calcification of the bioprosthesis (Figure 1B). Though virtual, the valve to coronary ostium distance was relatively short in both the right and left coronary arteries. We planned to implant a 26 mm SAPIEN 3 (Edwards Lifesciences) without coronary protection because she had a relatively enlarged sinus of Valsalva due to the Bentall procedure (Figure 1C). The 26 mm SAPIEN 3 was successfully implanted without any complications (Moving image 1, Moving image 2). Her dyspnoea disappeared, and she was discharged 7 days after the transcatheter aortic valve replacement (TAVR). Postprocedural echocardiography demonstrated a mean pressure gradient of 9 mmHg, and the index effective orifice area was 1.11 cm²/m². The postprocedural CT demonstrated a funnel-shaped expansion throughout the transcatheter aortic valve without the expected frame expansion of the INSPIRIS (Figure 1D).

We demonstrated a ViV procedure for early structural valve deterioration of the INSPIRIS, which might have been caused by inflammation due to repeated surgical replacements, including the Bentall procedure. The INSPIRIS RESILIA aortic valve has an expansion zone that is designed to open to allow for upscaling in case of future ViV procedures, though no clinical data on frame expansion in ViV procedures are currently available². In this case, however, the expansion zone of the INSPIRIS RESILIA did not expand, even after the implantation of a balloon-expandable valve. This might have happened because of an excessive amount of abnormal scar tissue caused by repeated surgical procedures, resulting in a rigid aortic annulus. Indeed, in the second aortic valve replacement for infective endocarditis, a bovine pericardial patch was used for the reconstruction of an abscessed aortic root, which might have interfered with the expansion. This is the first report of an unexpanded INSPIRIS frame during transcatheter valve-in-valve in a patient who underwent reconstruction of the aortic root.

Conflict of interest statement

Y. Watanabe is a clinical proctor of transfemoral TAV for Edwards Lifesciences and Medtronic. The other authors have no conflicts of interest to declare.

References

- 1. Bapat V. Technical pitfalls and tips for the valve-in-valve procedure. *Ann Cardiothorac Surg.* 2017;6:541-52.
- 2. Tamagnini G, Bourguignon T, Rega F, Verbrugghe P, Lamberigts M, Langenaeken T, Meuris B. Device profile of the Inspiris Resilia valve for aortic valve replacement: overview of its safety and efficacy. *Expert Rev Med Devices*. 2021;18:239-44.

Supplementary data

Moving image 1. Transcatheter heart valve implantation. **Moving image 2.** Final angiography after implantation.

The supplementary data are published online at: https://www.asiaintervention.org/doi/10.4244/AIJ-D-22-00079



Calcification with a figure of eight appearance found in routine coronary angiography



Ramanathan Velayutham*, MD; A. Shaheer Ahmed, MD, DM; Saurav Banerjee, MD

Department of Cardiology, Jawaharlal Institute of Postgraduate Medical Education and Research, Puducherry, India

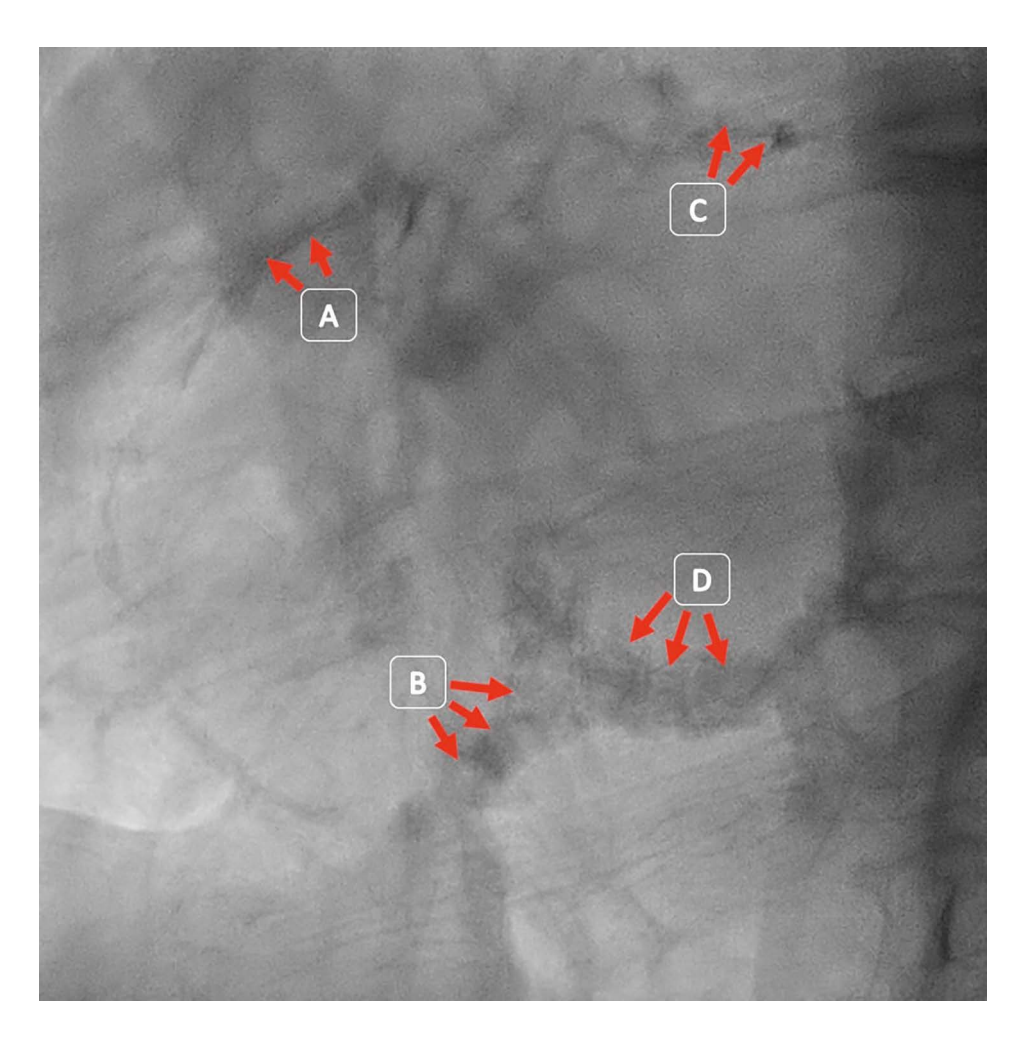


Figure 1. Fluoroscopic LAO view. This figure shows calcium deposits in a figure of eight along the right coronary artery (A), the tricuspid annulus (B), the left circumflex artery (C) and the mitral annulus (D). LAO: left anterior oblique

^{*}Corresponding author: Department of Cardiology, Jawaharlal Institute of Postgraduate Medical Education and Research, Jipmer Campus Road, Dhanvantari Nagar, Puducherry 605006, India. E-mail: nadalram@gmail.com

A 65-year-old female with recent anterior wall myocardial infarction presented with exertional angina. The examination found a pansystolic murmur at apex. Transthoracic echocardiography showed hypokinesia of the anteroseptal region and mitral annular calcification with severe mitral regurgitation.

Coronary angiography showed triple vessel disease. Fluoroscopy in the left anterior oblique (LAO) view demonstrated calcifications with a horizontal figure of eight appearance (Figure 1).

This image illustrates the importance of understanding fluoroscopic anatomy. Drawing an oblique line in the middle of the fluoroscopic LAO view helps to differentiate the right- and left-sided cardiac chambers¹. The lower semicircle of the figure 8 was formed

by annular calcification of the tricuspid valve and mitral valve annulus, while the upper half was completed by calcium along the right coronary artery and left circumflex artery on the right and left sides, respectively. The patient was referred for surgical mitral valve replacement with coronary artery bypass grafting.

Conflict of interest statement

The authors have no conflicts of interest to declare.

Reference

1. Thériault-Lauzier P, Andalib A, Martucci G, Mylotte D, Cecere R, Lange R, Tchétché D, Modine T, van Mieghem N, Windecker S, Buithieu J, Piazza N. Fluoroscopic anatomy of left-sided heart structures for transcatheter interventions: insight from multislice computed tomography. *JACC Cardiovasc Interv.* 2014;7:947-57.



Carotid artery interventions - endarterectomy versus stenting



Sasko Kedev*, MD

University Clinic of Cardiology, Faculty of Medicine, Ss. Cyril and Methodius University, Skopje, Republic of North Macedonia

KEYWORDS

- bare metal stent
- carotid
- drug-eluting stent
- stroke
- supra-aortic disease

Abstract

Current management of patients with carotid artery stenosis is based on well-established guidelines, including surgical procedures – carotid endarterectomy (CEA) and endovascular carotid artery stenting (CAS) – and optimal medical treatment alone. Outcomes in the postprocedural period after CAS and CEA are similar, suggesting strong clinical durability for both treatments. Recent advances, which include the emergence of novel endovascular treatment tools and techniques, combined with more recent randomised trial data shed new light on optimal patient selection and treatment in contemporary practice. Improved, modern technologies including enhanced embolic protection devices and dual-layered micromesh stents yield better outcomes and should result in further improvements in CAS. In centres of excellence, nowadays, the majority of patients with severe carotid artery stenosis can be successfully treated with either CEA or CAS.

^{*}Corresponding author: University Clinic of Cardiology, Faculty of Medicine, Ss. Cyril and Methodius University, Mother Theresa 17, 1000 Skopje, Republic of North Macedonia. E-mail: skedev@gmail.com

Abbreviations

ASR average surgical risk

CABG coronary artery bypass grafting

CAS carotid artery stenting **CEA** carotid endarterectomy

CTA computed tomography angiography

DAPT dual antiplatelet therapy
 DLMS dual-layer micromesh stents
 DUS duplex ultrasonography
 EPD embolic protection device

HSR high surgical risk

IEP integrated embolic protection

MACE major adverse cardiac events

MI myocardial infarction

MRA magnetic resonance angiographyMRI magnetic resonance imagingOMT optimal medical therapy

PCI percutaneous coronary intervention

RCT randomised controlled trial

TCAR transcarotid artery revascularisation

TIA transient ischaemic attack

Introduction

Severely stenosed carotid arteries are predisposed to stroke, and carotid artery revascularisation, with either carotid artery stenting (CAS) or carotid endarterectomy (CEA), can restore patency and reduce the long-term risk of ischaemic stroke. Open carotid endarterectomy completely removes the atheromatous material, but CAS (introduced as an alternative to CEA in 1994) is a less invasive procedure. Carotid endarterectomy 30-day stroke and death rates have decreased over the last 50 years, and similarly, carotid artery stenting 30-day stroke and death rates have declined in a similar magnitude in the last 30 years. Outcomes in the postprocedural period after CAS and CEA are similar, suggesting robust clinical endurance for both treatments.

Several randomised clinical trials, related meta-analyses, and expert opinions have reshaped the present guidelines on the diagnosis and treatment of carotid artery stenosis^{1,2}. Although the indications for carotid revascularisation are well defined, there is less consensus on the preferred revascularisation technique (CEA or CAS). In contemporary clinical practice, many patients are equally suitable for both treatment options.

Currently, CAS is a standard procedure performed by operators of different specialities (cardiologists, neuroradiologists, angiologists, vascular surgeons, and neurosurgeons)¹. Regardless of the medical speciality, the high proficiency of operators and site experience remain paramount for reducing periprocedural adverse cerebral events³. However, the guidelines still seem to underestimate the great importance of operator and site experience, as well as the impact of healthcare providers' decisions on outcomes^{1,2,4}.

According to clinical presentation, patients with extracranial carotid artery stenosis may be asymptomatic or symptomatic. Patients classified as recently symptomatic include those with

symptoms in the past 6 months. All patients with carotid stenosis should undergo an appropriate, independent neurological evaluation followed by duplex ultrasonography (DUS) as a first-line imaging modality in everyday clinical practice^{1,2}. Before any decision for revascularisation is made, additional aspects, such as a patient's surgical risk profile, life expectancy, degree of stenosis, and symptomatic neurological status, should be considered. Further clinical and imaging evaluations may be conducted if justified^{1,2,4}. The degree of carotid artery stenosis identifies patients who would benefit from revascularisation, and the DUS consensus criteria are used to determine stenosis severity according to current guidelines^{1,5}.

DUS is frequently combined with additional imaging modalities, such as computed tomography angiography (CTA) and magnetic resonance angiography (MRA), for improved accuracy of stenosis assessment¹. CTA or MRA can simultaneously delineate the aortic arch, supra-aortic trunks, carotid bifurcation, distal internal carotid artery (ICA) and intracranial circulation, which is particularly useful if CAS is being considered. Contrast-enhanced MRA has higher accuracy than non-contrast MRA but necessitates paramagnetic contrast agents (gadolinium). A combination of 2 imaging modalities (DUS + CTA or DUS + MRA) further improves accuracy and is routinely practised in many centres. Furthermore, postprocedural CTA or brain magnetic resonance imaging (MRI) are usually recommended to characterise the strokes that can occur as periprocedural complications of carotid revascularisation.

SYMPTOMATIC CAROTID STENOSIS

In patients with severe carotid artery stenosis, CAS and CEA both carry procedural risks, which are about twice as great for symptomatic as for asymptomatic patients. The clinical benefit of revascularisation for stroke risk reduction in patients with symptomatic carotid artery stenosis ≥70% is well established¹.².⁴. The revascularisation of symptomatic lesions with 50-69% stenosis should also be performed, but, due to the lower absolute stroke risk in these patients, the treatment value should always be balanced against the possible procedural risks, taking into consideration the patient's clinical presentation, age, and sex¹.².⁴. Exceptionally, in patients with recurrent symptoms despite best medical therapy and carotid stenosis <50% or near occlusion with distal vessel collapse, upon multidisciplinary team review, revascularisation may also be considered¹.⁴. As recommended in current guidelines, revascularisation should be performed within 2 weeks of the index event⁶.

The ongoing uncertainty for prevention of future strokes in patients with symptomatic carotid stenosis stands in defining the optimal candidates for either CEA or CAS. The current multisocietal guideline recommendations agree that in symptomatic high surgical risk (HSR) patients who qualify for carotid revascularisation, CAS is indicated and preferred over CEA.

Factors in favour of CAS include younger age, specific anatomical features (such as very distal ICA stenosis or contralateral occlusion), lack of ICA tortuosity, absence of or only minimal plaque calcification, and local tissue scarring due to previous neck

radiotherapy or complex surgery. Furthermore, a medical history of congestive heart failure, myocardial ischaemia, or severe pulmonary disease makes CAS preferable over CEA. Patients receiving anticoagulation for indications such as atrial fibrillation might also be more suitable for CAS without increasing access site bleeding complications (particularly with transradial CAS). However, CAS is still associated with infrequent periprocedural embolic cerebral complications, resulting in a slightly higher rate of peri- and early postprocedural (up to 30 days) minor ipsilateral strokes, compared to CEA⁷. Although the frequency of such events has been significantly reduced over the past years, cerebral embolisms remain the main weakness of CAS⁸.

Certainly, advantages of CEA over CAS may be found in patients >70 years of age, those with lesion elongation, extreme calcification, visible thrombus presence, or those with challenging anatomies (aortic arch type III or arch calcification)⁴.

ASYMPTOMATIC CAROTID STENOSIS

An asymptomatic carotid artery stenosis (ACS) indicates a stenosis which is detected in patients without any clinical history of ischaemic stroke, transient ischaemic attack (TIA), or other neurological symptoms which might be related to the carotid arteries. Among asymptomatic patients with severe carotid artery stenosis but no recent stroke or TIA, either CAS or CEA can restore patency and reduce long-term stroke risks.

The procedural risks of CAS and CEA have decreased over the decades, but there is still about a 1% risk of disabling stroke or death. There is also some procedural risk of non-disabling stroke (particularly with CAS) or of non-fatal myocardial infarction or cranial nerve palsy (particularly with CEA). Optimal medical therapy (OMT) can likewise reduce stroke rates; however, patients with severe carotid stenosis still have a 1% annual risk of disabling stroke or death.

In contrast to symptomatic carotid patients, the benefit of revascularisation to prevent future strokes in asymptomatic carotid artery stenosis patients is still very much debated. Contrary to the previous belief based on randomised trials comparing medical therapy to revascularisation⁹⁻¹², Howard et al demonstrated a strong and unique relationship between the risk of stroke and the degree of asymptomatic carotid stenosis¹³. Data from a prospective population-based cohort study (OxVasc) screening 2,178 asymptomatic patients with carotid ultrasound between 2002 and 2017 were used, as well as a systematic review and meta-analysis performed of previously concluded cohort studies on this subject between 1980 and 2020.

The observed discrepancy in the evidence from the cohort studies compared with earlier randomised trials could result from a potential recruitment bias in relation to the severity of stenosis, which would undermine any expected risk association in trial cohorts¹³. The authors observed that, in asymptomatic patients, the risk of stroke or TIA strongly correlated with the degree of ipsilateral carotid artery stenosis. The 5-year ipsilateral stroke risk was 18.3% in those with 80-99% stenosis compared with 1.0% in

those with 50-79% stenosis (p<0.0001). Therefore, the degree of asymptomatic carotid stenosis should be a primary consideration for patient selection for revascularisation.

Patients on OMT, featuring high-grade asymptomatic carotid stenosis (>70%), and particularly those with 80-99% artery narrowing, can greatly benefit from carotid revascularisation¹³. The importance of a prudent approach to asymptomatic patients is reflected in the most recent guideline updates. The German-Austrian S3 (2020), the European Stroke Organisation (2021) and the updated European Society for Vascular Surgery (ESVS; 2021) guidelines recommend the revascularisation of patients with asymptomatic high-grade stenoses, provided a meticulous preinterventional assessment is done.^{4,14,15}. The guidelines also recommend close monitoring of periprocedural stroke/death rate records to ensure that decision-making and clinical care are optimised and complications are kept to a minimum⁴.

Recent randomised clinical evidence reflecting real-world practice (the CREST, ACT-1, SPACE-2 and ACST-2 trials) demonstrates that CAS and CEA are both safe and effective in well-selected average surgical risk (ASR) asymptomatic patients ¹⁶⁻¹⁹. All randomised controlled trials (RCT) have shown comparable outcomes for CAS and CEA for periprocedural complications (death, stroke, and myocardial infarction [MI]) as well as rates of ipsilateral stroke during follow-up.

The largest and most recently published trial, the ACST-2 trial, randomised 3,625 patients and compared contemporary CAS versus CEA in asymptomatic patients with carotid artery stenosis.¹⁹. The main finding from the ACST-2 trial is that the effects of CAS versus CEA on disabling or fatal events are approximately equal in terms of procedural hazards (1.0% vs 0.9%; p=0.77). However, there was a slight excess of early non-disabling strokes after CAS and a slight excess of myocardial infarction after CEA. At 5 years, the risk of non-procedural fatal or disabling stroke was equivalent (2.5% vs 2.5%) and there was no significant difference for the incidence of any stroke (5.2% vs 4.5%) comparing CAS with CEA. The results were consistent across patient subgroups stratified by type of stroke, gender, age, and carotid artery diameter stenosis. The trial is scheduled to collect 10-year data which will provide additional evidence on the durability of their protective effects. Unfortunately, the ACST-2 study did not include an OMT arm, so the analysis of early procedural risk versus longterm benefit was not possible.

Furthermore, the investigators used the ACST-2 trial data to update a meta-analysis of long-term outcomes of RCTs comparing CAS versus CEA in patients with asymptomatic (ACST-2, CREST, SPACE-2, ACT-1) and symptomatic (ICSS, CREST, SPACE, EVA-3S) carotid artery stenosis. The meta-analysis confirmed that the protective effects of CAS and CEA are similar after the initial 30-day postprocedural period¹⁹.

One of the most important current questions regarding carotid revascularisation, whether OMT alone is as good as carotid revascularisation with OMT, still remains to be answered. The reports of a very low (\sim 1%) annual stroke rate in asymptomatic carotid

stenosis patients²⁰ has led to 2 ongoing trials (the CREST-2 and ECST-2 trials) investigating the potential benefit of revascularisation compared to modern OMT alone^{21,22}.

In conclusion, properly selected asymptomatic patients can greatly benefit from carotid artery revascularisation, and CAS is a safe and efficient revascularisation alternative to CEA in subjects at high risk for stroke on best available medical therapy.

OPTIMAL MEDICAL THERAPY

In patients with carotid artery disease, adequate concomitant medication is of paramount importance. OMT including antiplatelet agents, statins, blood pressure and diabetes control, smoking cessation, and a healthy lifestyle are critical components of any revascularisation strategy for stroke prevention.

Since atherosclerosis is a generalised condition, patients with carotid artery stenosis would benefit from optimal medical therapy, including antiplatelet and lipid-lowering drugs, irrespective of the revascularisation method^{1,2}.

After CAS, dual antiplatelet therapy (DAPT) with aspirin and clopidogrel is recommended for at least 3 weeks to 3 months after the procedure, followed by lifelong antiplatelet monotherapy thereafter^{1,2,4}. There are limited data on the value of novel P2Y₁₂ inhibitors (ticagrelor, prasugrel) after CAS. Some benefits from prolonged DAPT treatment, up to 12 months, may be expected in selected low bleeding risk CAS patients after recent myocardial infarction, as part of the secondary cardiovascular preventive strategy². The type and duration of antithrombotic treatment during and after CAS should be patient-tailored, always balancing the risk of cerebral ischaemic events against the bleeding risks, especially in patients on oral anticoagulation therapy¹. More dedicated clinical trials are needed to elucidate the optimal duration and type of antithrombotic regimen during and post-CAS to standardise current practice. Patients with severe carotid stenosis may further benefit from more aggressive preventive treatments and more frequent follow-up.

Arterial hypertension remains the most important, modifiable stroke risk factor and blood pressure control is among the most effective strategies for preventing both ischaemic and haemorrhagic stroke. Hypertension as a primary risk factor for stroke is also a risk factor for atrial fibrillation and MI, which both increase the likelihood of stroke. Statins, with ezetimibe as needed, should target low-density lipoprotein cholesterol (LDL-C) <70 mg/dL (<1.8 mmol/L) if not achieved with intensive statin therapy alone. Glycaemic control should target a glycosylated haemoglobin <7% if feasible.

NOVEL CAS TOOLS AND TECHNIQUES

CAS practices have evolved with better patient selection, further refinement of technique, and advanced technology to avoid periprocedural complications. Recently, several technical improvements and new tools have been introduced into CAS practice to further improve the treatment outcomes by providing better cerebral protection and optimal plaque scaffolding. However, anatomical difficulties, including aortic arch complexity, severe calcification and target vessel tortuosity, need to be considered before endovascular carotid artery revascularisation⁸. Selecting optimal treatment tools and approaches for a smooth and uneventful device delivery is of paramount importance for overall treatment success and favourable mid- to long-term outcomes.

EMBOLIC PROTECTION DEVICES

Primary stenting with self-expanding stents using embolic cerebral protection is a default strategy of endovascular carotid stenosis treatment¹. According to the latest recommendations for patients undergoing CAS, decisions regarding the choice of cerebral protection (filter, proximal flow reversal) should be at the discretion of the operator¹. Of note, technical performance based on embolic protection device (EPD) dwell time has been shown to be a significant predictor for 30-day outcome (death, stroke, MI)²³. The selection of EPD should be based on operator experience, lesion characteristics, anatomical factors and current availability of devices. Using different types of embolic protection devices in a more appropriate and individually tailored way may further improve CAS outcomes.

The embolic risk during CAS is highest during the post-dilation after stent deployment^{24,25}.

The majority of embolic particles are under 100 μm in size and may reach the cerebral circulation, despite the use of conventional distal filters, due to malapposition or through the filter pores (larger than 100 μm in most filters) and may contribute to the higher risk of procedural minor stroke seen with CAS²⁶. Recently, double filtration during CAS using a novel post-dilation balloon with an integrated embolic protection (IEP) filter with 40 μm pores showed a low 30-day death, stroke, or MI rate of $1\%^{26}$.

Another innovative approach in CAS is illustrated by the Neuroguard IEP (Contego Medical, Inc.), a 3-in-1 system comprising a carotid stent (with a closed-cell design), a post-dilation balloon and an IEP 40 µm filter, designed to reduce the number of CAS steps while maintaining macro- and microembolic cerebral protection²⁷. Results from the preliminary study demonstrated that the Neuroguard IEP system is safe and feasible for CAS of clinically significant carotid artery stenosis with a stroke/death rate of 0% at 30 days²⁷. A large pivotal study is currently underway.

TRANSRADIAL CAS

The transradial approach (TRA) has become the standard of care for cardiac catheterisation and coronary interventions. Its benefits are also well documented in peripheral interventions, including CAS, leading to a reduced risk of bleeding and access site complications, early ambulation and discharge and, ultimately, cost saving²⁸.

The technical failure of CAS through the femoral approach in most of the cases is due to a complex aortic arch. Features that increase the risk of complications during CAS procedures are some type 2 & 3 arches, bovine arch and plongeant innominate arteries²⁸.

TRA has been a subject of interest in CAS as part of the strategy to tackle some anatomical variants of the aortic arch and supraaortic vessels more safely. This alternative approach may reduce the time for catheter manipulation in the aortic arch and supraaortic vessels, thus directly limiting the CAS-associated stroke risk²⁹. Devices featuring low crossing-profile delivery systems are facilitating the TRA and yielding excellent results²⁸. However, large-bore devices can be used only selectively in patients with larger-size radial arteries. Furthermore, TRA CAS can be performed safely while the patient is taking anticoagulants plus antiplatelet therapy during the periprocedural period, without increasing access site bleeding complications.

While the adoption of transradial access has been increasing in CAS in recent years, more training initiatives and sharing of best practices are needed to bring its full potential to everyday clinical practice. Notably, the growing importance of alternative approaches (i.e., transradial and transcervical access) in modern CAS practice has recently been recognised in the latest ESVS guidelines update, with a recommendation that the 2 methods should be considered for cases in which the transfemoral (TF) route may confer a higher risk of complications¹.

TRANSCAROTID ARTERY REVASCULARISATION

Transcarotid artery revascularisation (TCAR) combines carotid artery stent placement with cerebral protection by clamping the proximal common carotid artery and reversing cerebral arterial flow. The major advantage of TCAR compared with TF CAS is avoiding catheter manipulation in the aortic arch with direct carotid artery access. Some relative contraindications include proximal lesions that are <5 cm cranial to the clavicle, severe target vessel tortuosity, a small or significantly diseased common carotid artery (CCA) or depth of the CCA, which makes access difficult. There are no randomised trials directly comparing TCAR with any other method of carotid revascularisation.

Two recent systematic reviews and meta-analyses reported on 4,852 patients from 10 prospective registries and 8 retrospective studies³⁰, and the second also included 2,110 patients in 18 reports of outcomes with TCAR³¹. Both reviews highlight low rates of periprocedural complications with TCAR; in symptomatic patients, the periprocedural risk of stroke or TIA was 2.5% compared with 1.2% in asymptomatic patients. Further comparative studies are warranted to overcome the potential for selection bias and ascertainment bias in these reports.

CONVENTIONAL CAROTID STENT DESIGN

Regarding the different conventional stent types, devices with open- and closed-cell designs are currently available. It has been shown that, during CAS, the new ipsilateral changes in diffusion-weighted brain MRI are reduced with the use of closed-cell versus open-cell stents (51% vs 31%; p<0.01)³². Consistently, the more recent meta-analysis confirmed that open-cell stents are associated with a 25% higher risk (p=0.03) of developing postprocedural new ischaemic lesions than closed-cell stents³³. No difference,

however, in the short- and intermediate-term risk of stroke or death was observed in patients during CAS with either open-cell or closed-cell stents.

Simplified categorisation into open-cell and closed-cell stent design might conceal true differences, since both stent types may feature different free cell areas and strut connections. The risk for postprocedural adverse cerebral events has been related to the size of the carotid stent free cell area, indicating a significant impact of carotid stent design on CAS outcome. Consistently, open-cell stents with a free cell area >7.5 mm² have been associated with an increased 30-day stroke risk³⁴.

Importantly, based on the CREST trial, around 40% of strokes in the CAS treatment arm occurred 24 hours post-procedure (median 3.5 days)³⁵. Significant incidence of serious cerebral ischaemic complications after removing embolic protection further highlights the importance of good plaque coverage for optimal CAS results.

DUAL-LAYER MICROMESH STENTS

Dual-layer micromesh stents (DLMS) are the next generation of carotid stents with an additional built-in protective micromesh which were specifically designed to provide sustained embolic protection after the stent implantation period. The feasibility and good clinical performance of DLMS have been confirmed in several CAS clinical studies^{36–38}. Currently, there are two DLMS available, Roadsaver (Terumo) and CGuard (InspireMD).

The CLEAR-ROAD study of the Roadsaver carotid stent reported a 2.1% rate of major adverse events at 30 days in 100 treated patients, with only 1 patient suffering a minor ipsilateral stroke due to atrial fibrillation with inadequate anticoagulation³⁹. An Italian multicentre registry reported excellent clinical performance with no cerebrovascular events within 30 days after CAS using the Roadsaver DLMS in 150 patients⁴⁰. Another multicentre Italian study including 200 patients implanted with the CGuard carotid stent resulted in 2 TIAs, 5 periprocedural minor strokes (2.5%), including 1 thrombosis – solved by surgery – up to 30 days post-procedure⁴¹.

Of note, results of studies reporting mid- to long-term outcomes (up to 6 years) of different DLMS support the efficacy and durability of this novel device class by showing relatively low ipsilateral stroke, in-stent restenosis, and target lesion revascularisation rates^{28,42-48}. Importantly, the latest German-Austrian S3 (2020) recommendations for management of carotid stenosis revascularisation updated the acceptable periprocedural (in-hospital) death/stroke incidence (as monitored by expert neurologists) to <2% for asymptomatic and <4% in symptomatic patients⁴. This is stricter than the most recent ESVS guideline update, which recommends 30-day death/stroke incidence thresholds of <3% and <6% for the two patient populations, respectively¹.

In this regard, it is important that an individual patient-level meta-analysis of 4 DLMS studies, including 556 asymptomatic or symptomatic patients treated either with the Roadsaver or CGuard carotid stents, showed very favourable 30-day safety results, with periprocedural stroke noted in 1.07% (0 major strokes), 30-day

stroke in 1.25%, and death in 0.17% of patients⁴⁹. Furthermore, no independent predictors of peri- or postprocedural adverse events, including symptomatic status, were identified. The investigators concluded that the low rate of adverse events, independent of clinical, anatomical and procedural characteristics, suggests that DLMS as a device class are safe for usage in guideline-based CAS and that they may have a possible clinical benefit over the conventional single-layer stents⁴⁹.

Comparably, a meta-analysis of 10 studies (combining the data on 635 asymptomatic or symptomatic patients) confirmed a low 30-day stroke and death rate of 2% (p<0.0001) with DLMS, without a major difference in the clinical performance of the 2 types of DLMS (CGuard vs Roadsaver)⁵⁰. Recently, other real-world studies have also confirmed the excellent safety and performance of DLMS during CAS in non-selected patient populations^{28,45,48,51,52}. Finally, the ROADSAVER study, the largest real-world DLMS study to date, with close to 2,000 elective patients enrolled, further complements the available clinical evidence on DLMS use in current CAS⁵³.

In this all-comers patient cohort, reflecting pan-European contemporary CAS practice, the Roadsaver DLMS results in 30-day death/stroke rates well below the strictest German-Austrian S3 recommendations⁴, 1.6% versus 2.0% in asymptomatic and 2.8% versus 4.0% in symptomatic patients (data not published).

While the current guidelines do not explicitly support the use of a particular stent type, stent designs providing better plaque coverage, including closed-cell stents and particularly DLMS, may actually limit plaque protrusion through the stent struts, thus lowering the incidence of cerebral embolisation during and after device implantation¹.

FUTURE PERSPECTIVES

A quality assurance program adopting competency in practicebased training and improvement, credentialing, and monitoring of procedural technique and outcomes can ensure high-quality CAS or CEA. A multidisciplinary team review (neurologists or stroke physicians, vascular surgeons and interventional cardiologists or radiologists) is recommended to reach consensus decisions regarding the indications and treatment of patients with carotid stenosis regarding CEA, CAS or OMT alone. Shared decision-making, including patient preferences after thoughtful informed consent, is vital in selecting the more appropriate procedure for individual patients. A thorough pre-revascularisation multidisciplinary assessment, using multimodality imaging, with particular emphasis on the degree of stenosis as one of the main factors determining the benefits of revascularisation, may be the most appropriate approach in eligible patients.

Based on current expertise, and considering recently published data, contemporary CAS and CEA can be considered as complementary methods for treating asymptomatic patients with 70-99% stenosis and symptomatic patients with 50-99% artery stenosis. Considering anatomical and medical factors, it is particularly important to identify patients who would benefit mostly from one approach or the other (**Table 1**).

A recent analysis suggested that high operator volume was associated with a lower risk of death or stroke following CAS54. Consequently, the importance of the centre's and operator's experience, particularly the annual operator volume (a better predictor of 30-day death or stroke rate after CAS than lifetime operator volume), in performing CAS should always be emphasised^{3,55}. Among appropriately trained, high-volume operators, satisfactory short- and long-term CAS outcomes can be achieved regardless of their specialisation⁵⁶. Continuous training of operators while maintaining a high procedural volume at both the centre and operator level are crucial for successful carotid revascularisation practice. In addition, quality assurance programs and continuous monitoring of complications are required to maintain high-quality management. Decisively, a collaboration between interventionalists, surgeons, and neurologists is essential to ensure proper patient selection and choose the optimal treatment approach.

Table 1. Revascularisation risks and benefits of CAS and CEA.

CAS preferred		CEA preferred		
Clinical history	Anatomical factors	Clinical history	Anatomical factors	
Congestive heart failure (NYHA Functional Class III/IV) Left ventricular ejection fraction ≤30%	Surgically inaccessible lesions: above C2 or below the clavicle Previous ipsilateral neck irradiation or complex neck surgery	• Elderly (>75 y)	Extreme access challenges	
Unstable angina Recent myocardial infarction (≤30 days) CAD with left main or multivessel CAD Planned open heart surgery (≤30 days)	Contralateral carotid artery occlusion Restenosis after CEA or CAS	Bleeding disorder, contraindication for DAPT	Complex and high-grade aortic arch atheroma Circumferential target lesion calcification Fresh thrombotic lesion	
Advanced COPD	Spinal neck immobility		Extreme ICA tortuosity	
Contralateral laryngeal palsy	Tracheostoma		Aneurismatic ICA morphology	
, , ,	• Iracneostoma	caratid artany stanting. CEA, caratid	1 65	

C2: second cervical spine vertebral body; CAD: coronary artery disease; CAS: carotid artery stenting; CEA: carotid endarterectomy; COPD: chronic obstructive pulmonary disease; DAPT: dual antiplatelet therapy; ICA: internal carotid artery; NYHA: New York Heart Association

Conclusions

The recent trials of CAS versus CEA have provided better evidence that both procedures carry similar risks and provide comparable long-term benefits. Comparisons between the two modalities often represent a false choice because the two therapies are better viewed as complementary approaches rather than competitive procedures. In centres of excellence, nowadays, the majority of patients with severe carotid artery stenosis can be successfully treated with either CEA or CAS. A multidisciplinary assessment with a careful patient and lesion analysis based on inclusion and exclusion criteria for both treatment options in high-volume centres of excellence in both strategies, are essential for selecting an optimal treatment approach. Finally, the evaluation should be done individually, tailoring the procedure to a specific patient in order to achieve the best risk-to-benefit balance.

Conflict of interest statement

The author has no conflicts of interest to declare.

References

- 1. Naylor R, Rantner B, Ancetti S, Gert J, de Borst GJ, De Carlo M, Halliday A, Kakkos SK, Markus HS, McCabe DJH, Sillesen H, van den Berg JC, Vega de Ceniga M, Venermo MA, Vermassen FEG, Esvs Guidelines Committee, Antoniou GA, Bastos Goncalves F, Bjorck M, Chakfe N, Coscas R, Dias NV, Dick F, Hinchliffe RJ, Kolh P, Koncar IB, Lindholt, Mees BME, Resch TA, Trimarchi S, Tulamo R, Twine CP, Wanhainen A, Document Reviewers, Bellmunt-Montoya S, Bulbulia R, Darling 3rd, RC, Eckstein HH, Giannoukas A, Koelemay MJW, Lindström D, Schermerhorn M, Stone DH. Editor's Choice European Society for Vascular Surgery (ESVS) 2023 Clinical Practice Guidelines on the Management of Atherosclerotic Carotid and Vertebral Artery Disease. *Eur J Vasc Endovasc Surg.* 2023;65:7-111.
- 2. Aboyans V, Ricco JB, Bartelink MEL, Björck M, Brodmann M, Cohnert T, Collet JP, Czerny M, De Carlo M, Debus S, Espinola-Klein C, Kahan T, Kownator S, Mazzolai L, Naylor AR, Roffi M, Röther J, Sprynger M, Tendera M, Tepe G, Venermo M, Vlachopoulos C, Desormais I; ESC Scientific Document Group. 2017 ESC Guidelines on the Diagnosis and Treatment of Peripheral Arterial Diseases, in collaboration with the European Society for Vascular Surgery (ESVS): Document covering atherosclerotic disease of extracranial carotid and vertebral, mesenteric, renal, upper and lower extremity arteriesEndorsed by: the European Stroke Organization (ESO)The Task Force for the Diagnosis and Treatment of Peripheral Arterial Diseases of the European Society of Cardiology (ESC) and of the European Society for Vascular Surgery (ESVS). Eur Heart J. 2018;39:763-816.
- 3. Stabile E, Esposito G. Operator's experience is the most efficient embolic protection device for carotid artery stenting. *Circ Cardiovasc Interv.* 2013;6:496-7.
- 4. Eckstein H-H, Kühnl A, Berkefeld J, Lawall H, Storck M, Sander D. Diagnosis, Treatment and Follow-up in Extracranial Carotid Stenosis. *Dtsch Arztebl Int.* 2020;117:801-7.
- 5. Arning C, Widder B, von Reutern G, Stiegler H, Görtler M. Ultraschallkriterien zur Graduierung von Stenosen der A. carotis interna Revision der DEGUM-Kriterien und Transfer in NASCET-Stenosierungsgrade. [Revision of DEGUM ultrasound criteria for grading internal carotid artery stenoses and transfer to NASCET measurement]. Ultraschall Med. 2010;31:251-7.
- 6. Kleindorfer DO, Towfighi A, Chaturvedi S, Cockroft KM, Gutierrez J, Lombardi-Hill D, Kamel H, Kernan WN, Kittner SJ, Leira EC, Lennon O, Meschia JF, Nguyen TN, Pollak PM, Santangeli P, Sharrief AZ, Smith SC Jr, Turan TN, Williams LS. 2021 Guideline for the Prevention of Stroke in Patients With Stroke and Transient Ischemic Attack: A Guideline From the American Heart Association/American Stroke Association. *Stroke*. 2021;52:e364-467.
- 7. Müller MD, Lyrer PA, Brown MM, Bonati LH. Carotid artery stenting versus endarterectomy for treatment of carotid artery stenosis. *Stroke*. 2021;52:e3-5
- 8. White CJ. Brott TG, Gray WA, Heck D, Jovin T, Lyden SP, Metzger DC, Rosenfield K, Roubin G, Sachar R, Siddiqui A. Carotid Artery Stenting: JACC State-of-the-Art Review. *J Am Coll Cardiol*. 2022;80:155-70.
- 9. Hobson RW 2nd, Weiss DG, Fields WS, Goldstone J, Moore WS, Towne JB, Wright CB. Efficacy of carotid endarterectomy for asymptomatic carotid stenosis. The Veterans Affairs Cooperative Study Group. *N Engl J Med.* 1993;328:221-7.

- No authors listed. Endarterectomy for asymptomatic carotid artery stenosis.
 Executive Committee for the Asymptomatic Carotid Atherosclerosis Study. JAMA.
 1995:273:1421-8.
- 11. Halliday A, Mansfield A, Marro J, Peto C, Peto R, Potter J, Thomas D; MRC Asymptomatic Carotid Surgery Trial (ACST) Collaborative Group. Prevention of disabling and fatal strokes by successful carotid endarterectomy in patients without recent neurological symptoms: randomised controlled trial. *Lancet*. 2004;363:1491-502.
- 12. Halliday A, Harrison M, Hayter E, Kong X, Mansfield A, Marro J, Pan H, Peto R, Potter J, Rahimi K, Rau A, Robertson S, Streifler J, Thomas D; Asymptomatic Carotid Surgery Trial (ACST) Collaborative Group. 10-year stroke prevention after successful carotid endarterectomy for asymptomatic stenosis (ACST-1): a multicentre randomised trial. *Lancet*. 2010;376:1074-84.
- 13. Howard DPJ, Gaziano L, Rothwell PM; Oxford Vascular Study. Risk of stroke in relation to degree of asymptomatic carotid stenosis: a population-based cohort study, systematic review, and meta-analysis. *Lancet Neurol.* 2021;20:193-202.
- 14. Bonati LH, Kakkos S, Berkefeld J, de Borst GJ, Bulbulia R, Halliday A, van Herzeele I, Koncar I, McCabe DJ, Lal A, Ricco JB, Ringleb P, Taylor-Rowan M, Eckstein HH. European Stroke Organisation guideline on endarterectomy and stenting for carotid artery stenosis. *Eur Stroke J*. 2021;6:I-XLVII.
- 15. AbuRahma AF, Avgerinos ED, Chang RW, Darling RC 3rd, Duncan AA, Forbes TL, Malas MB, Perler BA, Powell RJ, Rockman CB, Zhou W. The Society for Vascular Surgery implementation document for management of extracranial cerebrovascular disease. *J Vasc Surg.* 2022;75:26S-98S.
- 16. Brott TG, Hobson RW, Howard G, Roubin GS, Clark WM, Brooks W, Mackey A, Hill MD, Leimgruber PP, Sheffet AJ, Howard VJ, Moore WS, Voeks JH, Hopkins LN, Cutlip DE, Cohen DJ, Popma JJ, Ferguson RD, Cohen SN, Blackshear JL, Silver FL, Mohr JP, Lal BK, Meschia JF; CREST Investigators. Stenting versus endarterectomy for treatment of carotid-artery stenosis. *N Engl J Med.* 2010;363:11-23.
- 17. Rosenfield K, Matsumura JS, Chaturvedi S, Riles T, Ansel GM, Metzger DC, Wechsler L, Jaff MR, Gray W; ACT I Investigators. Randomized Trial of Stent versus Surgery for Asymptomatic Carotid Stenosis. *N Engl J Med.* 2016;374:1011-20.
- 18. Reiff T, Eckstein HH, Mansmann U, Jansen O, Fraedrich G, Mudra H, Böckler D, Böhm M, Brückmann H, Debus ES, Fiehler J, Lang W, Mathias K, Ringelstein EB, Schmidli J, Stingele R, Zahn R, Zeller T, Hetzel A, Bodechtel U, Binder A, Glahn J, Hacke W, Ringleb PA. Angioplasty in asymptomatic carotid artery stenosis vs. endarterectomy compared to best medical treatment: one-year interim results of SPACE-2. *Int J Stroke*. 2020;15:638-49.
- 19. Halliday A, Bulbulia R, Bonati LH, Chester J, Cradduck-Bamford A, Peto R, Pan H; ACST-2 Collaborative Group. Second asymptomatic carotid surgery trial (ACST-2): a randomised comparison of carotid artery stenting versus carotid endarter-ectomy. *Lancet*. 2021;398:1065-73.
- 20. Jaillant N, Thibouw F, Loucou JD, Pouhin A, Kazandjian C, Steinmetz E. A Prospective Survey of The Incidence of Cranial and Cervical Nerve Injuries After Carotid Surgery. *Ann Vasc Surg.* 2022;87:380-7.
- 21. Lal BK, Meschia JF, Brott TG. Clinical need, design, and goals for the Carotid Revascularization and Medical Management for Asymptomatic Carotid Stenosis trial. *Semin Vasc Surg.* 2017;30:2-7.
- 22. Featherstone R, Brown M. The Second European Carotid Surgery Trial. Endovasc Today. 2012;10:75-77. https://evtoday.com/articles/2012-oct/the-second-european-carotid-surgery-trial. Last accessed 14 June 23.
- 23. Shishehbor MH, Venkatachalam S, Gray WA, Metzger C, Lal BK, Peng L, Omran HL, Blackstone EH. Experience and Outcomes With Carotid Artery Stenting An Analysis of the CHOICE (Carotid Stenting for High Surgical-Risk Patients; Evaluating Outcomes Through the Collection of Clinical Evidence) Study. *JACC Cardiovasc Interv.* 2014;7:1307-17.
- 24. Hellings WE, Ackerstaff RG, Pasterkamp G, De Vries JP, Moll FL. The carotid atherosclerotic plaque and microembolisation during carotid stenting. *J Cardiovasc Surg (Torino)*. 2006;47:115-26.
- 25. Obeid T, Arnaoutakis DJ, Arhuidese I, Qazi U, Abularrage CJ, Black J, Perler B, Malas M. Poststent ballooning is associated with increased periprocedural stroke and death rate in carotid artery stenting. *J Vasc Surg.* 2015;62:616-23.
- 26. Langhoff R, Schofer J, Scheinert D, Schmidt A, Sedgewick G, Saylors E, Sachar R, Sievert H, Zeller T. Double filtration during carotid artery stenting using a novel post-dilation balloon with integrated embolic protection. *JACC Cardiovasc Interv.* 2019;12:395-403.
- 27. Langhoff R, Petrov I, Kedev S, Milosevic Z, Schmidt A, Scheinert D, Schofer J, Sievert H, Sedgewick G, Saylors E, Sachar R, Cremonesi A, Micari A. PERFORMANCE 1 study: Novel carotid stent system with integrated post-dilation balloon and embolic protection device. *Catheter Cardiovasc Interv.* 2022;100:1090-9.
- 28. Petkoska D, Zafirovska B, Vasilev I, Novotni G, Bertrand OF, Kedev S. Radial and ulnar approach for carotid artery stenting with RoadsaverTM double layer micromesh stent: Early and long-term follow-up. *Catheter Cardiovasc Interv.* 2023;101:154-63.

- 29. Maciejewski DR, Tekieli L, Trystula M, Tomaszewski T, Machnik R, Legutko J, Kazibudzki M, Musiał R, Misztal M, Pieniążek P. Clinical situations requiring radial or brachial access during carotid artery stenting. *Postepy Kardiol Interwencyjnej*. 2020;16:410-7
- 30. Galyfos GC, Tsoutsas I, Konstantopoulos T, Galanopoulos G, Sigala F, Filis K, Papavassiliou V. Editor's Choice Early and Late Outcomes after Transcarotid Revascularisation for Internal Carotid Artery Stenosis: A Systematic Review and Meta-Analysis. *Eur J Vasc Endovasc Surg.* 2021;61:725-38.
- 31. Paraskevas KI, Antonopoulos CN, Kakisis JD, Geroulakos G. An updated systematic review and meta-analysis of results of transcervical carotid artery stenting with flow reversal. *J Vasc Surg.* 2020;72:1489-98.e1.
- 32. Schnaudigel S, Gröschel K, Pilgram SM, Kastrup A. New brain lesions after carotid stenting versus carotid endarterectomy: a systematic review of the literature. *Stroke*, 2008;39:1911-9.
- 33. de Vries EE, Meershoek AJA, Vonken EJ, den Ruijter HM, van den Berg JC, de Borst GJ. A meta-analysis of the effect of stent design on clinical and radiologic outcomes of carotid artery stenting. *J Vasc Surg*. 2019;69:1952-61 e1.
- 34. Stabile E, Giugliano G, Cremonesi A, Bosiers M, Reimers B, Setacci C, Cao P, Schmidt A, Sievert H, Peeters P, Nikas D, Sannino A, de Donato G, Parlani G, Castriota F, Hornung M, Rubino P, Esposito G, Tesorio T. Impact on outcome of different types of carotid stent: results from the European Registry of Carotid Artery Stenting. *EuroIntervention*. 2016;12:e265-70.
- 35. Hill MD, Brooks W, Mackey A, Clark WM, Meschia JF, Morrish WF, Mohr JP, Rhodes JD, Popma JJ, Lal BK, Longbottom ME, Voeks JH, Howard G, Brott TG; CREST Investigators. Stroke after carotid stenting and endarterectomy in the Carotid Revascularization Endarterectomy versus Stenting Trial (CREST). *Circulation*. 2012;126:3054-61.
- 36. Musialek P, Mazurek A, Trystula M, Borratynska A, Lesniak-Sobelga A, Urbanczyk M, Banys P, Brzychczy A, Zajdel W, Partyka L, Zmudka K, Podolec P. Novel PARADIGM in carotid revascularisation: Prospective evaluation of All-comer peRcutaneous cArotiD revascularisation in symptomatic and Increased-risk asymptomatic carotid artery stenosis using CGuard MicroNet-covered embolic prevention stent system. *EuroIntervention*. 2016;12:e658-70.
- 37. Schofer J, Musialek P, Bijuklic K, Kolvenbach R, Trystula M, Siudak Z, Sievert H. A Prospective, Multicenter Study of a Novel Mesh-Covered Carotid Stent: The CGuard CARENET Trial (Carotid Embolic Protection Using MicroNet). *JACC Cardiovasc Interv.* 2015;8:1229-34.
- 38. Hopf-Jensen S, Marques L, Preiss M, Müller-Hülsbeck S. Initial clinical experience with the micromesh Roadsaver carotid artery stent for the treatment of patients with symptomatic carotid artery disease. *J Endovasc Ther.* 2015;22:220-5.
- 39. Bosiers M, Deloose K, Torsello G, Scheinert D, Maene L, Peeters P, Müller-Hülsbeck S, Sievert H, Langhoff R, Bosiers M, Setacci C. The CLEAR-ROAD study: evaluation of a new dual layer micromesh stent system for the carotid artery. *EuroIntervention*. 2016;12:e671-6.
- 40. Nerla R, Castriota F, Micari A, Sbarzaglia P, Secco GG, Ruffino MA, de Donato G, Setacci C, Cremonesi A. Carotid artery stenting with a new-generation double-mesh stent in three high-volume Italian centres: clinical results of a multidisciplinary approach. *EuroIntervention*. 2016;12:e677-83.
- 41. Speziale F, Capoccia L, Sirignano P, Mansour W, Pranteda C, Casana R, Setacci C, Accrocca F, Alberti D, de Donato G, Ferri M, Gaggiano A, Galzerano G, Ippoliti A, Mangialardi N, Pratesi G, Ronchey S, Ruffino MA, Siani A, Spinazzola A, Sponza M. Thirty-day results from prospective multi-specialty evaluation of carotid artery stenting using the CGuard MicroNet-covered Embolic Prevention System in real-world multicentre clinical practice: the IRON-Guard study. *EuroIntervention*. 2018;13: 1714-20.
- 42. Bosiers M, Deloose K, Torsello G, Scheinert D, Maene L, Peeters P, Müller-Hülsbeck S, Sievert H, Langhoff R, Callaert J, Setacci C, Wauters J. Evaluation of a new dual-layer micromesh stent system for the carotid artery. 12-month results from the CLEAR-ROAD study. *EuroIntervention*. 2018;14:1144-6.
- 43. Nerla R, Micari A, Castriota F, Miccichè E, Ruffino MA, de Donato G, Setacci C, Cremonesi A. Carotid artery stenting with a new-generation double-mesh stent in three

- high-volume Italian centres: 12-month follow-up results. EuroIntervention. 2018;14: 1147-9.
- 44. Mazurek A, Borratynska A, Malinowski KP, Brozda M, Gancarczyk U, Dluzniewska N, Czyz L, Duplicka M, Sobieraj E, Trystula M, Drazkiewicz T, Podolec P, Musialek P. MicroNET-covered stents for embolic prevention in patients undergoing carotid revascularisation: twelve-month outcomes from the PARADIGM study. *EuroIntervention*. 2020;16:e950-2.
- 45. Machnik RA, Pieniazek P, Misztal M, Plens K, Kazibudzki M, Tomaszewski T, Brzychczy A, Musiał R, Trystuła M, Tekieli LM. Carotid artery stenting with Roadsaver stent. Early and four-year results from a single-center registry. *Postepy Kardiol Interwencyjnej.* 2020;16:444-51.
- 46. Gray WA, Levy E, Bacharach JM, Metzger DC, Randall B, Siddiqui A, Schonholz C, Alani F, Schneider PA. Evaluation of a novel mesh-covered stent for treatment of carotid stenosis in patients at high risk for endarterectomy: 1-year results of the SCAFFOLD trial. *Catheter Cardiovasc Interv.* 2020;96:121-7.
- 47. Capoccia L, Sirignano P, Mansour W, Sbarigia E, Speziale F. Twelve-month results of the Italian registry on protected CAS with the mesh-covered CGuard stent: the IRON-Guard study. *EuroIntervention*. 2018;14:1150-2.
- 48. Sirignano P, Stabile E, Mansour W, Capoccia L, Faccenna F, Intrieri F, Ferri M, Saccà S, Sponza M, Mortola P, Ronchey S, Praquin B, Grillo P, Chiappa R, Losa S, Setacci F, Pirrelli S, Taurino M, Ruffino MA, Udini M, Palombo D, Ippoliti A, Montelione N, Setacci C, de Donato G, Ruggeri M, Speziale F. 1-Year Results From a Prospective Experience on CAS Using the CGuard Stent System: The IRONGUARD 2 Study. *JACC Cardiovasc Interv.* 2021;14:1917-23.
- 49. Stabile E, de Donato G, Musialek P, De Loose K, Nerla R, Sirignano P, Chianese S, Mazurek A, Tesorio T, Bosiers M, Setacci C, Speziale F, Micari A, Esposito G. Use of Dual-Layered Stents in Endovascular Treatment of Extracranial Stenosis of the Internal Carotid Artery: Results of a Patient-Based Meta-Analysis of 4 Clinical Studies. *JACC Cardiovasc Interv.* 2018;11:2405-11.
- 50. Sannino A, Giugliano G, Toscano E, Schiattarella GG, Franzone A, Tesorio T, Trimarco B, Esposito G, Stabile E. Double layered stents for carotid angioplasty: A meta-analysis of available clinical data. *Catheter Cardiovasc Interv.* 2018;91: 751-7
- 51. Sirignano P, Stabile E, Mansour W, Capoccia L, Faccenna F, Intrieri F, Ferri M, Saccà S, Sponza M, Mortola P, Ronchey S, Grillo P, Chiappa R, Losa S, Setacci F, Pirrelli S, Taurino M, Ruffino MA, Udini M, Palombo D, Ippoliti A, Montelione N, Setacci C, de Donato G, Ruggeri M, Speziale F. 1-Month Results From a Prospective Experience on CAS Using CGuard Stent System: The IRONGUARD 2 Study. *JACC Cardiovasc Interv.* 2020;13:2170-7.
- 52. Kahlberg A, Bilman V, Ardita V, Mascia D, Bertoglio L, Rinaldi E, Melissano G, Chiesa R. Contemporary Results of Carotid Artery Stenting Using Low-Profile Dual-Metal Layer Nitinol Micromesh Stents in Relation to Single-Layer Carotid Stents. *J Endovasc Ther.* 2021;28:726-36.
- 53. Kedev S, Müller-Hülsbeck S, Langhoff R. "Real-World Study of a Dual-Layer Micromesh Stent in Elective Treatment of Symptomatic and Asymptomatic Carotid Artery Stenosis (ROADSAVER)". Cardiovasc Intervent Radiol. 2022;45:277-82.
- 54. Kallmayer MA, Salvermoser M, Knappich C, Trenner M, Karlas A, Wein F, Eckstein HH, Kuehnl A. Quality appraisal of systematic reviews, and meta-analysis of the hospital/surgeon-linked volume-outcome relationship of carotid revascularization procedures. *J Cardiovasc Surg (Torino)*. 2019;60:354-63.
- 55. Calvet D, Mas JL, Algra A, Becquemin JP, Bonati LH, Dobson J, Fraedrich G, Jansen O, Mali WP, Ringleb PA, Chatellier G, Brown MM, Calvet D, Mas JL, Algra A, Becquemin JP, Bonati LH, Dobson J, Fraedrich G, Jansen O, Mali WP, Ringleb PA, Chatellier G, Brown MM, Algra A, Becquemin JP, Chatellier G, Mas JL, Fraedrich G, Ringleb PA, Jansen O, Brown MM; Carotid Stenting Trialists' Collaboration. Carotid stenting: is there an operator effect? A pooled analysis from the carotid stenting trialists' collaboration. *Stroke*. 2014;45:527-32.
- 56. Timaran CH, Mantese VA, Malas M, Brown OW, Lal BK, Moore WS, Voeks JH, Brott TG; CREST Investigators. Differential outcomes of carotid stenting and endarterectomy performed exclusively by vascular surgeons in the Carotid Revascularization Endarterectomy versus Stenting Trial (CREST). J Vasc Surg. 2013;57:303-8.

Letter: Limitless suffixes for bifurcation classification with the Movahed coronary bifurcation lesion classification system



Mohammad Reza Movahed^{1,2*}, MD

1. University of Arizona Sarver Heart Center, Tucson, AZ, USA; 2. University of Arizona, Phoenix, AZ, USA

With great interest, I read the paper by Shao-Liang Chen published in your Journal entitled "DEFINITION criteria for left main bifurcation stenting - from clinical need to a formula". The author correctly mentions the major limitations of the Medina bifurcation classification: "However, this classification also has limitations because it doesn't include important descriptive features of bifurcation lesions that could be helpful in determining the optimum stent treatment strategy. Therefore, the lack of a comprehensive stratification system defining the complexity of bifurcation lesions remains an unmet clinical need". Another detailed classification system, called the Movahed bifurcation classification system, exists that is simpler than the Medina classification in its basic structure and has unlimited suffixes that can be added in order to describe any given bifurcation lesion anatomy for clinical or research purposes. The Movahed classification^{2,3} simplifies bifurcation lesions into three categories: in the so-called B2 (B for bifurcation, 2 for both branches), both branches are involved; if only the main branch is involved, it is called B1m (B for bifurcation, 1m meaning only the main branch has disease); and if only

the side branch is involved, it is called a B1s lesion (B for bifurcation and 1s meaning only the side branch has the disease). Next, the Movahed classification adds additional optional suffixes that can describe any anatomical features of a given bifurcation classification that are needed for specific clinical or research purposes, enabling succinct definitions. For example, describing the angiographic criterion that was used in the DEFINITION study was a lengthy affair, whereas, using the Movahed bifurcation classification, it could have been summarised as follows: B2LM SBL ≥10 mm SBSD ≥70% CA MVD <2.5 TR MVL ≥25 (B2: both branches have the disease; LM: left main lesion; SBL ≥10 mm: side branch lesion length over 10 mm; SBSD ≥70%: side branch stenosis diameter ≥70%; CA: significant calcification; MVD <2.5: main vessel diameter <2.5 mm; TR: thrombus-containing; MVL \geq 25: main vessel lesion length \geq 25 mm). We believe the widely used Medina bifurcation classification should be abandoned in favour of the Movahed classification due to the complexity and lack of suffixes, in the former, for describing any needed anatomical description of a given coronary bifurcation lesion⁴⁻⁸. Figure 1

^{*}Corresponding author: University of Arizona Sarver Heart Center, 1501 North Campbell Avenue, Tucson, AZ 85724, USA. E-mail: Rmova@aol.com

Movahed	Medina
B2	1.1.1, 1.0.1, 0.1.1
B1m	1.1.0, 1.0.0, 0.1.0
B1s	0.0.1

Figure 1. Comparison of the Movahed to the Medina coronary bifurcation classification revealing the simplicity of the basic suffix of the Movahed classification.

and **Figure 2** describe the Movahed classification in comparison to the Medina classification with a detailed description of the Movahed classification when using additional suffixes.

Conflict of interest statement

The author has no conflicts of interest to declare.

References

- 1. Chen SL. DEFINITION criteria for left main bifurcation stenting from clinical need to a formula. *AsiaIntervention*. 2023;9:20-4.
- 2. Movahed MR, Stinis CT. A new proposed simplified classification of coronary artery bifurcation lesions and bifurcation interventional techniques. *J Invasive Cardiol.* 2006;18:199-204.
- 3. Movahed MR. Coronary artery bifurcation lesion classifications, interventional techniques and clinical outcome. Expert Rev Cardiovasc Ther. 2008;6:261-74.
- 4. Movahed MR. Quantitative angiographic methods for bifurcation lesions: a consensus statement from the European Bifurcation Group. Shortcoming of the Medina classification as a preferred classification for coronary artery bifurcation lesions in comparison to the Movahed classification. *Catheter Cardiovasc Interv.* 2009;74: 817-8

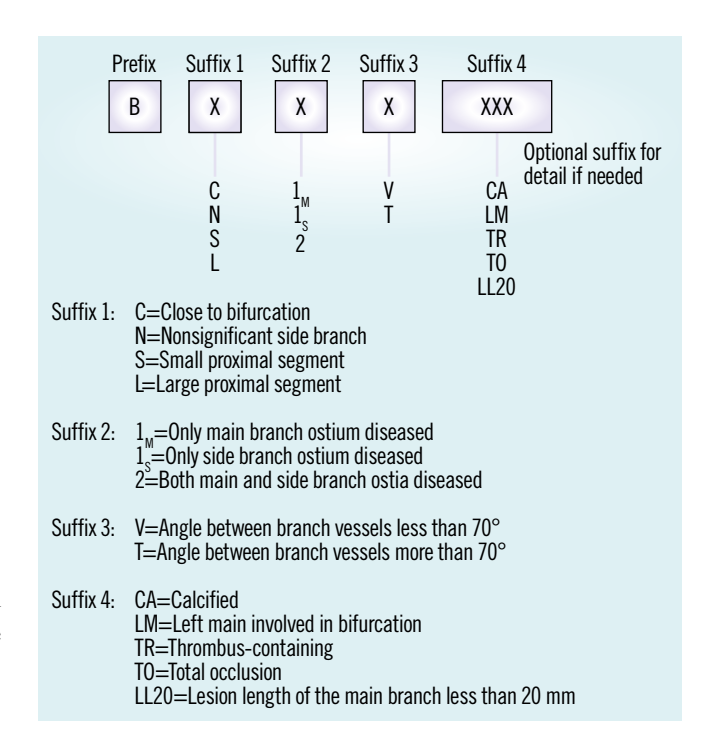


Figure 2. Details of the Movahed bifurcation classification with limitless optional suffixes.

- 5. Movahed MR. Studies involving coronary bifurcation interventions should utilize the most comprehensive and technically relevant Movahed coronary bifurcation classification for better communication and accuracy. *Am J Cardiol.* 2010;105:1204-5.
- Movahed MR. B2 lesions are true bifurcation lesions simply categorized as one group according to the Movahed bifurcation classification. *J Invasive Cardiol*. 2010; 22:252.
- 7. Movahed MR. Major limitations of randomized clinical trials involving coronary artery bifurcation interventions: time for redesigning clinical trials by involving only true bifurcation lesions and using appropriate bifurcation classification. *J Interv Cardiol.* 2011;24:295-301.
- 8. Movahed MR. Is it time to consider the Movahed classification as the preferred classification for coronary bifurcation lesions? *EuroIntervention*. 2010;5:652.

Reply: Limitless suffixes for bifurcation classification with the Movahed coronary bifurcation lesion classification system



Shao-Liang Chen, MD

Nanjing First Hospital, Nanjing Medical University, Nanjing, People's Republic of China

We appreciate the interest shown by Dr Movahed¹ regarding our review, "DEFINITION criteria for left main bifurcation stenting – from clinical need to a formula", which was recently published in AsiaIntervention².

The treatment of coronary bifurcation lesions is generally challenging, with Medina 1,1,1 and 0,0,1 subtypes associated with an increased risk of target lesion failure3. The Movahed bifurcation classification system tends to exclude the importance of Medina 0,1,1, but it indicates the importance of side branch lesions. Among the different classifications for coronary bifurcation lesions, the Medina stratification4 is the most extensively used, although it lacks some critical information correlated with clinical outcomes. Thereafter, serial classification systems were introduced, including the MADS (Main, Across, Distal, Side) classification system⁵ and the Mohaved classification system⁶. These stratifications guide the stenting selection based on the concept that a 2-stent technique is more frequently required for severely diseased side branches, and provisional side branch stenting may be associated with fewer clinical events for "simple" lesions. The remaining unresolved question is whether all "true" bifurcations are the same? This unmet need drove the birth of the DEFINITION criteria2. The subsequent DEFINITION II trial⁷ has further confirmed the utility of the DEFINITION criteria, represented by a higher rate of target lesion failure after provisional stenting for complex bifurcation lesions.

Coronary bifurcation lesions are relatively common among coronary artery lesions undergoing stenting. While the interventional community has achieved dramatic progress in understanding the mechanisms (particularly the abnormal distribution of shear stress), the importance of intravascular imaging guidance

and how to select a stenting approach, we are still facing a mass of unclear topics. Further research is warranted to promote patients with complex coronary bifurcation lesions.

Conflict of interest statement

The author has no conflicts of interest to declare.

References

- 1. Movahed MR. Letter: Limitless suffixes for bifurcation classification with the Movahed coronary bifurcation lesion classification system. *AsiaIntervention*. 2023;9:180-1.
- 2. Chen SL. DEFINITION criteria for left main bifurcation stenting from clinical need to a formula. *AsiaIntervention*. 2023;9:20-4.
- 3. Mohamed MO, Lamellas P, Roguin A, Oemrawsingh RM, Ijsselmuiden AJJ, Routledge H, van Leeuwen F, Debrus R, Roffi M, Mamas MA; e-Ultimaster investigators. Clinical Outcomes of Percutaneous Coronary Intervention for Bifurcation Lesions According to Medina Classification. *J Am Heart Assoc.* 2022;11:e025459.
- 4. Medina A, Suárez de Lezo J, Pan M. Una clasificación simple de las lesiones coronarias en bifurcación [A new classification of coronary bifurcation lesions]. *Rev Esp Cardiol.* 2006;59:183.
- 5. Louvard Y, Thomas M, Dzavik V, Hildick-Smith D, Galassi AR, Pan M, Burzotta F, Zelizko M, Dudek D, Ludman P, Sheiban I, Lassen JF, Darremont O, Kastrati A, Ludwig J, Iakovou I, Brunel P, Lansky A, Meerkin D, Legrand V, Medina A, Lefèvre T. Classification of coronary artery bifurcation lesions and treatments: time for a consensus! *Catheter Cardiovasc Interv.* 2008;71:175-83.
- 6. Movahed MR, Stinis CT. A new proposed simplified classification of coronary artery bifurcation lesions and bifurcation interventional techniques. *J Invasive Cardiol.* 2006:18:199-204.
- 7. Zhang JJ, Ye F, Xu K, Kan J, Tao L, Santoso T, Munawar M, Tresukosol D, Li L, Sheiban I, Li F, Tian NL, Rodríguez AE, Paiboon C, Lavarra F, Lu S, Vichairuangthum K, Zeng H, Chen L, Zhang R, Ding S, Gao F, Jin Z, Hong L, Ma L, Wen S, Wu X, Yang S, Yin WH, Zhang J, Wang Y, Zheng Y, Zhou L, Zhou L, Zhu Y, Xu T, Wang X, Qu H, Tian Y, Lin S, Liu L, Lu Q, Li Q, Li B, Jiang Q, Han L, Gan G, Yu M, Pan D, Shang Z, Zhao Y, Liu Z, Yuan Y, Chen C, Stone GW, Han Y, Chen SL. Multicentre, randomized comparison of two-stent and provisional stenting techniques in patients with complex coronary bifurcation lesions: the DEFINITION II trial. *Eur Heart J.* 2020;41: 2523-36

^{*}Corresponding author: Nanjing First Hospital, Nanjing Medical University, 68 Changle Road, Nanjing 210006, People's Republic of China. E-mail: chmengx@hotmail.com.